GRAVITY AND OTHER GEOPHYSICAL STUDIES RELATING TO THE CRUSTAL STRUCTURE OF SOUTH-EAST SCOTLAND

by

Evangelos Lagios
B.Sc., Athens University

Thesis presented for the degree of
Doctor of Philosophy
of the University of Edinburgh in the
Faculty of Science

OCTOBER 1979

DECLARATION

I hereby declare that the work presented in this thesis is my own unless otherwise stated in the text, and that the thesis has been composed by myself.

....

Evangelos Lagios

CONFESSIONS...

Twameva mata Chapita twameva
Twameva bundhu cha sukha twameva
Twameva vidya draminam twameva
Twameva sarvan mama deva deva
Twameva sarvan mama deva deva
Twameva sarvan mama deva deva

To

Elizabeth

ACKNOWLEDGEMENTS

I would like to express my sincere thanks to all those who helped me in any way to complete this thesis.

I am thankful to Professor K M Creer, Head of the Geophysics Department for allowing me full use of the Departmental facilities to carry out my project, and for his strong support for financial assistance.

I am grateful and particularly indebted to Dr Roger G Hipkin, my supervisor and initiator in Geophysics, not only for suggesting the project, but also for the kindness he has shown me during my stay in Edinburgh and his valuable help which I received in innumerable ways. Dr Hipkin accompanied me many times in fieldwork and particularly during the most difficult part of it, by walking up and down the hills at Lammermuir and Tweeddale in the Southern Uplands. I am thankful to him not only for his constant guidance and advice, but also for his extremely helpful and constructive criticisms during the progress of this thesis. For me it was a great pleasure and joy working with him.

I express my sincere thanks to Graham Dawes for his help and advice which I received in computing, especially during the implementation of the contouring routines and his occasional helpful company in fieldwork, which was fully appreciated and is gratefully acknowledged.

I am deeply indebted to my wife, Elizabeth, for her strong support, help in fieldwork and encouragement throughout my work.

I am pleased to extend my warm thanks to Drs Chris Swain and David Powell for their computer programs given to me for my work.

I am thankful to Drs Bruce Hobbs, Rosemary Hutton, Roy Gill and John Donato for useful discussions; especially to Dr Gill for giving me samples for density measurements.

I would like to thank Mr McQuillin, Head of Marine Geophysics Unit, IGS, for his permission to include in my thesis open-file IGS maps.

Also, I express my thanks to Professor J Drakopoulos, Athens University for his strong support for financial assistance and the encouragement he gave me to come to Edinburgh for post-graduate studies. The latter is gratefully acknowledged.

My friends and colleagues, K Dimitropoulos and K Makropoulos; the first for his assistance and useful discussions and the second for the strong support he has shown me for financial assistance.

I would like to thank my parents for their financial support and constant encouragement for which I will never be able to repay them.

The Schillizzi Foundation, the National Hellenic Research Foundation and the Royal Society of London for financial assistance.

Mr John McInnes for computing help with the SACM package.

Miss Routh Thomas who kindly did the susceptibility measurements.

All other members of the Geophysics Department and all my student colleagues, especially, Khalid Fahmi, for the enjoyable time I have had with them during the last three years.

Finally, Miss Linda Nisbet who kindly gave up many of her hours to type this thesis, an achievement for which I am indebted to her.

ABSTRACT

About 2500 gravity stations were established during a gravity survey of south-east Scotland. The reduction of the gravity observations, including computations of terrain corrections out to 22 km was made automatically by a sequence of computer programs and the Bouguer gravity anomaly map was plotted using different modern contouring routines.

The densities of about 200 rock samples were measured and a new method of estimating the surface density of rock formations, by fitting trend surfaces to the Bouguer anomaly, is described.

The gravity base network was adjusted manually but a least-squares analysis is also described which includes the instrumental drift. A computer program, based on this algorithm was written to perform the calculations and an RMS error of 0.096 g.u. was obtained for the adjustment of the network.

The Bouguer gravity anomaly map was interpreted with control from aeromagnetic and seismic information. The long-wavelength negative gravity anomaly of the Southern Uplands was interpreted as due to a granite batholith underlying the whole north-eastern part of the region. Particularly in the Tweeddale area, the detailed gravity model was also supported by aeromagnetic modelling. Three bosses near Peebles appear to come within 1½ km of the surface while another near Lammer Law may be shallower still. The interpretation with a granite batholith underlying the area and extending to a depth of 10 - 12 km

is generally compatible with other geophysical studies in the same area (seismic and magnetotelluric) and explains the formation of some interesting geological faulting features (the Southern Uplands Fault System) as well as the different rates of sedimentation between East Lothian and Midlothian.

The Devonian basins of Lauder, Eyemouth and Oldhamstocks have been studied gravimetrically. The first appears to be a simple V-shaped valley filled with Old Red Sandstone sediments, with a thickness of about 550 m near Lauder. The last two are faulted-bounded and have greater sediment thickness: about 900 m for Oldhamstocks and perhaps 1900 m for Eyemouth. The Cove and Innerwick Faults bounding the main Oldhamstocks Basin have estimated maximum throws of 800 m and 500 m respectively, while the Eyemouth and Coldingham Bay Faults both have throws of about 600 m. The Great Conglomerate of Monynut Edge, west of Oldhamstocks, has a thickness which is unlikely to exceed 400 m.

Finally, an investigation of the Lower Carboniferous volcanics in East Lothian and the inner Firth of Forth was based on combined gravity and magnetic models. The maximum thickness of the volcanics was found to be about 470 m, a few kilometres offshore from Aberlady. They were found not to be the main cause of the north-westerly gravity gradient in the area, which is an edge effect of the underlying granite batholith.

CONTENTS

Page

CHAPTER VI

DEVONIAN BASINS AND THE EAST LOTHIAN AREA

CHAPTER VII
CONCLUSIONS

APPENDIX A

APPENDIX B
NETWORK COMPUTER PROGRAM

APPENDIX C

APPENDIX D

APPENDIX E

BACK POCKET

LIST OF FIGURES

Page

Page

LIST OF TABLES

CHAPTER I

GEOLOGICAL AND GEOPHYSICAL REVIEW

1.1 Tectonic Review

The importance of the Caledonian earth movements becomes apparent when attempting to determine the tectonic history of the Midland Valley and the Southern Uplands from Pre-Cambrian to Upper Palaeozoic and onwards. Many plate tectonic models have been suggested to explain the geology of the southern terminations of the British Caledonides. Most of these models have been reviewed by Moseley (1977).

Wilson (1966) first published, after considerations of faunal evidence, the idea of a Proto-Atlantic ocean, which separated NW Scotland, NW Ireland and W Newfoundland from England-Wales, SE Ireland and E Newfoundland (Wright, 1976). The possible mechanism of its closure in late Ordovician times was suggested by plate tectonics. That Proto-Atlantic or Iapetus Ocean (Harland and Gayer, 1972) was an ocean of long standing (Wright, 1976) and, today, after the accumulation of so much supporting evidence (Williams, 1969, 1972, 1975), its existence is not in dispute, although the process which caused its closure is still not certain.

In the following a brief outline will be given of plate tectonic models associated with the Midland Valley and the Southern Uplands. In those models, the crustal composition under the Midland Valley and Southern Uplands, ie, whether it was of continental or oceanic crust, was a matter of controversy, at least at the beginning.

First, Dewey (1969, 1971) and Dewey and Pankhurst (1970) postulated that subduction took place both to the north-west near the Southern Uplands Fault and also, to the south-east, under the Solway-Northumberland basin. Subduction to the south-east received support from geochemical analysis of the regional magmatic variations in the Ordovician volcanic rocks of England, by Fitton and Hughes (1970). Subduction to the north-west was supported by Church and Gayer (1973). Garson and Plant (1973), in order to explain the calc-alkaline volcanicity in the Midland Valley in Lower Devonian times, accepted the existence of a northward Benioff zone between the Midland Valley and Southern Uplands. Therefore, the Southern Uplands was presented as overlying an oceanic crustal remnant. According to Jean's (1973) and Gunn's (1973) models, so was the Midland Valley.

This was the situation concerning the attempts at modelling by different workers without taking into consideration the full implications of the geophysical evidence, because , after that the idea of oceanic crust under the Midland Valley and Southern Uplands had to be abandoned.

Powell (1971, 1977b) and Agger and Carpenter (1965) pointed out using gravity, magnetic and seismic data, that continental crust underlies the Southern Uplands : the Moho lies at a depth of about 35 km, with overlying layers with a p-wave velocity of 6.4 km/s and 5.8 km/s. Consequently, the models of Dewey and Fitton and Hughes with oceanic crust under the Southern Uplands are unrealistic. These models were also strongly criticised by Gunn (1972).

Results from the Lithospheric Seismic Profile of Britain (LISPB) by Bamford et al (1976, 1977, 1978) have shown that continental crust underlies the Midland Valley. The seismic layering, including the 6.4 km/s refractor which outcrops in NW Scotland as Lewisian granulite, appears to be continuous as far as the Southern Uplands and may extend under them. An indication that granulite basement underlies the Palaeozoic sediments of the Midland Valley and Ireland has been pointed out by Upton et al(1976) in East Lothian, by Wilson (1918) in north-west Ayrshire , by Strongen (1974) in central Ireland and Phillips (1973) in north west Ireland. Also, recent work by Longman et al (1979) and Blaxland et al (1979) suggests evidence of Lewisian basement under the Midland Valley. Therefore, Gunn's (1973) speculation about oceanic crust under the Midland Valley is not valid, while Kennedy (1958) and George (1960) seem to have been right speculating that pre-Cambrian basement underlies the Midland Valley and probably the region further south.

In the following two of the most recent and comprehensive attempts to reconstruct the British Caledonides, by Mitchell and McKerrow (1975) and Phillips et al (1976), are discussed.

Mitchell and McKerrow observed that the tectonic evolution of the Caledonides in Britain is analogous to that of the Burma orogeny of Tertiary age. The Scottish Grampian Highlands, the Midland Valley and the Southern Uplands are comparable to the eastern Highlands, the central Lowlands and the Indoburman ranges of Burma respectively, although the corresponding events in the latter one took place after 400my. In figure 1.1 the model of the evolution of the Scottish

Caledonides is shown (Mitchell and McKerrow, 1975).

As can be seen, two Benioff zones are represented, one under the Southern Uplands and the other under the Midland Valley. The Iapetus Ocean was in existence until late Ordovician times, while by the Middle Devonian, it was finally closed.

Considering the Scottish Highlands and the eastern Highlands of Burma, high grade metamorphism characterises both regions. The Grampian Highlands, consisting of Dalradian basement, can be compared with the Kalaw syncline of eastern Burma, which consists of Mesozoic marine sedimentary deposits, mainly because of the turbidites and the thrusting in both areas. Hence, under the Scottish Highlands, according to the model, continental crust is depicted.

In the Midland Valley the igneous rocks of the Girvan area (serpentinite, eclogite etc), the turbidites along the southern part of the Midland Valley of Upper Ordovician and Lower Silurian age, and the sedimentary rocks of the Lower Old Red Sandstone are compared with the serpentinites, the oceanic and continental sedimentary rocks, throughout the Central Lowlands in Burma, of Upper Cretaceous to Miocene age. Therefore, under the Midland Valley oceanic or thin continental crust is assigned, as it can be seen also from figure 1.1.

Finally, it was considered that the Southern Uplands and the Indo-Burma Ranges, which are both characterised by highly thickened

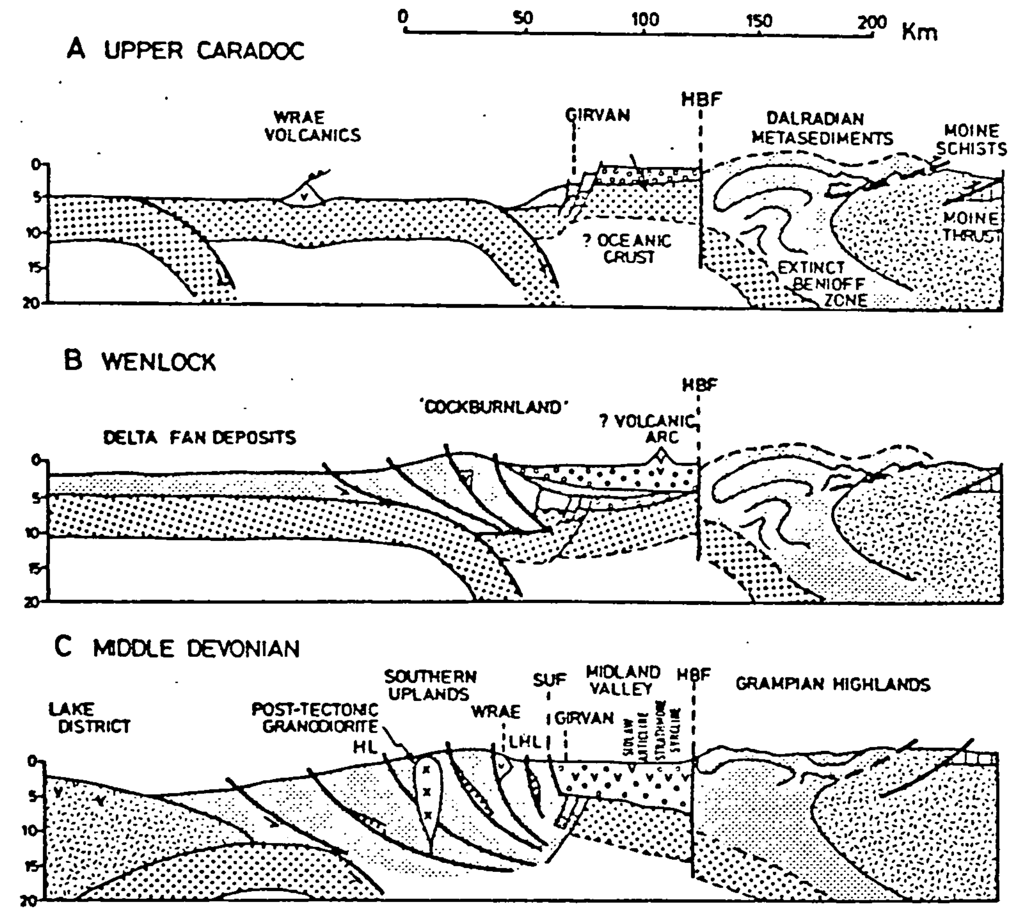

Fig. 1.1 Diagrammatic cross sections showing evolution of Scottish Caledonides. HBF = Highland Boundary Fault; SUF = Southern Upland Fault; HL = Hawick Line; LHL = Leadhills Line; (after Mitchell and McKerrow, 1975).

turbidites, were uplifted in Early to Middle Silurian and Oligocene times, respectively (Walton, 1965; Ziegler, 1970). In both cases the Midland Valley and the Irrawaddy Valley were separated from the ocean because of the uplift of the Southern Uplands and the Indo-Burman Ranges (Mitchell and McKerrow, 1975).

The most comprehensive reconstruction of the British Caledonides was proposed by Phillips et al (1976), which is also consistent with palaeomagnetic evidence, Briden et al (1973), Piper (1978). The innovation introduced by the model is that the two Benioff zones - one under the Southern Uplands and the other under northern England, are not parallel but at an angle (14^{o}-18^{o}) to each other. Therefore, the collision between the Southern Uplands and northern England occurs at a triple junction which migrates to the south-west.

Because the volcanicity in the Lake District ceased in Upper Ordovician times, while subduction to the south-west continued until early Devonian (Mitchell and McKerrow, 1975), dextral slip of 980km was adopted along the suture of Iapetus after its closure. Figure 1.2 shows the closure of Iapetus and the relative places of different crucial localities as the Southern Uplands, the Lake District etc.

As a conclusion, the author is inclined to believe that the closure of Iapetus was complete by the end of Silurian times, indicated from independent tectonic (Phillips et al, 1976) and magmatic evidence (Brown and Hennessy, 1978), but the position of the suture is still unclear.

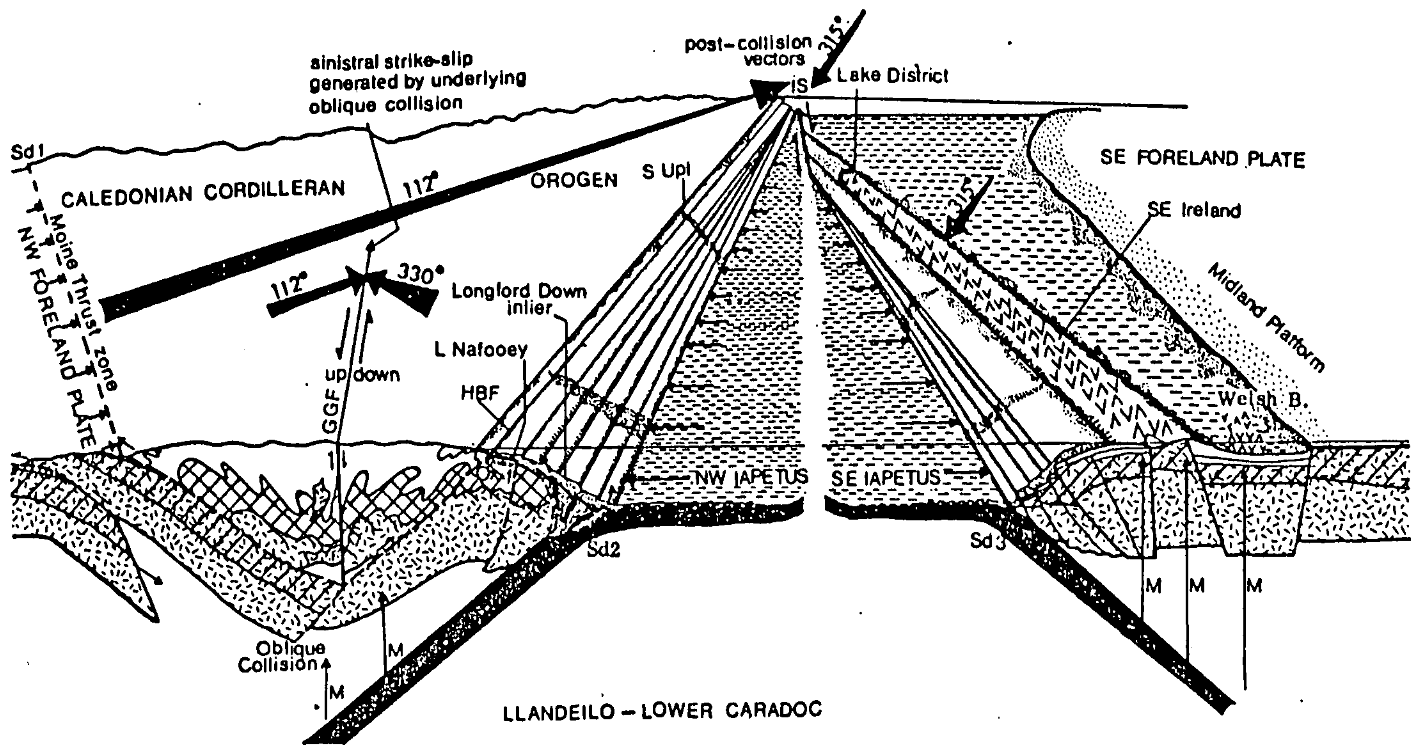

Fig. 1.2 Reconstruction of Iapetus closure (after Phillips et al, 1976).

Geophysical evidence from LISPB by Bamford _et al_ (1977) and electrical conductivity studies by Jones (1977), Jones and Hutton (1979b), indicate that the suture zone - defined as a mantle or upper crustal discontinuity - occurs under the Southern Uplands, while from sedimentological studies discussed by Phillips _et al_ (1976) the suture is put along the Solway. At this point, because of the post-collisional dextral slip along the "suture" and the fact that the Southern Uplands sedimentary sequence is allochthonous, "the palaeogeographical maps incorporating palinspastic reconstructions and showing two originally adjacent Southern Uplands units (basement and cover) would be particularly useful" as has been indicated by Dr Ingham in Phillips _et al_ (1976).

1.2 Geological History

In the following section, an attempt will be made to summarise briefly the geological history of that area, with more emphasis given mostly on south-east Scotland.

At the beginning of Ordovician times, the Iapetus Ocean was in existence and deposition of black shales and cherts was taking place, particularly on the continental margins. In Lower Ordovician times the Iapetus Ocean started closing. Subduction occurred under the continental margins (NW and SE) with the folding of shales, being scraped off the seabed and ophiolitic material detatched from oceanic crust and welded onto continental margins. During Caradocian times, with the Iapetus Ocean continuing to close, the Grampian Highland orogen was formed with intense metamorphism. Due to the SE subduction zone, the Lake District volcanicity took place and, generally, massive trench deposition of greywackes also took place. For more information of the above, see Gunn (1972).

During the Silurian, crustal warping and intense folding of the strata was marked until the end of Silurian times when the closure of the Iapetus was complete (Phillips et al., 1976).

Apparently following the closure of the Iapetus Ocean, cessation of the NW-SE stress resulted in a vast out-pouring of volcanic material (calc-alkaline) during Lower Devonian times, especially in the Cheviot region (Robson, 1977), the southern boundary of the Midland Valley and the remainder of south Scotland. There also appeared the SW-NE trending dykes (acid composition) of porphyrites, felsites, and diorites (Pringle, 1948), followed by massive igneous intrusion - with prevalent granodioritic or tonalitic magma - such as the three major outcropping granitic bodies in SW Scotland; Doon, Fleet, Criffel. At that time, shallow-water sediment deposition occured, which later covered the lavas at the bottom of the lakes. All this igneous activity after subduction was complete, suggests either an oversimplified tectonic model or an error in dating.

The absence of Middle Devonian rocks in the Cheviots, in the Midland Valley and in the district of Berwickshire generates an uncomformity on the base of the Upper Old Red Sandstone sediments which rest on the Lower Devonian sediments in that region. This phenomenon probably implies that uplift took place in Middle and possibly Upper Devonian times, particularly after the intrusion of the plutons in that area and the mass deficiency (Bott, 1974) they caused, followed by erosion, especially of the older rocks. Recent work (Leeder, 1973) has shown fluviatile origin of the Upper Old Red Sandstone sediments of SE Scotland.

The close of the Old Red Sandstone period was followed by an outbreak of intense volcanicity and the lavas can be traced over a considerable part of SE Scotland. During Lower Carboniferous or, especially, the Calciferous Sandstone Series, alkali basalts poured out sub-aerially from pipe-like vents and were intruded into sills with indications (Francis, 1965) that this type of volcanicity continued occasionally throughout the Carboniferous. The lavas of Garleton Hills, in East Lothian, the lavas of Greenlaw, in Berwickshire, Jedburgh, Burntisland and the Clyde Plateau lavas are related.

The deposition of the earliest Calciferous Sandstone Series over that area took place in an environment which was actually marine. The close of the Calciferous Sandstone times was marked by a widespread submergence of almost the whole region under the Carboniferous sea.

During the Upper Carboniferous, the igneous activity continued with the appearance of east-west trending quartz-dolerite dykes and sills over a much wider area than that of south Scotland. This activity is also associated with many east-west trending faults which were proved to be contemporaneous with the dykes and sills (Anderson, 1951).

At the end of the Lower Carboniferous period, especially in the Midland Valley, there was an uplift again leading to more denudation of the land areas. For more details about the deposition of the different subdivisions of the Upper Carboniferous rocks as well as the volcanic activity of that area, see McGregor and McGregor (1948), Francis (1961, 1965, 1968).

The late- and post-Carboniferous times are dominated by Hercynian movements which, in southern Scotland and northern England are represented by E-W compression, followed by folding (Holborn, Lemmington anticline) and, later, by the intrusion of the whin dykes and the Great Whin Sill (Robson, 1977).

Finally, in north-west Scotland the Tertiary period was marked by igneous activity, plateau basalts and dyke swarms. In the south of Scotland the dykes have a NW-SE trending direction. This period is characterised by N-S compression, but those forces were significantly less powerful than the Hercynian forces.

1.3 Geophysical Review

Although there is complete and very comprehensive geological mapping of Britain, the same is not true of geophysical work and exploration of the mainland. The aeromagnetic map of Britain, which has been published by the Institute of Geological Sciences and the parts of it concerning the Southern Uplands and the Southern Uplands Fault show features which are consistent with the surface geology. In particular, the Southern Uplands Fault is represented by a narrow line of magnetic highs (ending at (30,60) on Fig. 4.4) and the Southern Uplands are characterised by a linear magnetic high (near Galloway to Lauder (Fig. 4.5)) surrounded by two magnetic lows. The latter magnetic high was interpreted as being due to a smooth rise in a magnetic basement (about 5.5 to 10km deep) rather than to a fault or igneous feature

(Gunn, 1972). The line of broad highs in Silurian rocks is crossed obliquely by the magnetic lows caused by Tertiary dykes.

Important regional features can be separated and identified from the complex pattern of the aeromagnetic map which is due mainly to shallow magnetised sources, by applying an upward continuation filtering process. Therefore, filtered aeromagnetic maps have been produced by Hall and Dagley (1970) and Gunn (1972), approximating the magnetic field continued to a level of 2km above the flight level which was about 1000ft above ground level. Some of the significant features will be discussed later. A complete Bouguer gravity anomaly map has still to be published, especially for the south of Scotland-Borders region.

Detailed gravity and magnetic surveys have been carried out in some local areas of south Scotland and north England. In the discussion of some of them which follows attention will be given mostly to the work carried out in the Midland Valley and the Southern Uplands.

The Ballantrae Igneous Complex, in south-west Scotland, was studied by means of gravity and magnetic surveys by Powell (1970, 1977a). He finds that the strong magnetic highs over the Ballantrae Igneous Complex are mainly due to serpentinite, which contains secondary magnetite (Powell, 1970). The sub-circular positive anomaly in the Midland Valley, the Bathgate anomaly (Gunn, 1975), was interpreted by Gunn (1972) as due to a prismatic body of square plan section with its top at a depth of about 10km and its bottom at about 23km.

There was an alternative interpretation by Powell (1970) who considered it as being due to a body of 10 miles in diameter with its top only 3 miles deep. Recently, Hossain (1976) gave another interpretation. Conclusions about the origin of the Bathgate magnetic anomaly for the moment are speculative but a revised and, hopefully, a final interpretation is in preparation by McLean and Powell (pers. commun.); it places the causative body at a depth of 1.5km under the surface and its bottom at a depth of 7km.

Two gravity traverses across the Cairnsmore Fleet granite were made by Parslow (1968). A Bouguer gravity anomaly map of the Fleet region has been published by Parslow and Randall (1973). According to their interpretation, the Fleet granite represents a small exposure near the top of a batholith, extending not more than 15km in depth.

The negative gravity anomaly over the Criffell granodiorite has been interpreted, again, as due to a batholithic form, with its floor at least 11km deep (Bott and Masson-Smith, 1960).

The third major pluton in the south west part of Scotland, the Loch Doon granite, was studied by El-Batroukh (1975), by mainly gravity means. He has concluded that all the three granite batholiths, Doon, Fleet and Criffell are connected at a depth and form a huge batholith extending across the Caledonian trend (NNW to SSE).

The New Red Sandstone rocks around Dumfries and Lochmaben are associated with negative gravity anomalies and an estimated thickness of about 1km (Bott and Masson-Smith, 1960).

In the Sanquhar Coalfield, Ordovician greywackes underlie the relatively light Upper Carboniferous rocks and therefore a local gravity low is generated, superimposed on a steep regional field which decreases to the south-east. In this case, the residual Bouguer anomalies fit well to the structure of the Carboniferous rocks, but the regional field does not reflect a clear picture of the Ordovician basement (McLean, 1961).

Farther north, the distribution of the Upper Palaeozoic rocks and mainly the major structure of the Maucline Basin, are clearly reflected in the gravity anomalies (McLean, 1966). The presence of the NE-SW faults, as the Southern Uplands Fault, the Kerse Loch Fault give rise to large anomalies. According to gravity data, the Southern Uplands Fault and the Kerse Loch Fault existed in Middle Old Red Sandstone times and the hypothesis of a N-S compressional Armorican stress (George, 1960, Kennedy, 1958) does not seem to be correct (McLean, 1966).

Very recently, extensive geophysical studies (gravity, magnetic and seismic) carried out in the Firth of Clyde and a synthesis of the solid geology of the above region, has been published by McLean and Deegan (1978).

In the western Midland Valley and the neighbouring areas, ie, the SW part of the Grampians and the Southern Uplands, the regional Bouguer anomaly is characterised by a westwards gravity rise and by a gravity high over the Midland Valley, which decreases to the north (Grampian Highlands) and south (Southern Uplands) (McLean and Qureshi, 1966).

The latter regional gravity feature has been explained by a thickening of the crust under the Grampians and the Southern Uplands compared with the crust under the Midland Valley (McLean and Qureshi, 1966). The westwards increase of the regional gravity field in the west Midland Valley is a characteristic of the whole of western Scotland.

Another gravity survey further north on both sides of the western part of the Highland Boundary Fault was carried out by Qureshi (1970). There are steep gravity gradients across the Highland Boundary Fault and the gravity low west of Loch Lomond outlined a sedimentary basin partly filled by Lower Old Red Sandstone sediments with a maximum thickness, over that area, of between 1500-1800m.

Consideration of the isostatic anomalies over the western part of the Midland Valley suggests that they are a general feature of the continuation of the European gravitational field. The average positive values over the Midland Valley, the Highlands and the Southern Uplands are in qualitative agreement with the theory of isostasy (McLean and Qureshi, 1966).

The only gravity work which so far has been carried out in the eastern part of the south of Scotland is the gravity survey in the Midlothian Coalfield (Hipkin, 1977a, 1977b), covering the southern part of the Midlothian syncline and extending also into the Penicuik syncline. The interpretation of the gravity data gives detailed information on the structure and formation of the faulting features of that area. A Lower Devonian age of the Southern Uplands Fault (Leadburn Fault) is defined. The Roslin-Vogrie Fault system is considered to be of "major and long-standing proportions," truncating the Leadburn component of the Southern Uplands Fault (Hipkin, 1977b). Its throw is estimated to be, according to the model from gravity data, about 2700m and a great discrepancy from Tulloch and Watson's (1958) estimations is demonstrated.

Local seismic studies have been undertaken at various sites in the Midland Valley by Hall (1970, 1971, 1974) and near surface Lower Palaeozoic rocks are reported to have compressional wave velocity of 3.65-4.3km/sec.

Under the Southern Uplands, a distinct refracting horizon at 12km depth was found by Jacob (1969), using the Eskdalemuir seismic array. There is an increase in the seismic velocity from 5.54km/sec near the surface to 5.94km/sec at a depth of about 12km, with a sudden jump to 6.44km/sec.

About the same value of 6.4km/sec was recorded again for the Southern Uplands, by the Eskdalemuir stations from the Firth of Forth by Christie (1978). The results indicate a crust of normal continental thickness (approximately 30km depth).

Recently, a deep seismic refraction profile (LISPB) was carried out by an Anglo-German group, N-S across Britain. It was operated as four reversed lines and a preliminary result (Bamford et al, 1976) was reported: there is a clear Moho discontinuity under the Southern Uplands at an estimated depth of 32-36km. A more detailed analysis (Bamford et al, 1977 and Bamford et al, 1978) showed that the Moho discontinuity changes in nature from a sharp transition under the northern part of the Midland Valley to a gradual change under the Southern Uplands. Also, there might be a possible lateral change in the basement between the Southern Uplands Fault and the Stublick Fault, and the lower crustal layer appears to shallow beneath the Southern Uplands (figure 1.3). The latter could be due to a partial melting of the rocks at the crust-mantle boundary (Jones, 1977).

Low Poisson's ratios determined from LISPB associated with a layer on both sides, north and south of the Southern Uplands Fault, may be due to quartz enrichment or fracturing under the area, emphasising the tectonic activity which has been taking place on the margins of the Southern Uplands Fault (Assumpcao and Bamford, 1978).

Various electromagnetic studies have been made in the Southern Uplands, but the more recent one is of Jones (1977) and Jones and Hutton (1979a, 1979b). It is reported that under the Midland Valley there is a conducting layer at a depth of no greater than 12km. The conducting zone beneath the Southern Uplands is at a depth greater than 24km (Jones and Hutton, 1979b). However, a recent interpretation (Ingham, pers. commun.) puts the conducting zone under the Southern Uplands at a depth of only 10-12 km.

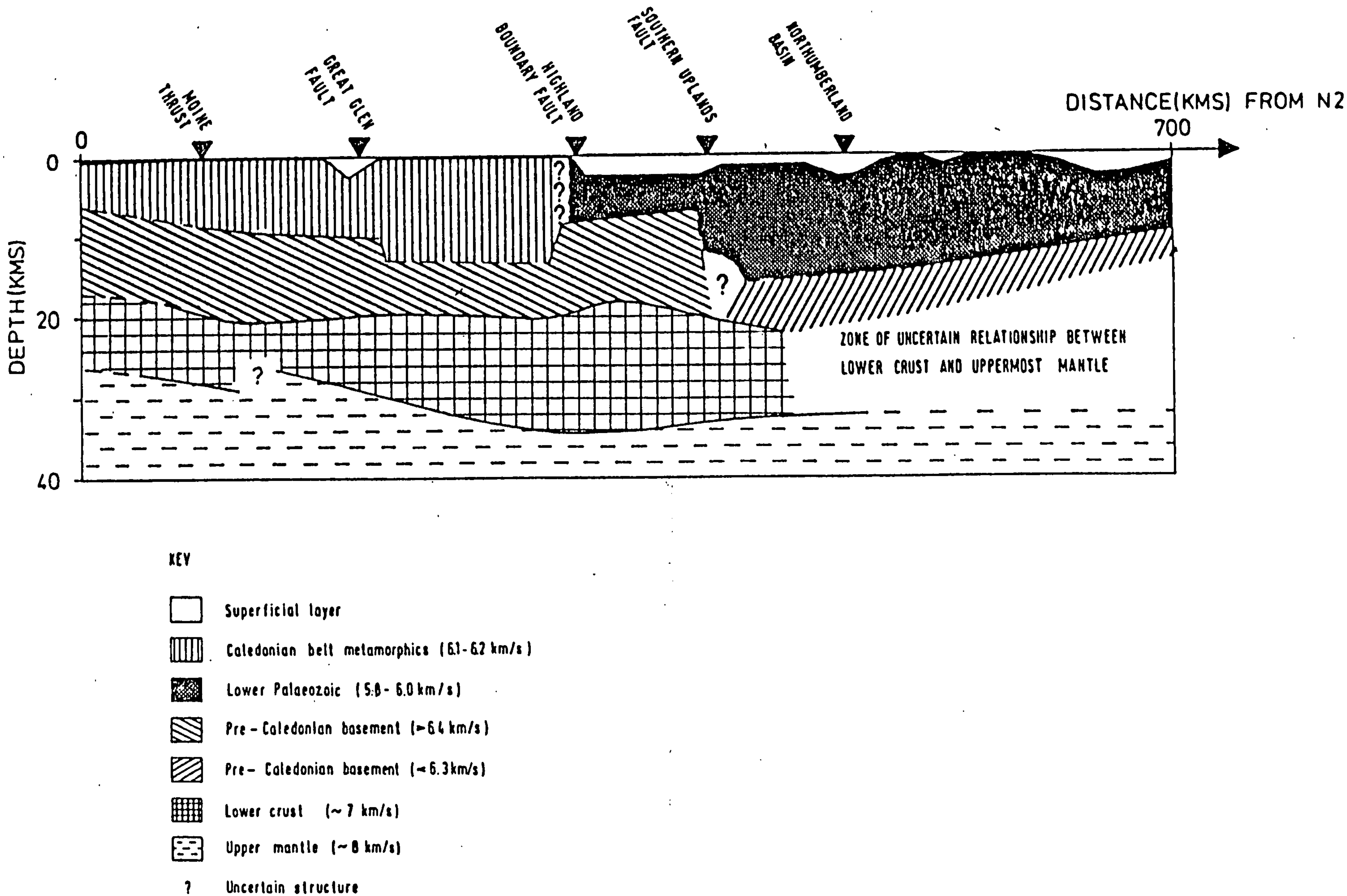

Fig. 1.3 Crustal section of northern Britain from P-wave interpretation (from Bamford et al. 1978).

Even after the LISPB experiment, the crustal structure of the Southern Uplands and their northerly margin, was still poorly determined. The relationship of the eastern part with that in the west, where the Ballantrae ophiolite sequence and the massive plutons are the central components of many tectonic models, was not known because similar exposures do not occur and very little detailed geophysical exploration had taken place in the south-eastern part of Scotland.

This project was intended to facilitate this comparison between the eastern and the western parts of southern Scotland and to test and perhaps to improve the structural model proposed by LISPB for the Southern Uplands.

CHAPTER II

FIELDWORK AND DATA REDUCTION

2.1. Locations of Gravity Measurements

The survey is delineated by National Grid Eastings 310 to 400km and Northings 620 to 710km. About 800 gravity stations had already been established around the Midlothian area and south of it by Dr R G Hipkin and other members of the Geophysics Department between 1974 and 1976. Most of these measurements were made along motorable roads and tracks. This area has the densest coverage of gravity stations. It involves detailed gravity profiles across the Southern Uplands Fault and a good coverage of the Midlothian Coalfield. In some cases, as for example the 10km National Grid square NT 25, the coverage is better than two stations per km^2.

The rest of the area, shown in Figure 2.1, was surveyed by the author. By the end of 1977 the East Lothian area and the Lauderdale and the Berwickshire area north of 650km N were covered and a map of the whole area was presented (Lagios, 1978). However, after the presentation of the marine gravity work in the Firth of Forth by Tully and McQuillin (1978), it was decided to extend the survey area: to the south from 650 to 620km N - the Cheviot area was excluded, NT 88 and NT 89 - and northwards to 710km N.

Also, many additional gravity measurements were taken in the Lammermuir Hills and in the Tweeddale area by the author and R G Hipkin. The fieldwork in this area was carried out on foot,

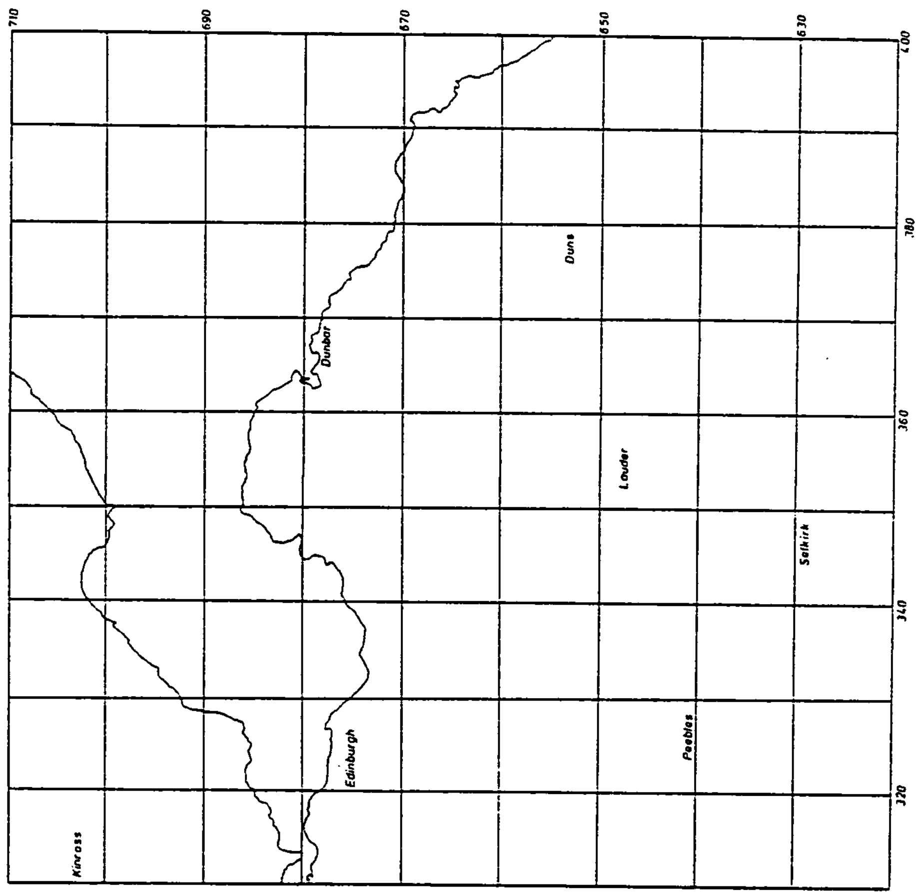

Fig. 2.1 Map showing the boundaries of the survey area.

climbing hills sometimes under unfavourable weather conditions. The second part of the fieldwork was completed by the end of 1978. A total number of 2500 new gravity stations were established over an area of 5800km^2.

2.2. Elevation and Position Measurements

Extra care was taken during the fieldwork to achieve a high degree of height control, as the final accuracy of the Bouguer anomalies is heavily dependent upon elevation accuracy. Four sources of elevation information were used:

(i) Bench marks, copied from 1:2500 maps. These are connected by spirit levelling traverses to the Ordnance Survey Datum at Newlyn Harbour, Cornwall, and are published to the nearest 0.01m or 0.01ft. The greatest part of the study area, that is, Midlothian, East Lothian, Lauderdale, Berwickshire and the Merse, was surveyed using this height control information, levelling from the nearest bench mark and hence maintaining an accuracy better than 0.1 g.u. from the point of view of elevation.

(ii) Levelled spot heights, copied from 1:25000 maps. These are unmarked intermediate stations on a levelling traverse between two bench marks, with the same precision as bench marks but published to the nearest 0.1 metre or foot. Almost all of the area south-east of 650km N and north-westwards of 680km N was surveyed using levelled spot heights, maintaining an accuracy better than 0.5 g.u.

(iii) In some cases the height was taken from 19th century bench marks, referred to the older Liverpool datum and given with accuracy of 0.1ft. These are assumed to be accurate, now, to about 0.3m, in the absence of resurvey information.

(iv) Unlevelled spot heights, copied from the same maps as (ii). These are identifiable but unmarked topographic features, such as tops of hills, measured either by triangulations (a precision of $\pm$ 0.3m is claimed) or by stereo aerial photographs (precision of $\pm$ 2m). The gravity stations which were established in the Lammermuir Hills and over the Tweeddale area, are based on spot heights measured by triangulation. Very few of these are stereographic spot heights.

The location of each gravity station was determined from 1:25000 maps with an accuracy better than $\pm$ 10m, for most of the gravity stations, which corresponds to an error of less than 0.1 g.u. in the latitude corrections.

2.3. Gravity Measurements

2.3.1 Instrument - Drift Characteristics

All the gravity measurements were made using the LaCoste and Romberg geodetic gravity meter G-275, which is thermostatically controlled at about 49°C with a world wide range and a reading accuracy of 0.02 g.u.

Although generally, the drift of LaCoste and Romberg gravity meters is very small, because drift tests of the G-275 had already been made, a brief description of the drift behaviour will be outlined below.

Interesting laboratory and field tests have shown that when the instrument is removed from its case, after storage for some hours, unclamped and read continuously, there is an initial phase of rapid increase of reading by 0.2 g.u. (20 μgal), lasting for about an hour (Hipkin, 1978b), until a plateau is reached, characterised by a slow and linear decrease - see upper part of Figure 2.2. The central part of Figure 2.2 shows that displacing the beam by only a few eyepiece divisions will quickly result in large jumps in reading, approximately 0.2 g.u. as the beam appears to be held near the position of the lower or upper stop. This suggests that there are different mechanisms applying in the case of clamping and beam displacement.

The result of testing the thermal response of the instrument (Hipkin, 1978 a, b) - see for example the lower part of Figure 2.2 - shows that thermal change effects are rather insignificant for the practical use of regional gravity surveying, where an accuracy of 0.2 g.u. is adequate.

As a conclusion, although drift effects are generally negligible, the 0.2 g.u. reading displacement can bias measurements referred to an initial value, as in the case of the observations at a base station

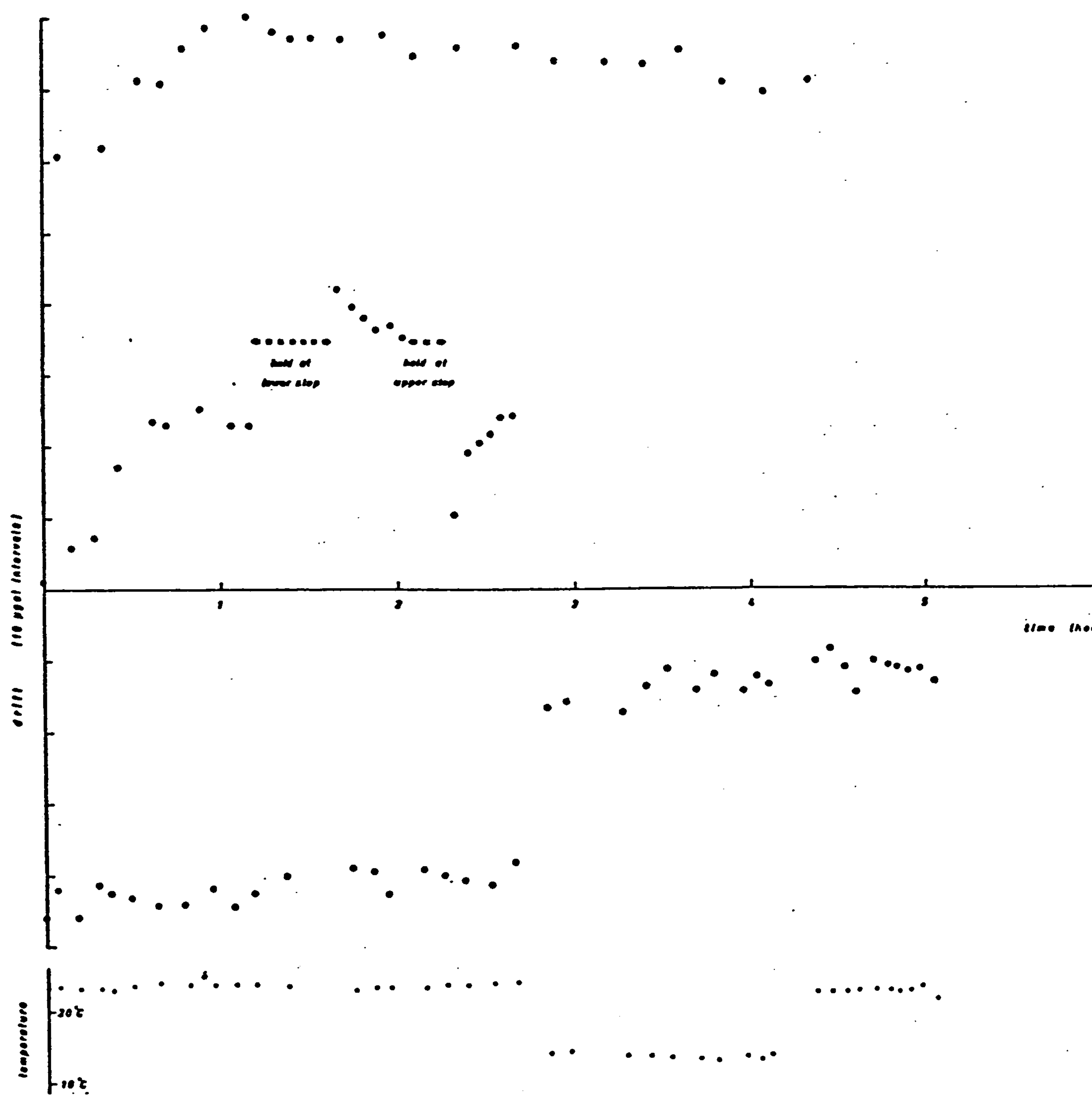

Fig. 2.2 Laboratory drift tests (after Hipkin, 1978b).

at the beginning of a day's fieldwork. For this reason it is suggested that the second measurement, taken at this base, be taken into consideration and not the first one.

2.3.2 Data Reduction

A general reduction computer program, GRAVØ1, written by R G Hipkin, was used for the reduction of the gravity observations. According to the program the following operations, described below, are taking place:

(1) The total number of gravity stations is read and the datum level - absolute value of gravity of a base - is defined.

(2) The input of data takes place in a manner described in a following paragraph.

(3) Eastings and Northings of each gravity station are converted to longitudes and latitudes, using the National Grid routine, from which the normal gravity is calculated using the constants of the Geodetic Reference System of 1967 (Morelli, 1976), instead of the International Gravity Formula of 1930.

(4) The meter readings are converted to g.u. using the manufacturer's calibration tables.

(5) The time of each observation is converted to days and decimals of a day elapsed since midnight December, 31st 1899-January 1st 1900, using the Gregorian Day number routine.

(6) Earth tide corrections are applied to the observed values of gravity for each station, based on the expansion of Cartwright and Tayler (1971), as corrected by Cartwright and Edden (1973).

(7) A linear drift curve is calculated and subtracted from the gravity values observed between successive base stations, generally one day's observations.

(8) Normal gravity, free-air and Bouguer corrections are calculated for each gravity station.

(9) Free-air and Bouguer anomalies are calculated for each gravity observation and,

(10) Output with all information concerning every station occurs.

For each station there is a line of literal description (format 18A4), then a line of numerical data using the following parameters: IREF, TIME, CIVIL, EAST, NORTH, GRAV, DENS, TERCF, where:

IREF: is the reference number of a gravity station.

TIME: is the time information of a gravity reading given as hours, minutes, day, month, year.

CIVIL: is the time difference in hours - local time minus Greenwich Mean Time.

EAST: NORTH: is the National Grid Easting and Northing given in metres and taken from 1:25000 maps with an accuracy of $\pm$ 5 metres.

GRAV: is the meter gravity reading.

DENS: is the factor which assigns the Bouguer density after being subtracted from the standard Bouguer density (2.67 g/cc).

TERCF: is the terrain coefficient, expressed in gravity units per unit density (g/cc).

By taking repeated readings at base stations every 3-4 hours, which was adopted during the survey, the tide factor can be removed as a linear drift, calculated by the program.

2.3.3 Terrain Corrections

Progress during the last decade in methods for reducing and processing geophysical data has been reflected by an increased use of computers. New and faster algorithms for making terrain corrections have been proposed by various authors and some of these have been reviewed by Grant (1972).

In the study area the terrain corrections were carried out applying a computer program, TERCOR, written originally by C J Swain and modified by the author. A similar program, used for the Kenyan data (Swain and Khan, 1978), covering a much larger area (300 x 300km) than ours, is described by Swain and Khan (1977). These programs use digitised topographic information, in which the area is divided into square blocks, each with the mean height assigned.

2.3.3.1 Digitisation Scheme

The idea of using rectangular arrays of squares of varying size and their application to the calculation of the terrain effect of gravity stations was proposed by Nagy (1966). Krohm (1976) suggested the idea of interpolating heights between a set of grid points and using these for an estimate of the local terrain correction, applying multiquadric surfaces. The size of the adopted grid plays an important role in the approximation of the actual terrain effect.

The whole study area was digitised with an accuracy of $\pm$20ft and 50ft from 1:25000 and 1:63360 maps respectively, assigning a mean value of elevation for every square block of topography, the size of one block depending on the digitisation scheme, as described below:

(1) 500m for the survey area and including 1km strip surrounding it.

(2) 1km for the area beyond this and up to 5km beyond the survey boundary.

(3) 2km up to 13km from the survey boundary.

(4) 5km from 13km to 23km.

Digitising the whole area and the surrounding strips was the most tedious and monotonous part of the task. All the digitised data were checked for probable errors and filed onto a tape by a filing routine, FTERCOR, kindly provided by C J Swain and modified by the author. The digitised value of each block was finally stored by FTERCOR in metres.

2.3.3.2 Description of the Terrain Correction, TERCOR, Computer Program

The program first reads the gravity stations, at which the terrain effect is desired, with their reference numbers co-ordinates (easting, northing) and heights in metres, taken from GRAVI2, a different version of GRAVØ1. Then, for each station, the terrain effect is calculated as follows:

(1) Local Terrain Effect. At this point the program TERCOR differs in two respects from Krohm's (1976) approach in calculating the local effect: (1) a 100m square grid is used for interpolating heights between the original grid of 500m. Considering a station falling in one of the central 25 blocks (each 500m in size) - see Figure 2.3 - either 100 or 225 heights are interpolated depending whether 4 or 9 blocks are taken into account. The latter depends on the maximum angle subtended at the station by each block. If this is very small then no interpolation is carried out.

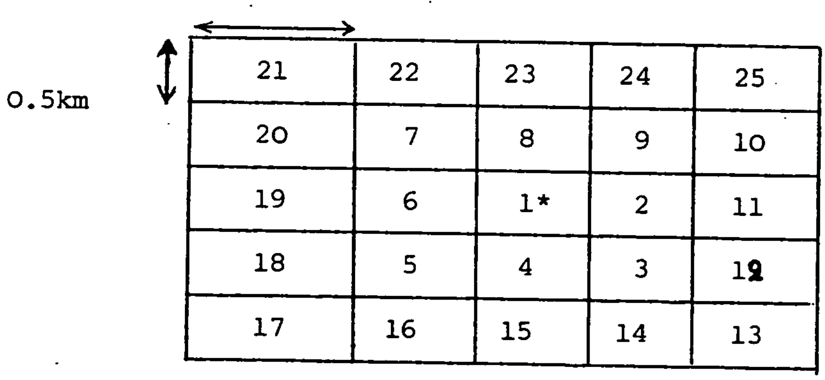

*Gravity station

Fig. 2.3 Diagram outlining the central 25 blocks from which the local terrain effect is calculated.

(2) Instead of multiquadric surfaces to carry out the interpolations, a paraboloid is fitted by weighted least squares because this was found to be much quicker (Swain, person. commun). Hence, the local topography is approximated by fitting a paraboloid to the 100 or 225

interpolated heights and the height of the station taken as control. The local terrain effect of each 100m block is calculated using the approximate formula for a segment of a hollow cylinder, developed by Bott (1959) with the form:

$$\Delta g = GA^2\rho \left[\frac{1}{r} - \frac{1}{(r^2 + \Delta h^2)^{\frac{1}{2}}} \right] \qquad (2.1)$$

where: G = gravitational constant

ρ = density

A = length of square (block) side

r = horizontal distance between the stations and the block centre

Δh = height difference between the gravity station and the estimated average block height.

(2) Outer Terrain Effect. This is calculated by the following scheme: (1) For blocks between 1 and 5km from the gravity station, the full prism formula is used, developed by Nagy (1966). (2) For blocks between 5 and 15km from the gravity station, the contribution is ignored if the angle subtended at the station by each block is less than 0.5 degrees; otherwise, Kane's (1962) formula is used to calculate the terrain effect of the block:

$$\Delta g = \frac{2GA^2\rho\ (1.26A + ((r - 0.63)^2 + \Delta h^2)^{\frac{1}{2}} - ((r + 0.63A)^2 + \Delta h^2)^{\frac{1}{2}})}{2.52rA} \qquad (2.2)$$

with the same notations used to describe formula (2.1).

These algorithms were used to calculate the terrain coefficients of all the gravity stations using all blocks whose centres are within 21.94km of the station, corresponding to the outer edge of Hammer Zone M. The height information was taken from the tape filed by the FTERCOR program. It took about12 seconds on ICL 4-75 computer for the calculation of the terrain coefficient of each gravity station.

2.3.4 Accuracy of Terrain Corrections

It was found that the most critical point of the calculations of the terrain corrections was the local effect. This is due to 4 or 9 blocks immediately surrounding each gravity station. If the topography within the 4 or 9 blocks is flat or varies in a smooth manner, then the local effect is small or rather insignificant. However, in cases where the latter is not applicable, then the local effect depends particularly on the shape of the topography: if the station is on the top of a hill, then the program TERCOR, by fitting the paraboloid, approximates the actual effect with a very good accuracy. However, in cases where the topography was very irregular, particularly for stations along a ridge of hills or along an elongated valley with steep slopes on both sides, it was found that the program gave unreliable results: the error in an extreme case was more than 80% of the near zone value. For this reason, in the Tweeddale area the local effect of the gravity stations was systematically calculated by hand using a Hammer chart. For the gravity stations elsewhere, the same approach was applied, where it was felt to be required, and then their local effects replaced the corresponding computer values.

There was, of course, a slight miss-match between the circular Hammer zone F - diameter 1.79km - and the square of the 9 central blocks (see Figure 2.3), but the error is likely to be within the limits of the accuracy of digitisation.

The 500m square block is approximately the same size as the compartment belonging to Hammer zone F (Hammer,1939), with outer radius at a distance 0.89km from the station. For blocks outside the outer radius of zone F, the program TERCOR will calculate their effects more accurately, as the area of each digitised block is smaller than the segment of any Hammer zone beyond zone F.

Table II-1 shows the difference of terrain coefficients between computer and Hammer chart corrections. The mean difference is 0.05 g.u. so there is no indication of bias. The mean absolute difference is 6.9% with an RMS difference of 9.2%, which is close to the limit of 10% according to Swain (person. commun.).

Walker (1977) used a version of Swain's program similar to the one described above for the calculation of the terrain corrections for the gravity stations in the Kavirondo Rift Valley, Kenya. He used a 1km digitisation scheme rather than the 500m one used in our survey area and he found that the error of the terrain correction was about ± 3 g.u.

TABLE II-1

Station Ref No.	Coordinates N.G. (km)	Height (m)	Terrain Coeff. Hand Corr. (I)	Terrain Coeff. Computer Corr. (II)	Difference (II-I)	Percentage Difference (II-I/I)100
00007	351.750 673.280	54.29	0.88	0.74	-0.14	-15.9
3566010	350.02 664.90	191.9	1.44	1.48	0.04	2.78
3566007	351.11 665.27	194.7	1.57	1.56	-0.01	-0.64
3566004	352.48 664.72	210.7	2.09	2.20	0.11	5.26
3566001	353.85 665.08	200.9	1.96	1.93	-0.03	-1.53
3566026	354.17 668.41	146.3	1.38	1.67	0.29	21.0
3566030	356.52 667.60	198.2	2.37	2.57	0.20	8.4
3566008	350.89 665.58	182.9	1.58	1.52	-0.06	-3.8
3566045	355.17 665.60	193.9	1.83	1.87	0.04	2.2
3567004	352.06 672.52	67.0	0.64	0.68	0.04	6.2
3567008	353.27 671.45	82.1	1.08	1.17	0.09	8.3

COMPARISON BETWEEN COMPUTER AND HAND-MADE TERRAIN CORRECTIONS

Also, Qureshi (1961) used a computer program for the terrain corrections, based on Bott's (1959) formula and he found an RMS difference of 4.8% between Hammer and computer values.

Since most of the gravity stations have terrain coefficients less than 1 g.u. and the majority of the rest between 1-10 g.u. (there are of course some stations in the Tweeddale area and also a very few in the Lammermuirs which have terrain coefficients between 10-25 g.u.), it appears that, applying a 10% error of the computer program, the error is between 0.1 to 1 g.u. Certainly, for most of the gravity stations, the error involved for the estimation of the terrain coefficients is less than 1 g.u.

2.4. Density Measurements

2.4.1 Laboratory Density Measurements

A number of rock samples were collected during the survey for the purpose of density determination. A few additional samples, particularly of porphyrites and granites from the Tweeddale district were collected by Dr R Gill, who, kindly, gave a portion of these samples for density measurements. Determination of density was made on a total number of about 200 specimens.

Specimens of usually less than 10 gm were used. They were left in water for some time, depending on the type of rock. Igneous rocks were left less time than sedimentary rocks. Usually in these cases, a vacuum is applied to the surface of the water, in which the samples are kept so that the air is removed from the pores more quickly. In our case, because of the small volume of the samples which were used, it was considered unnecessary; this because the diffusion time of the air is much smaller for small volume samples than that for larger volume samples. Nevertheless, some samples may not have been completely saturated, adding a small error to the results.

Thus the samples, after being in water for some time, were dried quickly and weighed in air (w_2) and then in water (w_3). Special caution was taken during their weighing in the water: the samples were suspended from a thin wire on which a mark was made, coinciding always with the horizontal surface of the water, for all the samples. At the end, the wire was weighed with the water surface at the same level with the marker on the wire. In that case, the surface tension effects on the wire were the same, with the samples on it and without them.

Following that, the samples were put into an oven (approximately 100°C) and kept overnight. They were then weighed (w_1) and the dry, saturated and grain density was calculated, applying the following formulae:

$$\text{Dry density, } d_d = \frac{w_1}{w_2 - w_3} d_w$$

$$\text{Saturated density, } d_s = \frac{w_2}{w_2 - w_3} d_w$$

$$\text{Grain density, } d_g = \frac{w_1}{w_1 - w_3} d_w$$

where: w_1 = Dry weight of sample in air,

w_2 = Saturated weight of sample in air,

w_3 = Saturated weight of sample in water, and

d_w = Density of water (1 g/cc).

The effective porosity P was calculated according to the formula:

$$P = (d_s - d_d)\ 100(\%)$$

All the density measurements were carried out using a Stanton micro-balance, which weighs up to 200 gm with 0.0001 gm accuracy. The result for each sample and its description is presented in Tables II-2 and II-3. The estimated value of the dry, saturated and grain density is given, with its standard deviation, actually representing variations in density and not errors of measurements, which were negligible.

As shown in Table II-3, the Lower Palaeozoic sediments (Ordovician and Silurian) have a mean saturated density of 2.708 $\pm$ 0.021 g/cc. This is very close to the value various authors (McLean, 1961a, Bott and Masson-Smith, 1960) have reported for the same type of rocks over the Southern Uplands.

Although our hand samples of Caledonian granites are only from four different localities over the Southern Uplands, it is apparent that there is a range from 2.63 to 2.72 g/cc, from coarse granite to microgranite, respectively. This was expected because the same result had been already obtained by other authors (eg Walker, 1924).

Sampling from six different localities of Upper Devonian sedimentary rocks has shown a variation of density from 2.47 to 2.67 g/cc, for sandstones to fine-grained sandstones, respectively, with a mean value generally greater than that for the same kind of sediments at the western part of the Midland Valley and Southern Uplands (McLean, 1961a).

TABLE II-2

SAMPLE NO	ROCK TYPE	GEOLOGICAL CLASSIFICATION	LOCALITY	NATIONAL GRID REFERENCE
1	Greywacke	Silurian	The Bell	NT 745 640
1a	"	"	Old Campus Quarry	NT 800 695
2	"	"	Hartside Quarry	NT 473 535
3	"	"		NT 208 241
4	"	"	Crosecleugh Bridge	NT 248 200
5	"	"	Earl's Hill	NT 253 188
6	"	Ordovician	Quarry Wear Heriot	NT 407 540
7	"	"	Lochurd Quarry	NT 335 505
8	"	"	Craigburn Quarry	NT 375 540
9	Felsite	Lower Old Red Sandstone	Kailzie Hill	NT 278 363
10	Porphyrite	"	Kirnie Law	NT 348 386
11	Porphyrite	"	Priesthope Hill	NT 360 400
12	Porphyrite	"	"	NT 360 400
13	Porphyrite	"	Preston Law	NT 253 348
14	Porphyrite	"	Juniper Craigs	NT 245 357
15	Sandstone	Upper Old Red Sandstone	Siccar Point	NT 813 708
16	Sandstone	Lower Old Red Sandstone	St Abb's Head	NT 317 678
17	Conglomerate	Lower Old Red Sandstone	St Abb's Head	NT 915 685

DENSITY MEASUREMENTS - SAMPLE DESCRIPTION

SAMPLE NO	ROCK TYPE	GEOLOGICAL CLASSIFICATION	LOCALITY	NATIONAL GRID REFERENCE
18	Great Conglomerate	Upper Old Red Sandstone	Monynut Water	NT 691 682
19	Fine-grained sandstone	Upper Old Red Sandstone	Dunbar	NT 673 794
20	Dolerite Sill	Lower Carboniferous	Aberlady Bay	NT 445 795
21	Black Chert	Ordovician	Broughton Heights	NT 125 405
22	Lava	Andesitic	St Abb's Head	NT 905 682
23	Basalt	Lower Carboniferous	Markle Quarry	NT 576 775
24	Pillow Lava	Ordovician	Broughton Heights	NT 125 405
25	Trachyte	Lower Carboniferous	Skid Hill Quarry	NT 508 764
26	Cornstone	Upper Old Red Sandstone	Dunbar (Bathing Pool)	NT 674 793
27	Sandstone	Upper Old Red Sandstone	Dunbar (Bathing Pool)	NT 673 793
28	Sandstone	Upper Old Red Sandstone	Near Bransley Hill	NT 667 704
29	Granite	Lower Old Red Sandstone	Broad Law Quarry	NT 344 539
30	Coarse Granite	Lower Old Red Sandstone	Kirnie Law	NT 348 387
31	Coarse Granite	Lower Old Red Sandstone	Kailzie Hill	NT 280 360
32	Microgranite	Lower Old Red Sandstone	Priesthope Hill	NT 344 390
33	Country Rock (altered greywackes)	Silurian	Priesthope Hill	NT 346 395
34	Slate	Silurian	S of Preston Law	NT 254 348
35	Country rock (altered greywacke)	Silurian	Near Broad Law Quarry	NT 344 540
36	Quartz-Dolerite	Lower Carboniferous	Musselburgh	NT 360 640

TABLE II-3

SAMPLE NO	NUMBER OF SPECIMENS	SATURATED DENSITY (g/cc)	DRY DENSITY (g/cc)	GRAIN DENSITY (g/cc)	POROSITY (%)
1	5	2.705 ± .002	2.694 ± .003	2.724 ± .003	1.1
1a	5	2.704 ± .009	2.695 ± .008	2.720 ± .011	0.9
2	5	2.676 ± .003	2.668 ± .006	2.689 ± .002	0.8
3	5	2.684 ± .002	2.679 ± .002	2.693 ± .003	0.5
4	5	2.721 ± .007	2.713 ± .007	2.734 ± .007	0.8
5	6	2.708 ± .028	2.698 ± .020	2.725 ± .029	1.0
6	6	2.722 ± .005	2.712 ± .009	2.739 ± .012	1.0
7	5	2.702 ± .007	2.694 ± .008	2.714 ± .007	0.8
8	5	2.754 ± .011	2.741 ± .011	2.776 ± .012	1.3
9	6	2.661 ± .017	2.657 ± .016	2.685 ± .018	1.0
10	6	2.661 ± .009	2.651 ± .010	2.678 ± .010	1.0
11	5	2.708 ± .009	2.705 ± .010	2.713 ± .010	0.3
12	5	2.675 ± .003	2.673 ± .003	2.679 ± .003	0.2
13	5	2.643 ± .007	2.641 ± .008	2.647 ± .007	0.2
14	5	2.626 ± .004	2.616 ± .004	2.643 ± .005	1.0
15	7	2.498 ± .023	-	-	-
16	4	2.695 ± .013	-	-	-
17	5	2.721 ± .023	-	-	-
18	5	2.619 ± .054	2.587 ± .058	2.672 ± .048	3.2

DENSITY MEASUREMENTS OF ROCK SAMPLES

SAMPLE NO	NUMBER OF SPECIMENS	SATURATED DENSITY (g/cc)	DRY DENSITY (g/cc)	GRAIN DENSITY (g/cc)	POROSITY (%)
19	5	2.673 ± .017	2.669 ± .017	2.681 ± .018	0.4
20	4	2.900 ± .015	2.895 ± .018	2.910 ± .011	0.5
21	5	2.631 ± .005	2.630 ± .005	2.632 ± .004	0.1
22	5	2.724 ± .007	2.709 ± .007	2.750 ± .036	1.3
23	6	2.722 ± .013	2.698 ± .012	2.763 ± .015	2.4
24	5	2.771 ± .010	2.754 ± .011	2.803 ± .008	1.7
25	6	2.604 ± .013	2.573 ± .014	2.655 ± .014	3.1
26	7	2.665 ± .012	2.651 ± .012	2.687 ± .014	1.4
27	6	2.471 ± .012	2.445 ± .009	2.509 ± .016	2.6
28	5	2.660 ± .012	2.633 ± .016	2.709 ± .011	2.7
29	5	2.712 ± .004	2.711 ± .006	2.717 ± .005	0.1
30	6	2.628 ± .006	2.621 ± .005	2.639 ± .007	0.7
31	5	2.627 ± .012	2.613 ± .014	2.648 ± .011	1.4
32	5	2.719 ± .004	2.715 ± .005	2.727 ± .004	0.4
33	7	2.818 ± .037	2.815 ± .038	2.824 ± .037	0.3
34	6	2.629 ± .022	2.583 ± .025	2.706 ± .024	4.6
35	5	2.703 ± .007	2.695 ± .007	2.717 ± .006	0.8
36	6	2.859 ± 0.018	2.831 ± 0.020	2.911 ± 0.016	2.8

Table II-4 shows a summary for most types of rocks in Table II-3 and compared with the values obtained by McLean (1961a) at the western part of South Scotland.

2.4.2 Least Squares Density Determination

Nettleton (1939) described a method of determining near surface densities by gravity observations along a profile over a topographic feature, a hill or valley with gentle slopes, unrelated to known geological structure. Although his method has been discussed by Parasnis (1952) and applied by various authors, it seems that, often, the results are unreliable.

However, in cases where there is an absence of exposures, a gravimetric method for the indirect determination of density may be necessary.

A computer program, DENS2, written by R G Hipkin, was used to estimate the density of rocks belonging to different geological classifications, by fitting a trend surface to the Bouguer anomaly.

According to the program, the Bouguer anomaly, BA, is fitted by least squares to the power series as follows:

$$BA = (BA)_o - (0.41923h - T)(d - d_o) = (Ax^2 + By^2 + Cxy + Dx + Ey + F) + e \qquad (2.3)$$

where: h = elevation (metres), T = terrain coefficient (g.u./g/cc), d = true density, d_o = assumed Bouguer density, A, B,...,E,F coefficients, e = error and $(BA)_o$ = the Bouguer anomaly calculated with the assumed density d_o.

TABLE II-4

Lithology	Number of		Mean Saturated Density (g/cc)	McLean's (1961a) Estimated Mean Density (g/cc)
	Localities	Specimens		
Ordovician & Silurian greywackes	9	47	2.708 ± 0.021	2.72
Lower Old Red Sandstone porphyrites-felsites	6	32	2.666 ± 0.028	2.58
Upper Old Red Sandstone sediments	6	35	2.598 ± 0.090	2.41
Lower Old Red Sandstone sediments	2	9	2.708 ± 0.018	2.61
Sills and Dykes (Quartz-Dolerite)	2	10	2.879 ± 0.029	2.90
Caledonian Granites	4	21	2.671 ± 0.050	2.67

SUMMARY OF DENSITY MEASUREMENTS OF THE MAIN ROCK TYPES

In this case, where the Bouguer anomaly is calculated with the assumed density d_o, the program gives the correction to the Bouguer density used. Using Free-Air anomaly the program gives the complete Bouguer density.

The program DENS2 was applied in some areas for an estimate of the near surface density of different type of rocks in various areas. The stations in each 10km National Grid square were taken for the calculation of the density. Because in some regions the gravity field approximated a 3^o surface better than a 2^o surface, an expansion of the DENS2 was made by the author and DENS3 fits the Bouguer anomaly to a third degree surface.

Some of the successful results applying DENS2 and DENS3 are shown in Table II-5. Generally, fitting a second degree surface has yielded better results and lower standard deviations than fitting a third degree surface on the gravity field over the Southern Uplands. From nine 10km squares within the Southern Uplands, the average near surface density is 2.709 $\pm$ 0.023 (g/cc), almost identical value with the saturated density of the Lower Palaeozoic sediments found in Table II-3.

The newly developed method has proved to be successful, particularly applying it over the Southern Uplands, where the results are very satisfactory.

2.5. Gravity Anomalies

Having all the parameters described in 2.3.2 as input to GRAVØ1, the

TABLE II-5

Geological Classification	NT	Number of Stations	Density from DENS2 (g/cc)	Density from DENS3 (g/cc)
Silurian Greywackes	12	23	2.699 ± .020	
Ordovician & Silurian Greywackes	13	21	2.670 ± 0.036	
Silurian Greywackes	23	48	2.746 ± 0.028	2.759 ± 0.027
Ordovician & Silurian Greywackes	24	54	2.709 ± 0.031	
Silurian Greywackes	32	32	2.685 ± 0.015	
Silurian Greywackes	33	32	2.721 ± 0.064	
Ordovician & Silurian Greywackes	34	17	2.727 ± 0.022	
Silurian & Upper Old Red Sandstone Sediments	65	29	2.726 ± 0.025	2.707 ± 0.013
Silurian & Upper Old Red Sandstone Sediments	76	25		2.699 ± 0.039
Silurian & Upper Old Red Sandstone Sediments	53	30	2.666 ± 0.057	2.662 ± 0.051
Carboniferous Limestones	47	53	2.557 ± 0.450	
Silurian & Upper Old Red Sandstone Sediments	54	53	2.750 ± 0.050	2.767 ± 0.047
Ordovician & Lower Old Red Sandstone Sediments	14	20	2.691 ± 0.086	

DENSITY ESTIMATIONS USING COMPUTER PROGRAMS

Free-Air and Bouguer anomalies were calculated using the following equations:

$$g_f = g_{obs} - g_n + 3.086h \qquad (2.4)$$

$$g_B = g_f - (0.41923h - TC)d \qquad (2.5)$$

where: g_f is the Free-Air anomaly (g.u.)

g_{obs} is the observed gravity (g.u.) corrected for drift

g_B is the Bouguer anomaly (g.u.)

h is the station elevations (m)

TC is the terrain coefficient (gu/unit density)

d is the density (g/cm^3)

g_n is the normal gravity, based on the Geodetic Reference System (1967).

$$g_n = 9780318.495(1 + 0.0052788944 \sin^2\varphi + 0.0000234631 \sin^4\varphi)$$

where: φ is the latitude. A density of 2.67 g/cm^3 was used in equation (2.5) as it is the usual value for computing Bouguer anomalies for crustal studies. The observed density of surface rocks was not used because the determination of the subsurface density structure is the task of gravity interpretation, not gravity reduction. Estimates of a locally appropriate density for the topography will be discussed in the chapters dealing with modelling.
All the above computations were carried out using the EMAS (Edinburgh Multi-Access System) ICL4-75 computer, in Edinburgh.

After the least squares adjustment of the gravity base stations, described in Chapter III, and the determination of the new values of the bases, the whole data set of the gravity measurements was rerun. The final values of the anomalies together with the relevant information for each gravity station is presented in Appendix C.

2.5.1 Error Estimation of the Gravity Anomalies

The error involved in the observed gravity (g_{obs}) arises mainly from the following factors:

(i) Reading error, which is really very small (approximately 0.03 g.u.).

(ii) The error involved in the absolute value of gravity of the Edinburgh F.B.M., to which all the gravity stations of the survey have been referred. It has been estimated as ± 0.33 g.u. (Masson-Smith et al, 1974).

(iii) The error due to the drift irregularity of the instrument, which is less than 20 μgal (0.2 g.u.). Since base station readings were made with ordinary gravity station readings interspersed between them, the standard deviation of the base station adjustment, found in Table III-4 to be 0.09569, is typical for any field station and could have been used instead.

(iv) The error due to the Earth tides: GRAVØ1 calculates the equilibrium tidal corrections with error ± 0.005 g.u., which is very small indeed. In coastal areas a marine tidal effect might be as large as 0.03 g.u. As has been mentioned elsewhere, this can be removed as a linear instrumental drift, visiting base stations every 3-4 hours.

(v) The error due to the manufacturer's calibration factor. This is only few parts in 10^4 g.u. As has been described in Chapter III, a fractional error of $(1.6 \pm 3.8) \times 10^{-4}$ was found for the calibration factor between Edinburgh and Hexham (Table III-6).

The largest gravity difference measured in the survey area with respect to Edinburgh F.B.M. was at Broad Law (NT1524) - 2072.24 g.u., resulting in a calibration error of 0.33 g.u.

Of the five cases considered here, the quoted errors for only (i) and (ii) are related to statistically determined standard deviations. The others are estimated maximum errors. All will be treated as if they were standard deviations, which will merely result in an over-estimate of the error. An arithmetic sum gives 0.92 g.u., while the RMS addition is 0.24g.u.

Therefore, from the five causes considered above, the error in the observed gravity, g_{obs}, is 0.92 g.u. with an RMS error of 0.24 g.u.

Heights determined from bench marks, levelled and other spot heights give an error contribution of $\pm$ 0.3 and $\pm$ 1 g.u. respectively, as described previously in section 2 of the present chapter. Again, from this section it is concluded that an error of $\pm$ 10m in latitude gives an error of less than 0.1 g.u. in the calculation of the normal gravity, g_n.

Assuming that the mean value of the terrain coefficient of the gravity stations is 2 g.u. per unit density (1 g/cm^3), then the error for the terrain coefficient is 0.2 g. u. per unit density. This value is a true standard deviation, but estimated from only a part of the data.

Treating all the above error estimates as standard deviations, including the probable maximum errors for station elevation, then the standard deviation of the Free-Air (FA) and Bouguer anomalies (BA)is estimated as follows, according to the errors propagation, Young (1962) :

$$S_{FA}^2 = S_{obs}^2 + S_{g_n}^2 + 3.086^2 \; S_h^2$$

$$S_{BA}^2 = S_{obs}^2 + S_{g_n}^2 + (3.086 - 0.41923)^2 \; S_h^2 + (2.67)^2 S_{TC}^2$$

where: S_{obs} is the standard deviation of g_{obs}

S_{g_n} is the standard deviation of the normal gravity g_n

S_h is the standard deviation of the height

S_{TC} is the standard deviation of the terrain coefficient, etc.

Using the above analysis and substituting in the above equations according to the height control information of a gravity station, the error is:

(1) From bench marks:

$S_{FA} = \pm 0.9$ g.u. and $S_{BA} = \pm 1.0$ g.u.

(2) From levelled spot heights:

$S_{FA} = \pm 1.2$ g.u. and $S_{BA} = \pm 1.3$ g.u.

(3) From other spot heights:

$S_{FA} = \pm 3.2$ g.u. and $S_{BA} = \pm 2.9$ g.u.

Therefore, the estimated individual Bouguer anomaly accuracy for most of the gravity stations is $\pm$ 1-1.5 g.u.

CHAPTER III

GRAVITY BASE STATION NETWORK ADJUSTMENT

3.1 Introduction

A gravity meter only measures differences in gravity and if a survey is extended outwards in an uncontrolled way, the errors will accumulate with distance. The network adjustment consists of correcting each measured difference between adjacent bases until the cumulative gravity difference between any two bases on the network is the same for all routes connecting them.

A few workers in the past have attempted to develop an algorithm for the adjustment of a gravity base station network. Pentz (1952) developed one which gives the most probable value for an arbitrary number of base stations in a gravity network, which is expanded when a value of a new base is assigned from two existing bases. As long as the number of conditional equations required to produce the necessary accuracy is maintained, the network of a finite but unknown bases is fully determined, when the conditions for the solution of the normal equations are satisfied.

Smith (1950), based on Gibson's (1937) paper developed a satisfactory graphical method for network adjustment, but it has the disadvantage of being slow.

Searle (1969) developed an analysis for altimetric traverses, but which could also be used for a gravity network, based on minimising the quantity $\Sigma w_i Q_i^2$, where $w_i \equiv$ weighting factor $= \frac{1}{\sqrt{N}}$ and N = number of height differences in each traverse; $Q_i = g_i' - g_i$ where g_i' and g_i are respectively the observed and adjusted height differences in a closing direction along the i^{th} traverse.

In none of these papers was the instrumental drift taken into consideration.

In the study area 52 bases have been established during the gravity survey. Twenty-five of them had already been set up in Midlothian and Tweeddale by Dr Hipkin, before the extension of the survey by the author. They are indicated by an asterisk in Table III-1, where the whole set of the bases is shown. A few of our bases belong to the National Gravity Reference Net - 1973 (Masson-Smith et al, 1974) and are marked by a double asterisk. Although all the bases and consequently the whole gravity net are referred to the Edinburgh Fundamental Bench Mark value (9815849.16 $\pm$ 0.33 g.u.), an alternative base was set up in the Geophysics Department in order to avoid delays due to traffic congestion in Edinburgh. This station, initially in 5 South Oswald Road and later in the James Clerk Maxwell Building, was frequently used for the more distant connections, eg. Thankerton and Mordington FBM's.

A manual adjustment as well as a least-squares one was made to the network, the analysis of which is described below.

Figure 3.1 shows the distribution of the base stations in the study area. Ties between the bases are shown in the data input file to program NETWORK, appendix A. Those ties which were made between bases before 1978, on which a manual adjustment was made, are also shown in figure 3.2. Later the network was extended and strengthened internally by more cross-ties.

3.2 Manual adjustment of the network

Most of the gravity base stations, established in the SE part of Scotland by the end of 1977, were initially adjusted by an empirical manual method. This network is shown in figure 3.2.

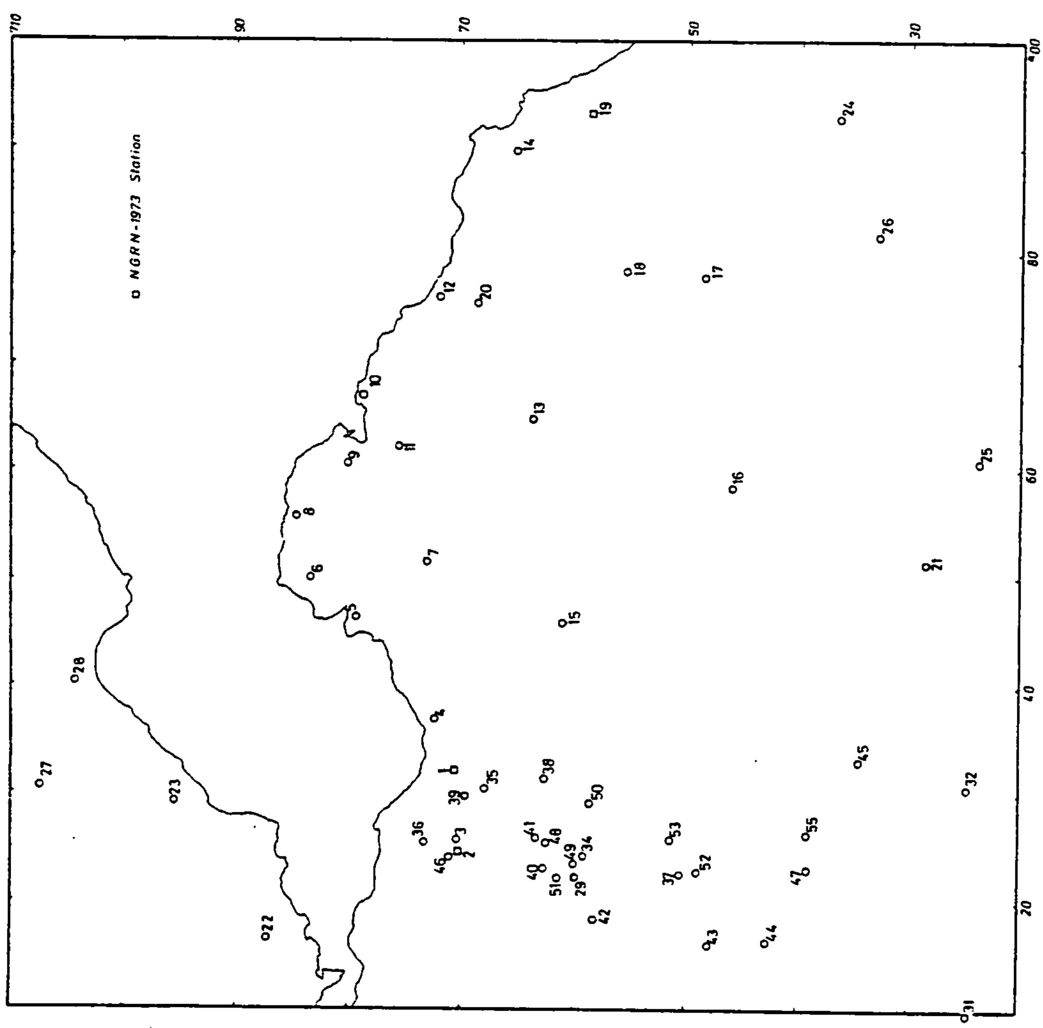

Fig. 3.1 Distribution of gravity base stations over the SE Scotland and Borders region.

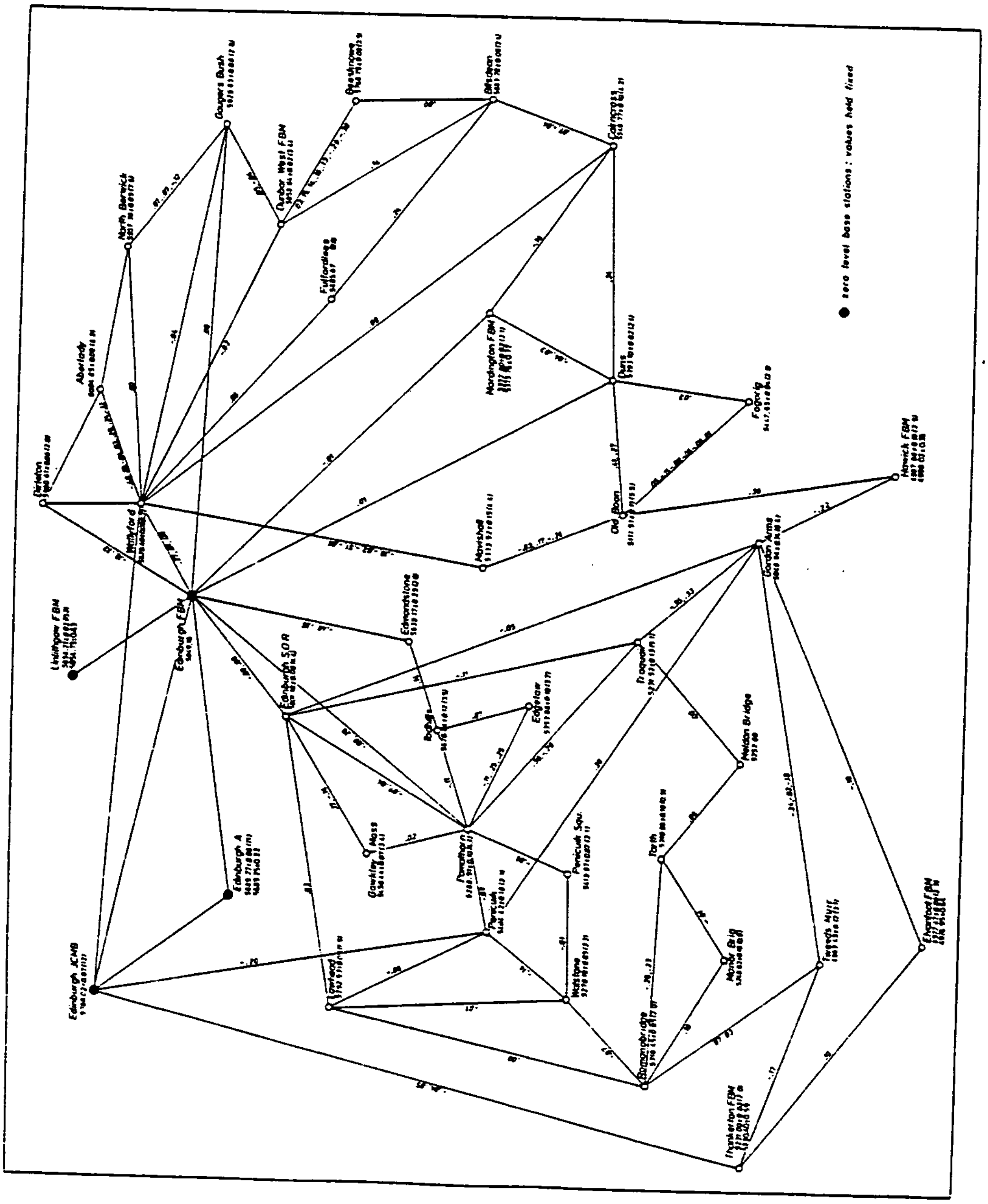

Fig. 3.2 Manual gravity base station adjustment.

Black circles represent "zero level" bases to which all the other bases are referred. Zero level bases were not included in the manual adjustment.

The value of gravity at Edinburgh F.B.M. was held fixed and the other zero-level bases separately determined with high precision by a special measurement program and a least-squares adjustment. Thereafter, the three zero-level bases in Edinburgh (Edinburgh F.B.M., Edinburgh A in the Royal Observatory of Edinburgh (Bullard and Jolly, 1936) and Edinburgh James Clerk Maxwell Building - J.C.M.B.) were held fixed for the manual adjustment of the network.

Those bases which are connected directly to one of the zero-level bases, are called "first-level" bases, such as Wallyford, Dirleton, Mordington F.B.M., Pomathorn etc.

Bases which are connected to zero-level bases via one other base are referred to as "second-level" bases. "Third-level" bases are those which are connected to zero-level with the intervention of two bases, etc.

The adjustment of a base of level N involved a weighted mean of the measured ties, achieved with fewer than M links ($M \leqslant 2$), between it and every other base of level N-1. The weight assigned to such a tie was $\frac{1}{(N + M-1)^{\frac{1}{2}}}$. For example, the adjustment of base 4 (Wallyford, level 1) which involved links with base 3 (Edinburgh J.C.M.B.), base 1 (Edinburgh F.B.M.) and base 9 (Gauger's Bush, level 1) is outlined below:

No of links	Wallyford (4) Links between Bases	Observed Value	Weight
3	1-4	9815829.13	1
	1-4	9815829.39	1
	1-4	9815829.40	1
1	3-4	9815829.60	1
1	1-9-4	9815829.50	$1/\sqrt{2}$

Weighted Mean: 9815829.398 Total Weight: 4.707

The procedure becomes increasingly complex for higher level bases but the results were in reasonable agreement with later work. Figure 3.2 shows the adjusted mean for each base and its standard deviation with its total relative weight in parenthesis.

3.3 Least-Squares Adjustment

3.3.1 Introduction

Because new base stations were established during the expansion of the survey, as described in Chapter II and, also, additional ties made between the bases, it was considered necessary to make a computer adjustment of the network, using the least-squares technique. This was inevitable because the addition of the new bases and internal cross-ties required the whole manual adjustment to be repeated. A least-squares technique was suggested by R G Hipkin and a description of the setting up of the normal equations is outlined below. Subsequently, an error analysis was made and a computer program, NETWORK, was written to perform the adjustment.

In the adjustment, errors are distributed amongst all the gravity stations, including Edinburgh FBM, and the drift rate for each day's observations is recomputed, by least-squares. The datum level is set by constraining only the mean observation at Edinburgh FBM, rather than every reading, to be 9815849.16 (g.u.), so that a standard deviation can be attributed to it.

3.3.2 Definitions

Base station is any point at which repeated observations have taken place.

Traverse is a sequence of observations to which a single drift curve is to be fitted.

Gravity observation (g) is obtained by converting the meter dial turns to gravity units and correcting for Earth tides. An (arbitrary) datum value and, possibly, a linear drift correction, which are the same for all stations on the same traverse, may have been applied. The quantity "observed gravity," computed by GRAVØ1 is a suitable measure for g.

3.3.3 Notation

The following notation has been used:

M total number of base stations

m index specifying the base station ($m = 1, 2, \ldots, M$)

K total number of traverses

k index specifying the traverse ($k = 1, 2, \ldots, K$)

p index specifying an observation on k^{th} traverse at station m

P_{km} number of observations at m^{th} base station during the k^{th} traverse

$Q_m = \sum_{k=1}^{K} P_{km}$ total number of observations at m^{th} base station

$R_k = \sum_{m=1}^{M} P_{km}$ total number of observations on k^{th} traverse

G_m adjusted value of gravity at m^{th} base station

a_k datum constant of k^{th} traverse

b_k drift rate for k^{th} traverse

[ ] enclose observed quantities

$\langle\ \rangle$ indicate mean value

3.3.4 Observational equation

For each observation, p, at base m on traverse k, the observed value of gravity g_{pkm} has the form:

$$g_{pkm} = G_m - a_k + b_k \, t_{pkm} + \xi_{pkm} \tag{3.1}$$

where t_{pkm} and ξ_{pkm} are the time and error for that particular observation.

3.3.5 Variance

From equation (3.1) summing the square of ξ_{pkm} for all the observations at all bases on all traverses, the variance of the network is:

$$\Sigma(\xi^2) \equiv \sum_{k=1}^{K} \sum_{m=1}^{M} \sum_{p=1}^{P_{km}} (\xi_{pkm})^2 = \sum_{k=1}^{K} \sum_{m=1}^{M} \sum_{p=1}^{P_{km}} (g_{pkm} - G_m + a_k - b_k t_{pkm})^2 \tag{3.2}$$

3.3.6 Normal equations

The quantity $\Sigma\xi^2$ has to be minimised. Therefore, three sets of equations are produced by setting the partial derivatives of the variance equal to zero. From $\frac{\partial \Sigma \xi^2}{\partial a_k}$ we have K equations where k = 1,2,...., K:

$$\left[\sum_{m=1}^{M} \sum_{p=1}^{P_{km}} g_{pkm}\right] = \sum_{m=1}^{M} \left[P_{km}\right] G_m + \left[-R_k\right] a_k + \left[\sum_{m=1}^{M} \sum_{p=1}^{P_{km}} t_{pkm}\right] b_k \tag{3.3}$$

In the above equations we shall replace the sums $\sum_{p=1}^{P_{km}}$ and $\sum_{k=1}^{K}$ and $\sum_{m=1}^{M}$ by $\sum_p$ and $\sum_k$ and $\sum_m$ respectively, and thereafter this notation will be held in the following:

From $\frac{\partial \Sigma \xi^2}{\partial b_k}$ we have K equations for k = 1,2,..., K:

$$\left[\sum_m \sum_p g_{pkm}\, t_{pkm}\right] = \sum_m \left[\sum_p t_{pkm}\right] G_m - \left[\sum_m \sum_p t_{pkm}\right] a_k + \left[\sum_m \sum_p (t_{pkm})^2\right] b_k \qquad (3.4)$$

From $\frac{\partial \Sigma \xi^2}{\partial G_m}$ we have M equations, when m = 1,2,..., M:

$$\left[\sum_k \sum_p g_{pkm}\right] = \left[Q_m\right] G_m + \sum_k \left[-R_k\right] a_k + \sum_k \left[\sum_p t_{pkm}\right] b_k \qquad (3.5)$$

Considering equations (3.3), (3.4), (3.5), we have a total number of M + 2K equations, which equals the numbers of unknowns G_m, a_k, b_k; but only (M + 2K)-1 of them are independent. For, the sum over all bases ($\sum_{m=1}^{M}$) on set (3.5) is equal to the sum for all traverses ($\sum_{k=1}^{K}$) on set (3.4). It appears then that the whole set of equations is under-determined, for there are (2K + M)-1 linearly independent equations with (2K + M) unknowns: an additional equation is required.

This is provided by defining the datum for the survey, which otherwise is entirely relative and could not determine absolute values G_m.

If the base station m = 1 has to (absolute) gravity value ζ_o, the additional required equation is simply $G_1 = \zeta_o$ and the equation with m = 1 from (3.3) can be omitted.

Summarising the above, we have that the (M + 2K) set of normal equations has the form:

$$[1]\, G_1 = [\zeta_o]$$

$$[0]\, G_1 + [Q_2]\, G_2 + \ldots + [-P_{21}]\, a_1 + [-P_{22}]\, a_2 + \ldots + \left[\sum_p t_{p12}\right] b_1 + \left[\sum_p t_{p22}\right] b_2 + \ldots = \left[\sum_{kp}\sum g_{pk2}\right]$$

$$[0]\, G_1 + [0]\, G_2 + [Q_3]\, G_3 + \ldots + [-P_{31}]\, a_1 + [-P_{32}]\, a_2 + [-P_{33}]\, a_3 + \ldots + \left[\sum_p t_{p13}\right] b_1 + \left[\sum_p t_{p23}\right] b_2 + \ldots = \left[\sum_{kp}\sum g_{pk3}\right]$$

....

$$[P_{11}]\, G_1 + [P_{12}]\, G_2 + \ldots + [-R_1]\, a_1 + [0]\, a_2 + [0]\, a_3 + \ldots + \left[\sum_{mp}\sum t_{p1m}\right] b_1 + [0]\, b_2 + [0]\, b_3 + \ldots = \left[\sum_{mp}\sum g_{p1m}\right]$$

$$[P_{21}]\, G_1 + [P_{22}]\, G_2 + \ldots + [0]\, a_1 + [-R_2]\, a_2 + [0]\, a_3 + \ldots + [0]\, b_1 + \left[\sum_{mp}\sum t_{p2m}\right] b_2 + [0]\, b_3 + \ldots = \left[\sum_{mp}\sum g_{p2m}\right]$$

....

$$\left[\sum_p t_{p11}\right] G_1 + \left[\sum_p t_{p12}\right] G_2 + \ldots + \left[-\sum_{mp}\sum t_{p1m}\right] a_1 + [0]\, a_2 + \ldots + \left[\sum_{mp}\sum (t_{p1m})^2\right] b_1 + [0]\, b_2 + [0]\, b_3 + \ldots = \left[\sum_{mp}\sum g_{p1m} t_{p1m}\right]$$

$$\left[\sum t_{p21}\right] G_1 + \left[\sum_p t_{p22}\right] G_2 + \ldots + [0]\, a_1 + \left[-\sum_{mp}\sum t_{p2m}\right] a_2 + \ldots + [0]\, b_1 + \left[\sum_{mp}\sum (t_{p2m})^2\right] b_2 + \ldots = \left[\sum_{mp}\sum g_{p2m} t_{p2m}\right]$$

....

3.3.7 Error Analysis

Considering equations (3.1) where G_m is a function of the uncorrelated measured variables g_{pkm} and t_{pkm}, we have (Bevington, 1969):

$$(\xi_{pkm})^2 = \left(\frac{\partial G_m}{\partial g_{pkm}}\right)^2 (\xi g_{pkm})^2 + \left(\frac{\partial G_m}{\partial t_{pkm}}\right)^2 (\xi t_{pkm})^2 \qquad (3.6)$$

Assuming that all the observations of gravity (g_{pkm}) and time (t_{pkm}) at all bases on all traverses, belong to the same population then the expected value of any ξg_{pkm} and any ξt_{pkm} will be as follows:

$$\left\langle \xi g_{pkm}^2 \right\rangle = s_{g_m}^2 \text{ and } \left\langle \xi t_{pkm}^2 \right\rangle = s_{t_m}^2 \tag{3.7}$$

for any observation on any traverse; ξ_{g_m} and ξ_{t_m} are the standard deviations of the gravity observations and time at a base m, respectively.

Assuming P_{km} observations at the m^{th} base station for the k^{th} traverse, a total number of Q_m observations at the same base for all the traverses, and summing for all traverses and observations, from (3.6) we have:

$$\sum_{k}\sum_{p}(\xi_{pkm})^2 = \sum_{k}\sum_{p}\left(\frac{\partial G_m}{\partial g_{pkm}}\right)^2(\xi g_{pkm})^2 + \sum_{k}\sum_{p}\left(\frac{\partial G_m}{\partial t_{pkm}}\right)^2(\xi_{t_{pkm}})^2$$

and from (3.7)

$$\sum_{k}\sum_{p}(\xi_{pkm})^2 = Q_m\, s_{g_m}^2 + \left(-\sum_{k} P_{km} b_k\right)^2 s_{t_m}^2 \tag{3.8}$$

Because the contribution of the second term on the right hand at the above equation is negligible it can be omitted.

Hence, the error for each base is expressed in terms of the total number of observations at that base station. The greater the number of visits to a base, the better the estimation of its error.

The root mean square error of the adjustment S_{RMS} can be derived as the square root of the total variance divided by the total number of observations on all the bases, NOBS, minus one:

$$S_{RMS} = \left(\frac{\Sigma \xi^2}{NOBS - 1} \right)^{\frac{1}{2}}$$

Because the number of observations at almost any base is relatively small, it is more desirable to estimate confidence limits on the adjusted value, G_m, rather than simply quote an apparent standard deviation or standard error.

For example, over what range is there a 95% probability that the true mean μ_{G_m} will be within this confidence interval on either side of our adjusted mean G_m.

Thus, the confidence interval within which μ_{G_m} falls with 100(1-a)% confidence is (Bendat and Piersol, 1971);

$$G_m - \frac{S_{g_m} \, t_{n,a/2}}{\sqrt{\varrho_m}} \leqslant \mu_{G_m} < G_m + \frac{S_{g_m} \, t_{n,a/2}}{\sqrt{\varrho_m}} \tag{3.10}$$

and the true variance $\sigma^2_{G_m}$ of μ_{G_m} based upon the standard deviation S_{g_m} of G_m is:

$$\frac{ns^2_{g_m}}{\chi^2_{n,a/2}} \leqslant \sigma^2_{G_m} < \frac{ns^2_{g_m}}{\chi^2_{n,1-a/2}} \tag{3.11}$$

where $n = Q_m - 1$ and a can be found from tables showing the percentage points of Student's t distribution - see Bendat and Piersol (1971), p. 389 - and chi-square distribution.

Taking the square root on both sides of equation (3.11), we can have an estimate of a lower and upper limit of the standard deviation of μ_{G_m}. This was done with a 95% confidence interval for the μ_{G_m} and σ_{G_m}, taking the values of the student t and chi-square distribution from tables given by Bendat and Piersol (1971).

3.3.8 Programming - results

A Fortran IV computer program, NETWORK, was written based on the analysis presented in the previous sections. A listing of the program and a description of it is outlined in Appendix B.

The input data to NETWORK are presented in Appendix A. They consist of the reference number of a base station, followed by the observed value of gravity at that base and the time, expressed in number days, using the Gregorian day number routine of the GRAVØ1 program. It is also possible to see the ties between different base stations.

To solve the M + 2K = 221 normal equations (M = 57, K = 82) with a total number of NOBS = 364 observations, for all the traverses, took something less than six minutes for 4-75 ICL computer on EMAS and 40 seconds on the 2980 ICL machine.

The results are presented in Table III-1, where for each base the adjusted value, its standard deviation and standard error is shown.

Table III-2 shows the upper and lower 95% confidence limits of the base station values, after the application of the t test, while Table III-3 shows the same upper and lower limit of the standard deviation of the value of each gravity station, with the number of visits defined in parenthesis.

TABLE III-1	Adjusted Values of Gravity Base Stations.
TABLE III-2	Lower and Upper Limits of Base Values with 95% Confidence.
TABLE III-3	Lower and Upper Limits of St. Deviation with 95% Confidence. Values in parentheses are number of visits at this base.

TABLE III-1

REFERENCE NUMBER		BASE STATION	ADJUSTED VALUE	STANDARD DEVIATION	STANDARD ERROR
1	**	EDINBURGH FBM	9815849.16	0.14	0.03
2		EDINBURGH A	9815689.68	0.11	0.05
3		EDINBURGH-JCMB	9815787.87	0.06	0.01
4		WALLYFORD	9815829.30	0.09	0.02
5		ABERLADY	9816004.56	0.12	0.04
6		DIRLETON	9815960.63	0.12	0.05
7		HADDINGTON	9815786.01	0.08	0.03
8		NORTH BERWICK	9815957.31	0.06	0.03
9		GAUGER'S BUSH	9815929.53	0.07	0.03
10		DUNBAR WEST FBM	9815859.64	0.03	0.01
11		BEESKNOWE	9815768.85	0.13	0.05
12		BILSDEAN	9815663.76	0.08	0.03
13		PRIESTLAW	9815230.78	0.03	0.01
14		CAIRNCROSS	9815548.82	0.11	0.04
15		MAVISHALL	9815333.95	0.07	0.02
16		OLD BOON	9815111.55	0.10	0.03
17		FOGORIG	9815447.86	0.08	0.03
18		DUNS	9815393.22	0.14	0.05
19	**	MORDINGTON FBM	9815372.82	0.12	0.04
20		FULTORDLEES	9815485.46	0.04	0.02
21		SELKIRK	9815093.23	0.11	0.06
22		ABERDOUR	9815721.27	0.06	0.03
23		THORNTON	9815879.93	0.08	0.04
24		FLODDEN LODGE	9815477.46	0.04	0.02
25		ANCRUM	9815335.92	0.07	0.03
26		HOSELAW	9815220.40	0.05	0.02
27		KETTLEBRIDGE	9816016.46	-	-
28		HATTON-LARGO	9815941.86	0.06	0.03

29	* JOHN'S ST-PENICUIK	9815404.34	0.06	0.02
30	** THANKERTON FBM	9815230.86	0.11	0.06
31	* TWEEDSMUIR	9814983.28	0.15	0.08
32	* GORDON ARMS	9815049.69	0.12	0.04
33	** ELVANFOOT FBM	9814977.11	0.04	0.03
34	* POMATHORN	9815288.86	0.07	0.01
35	* TODHILLS	9815669.93	-	-
36	* APPLETON TOWER	9815808.18	0.01	0.01
37	* COWESLINN	9815214.94	0.07	0.05
38	* DALHOUSIE	9815560.77	0.07	0.05
39	* OLD DALKEITH RD	9815639.47	0.03	0.02
40	* HOUSE OF MUIR	9815415.31	-	-
41	* GOWKLEY MOSS	9815456.52	0.25	0.15
42	* WALSTONE M.S.	9815270.11	0.02	0.01
43	* ROMANOBRIDGE	9815316.33	0.08	0.03
44	* TARTH WATER	9815310.84	0.18	0.13
45	*TRAQUAR WAR MEM	9815231.54	0.28	0.12
46	* S. OSWALD RD	9815800.78	0.25	0.09
47	* OLD MANOR BRIG	9815246.78	0.13	0.06
48	* PILLAR-ROSLIN	9815459.53	-	-
49	* SQUARE-PENICUIK	9815419.87	-	-
50	* EDGELAW COTTAGE	9815353.93	0.06	0.04
51	* LAWRIES DEN RD	9815292.41	0.04	0.03
52	* CLOICH FOREST	9815163.91	0.04	0.03
53	* WESTLOCH FARM	9815217.25	0.02	0.01
54	** HAWICK FBM	9814997.64	0.07	0.04
55	* GALLOWS HILL	9815214.26	-	-
56	** WETHERAL FBM	9814938.34	-	-
57	** HEXHAM FBM	9814708.32	-	-

TABLE III-2

BASE	LOWER LIMIT	ABS. GRAVITY	UPPER LIMIT
1	9815849.09	9815849.16	9815849.23
2	9815689.54	9815689.68	9815689.82
3	9815787.85	9815787.87	9815787.89
4	9815829.27	9815829.30	9815829.34
5	9816004.48	9816004.56	9816004.65
6	9815960.50	9815960.63	9815960.76
7	9815785.95	9815786.01	9815786.07
8	9815957.23	9815957.31	9815957.39
9	9815929.47	9815929.53	9815929.58
10	9815859.61	9815859.64	9815859.67
11	9815768.74	9815768.85	9815768.96
12	9815663.69	9815663.76	9815663.82
13	9815230.76	9815230.78	9815230.81
14	9815548.72	9815548.82	9815548.93
15	9815333.91	9815333.95	9815333.99
16	9815111.49	9815111.55	9815111.60
17	9815447.80	9815447.86	9815447.92
18	9815393.11	9815393.22	9815393.33
19	9815372.73	9815372.82	9815372.91
20	9815485.42	9815485.46	9815485.50
21	9815093.08	9815093.23	9815093.39
22	9815721.21	9815721.27	9815721.34
23	9815879.81	9815879.93	9815880.04
24	9815477.38	9815477.46	9815477.54
25	9815335.83	9815335.92	9815336.02
26	9815220.34	9815220.40	9815220.45
27	9816016.46	9816016.46	9816016.46
28	9815941.75	9815941.86	9815941.97

29	9815404.29	9815404.34	9815404.39
30	9815230.63	9815230.86	9815231.08
31	9814982.99	9814983.28	9814983.58
32	9815049.59	9815049.69	9815049.78
33	9814976.84	9814977.11	9814977.38
34	9815288.83	9815288.86	9815288.89
35	9815669.93	9815669.93	9815669.93
36	9815808.17	9815808.18	9815808.20
37	9815214.48	9815214.94	9815215.39
38	9815560.31	9815560.77	9815561.23
39	9815639.41	9815639.47	9815639.53
40	0.00	9815415.31	0.00
41	9815456.01	9815456.52	9815457.03
42	9815269.99	9815270.11	9815270.23
43	9815316.26	9815316.33	9815316.39
44	9815309.68	9815310.84	9815312.01
45	9815231.23	9815231.54	9815231.85
46	9815800.59	9815800.78	9815800.98
47	9815246.64	9815246.78	9815246.92
48	0.00	9815459.53	0.00
49	0.00	9815419.87	0.00
50	9815353.57	9815353.93	9815354.30
51	9815292.17	9815292.41	9815292.65
52	9815163.65	9815163.91	9815164.16
53	9815217.13	9815217.25	9815217.37
54	9814997.49	9814997.64	9814997.79
55	0.00	9815214.26	0.00
56	0.00	9814938.34	0.00
57	0.00	9814708.32	0.00

TABLE III-3

BASE	LOWER LIMIT	ST DEVIATION	UPPER LIMIT
1(21)	0.11	0.14	0.21
2(5)	0.07	0.11	0.32
3(43)	0.05	0.06	0.08
4(26)	0.07	0.09	0.12
5(10)	0.08	0.12	0.21
6(5)	0.06	0.11	0.31
7(9)	0.05	0.08	0.14
8(4)	0.03	0.05	0.19
9(7)	0.04	0.06	0.14
10(6)	0.02	0.03	0.06
11(7)	0.08	0.12	0.27
12(7)	0.05	0.07	0.16
13(6)	0.02	0.03	0.06
14(6)	0.06	0.10	0.25
15(18)	0.05	0.07	0.11
16(12)	0.06	0.09	0.15
17(9)	0.05	0.07	0.14
18(8)	0.09	0.13	0.27
19(8)	0.07	0.11	0.22
20(6)	0.02	0.04	0.09
21(4)	0.06	0.10	0.37
22(5)	0.03	0.05	0.15
23(4)	0.04	0.07	0.27
24(3)	0.02	0.03	0.21
25(4)	0.03	0.06	0.21
26(5)	0.02	0.04	0.12
27(2)	0.00	0.00	0.01
28(3)	0.02	0.05	0.29

29(9)	0.04	0.06	0.12
30(3)	0.05	0.09	0.56
31(3)	0.06	0.12	0.75
32(8)	0.07	0.11	0.23
33(2)	0.01	0.03	0.98
34(24)	0.06	0.07	0.10
35(2)	0.00	0.00	0.00
36(4)	0.01	0.01	0.05
37(2)	0.02	0.05	1.61
38(2)	0.02	0.05	1.64
39(3)	0.01	0.02	0.15
40(1)	0.00	0.00	0.00
41(3)	0.11	0.21	1.29
42(2)	0.01	0.01	0.44
43(7)	0.05	0.07	0.16
44(2)	0.06	0.13	4.14
45(5)	0.15	0.25	0.72
46(8)	0.15	0.23	0.47
47(5)	0.07	0.12	0.33
48(1)	0.00	0.00	0.00
49(1)	0.00	0.00	0.00
50(2)	0.02	0.04	1.30
51(2)	0.01	0.03	0.84
52(2)	0.01	0.03	0.90
53(2)	0.01	0.01	0.43
54(3)	0.03	0.06	0.38
55(1)	0.00	0.00	0.00
56(1)	0.00	0.00	0.00
57(1)	0.00	0.00	0.00

Table III-4 shows the histogram of the errors of the observations, calculated from each observational equation. They are expected to follow the normal distribution. They seem to form a symmetrical normal distribution curve.

Table III-5 summarises the results found from our adjustment and the NGRN-73 gravity values.

3.3.9 Calibration factor tests

The difference of absolute gravity values between Edinburgh and Hawick and also the difference between Edinburgh and Hexham found from our adjustment and the NGRN-73 are shown in Table III-6.

Both the local measurements suggest that the manufacturer's calibration factor is too large for the LaCoste and Romberg gravity meter G-275, but neither is statistically significant.

Tests which have been carried out along the short calibration line near Macclesfield (Masson-Smith et al, 1974) with the G-274 gravimeter between North Rode and Cat and Fiddle (NRCF) and the newer one, Hatton Heath and Prees (HHP), are also shown in Table III-6. In contrast to the local measurements. these results suggest that the manufacturer's calibration factor is too small. The two calibration line results are not statistically consistent either with each other or with the Scottish measurements.

TABLE III-4
HISTOGRAM OF RESIDUALS

```
                       RMS RESIDUAL      0.09569 GU
LOWER LIMIT OF HISTOGRAM = -0.478
UPPER LIMIT OF HISTOGRAM =  0.478
HISTOGRAM INTERVAL =  0.096

                              HISTOGRAM
THEORETICAL
 FREQUENCY   .1    .5     8    49   124   124    49     8    .5    .1

OBSERVED
FREQUENCY     1     1     7    28   145   138    35     7     1     1
------------------------------------------------------------------------
EACH *EGALS  3 POINTS

    144                              *
    141                              *
    138                              *     *
    135                              *     *
    132                              *     *
    129                              *     *
    126                              *     *
    123                              *     *
    120                              *     *
    117                              *     *
    114                              *     *
    111                              *     *
    108                              *     *
    105                              *     *
    102                              *     *
     99                              *     *
     96                              *     *
     93                              *     *
     90                              *     *
     87                              *     *
     84                              *     *
     81                              *     *
     78                              *     *
     75                              *     *
     72                              *     *
     69                              *     *
     66                              *     *
     63                              *     *
     60                              *     *
     57                              *     *
     54                              *     *
     51                              *     *
     48                              *     *
     45                              *     *
     42                              *     *
     39                              *     *
     36                              *     *
     33                              *     *     *
     30                              *     *     *
     27                        *     *     *     *
     24                        *     *     *     *
     21                        *     *     *     *
     18                        *     *     *     *
     15                        *     *     *     *
     12                        *     *     *     *
      9                        *     *     *     *
      6                  *     *     *     *     *     *
      3                  *     *     *     *     *     *
------------------------------------------------------------------------
INTERVAL      1     2     3     4     5     6     7     8     9    10
 CLASS
```

TABLE III-5

Adjusted and NGRN-73 Values of Some Stations

FBM NAME	ADJUSTED VALUE (gu)	NGRN-73 VALUE (gu)
Edinburgh	9815849.16 ± 0.14	9815849.16 (±0.33)*
Modrington	9815372.82 ± 0.12	9815373.76 (±0.77)
Thankerton	9815230.86 ± 0.11	9815230.40 (±0.59)
Elvanfoot	9814977.11 ± 0.04	9814976.95 (±0.64)
Hawick	9814997.64 ± 0.07	9814998.02 (±0.35)
Wetheral	9814938.34 -	9814938.11 (±0.22)
Hexham	9814708.32 -	9814708.50 (±0.25)

* Values in parenthesis indicate standard error.

TABLE III-6

Scale Calibration Results

Link	Manufacturer's Scale gu	NGRN 73 gu	Discrepancy gu	Calibration factor correction
Edinburgh-Hawick	851.52 ± 0.17	851.14 ± 0.48*	0.38 ± 0.51	0.99955 ± 0.00059
Edinburgh-Hexham	1140.84 ± 0.17**	1140.66 ± 0.40*	0.18 ± 0.43	0.99984 ± 0.00038
North Rode-Cat & Fiddle	604.249 ± 0.040	604.53 ± 0.08*	-0.281 ± 0.089	1.00047 ± 0.00015
Hatton Heath-Prees	555.784 ± 0.034	556.51 ± 0.09*	-0.726 ± 0.095	1.00131 ± 0.00017

* Standard errors: all other errors are standard deviations.

** Predicted error from the least squares adjustment.

If the factor deduced from the HHP calibration line measurement, which is the line now preferred by IGS, is used for the network adjustment, there are now statistically significant discrepancies with local NGRN stations; eg, Edinburgh-Hawick 1.50 $\pm$ 0.53 gu

Edinburgh-Hexham 1.68 $\pm$ 0.47 gu.

Therefore, in spite of their apparent good quality, the calibration line measurements have been ignored and the manufacturer's calibration tables were used throughout.

Without further investigation, the calibration discrepancy cannot be explained: it may be due to non-linearity of the meter scale, or perhaps to a change or error in one of the national calibration lines.

CHAPTER IV

THE BOUGUER GRAVITY ANOMALY MAP AND CONTOURING ROUTINES

4.1 Introduction

This chapter deals with the construction and description of the Bouguer gravity anomaly map and its correlation with the geological map of the area. Also, an attempt was made to compare different contouring routines and a regional-residual separation of the gravity map in terms of simple or orthogonal polynomials.

4.2 Bouguer Gravity Anomaly Map

4.2.1 Construction

After the least squares base station adjustment of the network, the adjusted values of the bases were used as a control to rerun the gravity data using a different version of GRAVØ1 and a suitable output was obtained - with the reference number, co-ordinates and value of each gravity station - as an input to the contouring routines used to plot the data. Various contouring routines were used, described below, in paragraph 4.3, which generate a regular grid of values from the irregularly spaced gravity data, the spacing of the grid interval playing an important role in the more realistic representation of the gravity map. Figure 4.1 shows the gravity data plotted by the General Purpose Contouring Program (GPCP) of the CALCOMP package with a grid interval of 1.5km. Figure 4.2 shows the same gravity data, plotted with a grid size of 2km, superimposed on the geological map. All the Bouguer gravity anomaly maps mentioned above were compiled with a

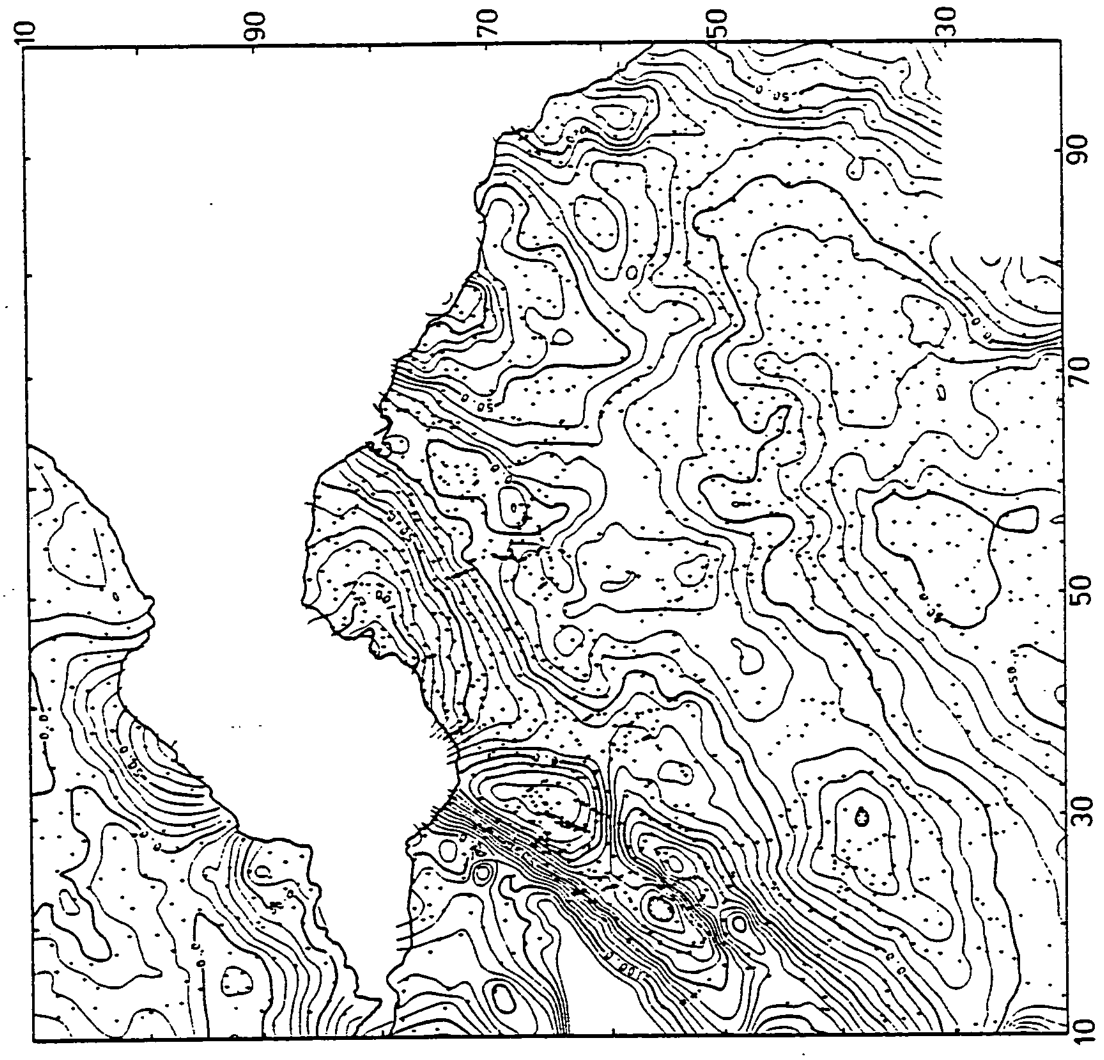

Fig. 4.1 Bouguer gravity anomaly map. Contour interval 10 gu. Plotted by GPCP using 1.5km grid size. Crosses represent gravity stations.

Fig. 4.2 Bouguer gravity anomaly map superimposed on the geological map.

50
100
-50
50
-50
SELKIRKSHIRE

Bouguer density of 2.67 g/cc.

Also, it was decided to incorporate marine data by digitising the offshore contours produced by Tully and McQuillin (1978). These are shown in figure 4.3 with a better representation of them in figure 4.9.

4.2.2 Description and correlation with the geology

Considering the features of the gravity map (figure 4.1) over the study area, there are positive and negative closures associated with different geological formations.

Starting with negative gravity anomalies, the most predominant feature of the gravity map (figure 4.1) is the gravity low which runs SW-NE over the Lower Palaeozoic rocks of Ordovician and Silurian greywackes, reaching values of -50 gu over the Tweeddale area, -40 gu over the Lauderdale area and -110 gu over the area of Cockburnspath. This long wavelength negative gravity anomaly is the subject of study in Chapter V, where it has been interpreted as being caused by a granite batholith underlying this area. To the north-west of Lauder, there is an offset and widening of the main negative feature caused by the superposition over the Lower Palaeozoic rocks of the Upper Old Red Sandstone sediments. The main negative anomaly is also enlarged by the Calciferous Sandstone series and Upper Devonian sediments of the Cockburnspath-Oldhamstock basin in the north-east of the area. These basins are discussed in detail in Chapter VI.

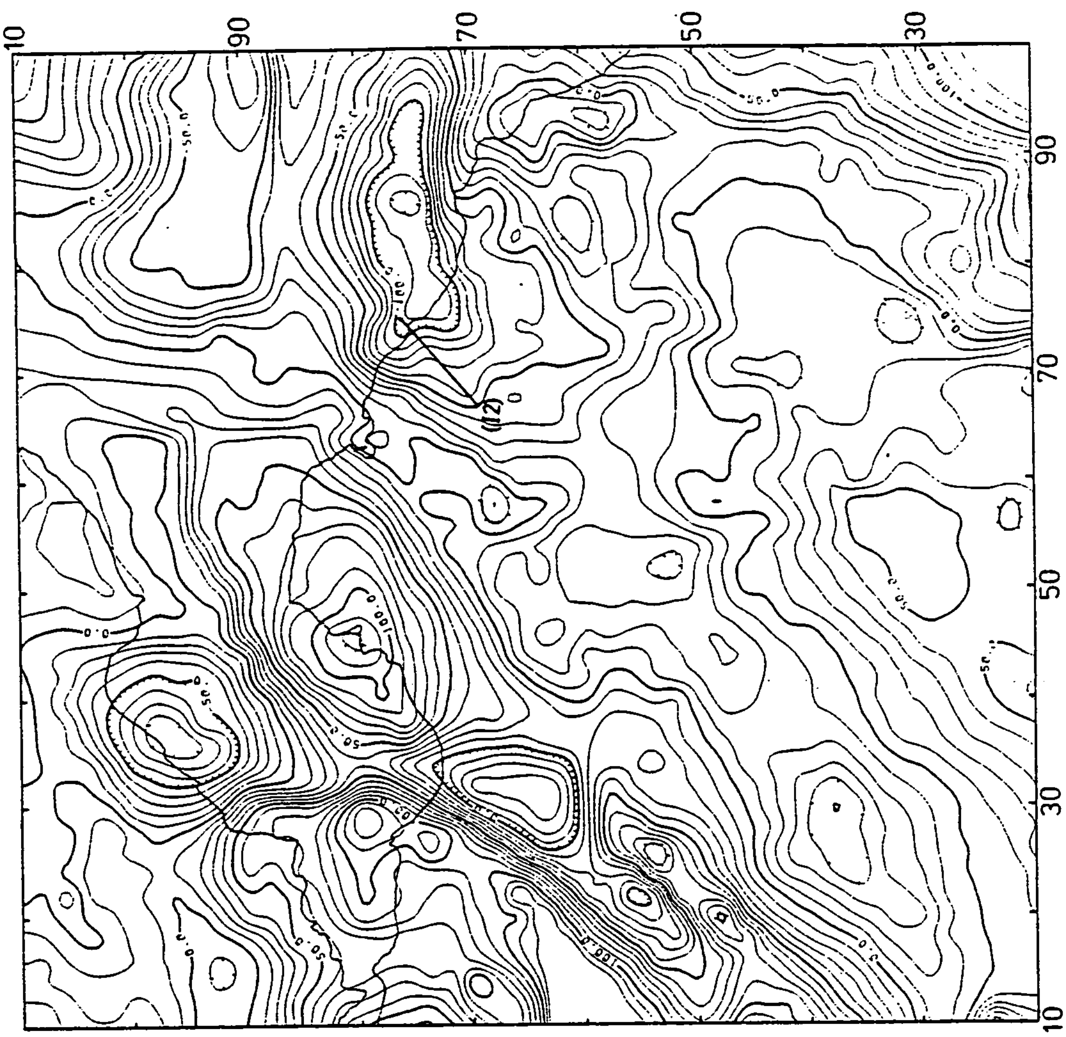

Figure 4.3 Bouguer gravity anomaly map compiled with marine data (Tully and McQuillin, 1978) and plotted by CALCOMP-GPCP at 10 gu in grid size 2km.

The second in size of the large negative gravity anomalies is the one associated with the Leven Coalfield with another marking the Midlothian Coalfield. The gravity map suggests that the Leven Coalfield on the western coast of the Firth of Forth is continuous under the sea, covering an area almost the same as on-shore; it is characterised by a large (at least -70 gu) negative gravity anomaly. The Midlothian Coalfield is clearly correlated with a low of -30 gu amplitude and it appears, probably mis-leadigly, from figure 4.3 that it does not continue far into the Firth of Forth.

There are also some other small negative gravity closures on the gravity map (figure 4.1) which are associated with the Devonian basins at Kinross and Eyemouth. The Devonian basin at Eyemouth is discussed in detail in Chapter VI.

Considering the positive gravity anomalies of the gravity map (figure 4.1), there is a positive anomaly of relatively long wave-length over the East Lothian area with an amplitude of 120 gu at Aberlady Bay. A few stations along the seashore of Aberlady indicate anomalies of more than 120 gu and, in the author's opinion, the gravity field continues to increase offshore although its maximum amplitude probably occurs not far from the coast. All of the East Lothian area is characterised by a high with steep gradients of about 10-12 gu/km, towards the Aberlady region. It is suggested that the gravity maximum marks a volcanic centre in Aberlady Bay rather than at the Garleton Hills where there are extrusive trachytes and basalts of Lower Carboniferous age.

Comparing the gravity pattern with the aeromagnetic one (Bullerwell, 1968), figure 4.4, it is concluded that both gravity and magnetic positive anomalies are caused by a Lower Carboniferous basic volcanic centre around Aberlady Bay. This seems to be continuous under the Firth of Forth and is probably connected at depth with the Burntisland lavas through a narrow east-west volcanic belt, truncating the northern end of the Midlothian Coalfield and marking the southern boundary of the Leven Coalfield, something which has already been suggested by Francis (1961). Another possibility is that both the Coalfields are continuous under the Firth of Forth but their gravity effect is marked by a superimposed positive anomaly due to an E-W trending offshore volcanic belt.

The aeromagnetic map, figure 4.4, shows two positive extensions, perhaps due to a sill or lava flow to the north-east and north of the Garleton Hills, one forming a narrow belt, extending several kilometres north-eastwards into the North Sea, while the other one to the north, suggests a small feature, confidently identified as a sill of relatively small vertical thickness (Gunn, 1972). This idea is supported by a small island (Island of May, NT 6699) to the north, which has been marked in the geological map as basalt. As has been suggested by Gunn (1972), the narrow magnetic belt to the north-east of Dunbar may be caused by ophiolitic material, as it lies along the offshore extension of the Southern Uplands Fault (Lammermuir Fault), although there is no clear gravity support in this case.

In the East Lothian area there is also a minor elongated gravity high south-west of Traprain Law (NT 6277), which appears to be

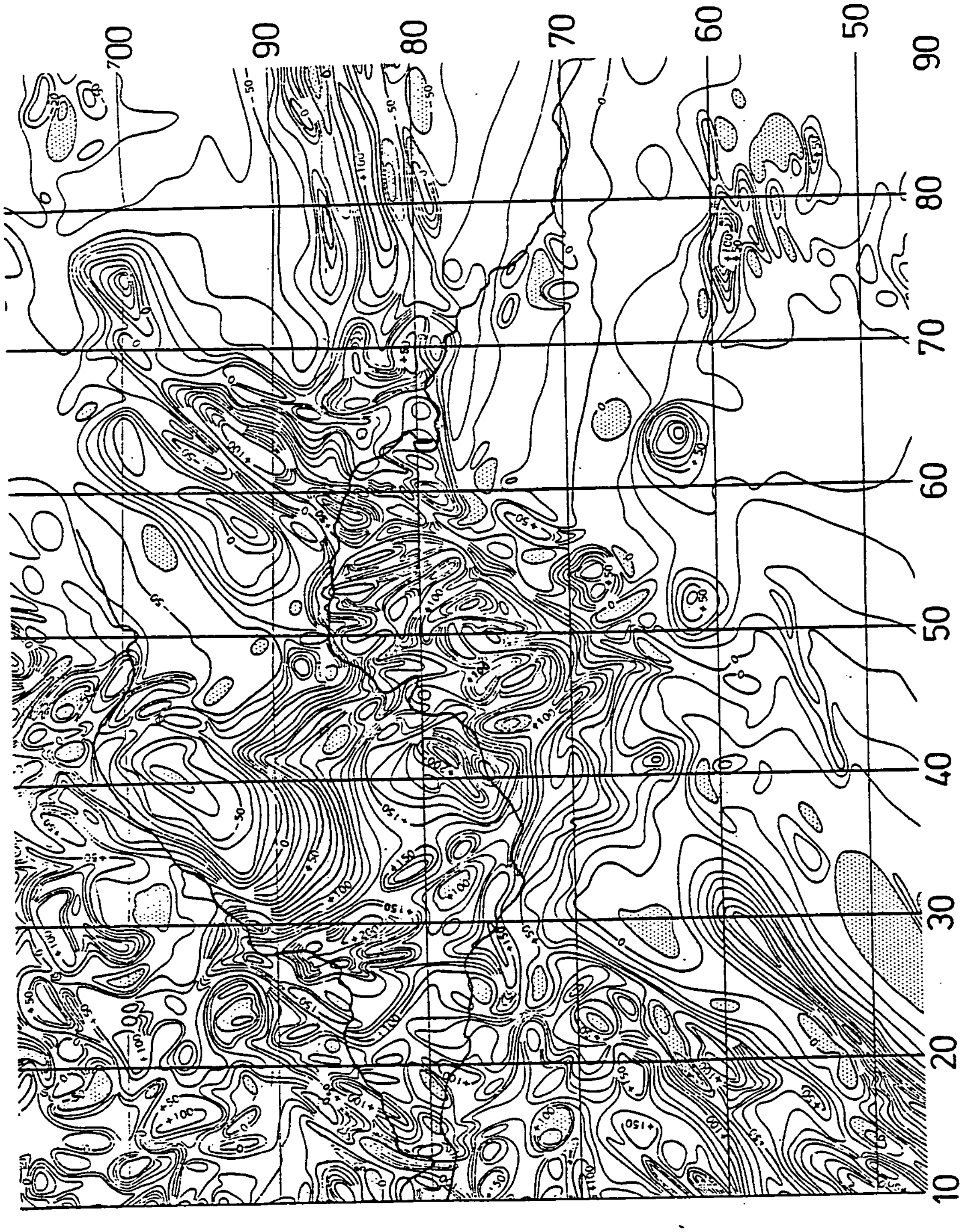

Fig. 4.4 Aeromagnetic map; part of Sheet 11 (after Bullerwell, 1968). Contour interval 10 nT.

correlated with the phonolite intrusion. It is also associated with a large positive magnetic anomaly, as has been shown by the ground magnetic traverses of the vertical component of the earth's field by Bennett (1969). From those studies it was concluded that there are more intrusions to the south-west of Traprain Law, apart from the basalts and trachytes extrusives of Lower Carboniferous age marked on the geological map. The intrusions, which are delineated by the small elongated gravity high (figure 4.1), are caused by basic material, probably of Carboniferous rather than of Permian age (Bennett, 1969).

Going to the western part of the study area, the gravity and aeromagnetic pattern also suggest by their continuity that all the numerous dolerite intrusions around the Edinburgh area and to the west and north-west of it have the same origin and are connected at depth. This belt of high gravity is similar in form to the upward continued aeromagnetic pattern (figure 4.5). The positive aeromagnetic anomaly connects with others to the west, north-west and south-west of the Edinburgh area and is the north-east part of a major feature which dominates the whole of the Midland Valley.

Recent gravity work on the western part of the Midland Valley (Alomari, Geology Department of Glasgow University, person. commun.) shows that there is a gravity high running from the Island of Arran, a Tertiary igneous centre, through the Clyde Plateau lavas to the Bathgate region, where the largest positive gravity and magnetic anomalies over the Midland Valley and Southern Uplands are met, and from there to the Burntisland-Aberlady area. The Arran intrusion is much younger than the other features and not genetically related to them.

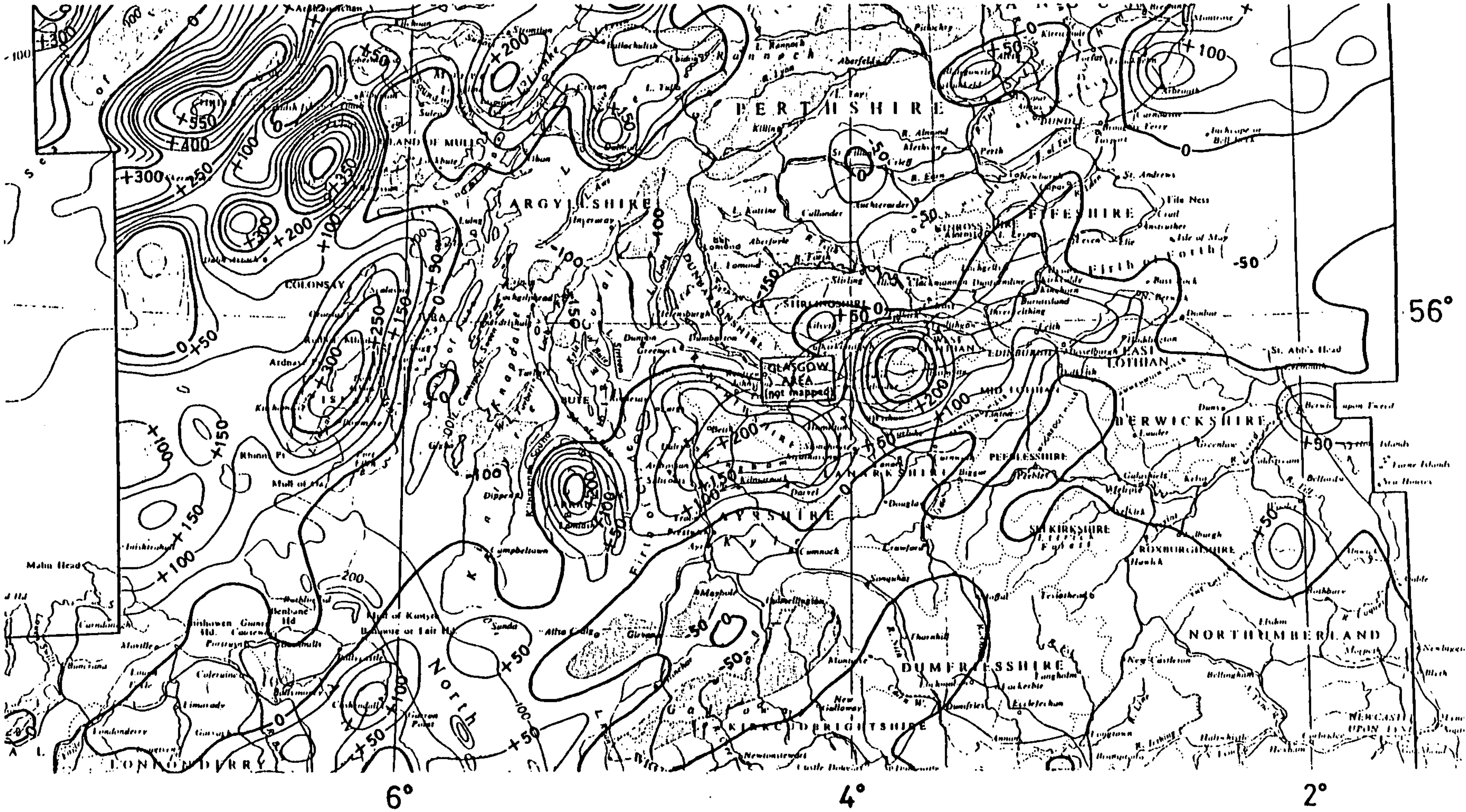

Fig. 4.5 Smoothed aeromagnetic map (after Hall and Dagley, 1970).

In the southern part of the study area, the gravity high of 50 gu near Selkirk and Melrose is discussed in detail in Chapter V. At this point it should be noted that the western flank of the Upper Old Red Sandstone basin of the Lauderdale area lines up with the 50 gu contour in Selkirkshire, and the relatively steep gradient east of Melrose, is perhaps indicative of a fault with relatively small dimensions.

In Berwickshire there is a steady decrease of the gravity field south-eastwards towards the Cheviot suite of the granite exposure.

Major and minor fault components exist in various parts of SE Scotland. The Leadburn Fault, the north-east component of the Southern Uplands Fault, is associated with a narrow elongated belt of gravity and magnetic highs. This was interpreted (Gunn, 1972) as due to ophiolitic material emplaced at depth during the Caledonian earth movements and closure of the Iapetus Ocean.

Steep gravity gradients correlated with the Roslin-Vogrie Fault system and the Pentland Fault which bound the Midlothian Coalfield to the south and west respectively, confirm that they are major features with a relatively large throw. From the offshore extrapolation of the gravity field north of the Midlothian Coalfield, the anomaly due to the Pentland Fault does not continue very far into the Firth of Forth and terminates where the offshore northern (faulted?) boundary of the Midlothian Coalfield is.

The Eyemouth Fault, marking the south-eastern boundary of the Eyemouth Old Red Sandstone basin is an unexpectedly strong feature in contrast to the Lammermuir and Dunbar-Gifford Faults - probable components of the Southern Uplands Fault system to the north-east, which are not associated with any significant gravity gradients. These faults are discussed in detail in Chapter VI.

4.3 Automatic Contouring Routines

The routines which produce contour maps are generally divided into three categories, which will be discussed below.

The first is that a rectangular grid is superimposed over the map area and a value assigned at each grid point. For this stage, estimation techniques vary widely. They usually consist of selecting a number of neighbouring data points and then calculating a weighted average from them, after choosing a weighting function which gives less weight to more distant points. Once the grid values are obtained then straight or curved line segments are drawn by conventional methods for a desired contour level by interpolation from the values at the corners of each rectangular unit.

The second technique consists of triangular structures. A set of irregular triangles is superimposed on the map area, each vertex corresponding to a data point. Once this network is constructed then the contouring procedure is straightforward. This method is rarely used nowadays.

The third category is the so-called 'universal kriging.' This is an estimation procedure developed as an alternative mean of grid generation. It is an empirical observational theory originated by D G Krige in the estimation of ore problems (Krige, 1966). Later, G Matheron expanded Krige's estimation methods introducing the theory of generalised variables, in which a complete error estimation theory was also developed.

Because universal kriging is associated with a large and a very complicated mathematical analysis, it will not be described here; a review by Olea (1975) is recommended as a further reference. It was considered necessary to mention it because universal kriging overcomes all the disadvantages appearing in weighted average techniques (which are highly empirical, non-optimal, etc) and trend surface analysis. It is an exact interpolation procedure which can also take into account the volume which data observations may have, providing an error estimate at all generated grid points too.

SURFACE II graphic system (Sampson, 1975) is a Fortran-IV package in which the universal kriging technique has been applied. This package has been implemented at the Rutherford Laboratory, but it was impossible for the author to have access to it.

There are essentially two problems appearing with the first technique of using a grid superimposed over the map area. The first is the definition of the weighting function. Frequently, it has the form of $1/d^n$, where d is the distance of the data point from the point whose value is to be determined and n equalls to 2 or, rarely, 3 etc.

In other cases the weighting function has a different form varying from package to package. Those routines applying weighting functions often suffer from having singularities or inflections at the data points. The second difficulty eventually occurs in the definition and collection of the neighbouring data points. Testing and collection of data points is one of the most time-consuming operations on a computer, particularly when the grid is to be generated from irregularly spaced data. Again, at this point different methods are applied. One uses a constant "search radius" which takes into consideration those data points which fall within the region defined by a circle centred on the grid point or, by another method, defining neighbouring points as a standard number of the closest data points.

For the production of good quality maps the determination of the grid size is of great importance and it is recommended that the grid size should have a value close to the average spacing of the data points. Then the next, not so critical, action is the determination of the number of the neighbouring data points or the size of the search radius, although, from the author's experience, the latter mainly affects the degree of smoothing, depending on the weighting function used.

In the case of imposing triangles on the data points, the user does not have much opportunity for personal judgement, and the quality of the map depends mainly on the distributions of the data points. If they are evenly distributed, then the shape of the triangles is not so irregular and distortion and local irregularity of the contours is avoided.

In these three techniques for contouring irregularly-spaced data, the non-uniqueness of the problem is obvious. However, this is of less importance when the user is contouring a large amount of data, where the use of the machine becomes necessary. Eventually the cost of an automatically contoured map is competitive with that of a manually contoured map and the variability and inconsistency involved in manual draughting are mostly avoided.

Since in Edinburgh there was access to some very modern contouring packages, the production of automatically contoured gravity anomaly maps by the implementation of those packages was considered advantageous at once. One of the most significant benefits was the possibility of updating maps at a low marginal cost.

Most of the author's needs were covered by the use of the CALCOMP's (1973) GPCP implemented in ERCC. Another routine, TRIANG, used at the beginning, was based on a triangular data structure and developed by C Gold, Geology Department, University of Alberta. It was implemented in the Geophysics Department of Edinburgh University and a modified version of it by the author, was used. Also, the SACM package (Surface Approximations and Contour Mapping) available by NERC at Rutherford Laboratory was tried.

Swain (1976) published a program which interpolates irregularly-spaced data onto a regular grid. The grid values are approximated by the smoothest surface which passes through every data point, applying Brigg's (1974) method of mimimum curvature. The implementation of this program was tried but it did not work, even adding the missing line in the published program (Swain, person. commun.). Minor corrections were made and the program ran successfully but without satisfactory results on real data. Similar corrections which were also made by Dr Sowerbutts (person. commun.) were tried without satisfactory results. Then, the attempts to run the program successfully were abandoned. Hopefully, Tobler's (1977) corrections will prove to be more effective.

4.3.1 CALCOMP's General Purpose Contouring Program (GPCP)

The grid-value generation as well as the weighting function applied to the neighbouring data points (NP) is described in CALCOMP's (1973) user's manual.

It was found that, choosing a small grid size and a large number of neighbouring data points (NP) is very time-consuming on the computer. The gravity data were run using a grid of 1, 1.5, 2km and NP = 18. This was done because the distribution of gravity stations over the map area is not even and these grid sizes reflect locally the average spacing of the stations. The maps are presented in figures 4.6, 4.1, 4.3. It appears that by increasing the grid size the contours become smoother and some of the local very small closures disappear with a larger grid size.

4.3.2 TRIANG Routine

This routine, written initially by C Gold, contours irregularly-spaced data. First a large triangle, big enough to enclose the

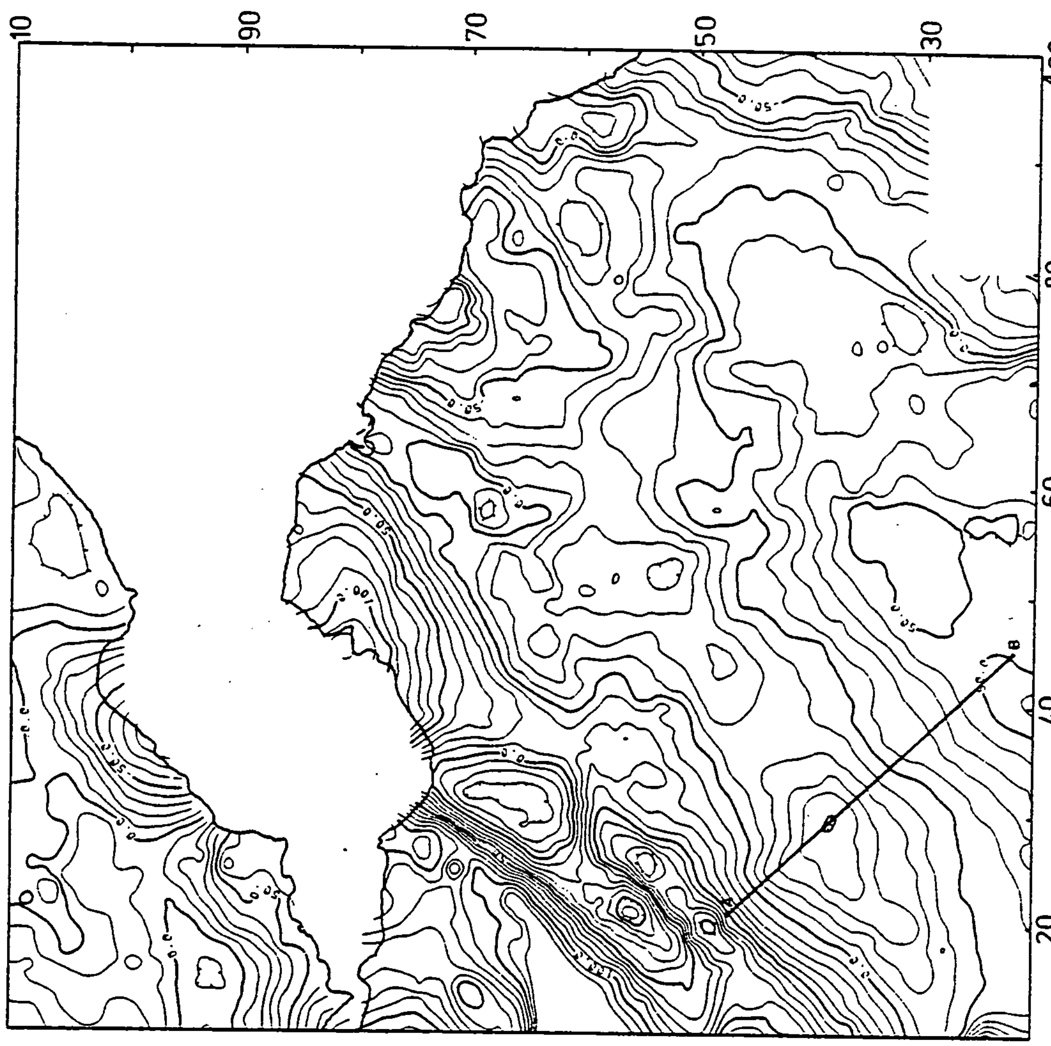

Fig. 4.6 Bouguer gravity anomaly map, plotted by GPCP with grid size of 1km at a contour interval of 10 gu; smoothing factor 15.

map area, is generated. Then, each data point, one at a time, is entered. Consequently, the big triangle is divided into three new triangles with the inserted point at a vertex of each triangle. This process continues until all the data points are entered. The resulting triangles, which are continuous over the map area, may not have a desirable shape. For this purpose, an optimisation routine checks each triangle against its neighbours to see if the quadrilateral thus formed should be divided the other way on the basis of minimising the length of the dividing line. This has an effect of reducing considerably the number of sharp triangles. As is obvious, this procedure is very time-consuming.

The program was modified so that the triangle structure is plotted and, therefore, the sharp triangles can be identified. By interfering, their shape can be changed, locally, or, more effectively, some data points can be omitted altogether. This was not always found effective depending particularly on the distribution of the adjacent data points; for example, it was ineffective along dense profiles.

Part of the area was plotted using the TRIANG routine and the map is shown in figure 4.7.

From the experience of using this routine, the following conclusions may be drawn:

1. It is a very slow and expensive routine and, therefore, not satisfactory.

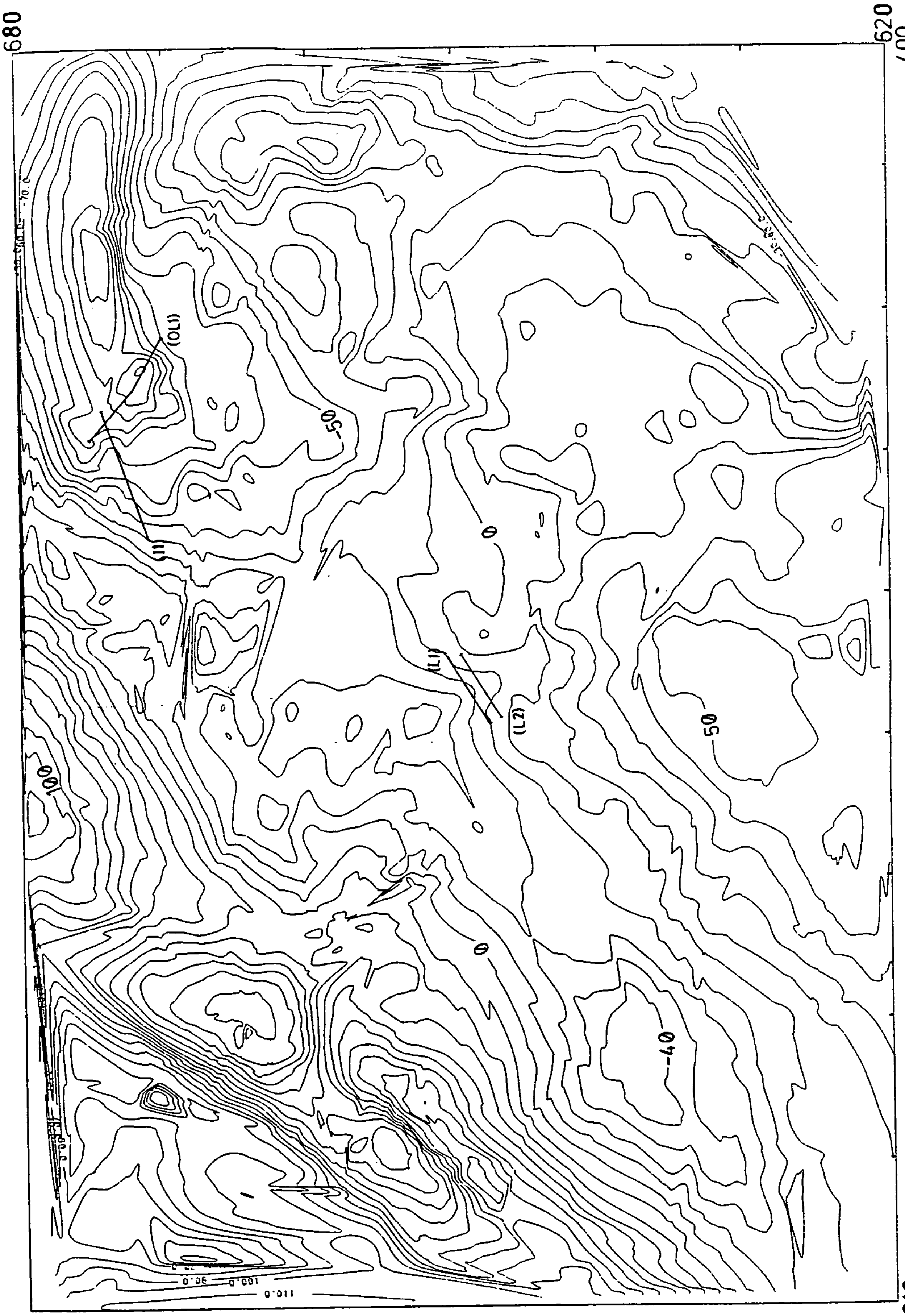

Fig. 4.7 Bouguer gravity anomaly map plotted by TRIANG at 10 gu interval.

2. It is recommended for a small number of data points, but not for a large number.

3. If no other contouring routine is available, then the contouring map should be retraced, applying visual smoothing where the contours have been distorted by sharp local triangles.

4. The map is satisfactory where the data point distribution is even.

In figure 4.8, the station distribution in the eastern Berwickshire, the Merse and generally the south-eastern part of the study area is quite evenly spaced and therefore the contours, except in some local places, have a satisfactory appearance. In places where the area is densely covered (Midlothian) or where dense gravity profiles are present, the program almost fails in the plotting procedure, besides the fact that it becomes extremely slow and expensive. This was the reason why many of the stations in the Midlothian area were omitted. Some of the dense profiles were deliberately left untouched, for instance, the profiles along the Lammermuir Fault and Dunbar-Gifford Fault, so keeping their effect on the contours.

4.3.3 SACM

SACM is one of the very modern contouring packages (as is SURFACE II), which is available to Science Research Council (SRC) users by NERC and implemented at the Rutherford Laboratory.

From Edinburgh there is access through the Institute of Geological

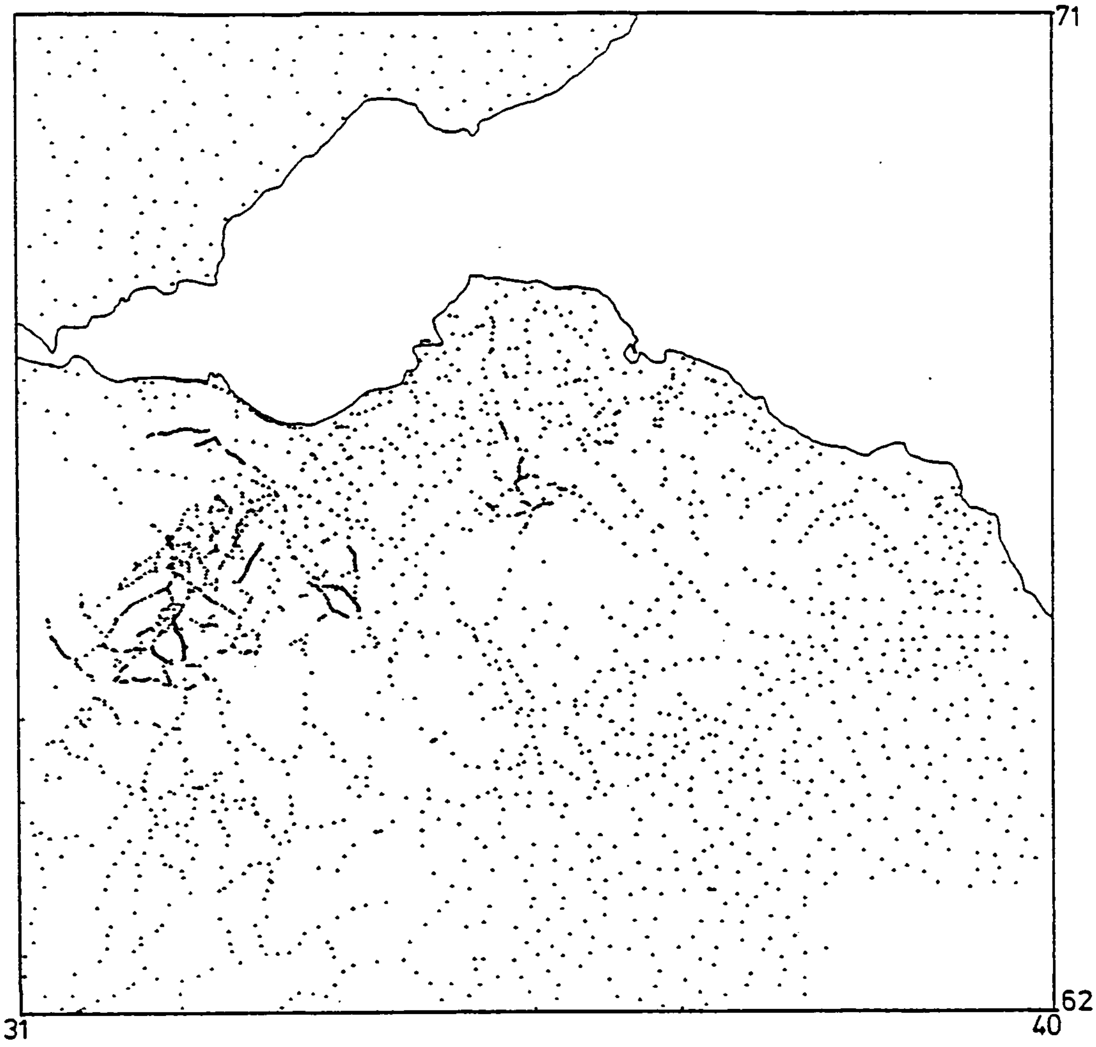

Fig. 4.8 Gravity observations over the SE part of Scotland and Borders region.

Sciences. It was possible to contour the gravity data using this package and, as it is described below, to produce trend surface maps since that facility is also provided by the package.

Apart from a manual for running the package, no description of the algorithm of SACM was available, as occurs with most commercial contouring packages whose algorithms have not been made public. Therefore, the data structure and interpolation function used for SACM are unknown.

The gravity data plotted by the SACM package are presented in figure 4.9. No smoothing was applied. The similarity of the map when compared with the map plotted by GPCP with the same grid interval (figure 4.3) is remarkable. SACM approximates the off-shore digitised contours in a better way than GPCP. Also, the local closures produced by SACM are fewer than by GPCP, for example, along the broad high near the Southern Uplands Fault.

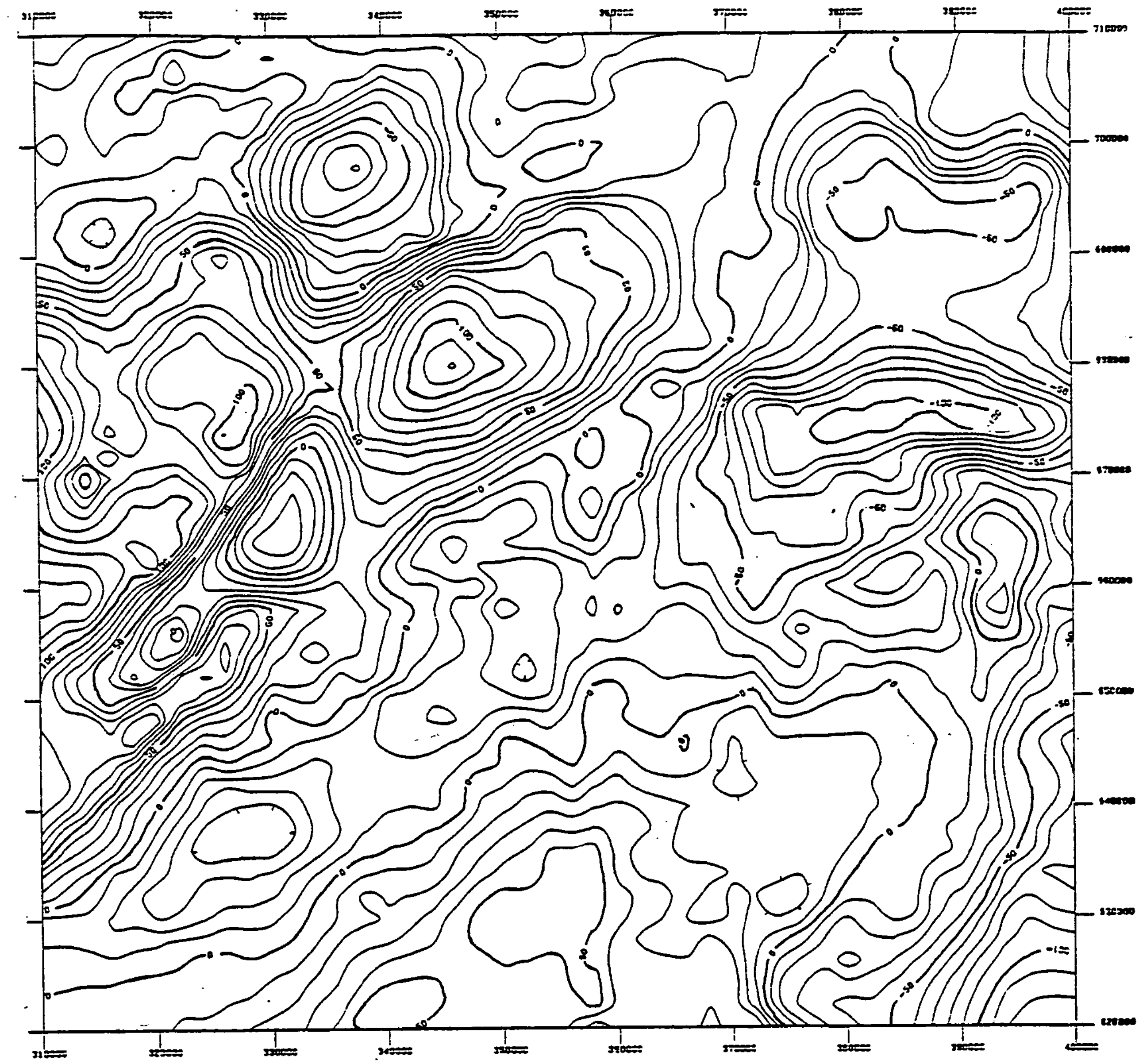

Fig. 4.9 Bouguer gravity anomaly map plotted by SACM; grid size 2km, contour interval 10 gu.

4.4 Regional-Residual Separation

In practical situations, gravity anomalies from sources at different depths and different horizontal scales are superimposed. To interpret any one of them, it must be separated from the others. One approach is to postulate the other structures or to determine them by a different technique and then subtract their calculated attraction as a regional field; another makes use of the different wavelength characteristics of deep and shallow sources, hoping that the shorter wavelength residual anomalies left after the longer wavelength "regional" anomalies have been removed properly reflect the local structure under investigation.

As an example of the first approach, the calculated attraction of the LISPB seismic model was removed for the interpretation of the anomalies due to the granite batholith in the Southern Uplands (Chapter V). In this section, examples of the second approach are considered even though, in the end, not much use was made of it.

Apart from the graphical and smoothing methods, techniques have also been developed using digital computers by filtering, by using the second derivative method and by fitting trend surfaces described by orthogonal or non-orthogonal polynomials.

Many algorithms producing trend surface maps from regularly or irregularly spaced data have been developed during the last few years, using orthogonal or non-orthogonal polynomials. There is quite an extensive bibliography on this subject, here exemplified by a recent algorithm produced by Whitten (1974).

It uses orthogonal polynomials applied to irregularly spaced data. Because Whitten's (1974) program seemed very impressive, its implementation was attempted on EMAS. Unfortunately, there were many errors, perhaps in typing, and it was impossible to compile it successfully. After a while this attempt was abandoned.

However, a picture of the regional-residual gravity field of the area was desirable. For this purpose, the SYMAP (1975) package was used for the picture of the regional field of different degrees. It fits monorthogonal polynomials by least squares to the data points. This package has been implemented by ERCC. The maps are obtained on a line printer; the trend surface maps are usually clearly readable but the same is not true for the residual maps, whose display on a line printer is difficult to visualise. Another disadvantage is that because the least squares surface is constrained only at each data point, the approximation by a certain degree surface is very poor in areas where there are very few data points, since the trend surface becomes very unstable away from data points.

In our area a contrast appears for the density of gravity stations on land and offshore, where only at 20 or 50 gu intervals contours (Tully and McQuillin, 1978) have been digitised. Because of that, the gravity field will not be approximated realistically. This was another reason why no SYMAP maps of the residual or regional field are shown.

Instead of SYMAP, the SACM package was used. There, from the data points a grid array is calculated and a least square fit using Chebychev polynomials is applied. Trend surfaces of first, second and third degree were made. They are shown in figures 4.10, 4.11, 4.12. It is clear from these figures that there is an eastwards decrease of the regional field. The gravity gradient varies from 0.9 gu/km for the linear trend to 1.25 gu/km for quadratic trend and 1.66 gu/km for third degree trend, always in a direction east-west.

Figures 4.13, 4.14 and 4.15 show the residual gravity field anomalies over the study area. In all three maps the general correlation with the geological features of the area is more or less the same. For example, the Midlothian Coalfield, the Aberlady high, the East Fife Coalfield, the Oldhamstocks sedimentary basin, the gravity low along the Caledonian Trend and the Melrose high are a few of the main features which appear almost the same in all three residual maps.

In the following chapters, where the interpretation of some of these features is presented, residual maps obtained by SACM will not be used for two main reasons:

1. A regular access to the SACM package was not possible.

2. Trend surfaces, because they are a pure mathematical abstraction, are usually without any physical or geological meaning; although the residual maps do show correlation with the geology, there is no better indication of the real amplitude of local anomalies.

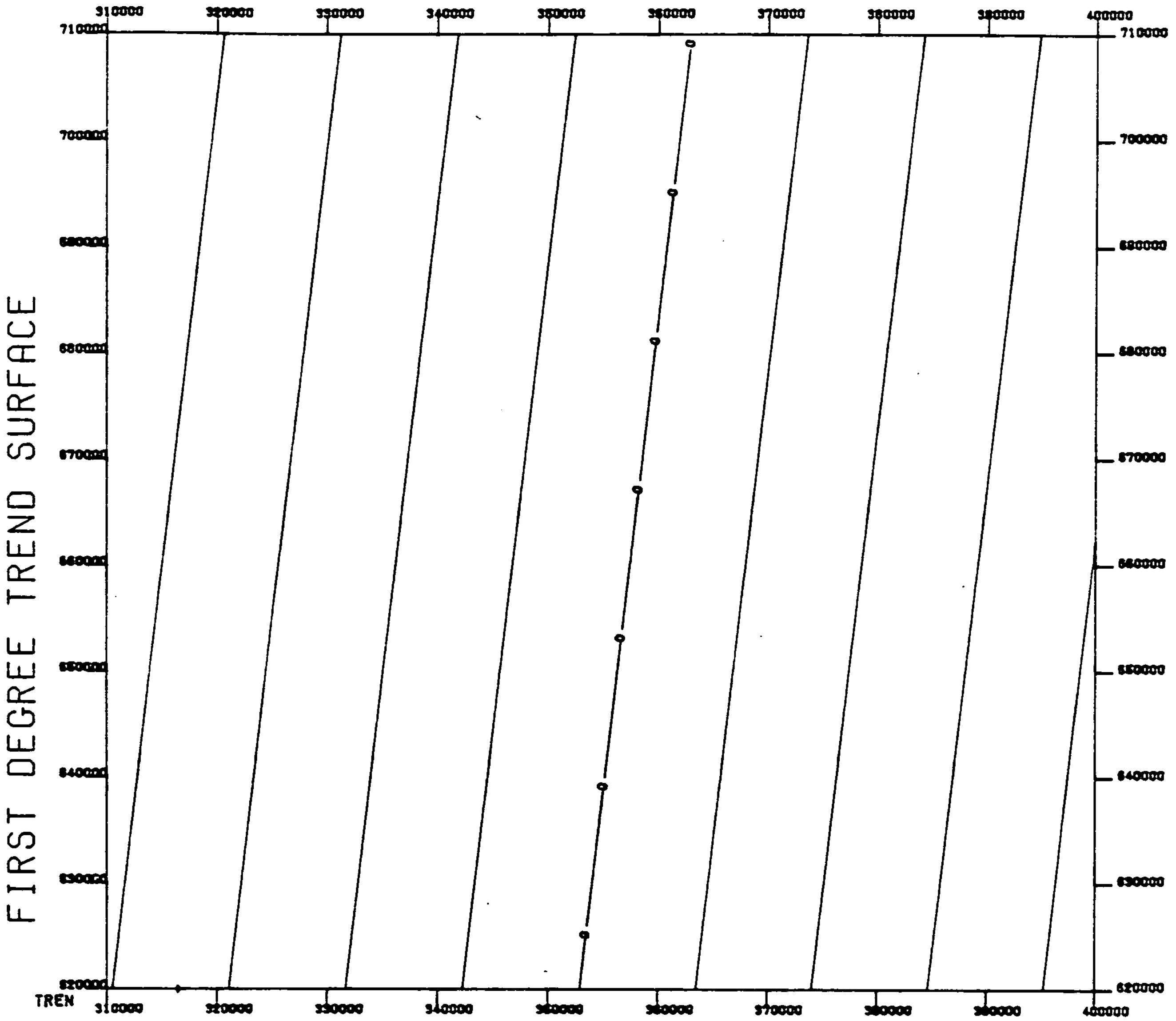

Fig. 4.10 First-degree trend surface of the gravity field of figure 4.9. Contour interval 10 gu.

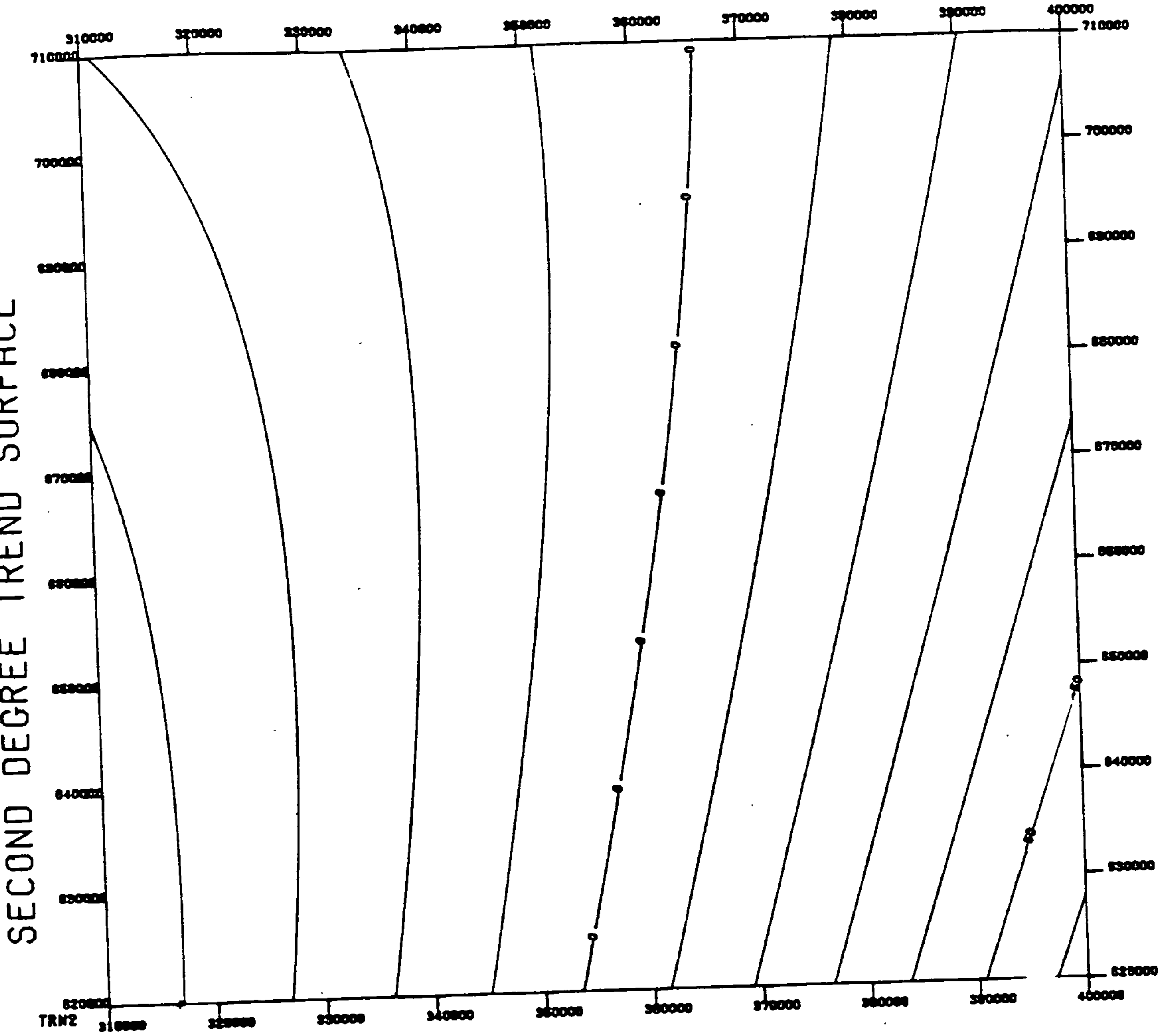

Fig. 4.11 Second-degree trend surface of the gravity field (figure 4.9); contour interval 10 gu.

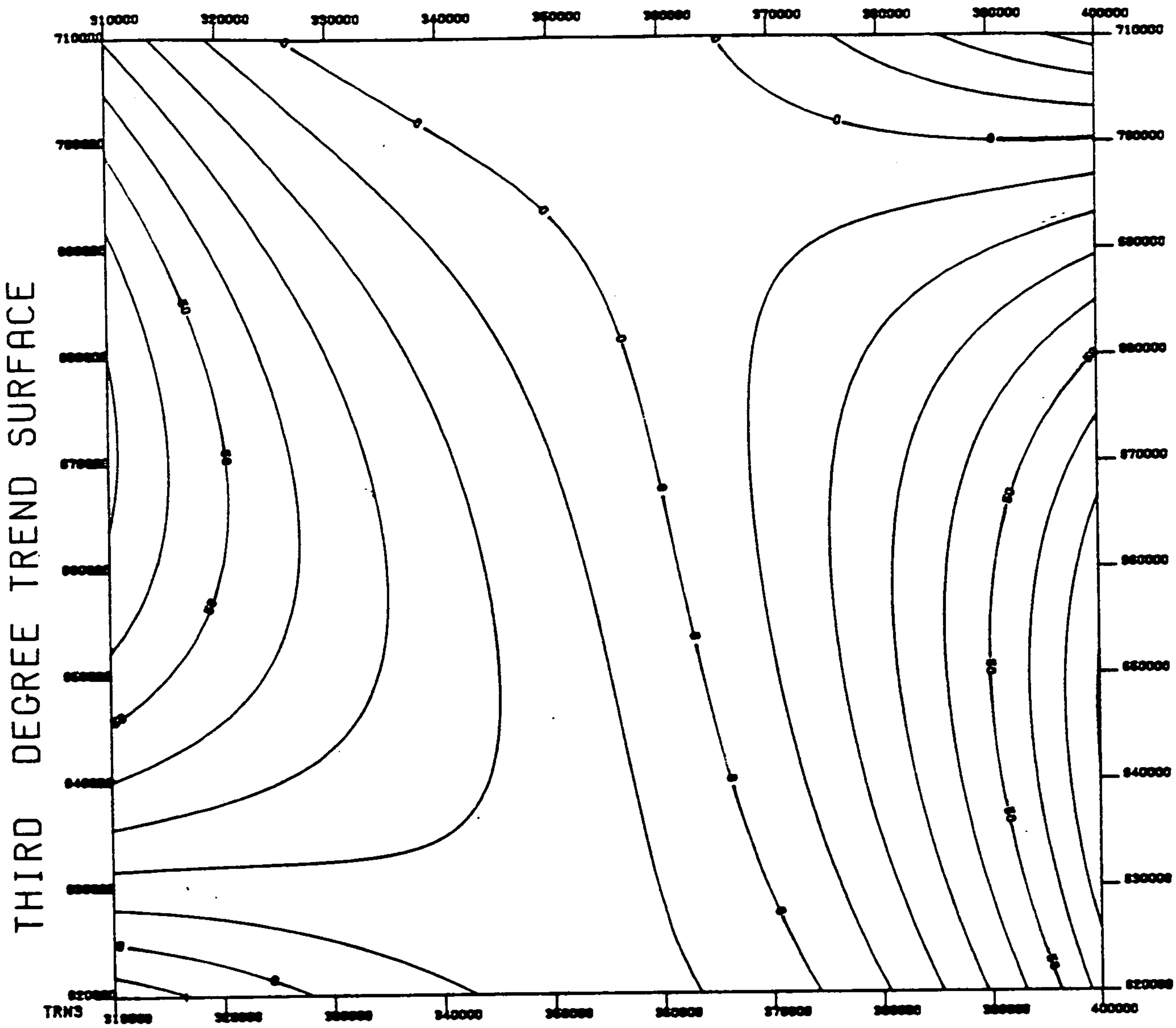

Fig. 4.12 Third-degree trend surface of the gravity field (figure 4.9); contour interval 10 gu.

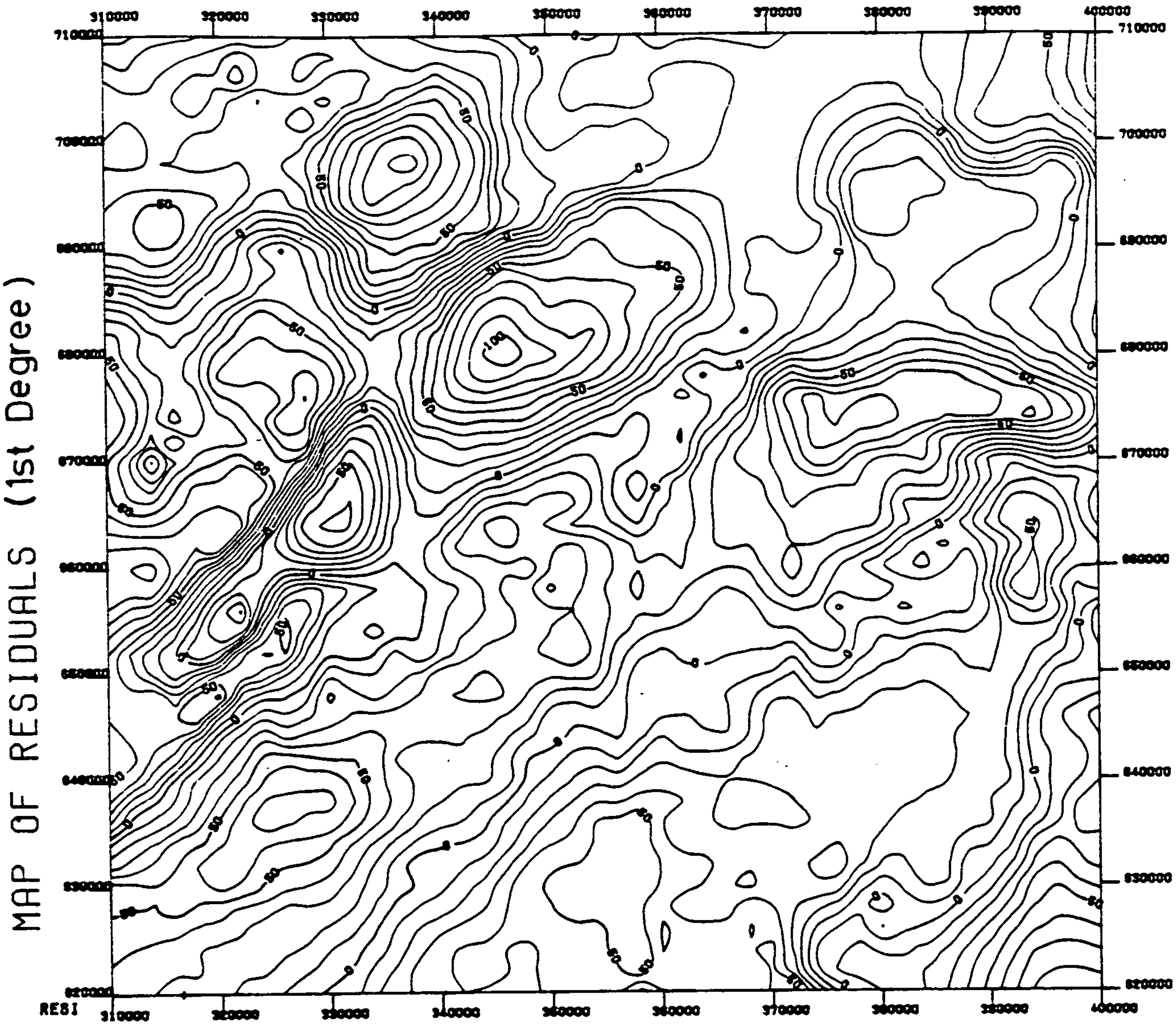

Fig. 4.13 First-degree residual Bouguer gravity anomaly map. Contour interval 10 gu.

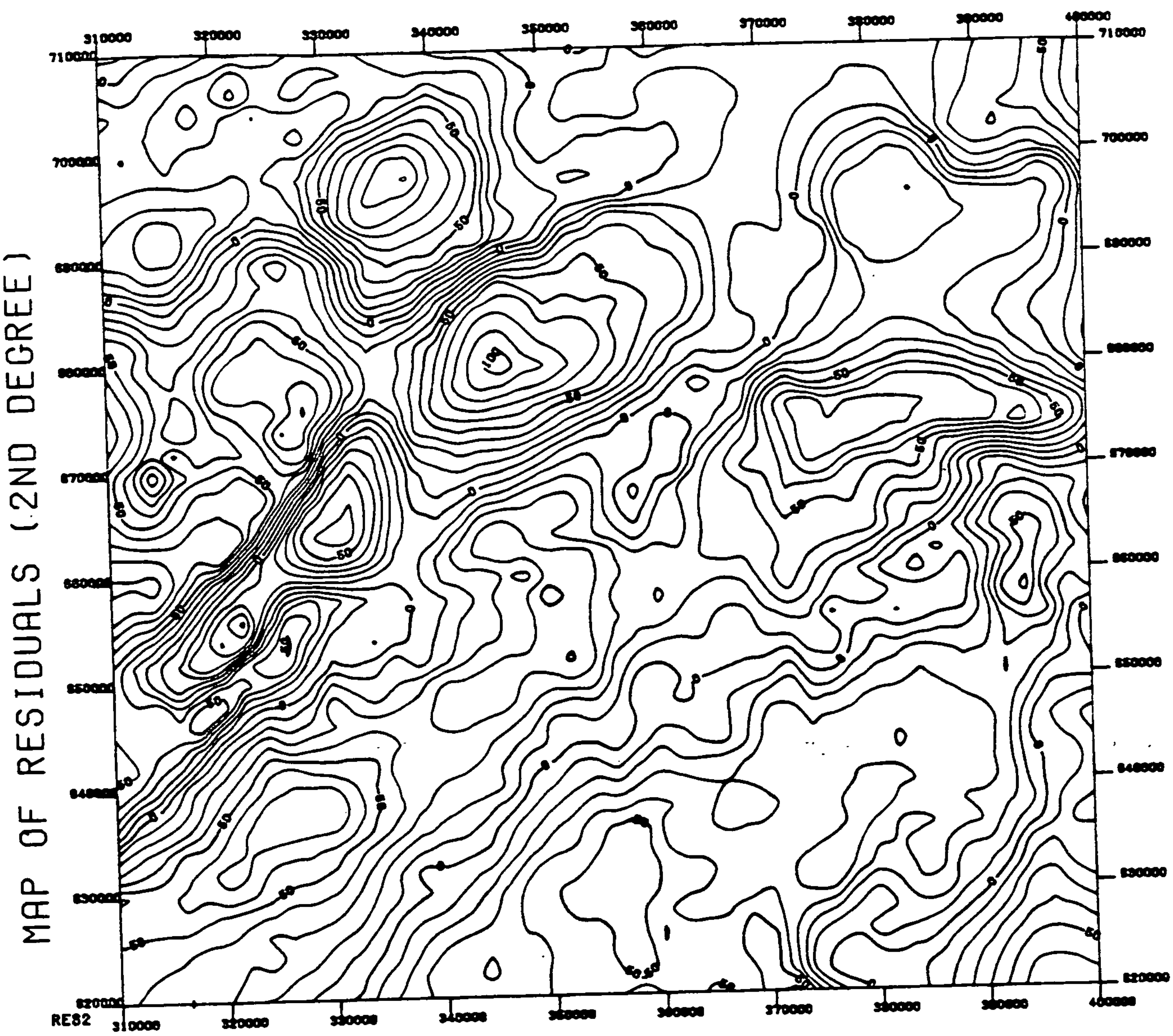

Fig. 4.14 Second-degree residual Bouguer gravity anomaly map. Contour interval 10 gu.

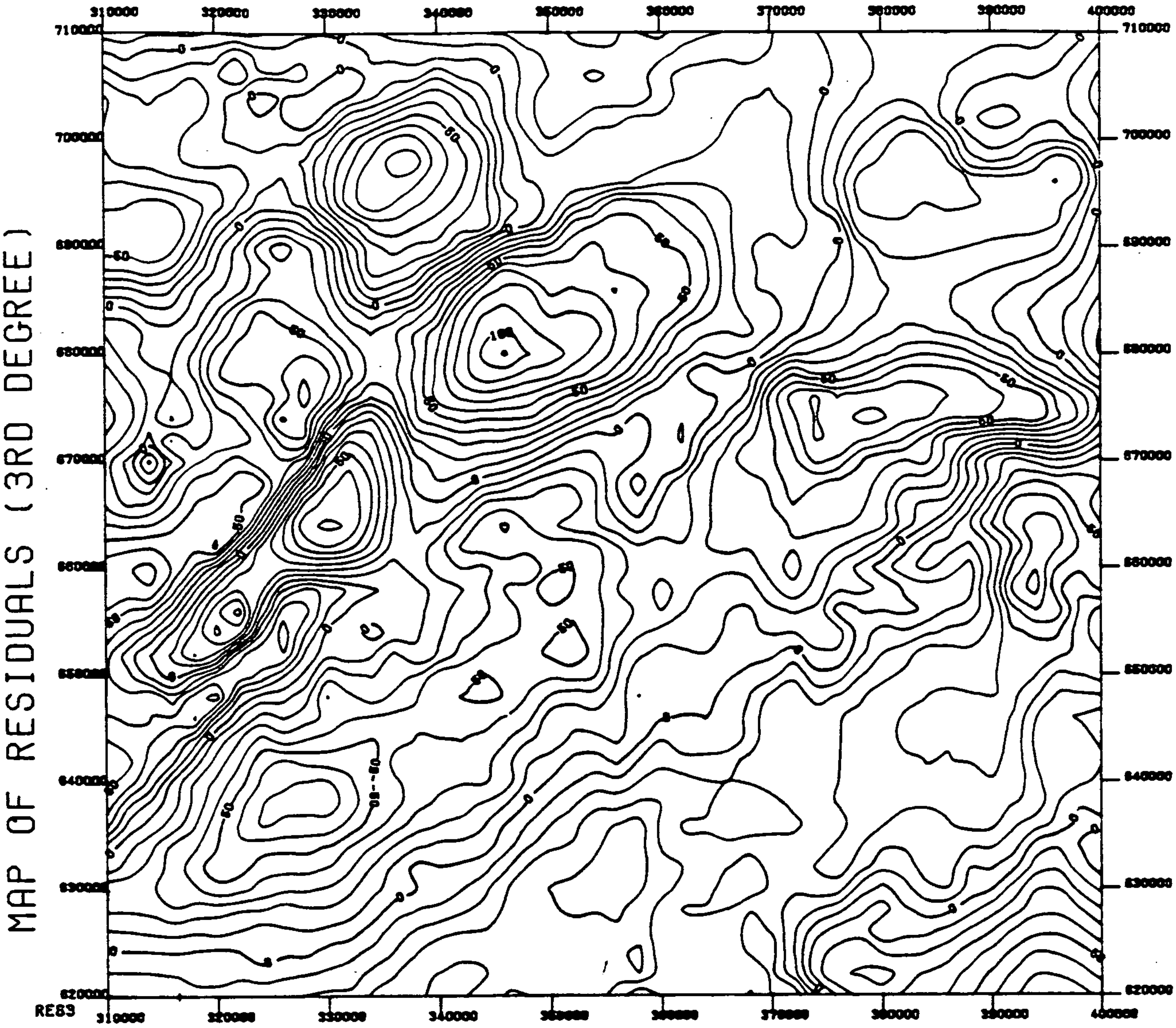

Fig. 4.15 Third-degree residual Bouguer gravity anomaly map.
Contour interval 10 gu.

CHAPTER V

GRANITES AND OTHER DEEP IGNEOUS INTRUSIONS

5.1 Introduction

This chapter deals mainly with the regional interpretation of the long-wavelength gravity anomaly which runs SW to NE parallel to the Caledonian trend, along the Southern Uplands. The latter is interpreted as being due to a large granitic intrusion underlying the area and a detailed modelling attempt was made over the District of Tweeddale. The interpretation of some of the other features of the gravity and aeromagnetic map over the rest of the NE part of the Southern Uplands is also discussed.

5.2 Tweeddale (Peeblesshire)

5.2.1 Brief geological account

Nicol (1843) first described the geology around the County of Peebles in the last century. The surface geological exposure to the SE of the Southern Uplands Fault is relatively uniform (see figure 5.1a); the Ordovician greywackes and shales form part of the SW-NE trending Northern Belt (Walton, 1965), and are followed to the south by similar Silurian sediments (Central Belt). Walton (1955) has made a detailed study of the Silurian greywackes over that region.

Within the Lower Palaeozoic and particularly within the Ordovician, there are the occasional small lenses of black shales and radiolarian cherts. Ashes of Caradocian age are met at Hamilton Hill and Winkston Hill, just north of Peebles, with thicknesses of 45m and 100m respectively (Ritchie and Eckford, 1931), while pillow lavas of Llandeilian age occur in the Northern Belt near the Southern Uplands Fault. The most predominant of the sporadic small igneous intrusive features are the numerous felsite and porphyrite veins in the greywacke strata. Their dimensions vary from 1 to 30ft, but others occur in much larger dimensions (Nicol, 1843), sometimes forming whole or part of a mass of a hill, notably the porphyritic exposures at Priesthope Hill (NT 3540) and at Juniper Craigs (NT 2536). Nicol (1843) has estimated the total thickness of the porphyritic sheets over that area and reported a number of 200-250m.

There are also boulders of granite in the nearby drift - Kailzie Hill (NT 2836), Kirnie Law (NT 3539) - believed to be locally derived (Gill, person. commun.). These outcrops can also be seen on the Geological Survey map (Sheet 24).

5.2.2 Residual Bouguer gravity anomaly map

All the gravity stations in the Tweeddale area were used for the construction of the Bouguer gravity map (more specifically, stations falling within the 10km National Grid squares NT 12, NT13, NT14, NT22, NT 23, NT 24, NT 32, NT 33, NT 34, and part of the NT25, NT 35, NT 45).

Since the geology to the north-west of the Southern Uplands Fault is not uniform and in order to avoid taking the Devonian sediments and the andesitic lavas to the north-west of the Southern Uplands Fault into account in the modelling procedure, it was decided to rotate the boundaries of the data through 45°. The map is presented in figure 5.1. The Southern Uplands Fault runs parallel, just 1km off the upper margin of the map. The

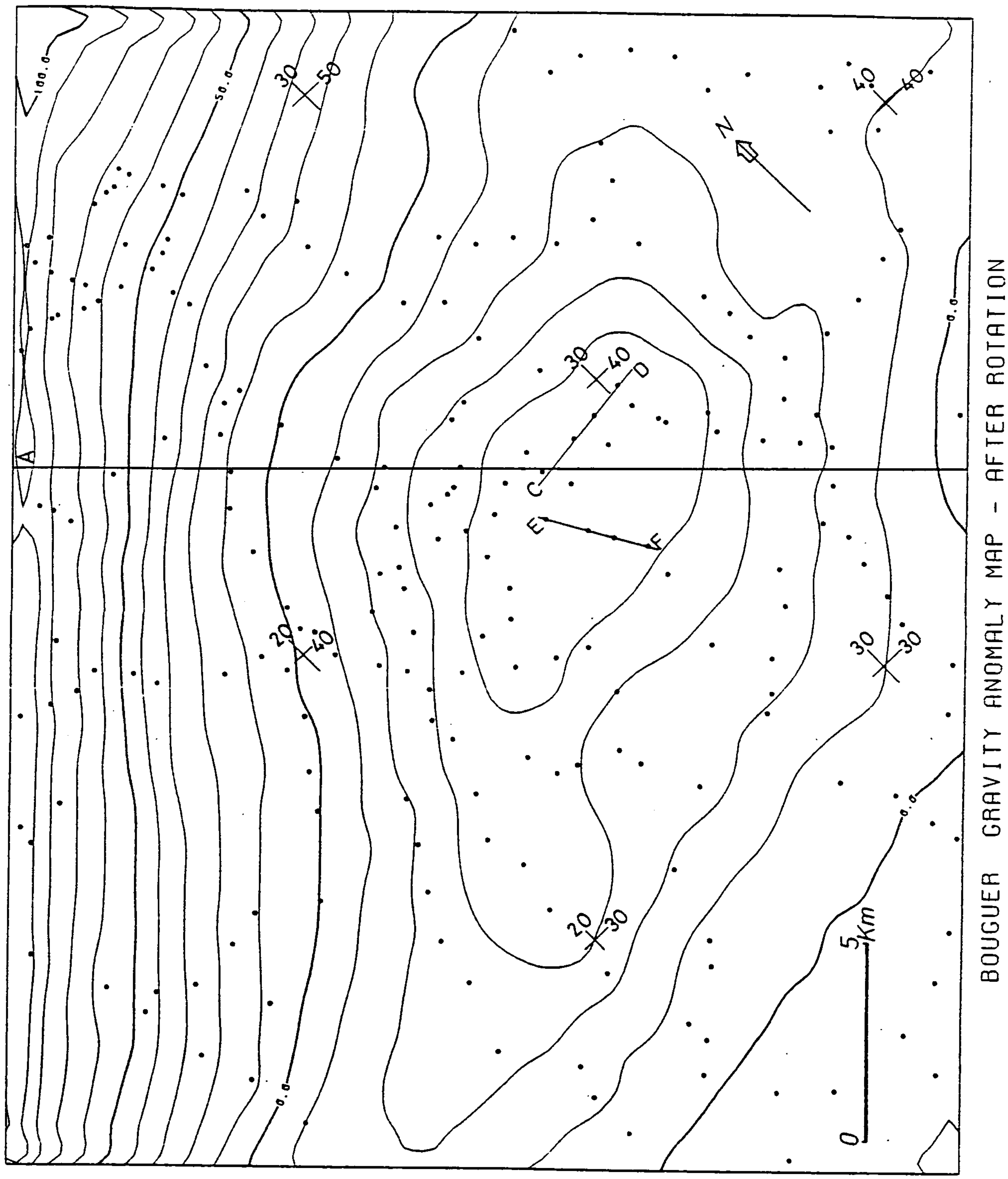

Fig. 5.1 Bouguer gravity anomaly map of Tweeddale area and gravity station distributions (circles). Line from NW to SE represents the beginning of profile AB. Contour interval 10 gu. EF & CD represent lines along which 3-point depth rules were applied (equation 5.2).

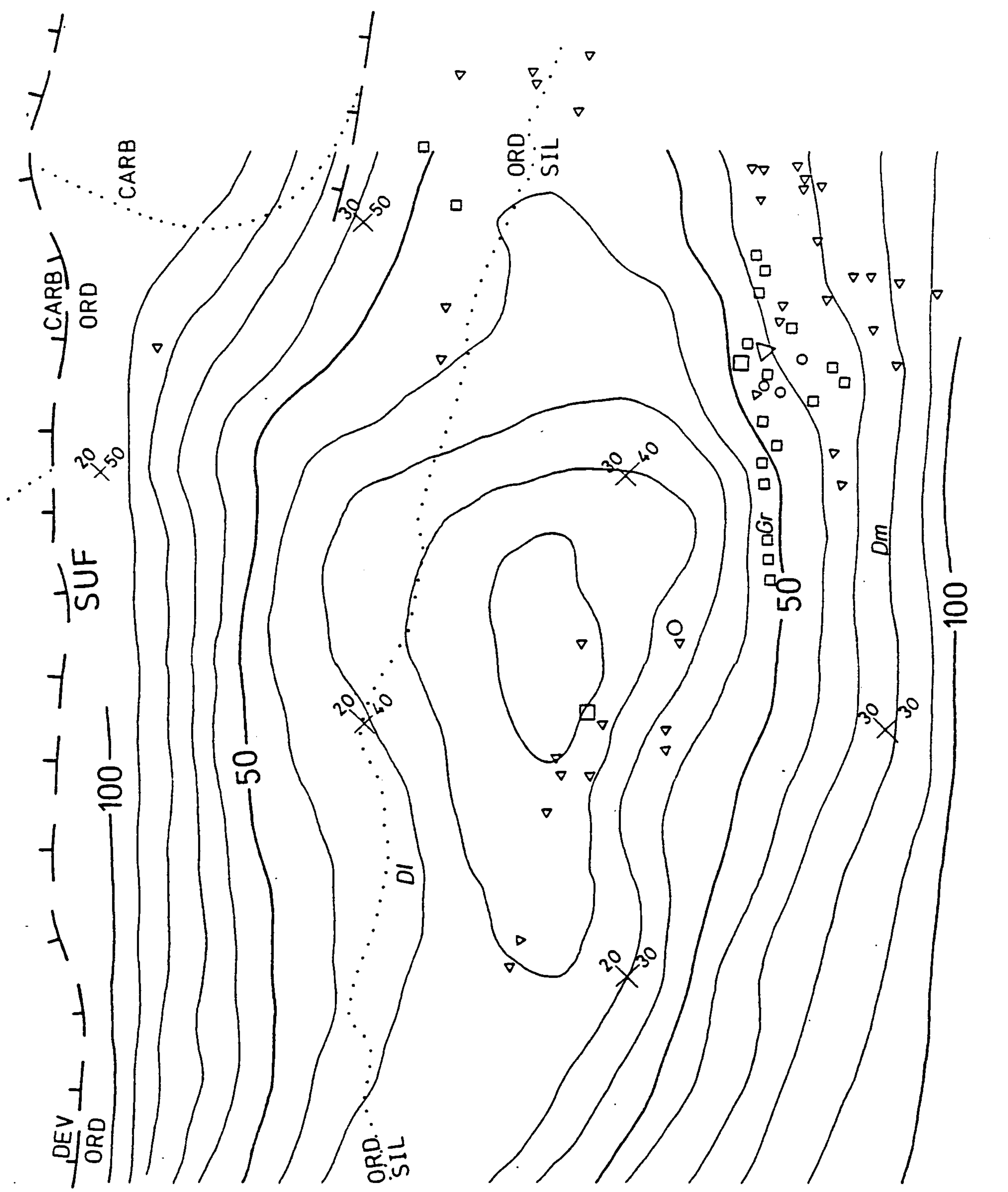

Fig. 5.1a **Residual Bouguer anomaly map of the Tweeddale area, superimposed upon a geological sketch map. (ORD: Ordovician; SIL: Silurian; DEV: Devonian; CARB: Carboniferous; SUF: Southern Uplands Fault; Dl: Dalwick; Gr: Grieston; Dm: Dumbetha; △ : felsite; □ : Porphyrite; ○ : granite. Contour interval 10 gu).** The LISPB(figure 5.3) linear trend was subtracted.

GPCP was used to contour the data, with a 1km grid interval, since this represents the density of the stations, at least at the centre of the feature, where greatest detail is required.

For the construction of the residual Bouguer gravity map it is necessary to have an estimate of the regional picture of the gravity field. Because the geology over the Tweeddale area appears to be relatively uniform, it was decided that the model from LISPB (Bamford et al, 1977, 1978) should be adopted, since the LISPB line passes through this area.

For this purpose the refracting horizons of the LISPB model were digitised and the gravitational attraction of these layers was calculated using the TALG2D program. The Nafe-Drake curve (Nafe and Drake, 1963) was used for the translation of seismic velocities to densities. The superficial layer of LISPB was not taken into consideration. Figure 5.2 shows the picture of the regional field. For computational reasons, the part of this regional field over the survey area was represented by either a linear or quadratic approximation. The LISPB model was assumed to be two-dimensional striking parallel to the Caledonian trend.

The area between the dashed lines (figure 5.2 and figure 5.3) represents a region 40km wide to the SSE of the Southern Uplands Fault, whilst the area covered by the gravity map in figure 5.1 is only 25km to the south-east of the Southern Uplands Fault. The regional field between the dashed lines in figure 5.2 is shown in a larger scale in figure 5.3.

A linear gradient of 3.7 gu/km approximates the calculated effect over the first 25km to the south-east of the Southern Uplands Fault.

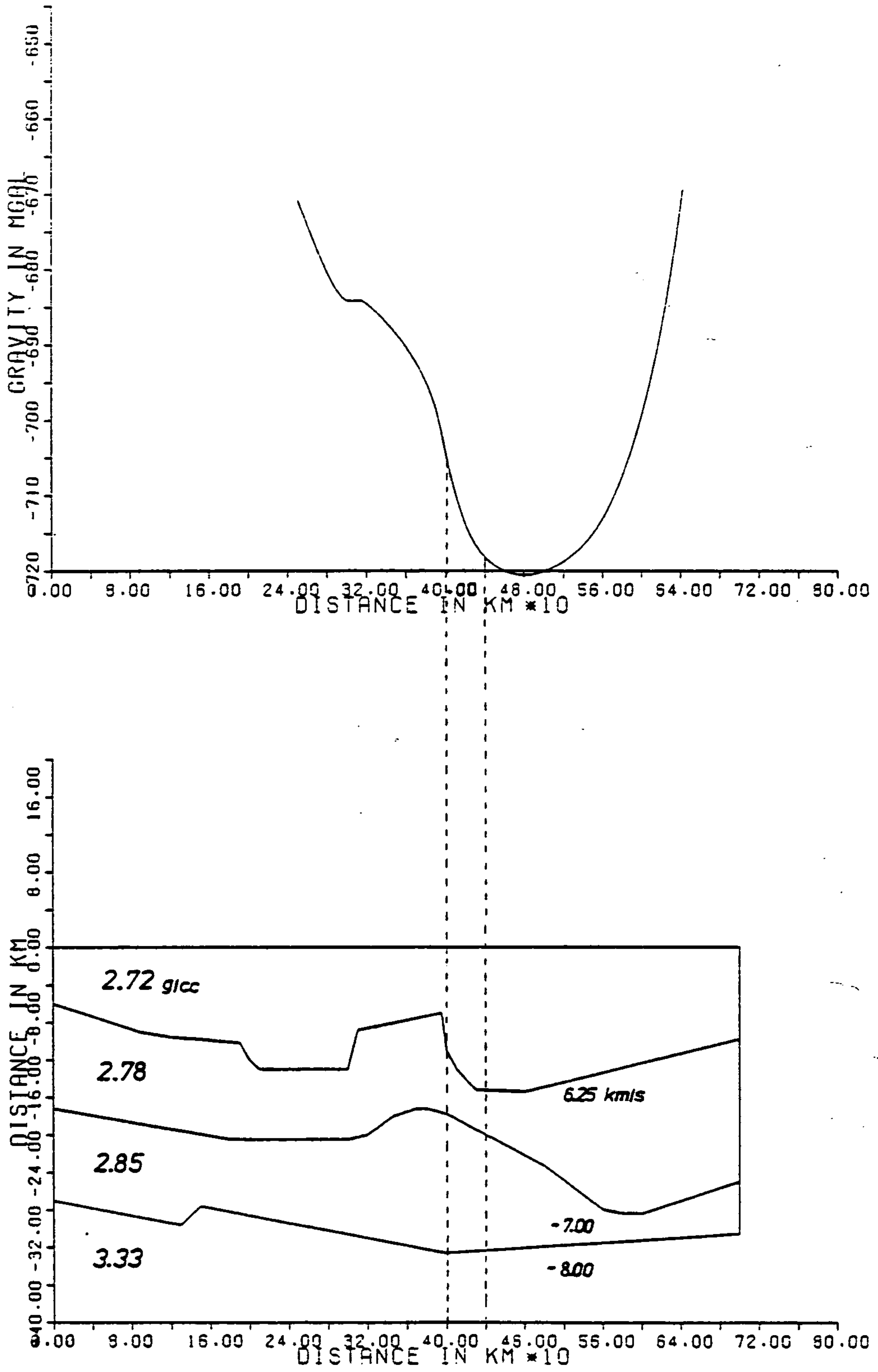

Fig. 5.2 Gravitational attraction (upper part) of the LISPB model, after digitising the refraction horizons and translating the seismic velocities into densities using the Nafe and Drake (1963) curve. The region between the dashed lines represents 40km to the SSE of the Southern Uplands Fault.

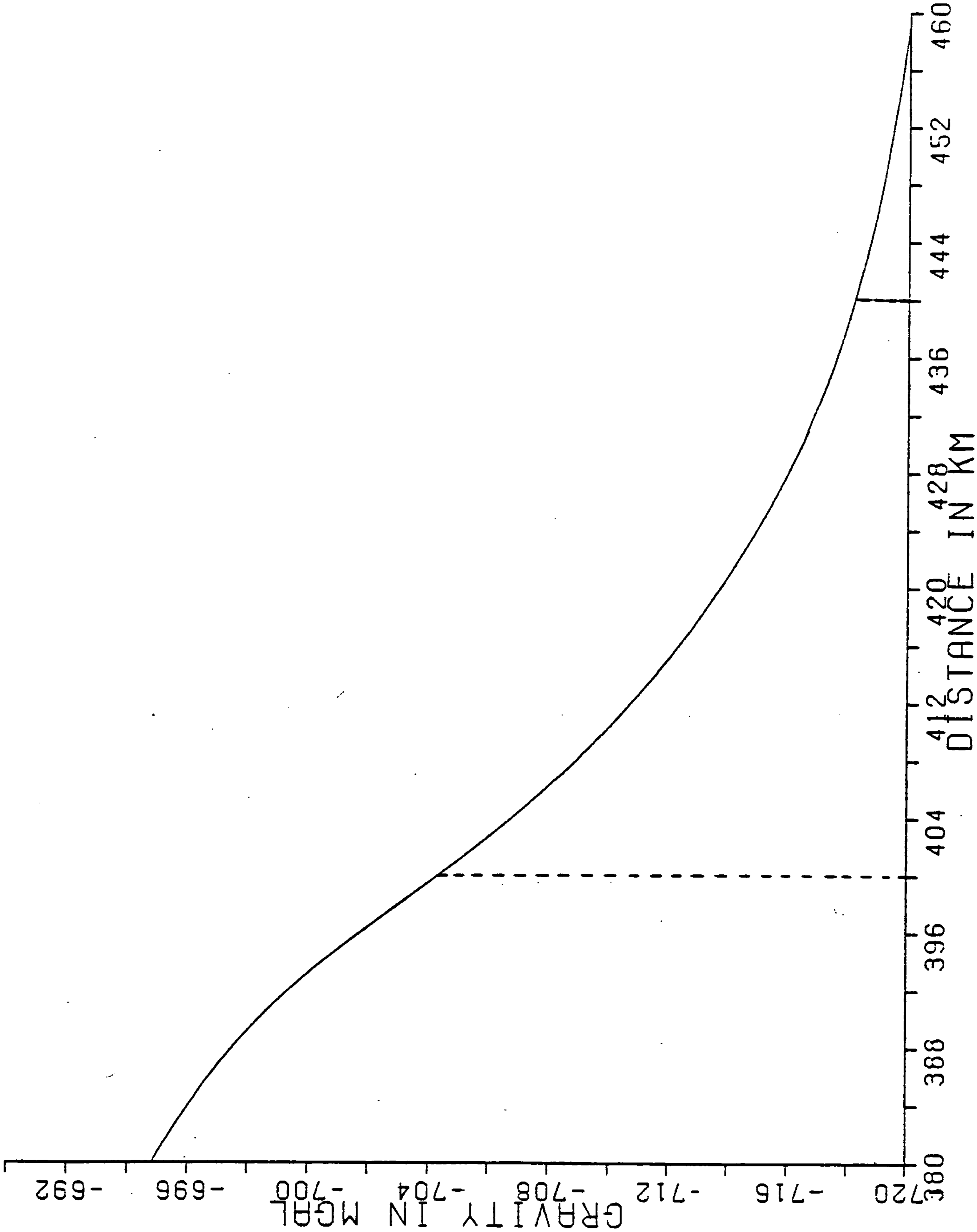

Fig. 5.3 Variation of the regional gravity field calculated from LISPB. Region between dashed lines represents 40km SSE to the Southern Uplands Fault.

This is the value of the regional trend along the LISPB line. However, because we are interested in the value of the field perpendicular to the strike of the anomaly, the estimation of that was made as follows:

$$\text{gradient across strike} \equiv \frac{\Delta g}{\Delta x'} = \left(\frac{\Delta g}{\Delta x}\right)\frac{1}{\cos\theta} \equiv (\text{gradient along LISPB})\frac{1}{\cos\theta},$$

where Δx represents distance along the LISPB line, and θ = angle between LISPB line and the direction perpendicular to the strike of the anomaly (approximately 25^{o}).

Consequently, a linear trend of 4.06 gu/km was added in the south-east direction across the Caledonian trend, and the residual Bouguer gravity anomaly map over the same area is shown in figure 5.4 as well as superimposed on figure 5.1a.

As an alternative, a quadratic approximation to the regional field estimated by LISPB (figure 5.3) was calculated and the residual gravity anomaly map is shown in figure 5.5 .

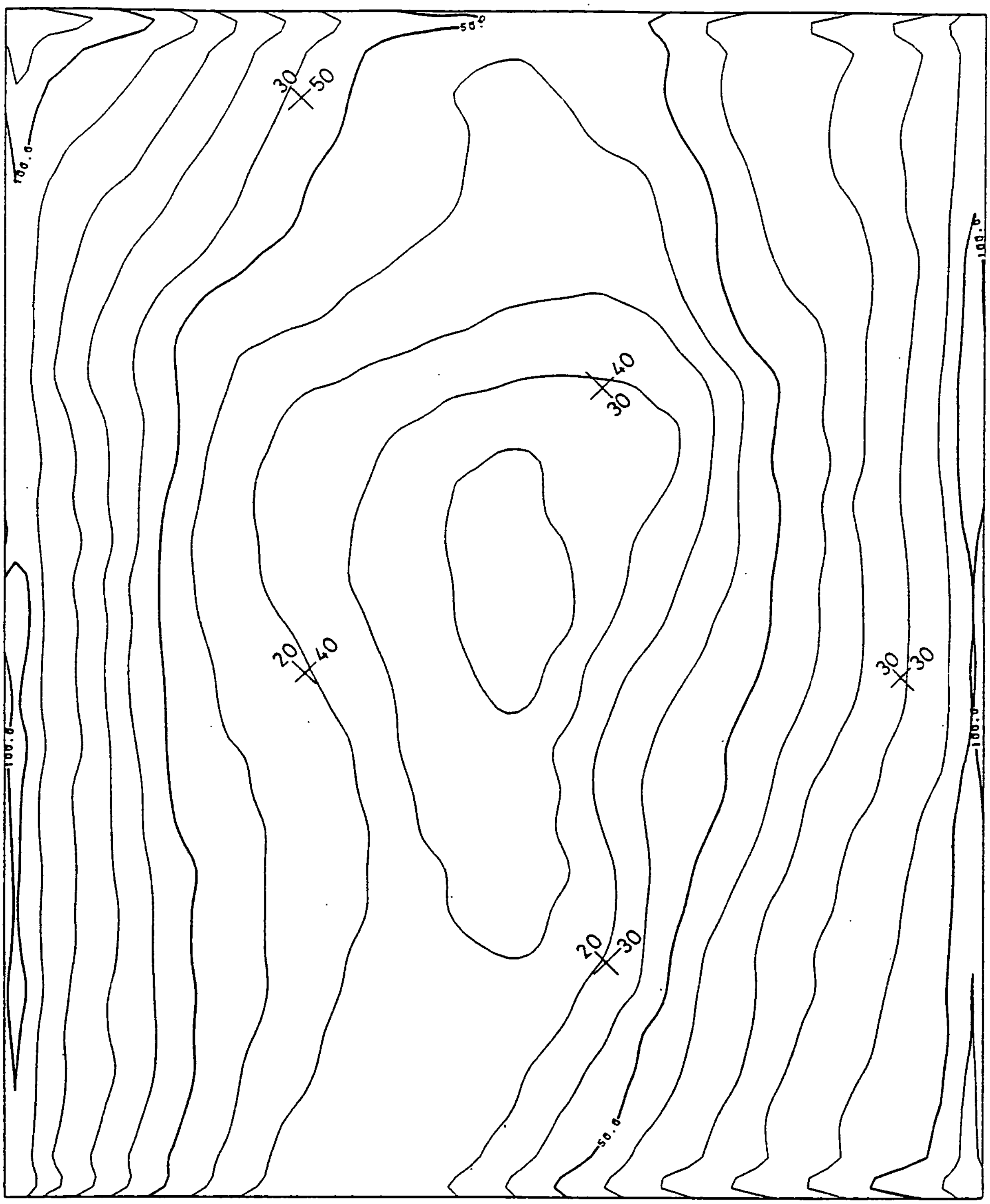

Fig. 5.4 Residual gravity map of the Tweeddale area, after subtraction of a linear trend calculated by LISPB (figure 5.3). Contour interval 10 gu.

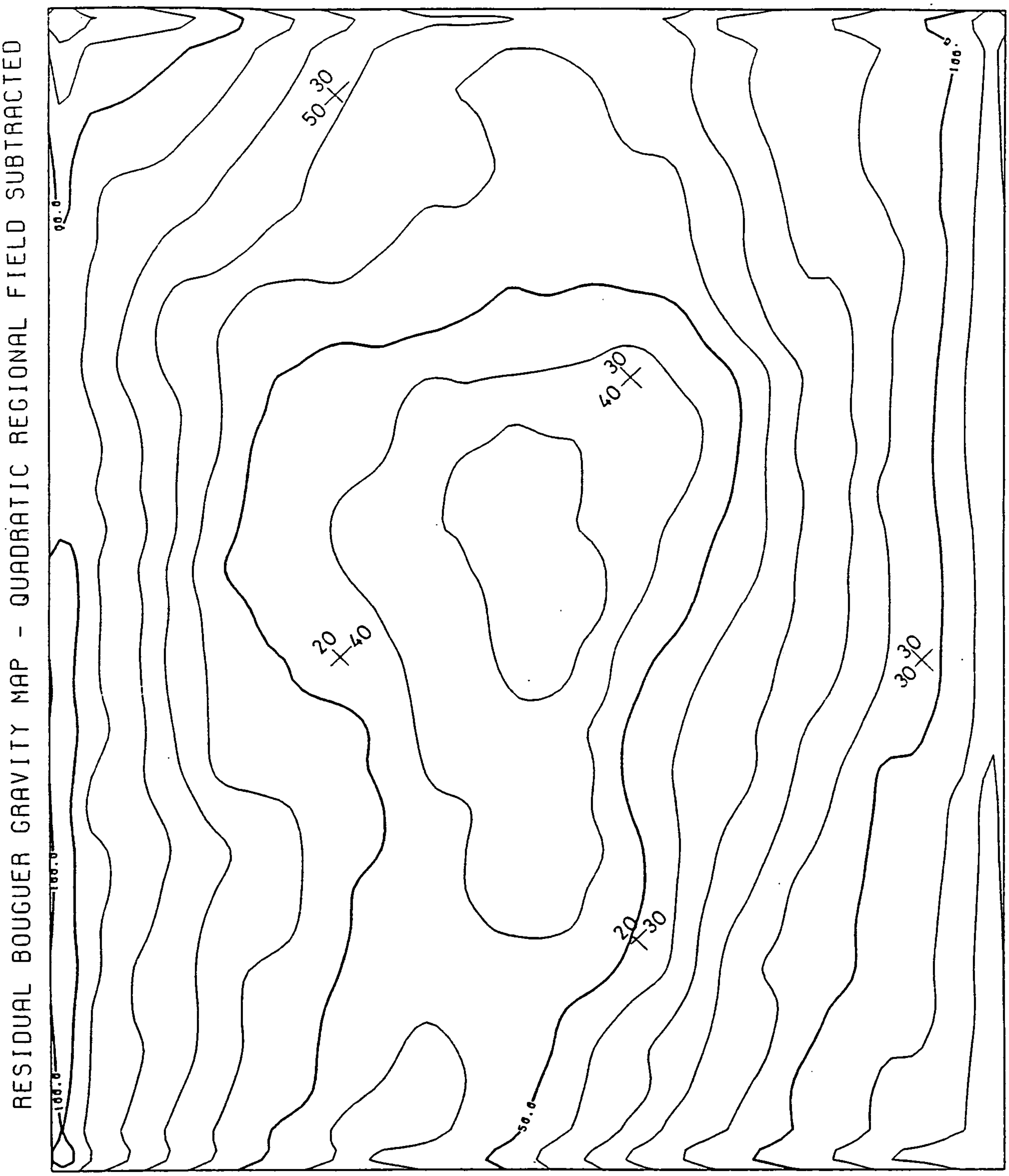

Fig. 5.5 Residual gravity map of the Tweeddale area subtracting the quadratic trend calculated by LISPB (figure 5.3). Contour interval 10 gu.

5.2.3 Interpretation

The general trend of the gravity low in the eastern Southern Uplands is NE-SW, coincident with the main trend of surface features like the age zones, the folds and thrust faults and the bounding Southern Uplands fault. These all follow and help to define a "Caledonian trend". The coincidence of trend suggests a source related to the closure of the Iapetus Ocean.

If, as many authors have proposed, the suture lies under or near to the Southern Uplands, the gravity low could be caused by an obducted sedimentary prism overlying a denser basement; alternatively, the suture might have trapped a zone of lower density sediments between the two opposing basements; finally, the low might be due to a granite, resulting from the subduction. An extensive sediment-filled gap in the basement ought to have been plainly seen by LISPB.

Detailed and analytical studies on the granite batholiths have been made by Bott (1953, 1956) and Bott and Smithson (1967), while a criterion for distinguishing gravity lows due to either sedimentary basins or igneous intrusions has been outlined again by Bott (1962). In this section, considering the geology of the area, which in a large scale is not different from the general geological picture of the Northern and Central Belts of the Southern Uplands, the interpretation of that long-wavelength negative gravity anomaly will be discussed in terms of three factors which could be responsible for it:

(i) Variation in the density of the Lower Palaeozoic sediments

(ii) variation in the sediment thickness and,

(iii) an igneous intrusion.

5.2.3.1 Density Variation of the Sediments

The sediments exposed in the Southern Uplands show an overall decrease in age southwards and while there is no major change in lithology, there is a trend with increasing thickness of trench sediments from north to south. Consequently there is no visible symmetry of rock type about the centre of the anomaly and no corresponding symmetrical density variation would be expected.

From hand samples of rocks taken from different localities over the Southern Uplands, laboratory density measurements have shown that there is not such a considerable systematic density variation in Silurian and Ordovician greywackes. A mean value of 2.708 ($\pm$ 0.021)g/cc saturated density was found (Table II-4) for the greywackes which is not so far from McLean's (1961a) and Bott and Masson-Smith's (1957) values over the Southern Uplands. Nevertheless, a more systematic approach was made by applying Nettleton's (1939) method, fitting a quadratic surface to all the gravity stations falling in each 10km National Grid square. The results have been shown in Table II-5 and summarised in Table V-1, for the Tweeddale area. A mean value of 2.711 $\pm$ 0.026 g/cc was found.

TABLE V-1

NT14	NT24	NT34
2691 ± 86 (20)	2709 ± 31 (54)	2727 ± 22 (17)
NT13	NT23	NT33
2670 ± 36 (21)	2746 ± 28 (48)	2721 ± 64 (32)
NT12	NT22*	NT32
2699 ± 20 (23)	2749 ± 36 (20)	2685 ± 15 (32)

Computed Bouguer density (kg m^{-3}) in each 10 km National Grid square, with its standard deviation and the number of gravity stations, obtained by fitting a quadratic surface to the Bouguer anomaly.
*(Because of the unsuitable distribution of stations, a linear surface was fitted in square NT22).

5.2.3.2 Sediment thickness variation

The original idea (Hipkin and Lagios, 1978) was to interpret the long-wavelength negative gravity anomaly in the Southern Uplands in terms of an obductive sedimentary prism marking the area of the suture of Iapetus.

The first attempt made was the interpretation of a NW-SE trending gravity profile over the Tweeddale area. At that time, because the survey had not been completed in that region, there was not very good control of the profile at the centre of the anomaly. Modelling attempts revealed a great thickness for the greywackes at the centre of the anomaly with unacceptable depths greater than 20km. Even today, trying to model the gravity low in terms of thickness variations of the greywackes, relatively large residuals were found at the centre of the anomaly. Figure 5.6 shows such an attempt with density contrast of -0.06 g/cc. Such a sediment density of 2.65 g/cm^3 is already lower than implied by the density measurements but a smaller density contrast will cause the sedimentary prism to extend into the 6.4 km/s layer assumed for the regional calculation.

These two results reflect the short wavelength features of the anomaly near its centre which cannot be modelled by a deep interface like the one generated by a sedimentary prism. This is demonstrated quantitively by the maximum depth estimates discussed in section 5.2.4.1. Therefore, it was difficult to accept such an interpretation, furthermore, it was not in agreement with evidence of the seismic horizons under the Southern Uplands (LISPB).

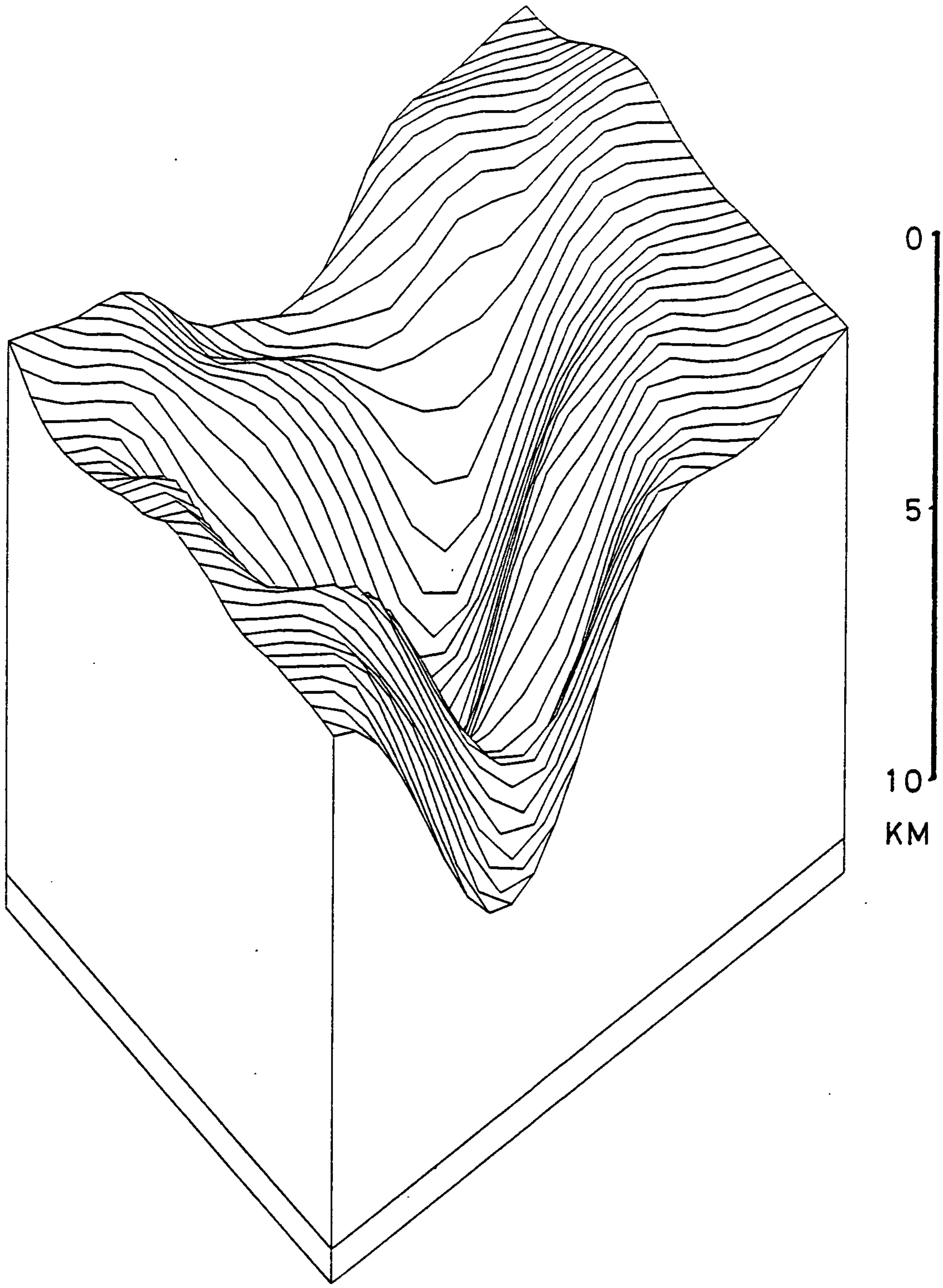

Fig. 5.6 Three-dimensional representation of the residual gravity map of the Tweeddale area modelled as a sedimentary basin with density contrast -0.06 g/cm^3. It covers the same area as the residual anomaly map in figure 5.5 viewed from the west.

5.2.3.3 Igneous intrusion

It is well known that granite batholiths are associated with elevated ground (Highlands, Lake District, Cheviot Hills, Northern Pennines) as has been shown by many authors, Bott (1956), Bott and Masson-Smith (1957), Bott et al (1978), Scrutton and Dingle (1973) etc, and sedimentary basins usually by low ground. The Southern Uplands are characterised by high elevation and particularly over the Tweeddale area there are spots with elevation more than 2700ft and Broad Law (NT 1423) has the highest elevation (2755ft) in the whole Southern Uplands. In fact, Peeblesshire has the highest mean elevation of any Scottish county.

There are granitic exposures all the way along the Caledonian trend, and particularly in the south-western part of Scotland where detailed studies have already been carried out and described in Chapter I. It has been shown (El-Batroukh, 1975) that the three principal plutons of the south-west of Scotland are connected at depth forming a huge granitic layer extending parallel to the Caledonian strike under the Lower Palaeozoic sediments.

The existence of a granite batholith, both in SW Scotland and along strike in SE Scotland is consistent with recent plate tectonic models for the British Caledonides (Mitchell and McKerrow, 1975; Phillips et al, 1976). The Southern Uplands have been persistently elevated, at least since Upper Silurian times, when it formed part of Cockburnland (Walton, 1965, McKerrow et al, 1977) and, therefore, the existence of a granite batholith also along the NE part of the Southern Uplands should not be considered as a surprise.

It is worth mentioning that the porphyritic and felsite veins and dykes occur not only in SW Scotland but extend parallel to the strike to the north-east until they reach the Oldhamstocks basin. Although it is believed that these dykes or veins are not all contemporaneous, a high proportion of them are associated with granitic masses and they seem to have been intruded rather later than the formation of those granitic bodies and are clearly associated with granite emplacement in Connemara, Donegal, west and south-west Scotland (Watson, 1964). Felsites and porphyrites are widespread in the region between the Highland Boundary Fault and the Great Glen Fault where granitic exposures occupy about one fourth of the land and, recently, it was shown that they continue under the Moray Firth Basin (Dimitropoulos and Donato, 1979). In the Southern Uplands these dykes were intruded during Lower Old Red Sandstone times (Kelling, 1962) after the compression normal to the Caledonian strike.

Further strong support in favour of a granite batholith comes from the carbonisation and graphitisation of the organic material of the Moffat shales (Peach and Horne, 1899). This has been attributed (Watson, 1976) to thermal effects from regional metamorphism and a deep seated igneous body, centred at depth in the vicinity of Hartfell (NT 1213) which is only 7-8 km south-west of the area under consideration. The thermal effects of this body can be detected on a regional scale from reflectivity measurements on graptolite fragments: Watson (1976) deduced from temperature computations outside a cooling pluton and their relationship with reflectivity that the igneous body occupied a radius of 8km from Hartfell, assuming 700° for the initial temperature of magma, but his data did not define the northern boundary of his intrusion

Mineralisation associated with buried granites is usually expected, but it is only sporadic in the Southern Uplands and in the area of Tweeddale not strongly developed. It has been reported (Hardy, 1892; Wilson and Flett, 1921) that lead ore has been worked at several localities in the Tweed Valley and its tributaries. The most extensive workings were at the abandoned Grieston Mine (NT 3136) near Traquair (NT 3335), at Dalwick (NT 1734) near Stobo and at Dumbetha (NT 3433), see figure 5.1a.

Elsewhere in the Southern Uplands it is reported (Wilson and Fleet, 1921) that abandoned copper mines exist in the Lauderdale district and at Pristlaw Hill (NT 645635); also, in Berwickshire near Elba (NT 787613) and at Ellenford (NT 730600), two old abandoned mines exist, near the Cockburnlaw granitic exposure.

The LISPB experiment determined a seismic velocity of 5.84 ± 0.02 km/sec for the layer of supposedly Lower Palaeozoic sediments, which is the same as the one found by Holder and Bott (1971) for the granite batholith at the south-western part of England. Because that value is a typical one found generally for granites (Woollard, 1962; Powell, 1971), it does not contrast with the velocity of the Lower Palaeozoic greywackes (Powell, 1971), and therefore, although the LISPB line crosses the

Tweeddale area, it is not expected to show the lateral extent of any supposed granite batholith.

The low Poisson's ratio found (Assumpcao and Bamford, 1978) from S-wave arrivals to the south-east of the Southern Uplands Fault, is consistent with quartz enrichment, something that is supported by Nicol (1843) in his accounts on the quartz veins over the area.

5.2.4 Modelling Procedure

5.2.4.1 Gravity

As has been discussed in the previous sections, the evidence in favour of a granite batholith underlying the area of consideration seems strongest and this is how the structure is going to be modelled.

The residual Bouguer gravity map shown in figure 5.4 and figure 5.5 was made using GPCP and the grid size of the array was determined at 1km, which reflects the spacing of the gravity stations in the centre of the anomaly, although this is not true for other regions of the same area, particularly towards the margins of the map.

A three-dimensional attempt was made to model the batholith, using MODG3D program. For this purpose two conditions were required: (1) the density contrast between the Lower Palaeozoic rocks and the igneous rocks and (2) the depth, at which a fixed point of the model had to be constrained.

As has been discussed previously, a density of 2.72 g/cc for the

Lower Palaeozoic sediments seems to be very reasonable, although this value can be greater (approximately 2.73 g/cc) at greater depths than that determined from surface hand samples.

Published densities of exposed granitic rocks in south-east Scotland (Walker, 1928) vary between 2.63 and 2.80 g/cc and, therefore, do little to constrain the interpretation. From a few massive boulders on Kailzie Hill and Kirniew Law, a saturated density of 2.628 $\pm$ 0.009 g/cc (11 samples) was found, with 2.663 $\pm$ 0.027 g/cc (42 samples) for nearby porphyrites and felsites. In south-west Scotland the Griffel granodiorite was interpreted (Bott and Masson-Smith, 1960) with a gradational density between 2.64 and 2.71 g/cc, while the Fleet granite was modelled (Parslow and Randall, 1973) with a density of 2.63 g/cc.

Apart from the author's density measurements of porphyrites and felsites, it is reported (Nicol, 1843) that those varieties do not vary much in density over the Tweeddale area and "representative values of 2.600 and 2.552 g/cc" are given, respectively.

Density contrasts, between Lower Palaeozoic sediments and the igneous intrusion of 0.06,0.07, 0.08 were chosen for modelling purposes (density contrasts always in g/cc).

A profile AB (figure 4.6) was constructed across the strike of the feature, figure 5.7a. The points for the first 24km were taken from the array generated by GPCP from the residual map and the remainder from the contours of the map. A maximum

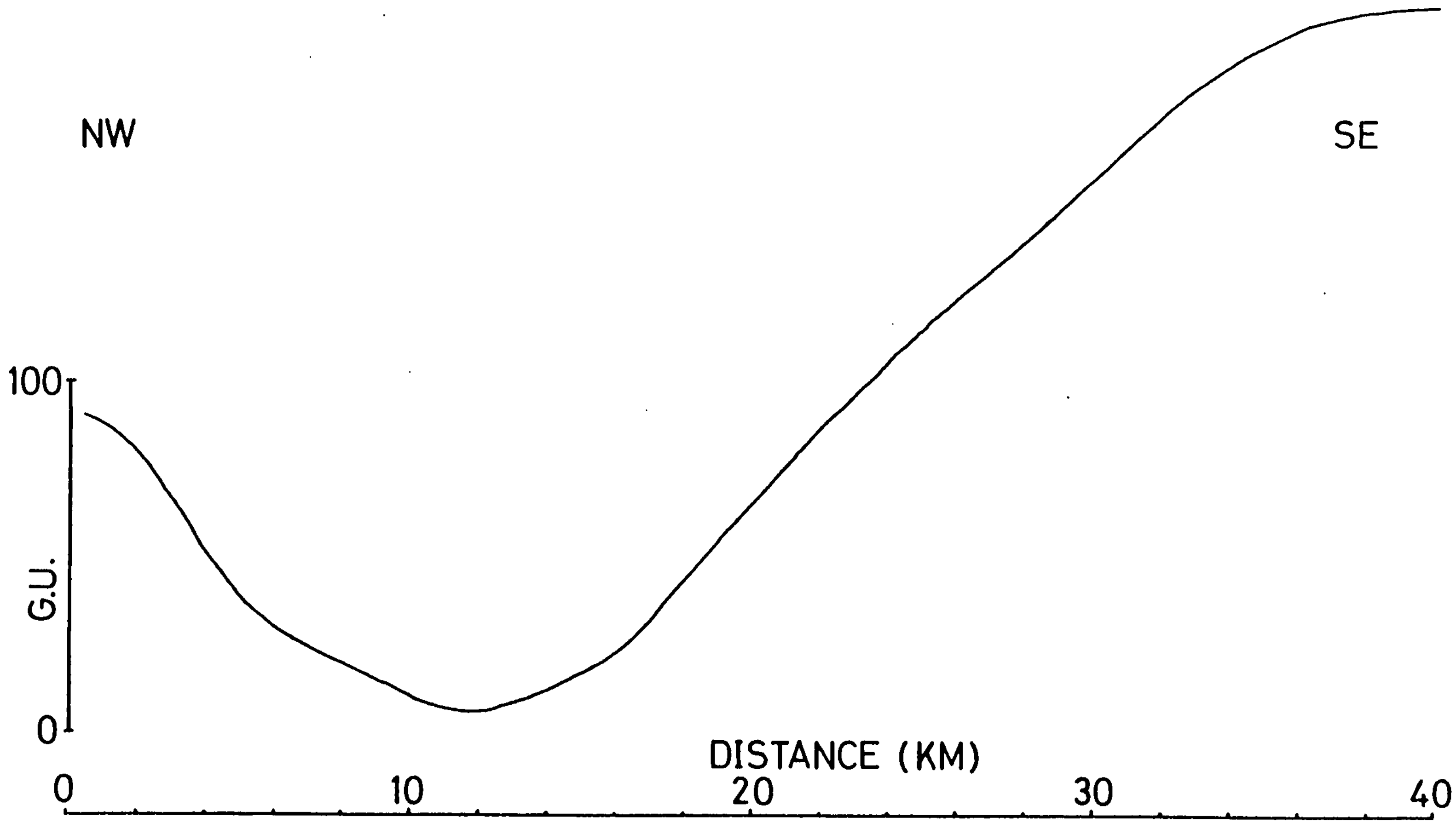

Fig. 5.7a Gravity profile AB, coordinates of the end points of the profile are NT 210 472 and NT 452 217.

gradient of about 13 gu/km is observed. For an estimate of the depth of the centre of the mass which causes the anomaly, the formula amplitude/maximum-gradient was applied (Bott and Smith, 1958):

$$h \leqslant 0.86 \frac{\left[\Delta g\right]_{max}}{\left[d(\Delta g)/dx\right]_{max}} \tag{5.1}$$

Allowing a maximum amplitude of about 90 gu of the anomaly due to the granite and taking the above mentioned maximum gradient, then $h \leqslant 6$km.

For an estimate to the top of the body the following formula was applied (Bott and Smith, 1958):

$$\text{if } \mu = \frac{2\Delta g(x)}{\Delta g(x+d) + \Delta g(x-d)} > 1 \rightsquigarrow h \leqslant d\left(\mu^{2/3} - 1\right)^{-\frac{1}{2}} \tag{5.2}$$

where $\Delta g(x-d)$, $\Delta g(x)$, $\Delta g(x+d)$ is the value of gravity at places x-d, x, x+d along a straight line, respectively. This rule, which has the advantage of giving results unbiased from the regional gradient, was applied on stations falling approximately along the lines CD, EF (figure 5.1) after the interpolation of some values. Along the line EF, $h \leqslant 4.6$km was found and from stations along the line CD values of 3.4 and 2.6km for maximum depth was found. Thus, it appears that the depth, h, to the top of the granitic body should be:

$$h \leqslant 3\text{km}$$

while the centre of mass is at a depth of something less than 6km.

Program MODG3D was used for a three-dimensional inversion model. The interface was approximated with vertical prisms of 1km side (the grid size of the residual map). Different density contrasts were applied. Figure 5.7 shows a contouring of the model inversion with a fixed depth near the centre of the anomaly of 1.5km and a density contrast of 0.07 g/cc. It is from the third iteration with root mean square residual of 4.4 gu. It was observed that increasing the fixed depth of the body, the model was converging very slowly, particularly at the top and bottom margin of the modelling area. Using the data array of the isodepth contours of the batholith of figure 5.7, SYMVU was used to produce a three-dimensional picture, shown in figure 5.8a.

As can be seen from the model, there are three main bosses, on a body whose shape is typical for a granite batholith, with outward sloping sides, extending to a depth of more than 10km and possibly more than 12km. One of the bosses, which is the main one, appears near where the minimum anomalies occur (-49.97 and -49.25 gu) around the area of Cardrona Forest. The middle one is near the Juniper Craigs porphyritic exposure and the third one near Posso Craig (NT 2032) where again some felsites have been marked on the one inch geological map.

From the distribution and the accuracy of the gravity data over that area, it is concluded that the boss which comes near the surface under Cardrona Forest, just 2km north-west of the Grieston Quarry, is the most confident one.

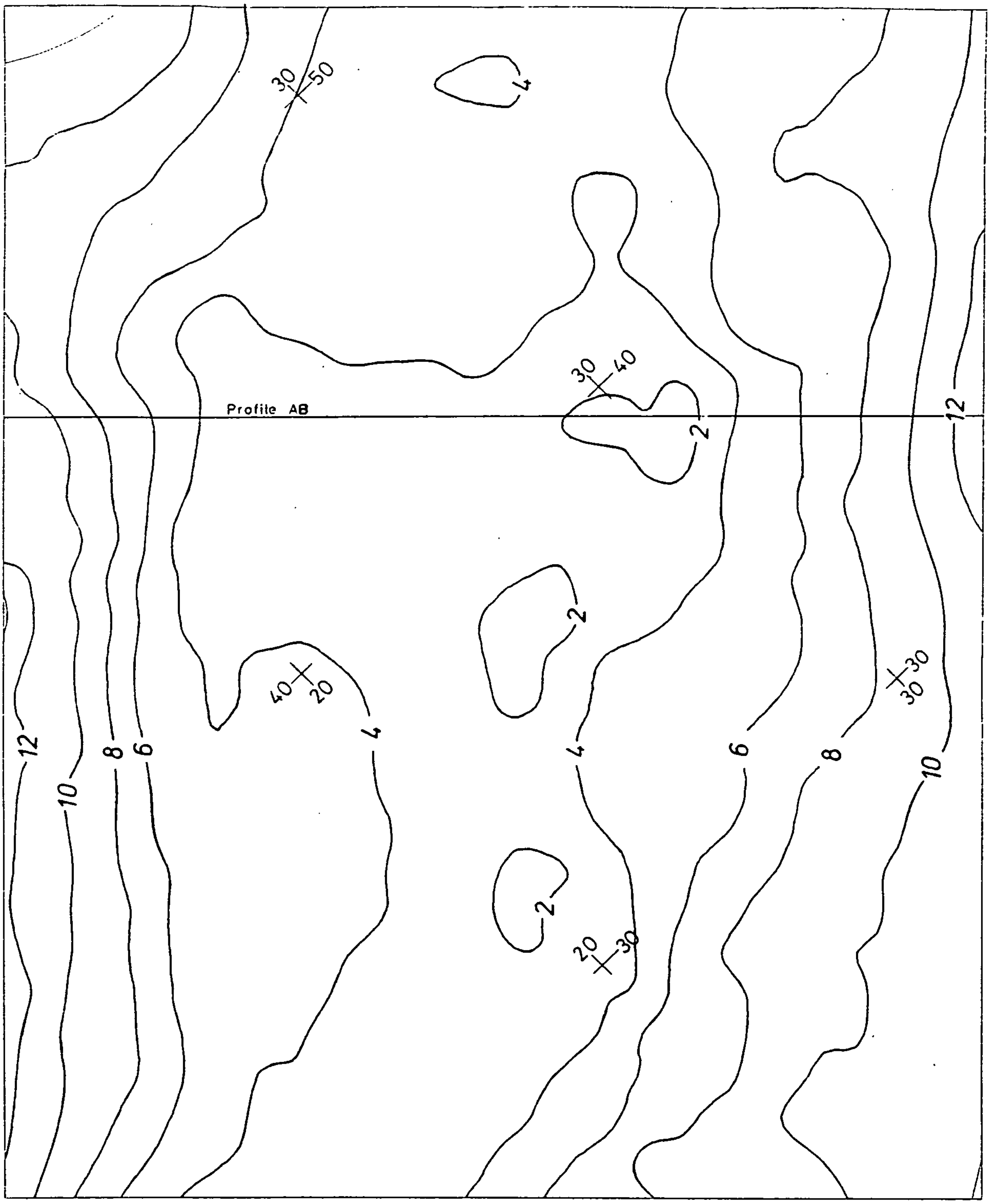

Fig. 5.7 Isodepth map of the Tweeddale Granite; contour interval 2km. Intersections represent 10km National Grid square.

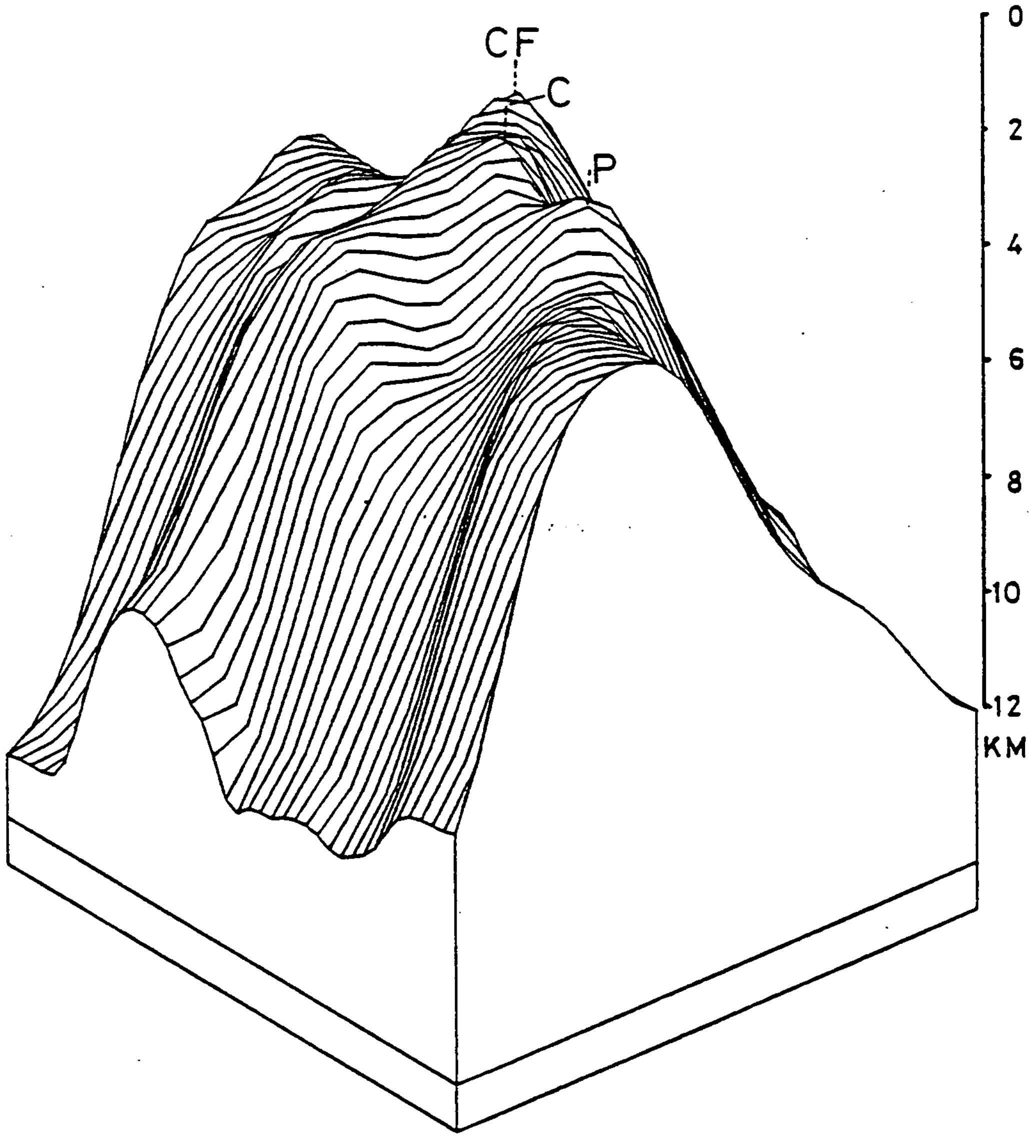

Fig. 5.8a Three dimensional model of the upper surface of the Tweeddale Granite, viewed from the west. The computation includes infinite extensions from all edges of the model, the beginnings of which in the SW-NE direction are included in the drawing. CF : Cardrona Forest; P : Posso Craig; C : Crookston (NT 2537).

Models were also produced with a quadratic regional field (represented in figure 5.3), subtracted from the original Bouguer gravity map of the area (figure 5.1). Figure 5.8 represents a three-dimensional picture of that attempt. From the latter figure it is concluded that the resulting model does not differ significantly from the models produced after the subtraction of a linear trend, and, generally, in all those models the boss near Cardrona Forest appears to be the most predominant one.

Also, various models were tried. Figures 5.9, 5.10 and 5.11 show the three-dimensional picture of various models with density contrast -0.06, -0.07, -0.08 g/cc fixed at a depth of 1km.

5.2.4.2 Magnetic

Looking at the aeromagnetic map over the Tweeddale area, a mean positive linear magnetic feature appears to be running in a direction NE-SW within the belt of the gravity low. The northern zero magnetic contour seems to form the same offset to the north-west, before approaching the Lammer Law (NT 5261) area, as does the gravity pattern. A magnetic profile (M1) was traced (figure 5.12) along the same direction as the gravity profile AB, and a two-dimensional modelling attempt was made. The computer program MODM2D was used. The co-ordinates of the corners of the body shown in figure 5.13 were taken from the gravity model with a density contrast of 0.07 g/cc as shown in figure 5.7.

It was found that an intensity of magnetisation* of 9.5 nT resulted in a very good match to the observed profile (M1), figure 5.13. The body was assumed to be normally magnetised

---

(*) 'Magnetization' is used throughout for the product $\mu_o M$ so that it is measured in units of magnetic induction, eg. nT.

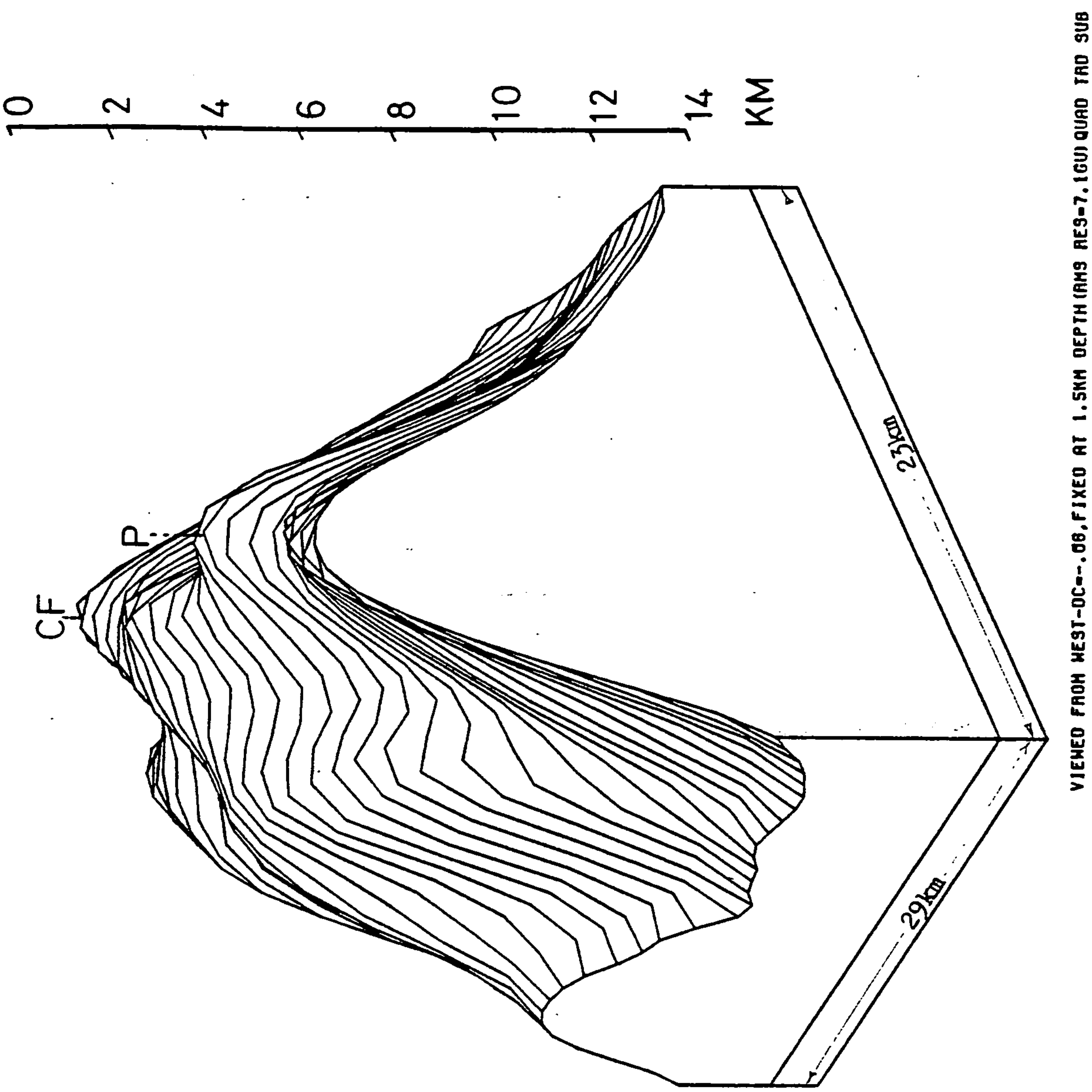

Fig. 5.8 Three-dimensional model of the upper surface of the Tweeddale Granite viewed from the west. Density contrast 0.06 g/cm^3. CF: Cardrona Forest; P: Posso Craig.

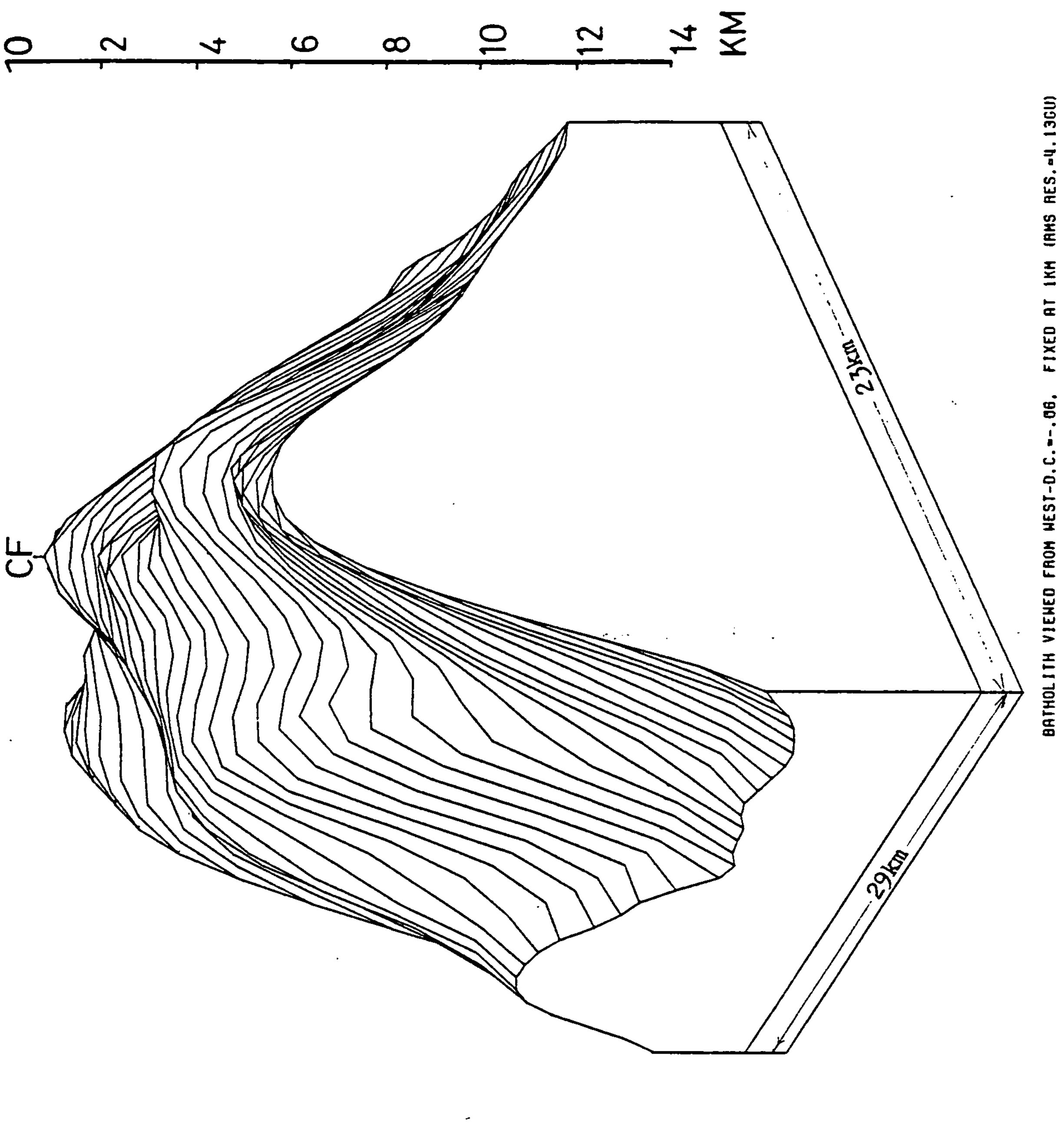

Fig. 5.9 Three-dimensional model of the upper surface of Tweeddale Granite, viewed from the west; density contrast 0.06 g/cm^3, fixed at a 1km depth. CF: Cardrona Forest.

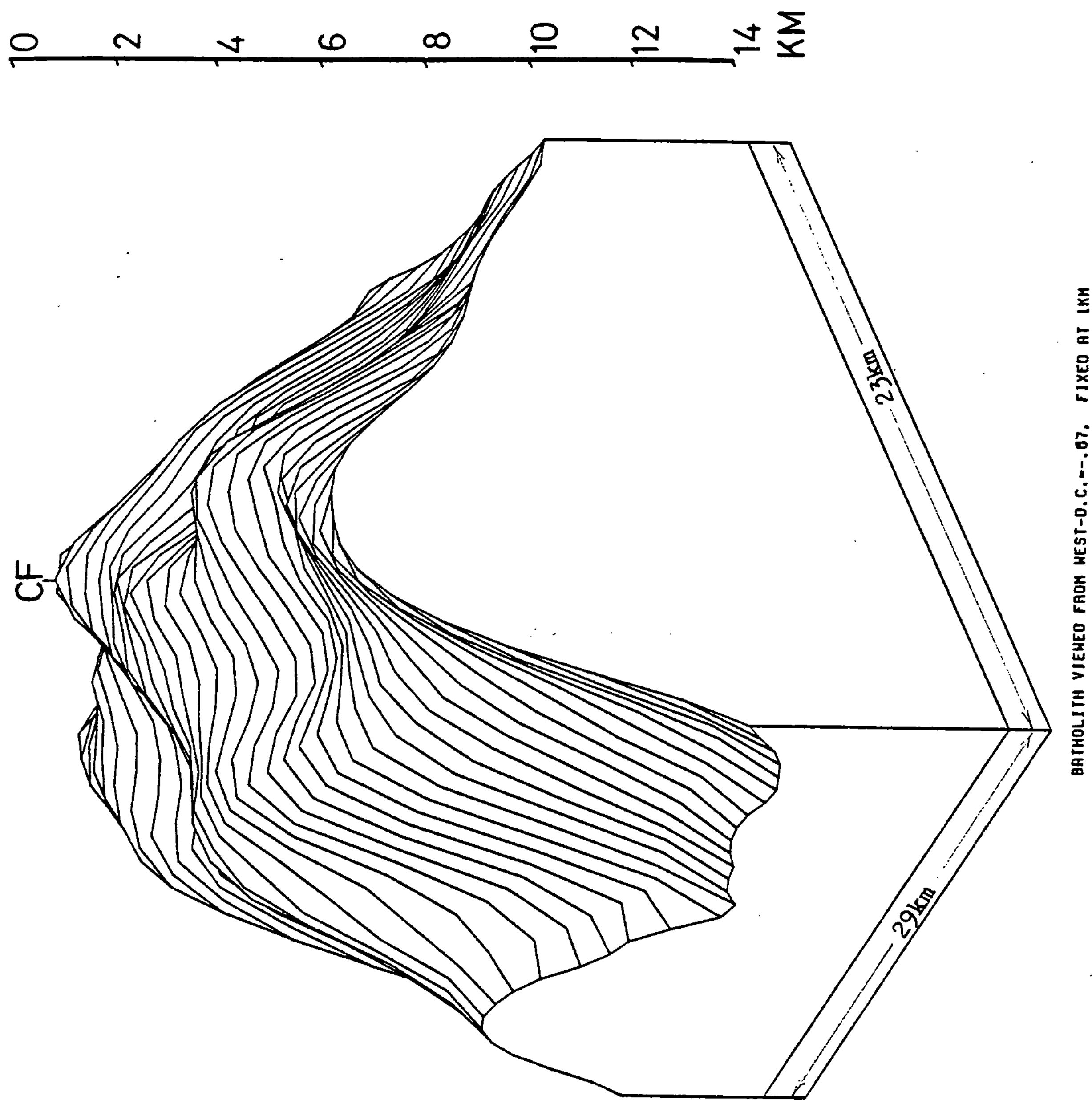

Fig. 5.10 Three-dimensional model of the upper surface of Tweeddale Granite, viewed from the west; density contrast 0.07 g/cm^3, fixed at 1km depth. CF: Cardrona Forest.

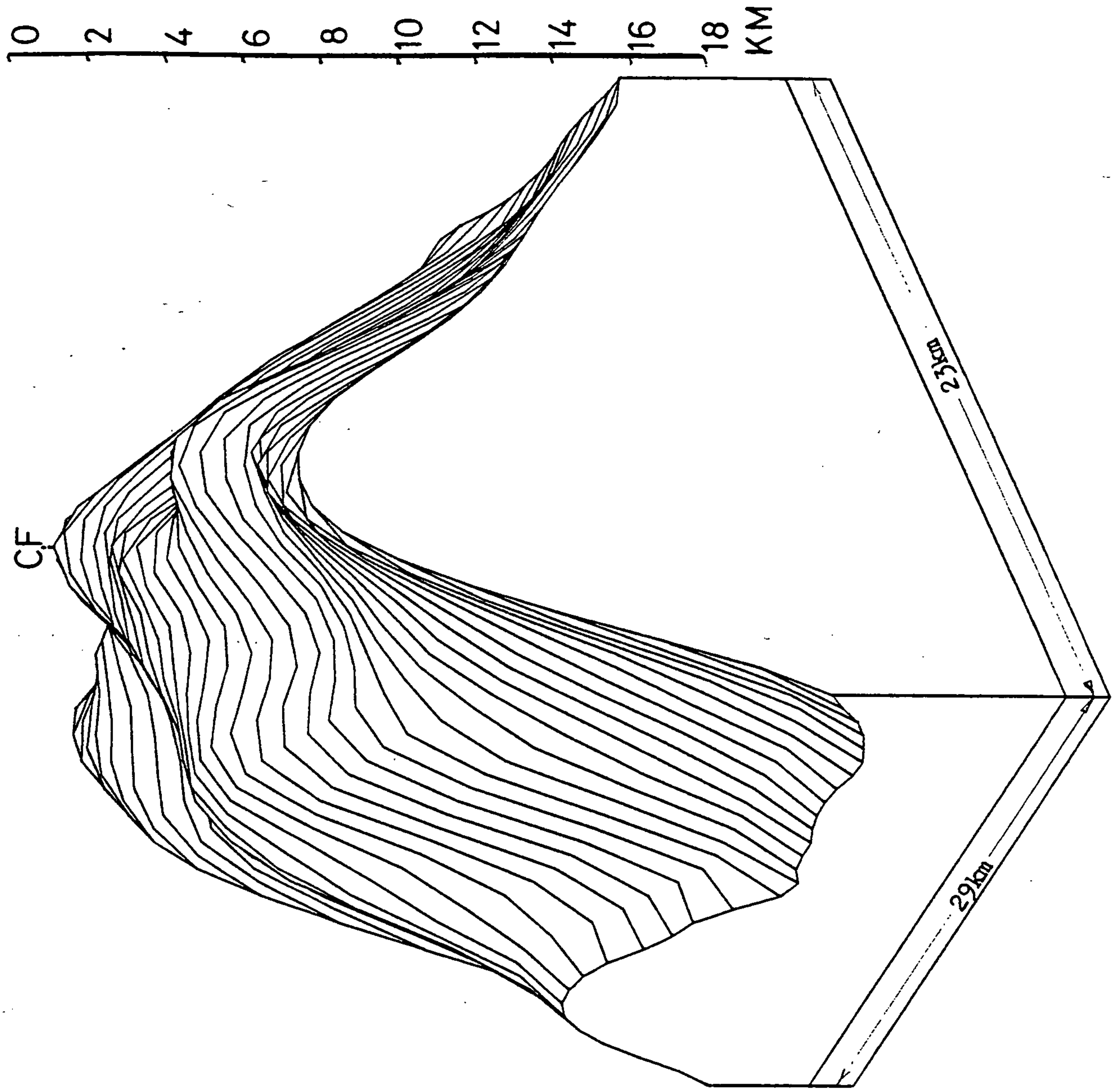

Fig. 5.11 Three-dimensional model of the upper surface of Tweeddale Granite, viewed from the west; density contrast 0.08 g/cm^3, fixed at 1km depth. CF: Cardrona Forest.

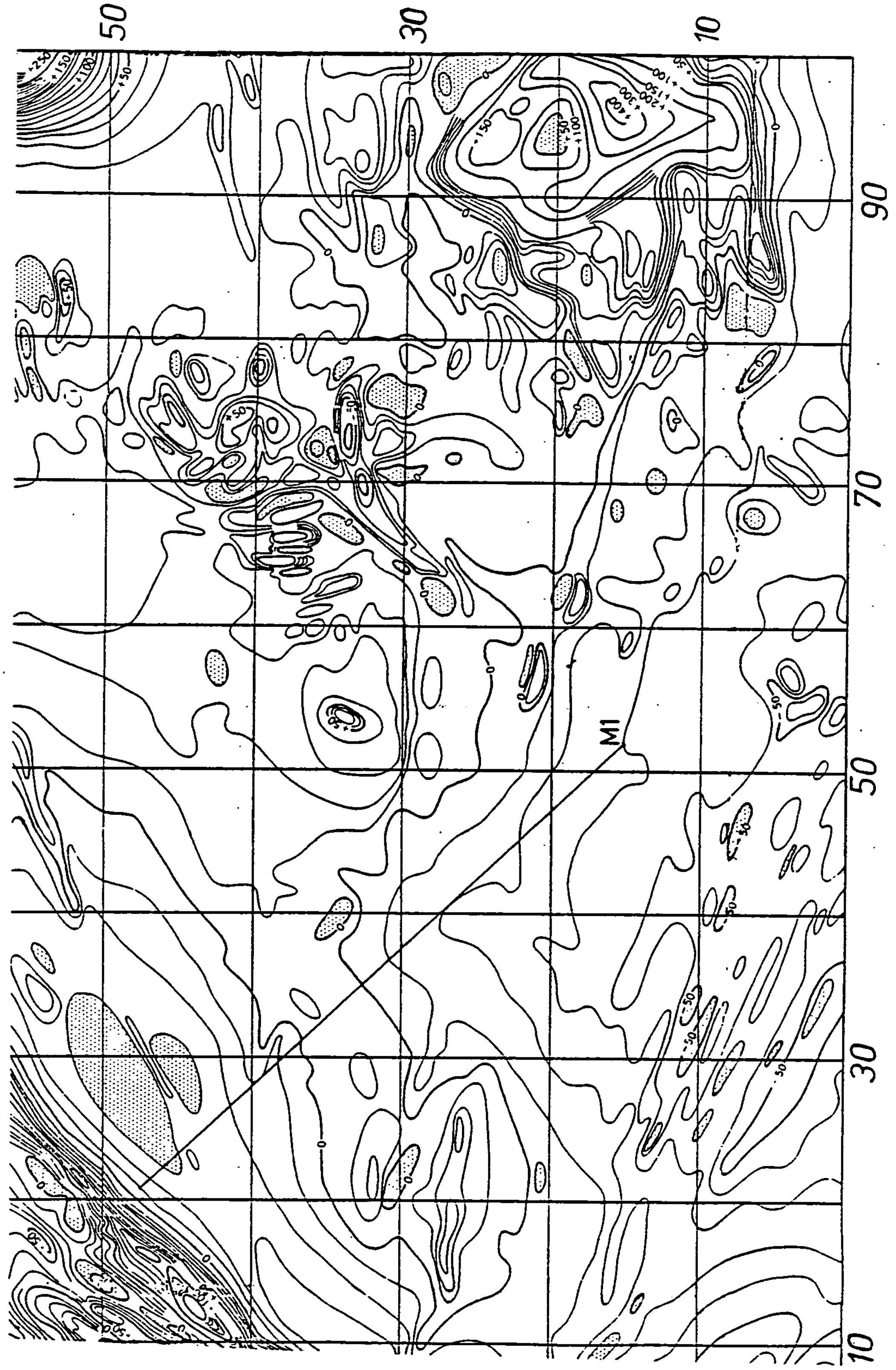

Fig. 5.12 Aeromagnetic map (after Bullerwell, 1968) of part of SE Scotland. Contour interval 10nT.

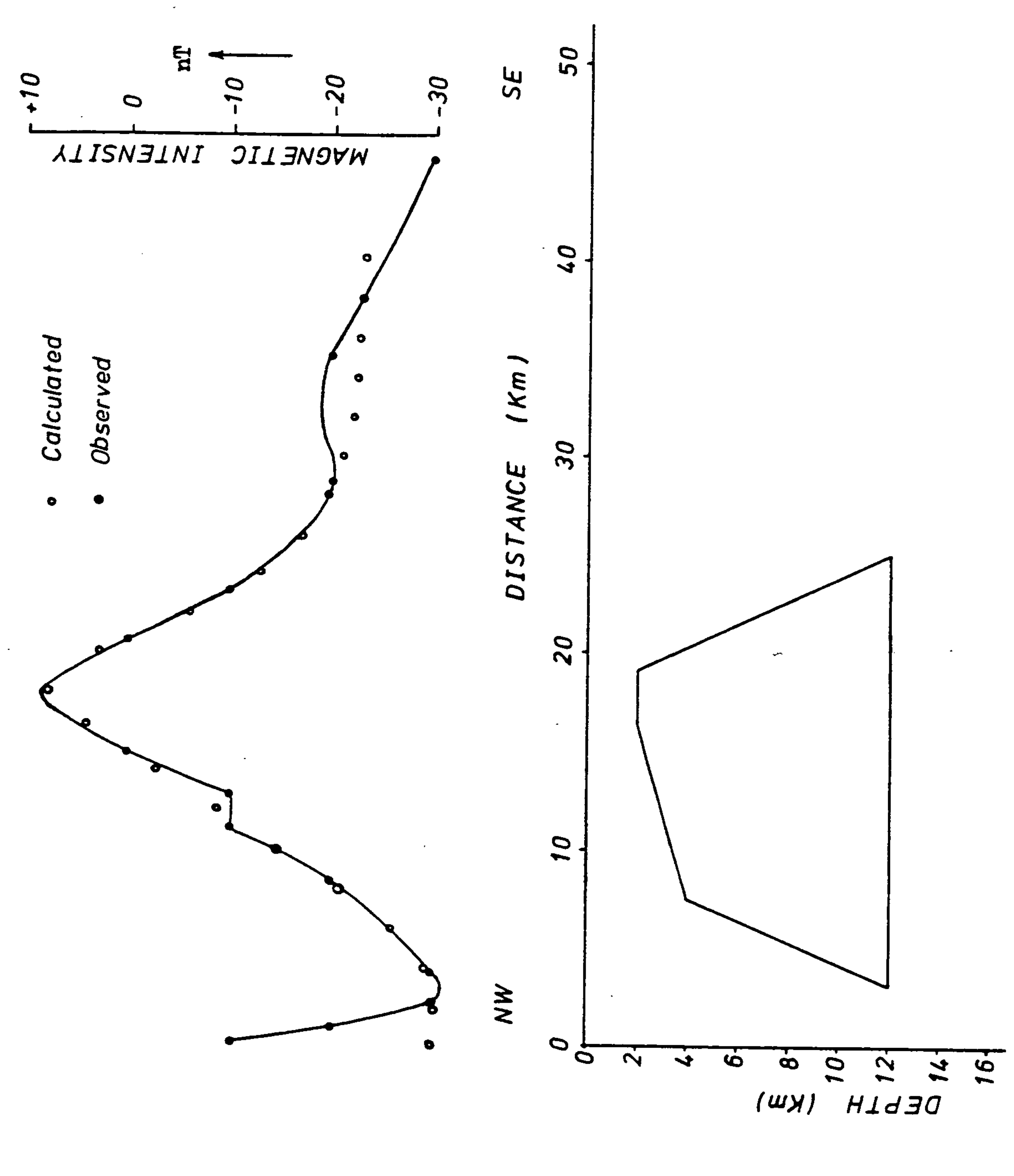

Fig. 5.13 Magnetic profile (M1) across the Tweeddale batholith. The corners of the model were taken from the gravity model (figure 5.7); assigned intensity of magnetisation 9.5 nT. Coordinates of the profile are NT 210472 and NT 520150.

according to the earth's present magnetic field. The very good agreement of the predicted and observed profiles adds support to the gravity model. This magnetisation compares with values of about 10 nT found by Powell (1970) for the Fleet and Dee granites and about 100 nT for Criffel.

5.2.4.3 Discussion

Observing those different models, it is concluded that the granite is extended to the north-east and south-west and has a trend parallel to the Caledonian trend. It appears that the batholith comes near the surface again at the south-west margin and reaches a depth of about 2km, but this is not certain as the gravity stations coverage over that area is rather poor and there is not good control. Therefore, the picture over that part is rather dubious, but certainly the body extends to the south-west.

Looking at the profile AB (figure 5.7a) a gradational change in the density contrast might be happening at the south-eastern part of the granite, observing the longer constant slope of the curve, compared to the north-western part. Such an increase in density going outwards from the centre of the body has been observed in hand samples across the outcrop of the Criffell granodiorite (Bott and Masson-Smith, 1960). In all the models which have been produced, it has been assumed that the density contrast between granite and country rock was constant. This might be considered as unlikely in view of possible changes of the composition of granite in depth or of increase of the density of the sediments due to compaction. Thus, estimates of the depth to which the granite extends from surface density measurements of the rocks and gravity anomalies seems to be uncertain. However, a rough estimate can be made using information from other geophysical work over the area. Magnetotelluric measurements (Jones and Hutton, 1979a,b; Jain and Wilson, 1967) suggest that a conducting zone within the crust underlies the Southern Uplands and channels the flow of earth currents induced in the adajcent areas (the North Sea and Solway Firth). Jones and Hutton (1979b) had estimated the top of the conducting body at a depth of 24km under the Southern Uplands. However, more recent interpretation of the magnetotelluric data at sites Earlyburn (NT 2249), Peebles (NT 2740), Yarrow (NT 2924) and Borthwick Brae (NT 3616) (these sites are almost in a straight line across the granite) have shown with a one-dimensional inversion that the conductor (10^2 Ωm) is at shallower depth, 10-12km and underlies a highly resistive layer (10^4 Ωm) which the author considers as the lower part of the batholith. The depth is consistent also with seismic evidence (Jacob, 1969) **of a refractor at 12 km depth.**

5.3 Selkirkshire

In this section, an attempt will be made to interpret the gravity high south of Melrose and south-east of Selkirk. It forms a plateau with an area of more than $20km^2$ which, from the distribution and density of the gravity stations, is well defined. It runs parallel along the strike of the gravity low to the north-west and terminates at the south-western margins of the Lauderdale Upper Old Red Sandstone basin. Although its limits to the north-east are well defined, to the south-west the situation is not so clear. From Bullerwell's unpublished gravity map (**personal communication**) it is obvious that this gravity high continues to the south-west and attains higher values (approximately 100 gu) particularly around the Lower Carboniferous extrusive basalts at Lockerbie. Thus, it appears that this high might be due to intrusive intermediate or basic volcanic rocks with their thickness becoming progressively larger to the south-west.

Over the area of Melrose in particular, an analytical petrographical study was made (McRobert, 1914) on the acid and other intrusions, marked on the geological map as intrusive basalts, intrusive felstones and volcanic agglomerates in necks of Calciferous Sandstone age. It is suggested that the Eildon Hills (NT 5532) are probably the denuded remains of a composite laccolith and the presence of lavas underneath may be inferred from the stratiform appearance of those hills, while the geochemical resemblance to the Eildon suite of intrusions of a group of dykes and sills about a mile south-west of the Chiefswood (NT 5434) agglomerate neck, may be considered as a positive sign of continuation at depth between these two formations (McRobert, 1914).

Quantitative attempts were made for the interpretation of this high which appears in the observed profile AB (figure 5.7a). The steep gradient at the south-east margin of the granite continues with almost the same slope then nearly flattens in an area where there is not a very good control of gravity stations but, as mentioned previously, the continuation of this high is clear to the south-west.

The generation of this steep gradient of the margin of the granite batholith can be attained either by putting a denser mass at a depth between 6-12km or fixing it near the surface. In figure 5.14 to figure 5.17 representative models are shown. Thus, the interpretation has been approached either (1) by basement (2.78 g/cc) uplift or (2) by an intrusion near the surface. Both cases are discussed.

5.3.1 Basement uplift

Figure 5.14 and figure 5.15 represent quantitative models which match the observed profile. Gunn (1972) has interpreted the magnetic high over the Southern Uplands along a north-west south-east profile in south-west Scotland as due to a rise in the magnetic basement from 10 to 5km depth. Although the profile AB coincides with Gunn's magnetic high, his interpretation seems rather unlikely as it is not consistent with the seismic data (Jacob, 1969), which places a distinct refraction horizon at a depth of about 12km.

5.3.2 Near surface intrusion

In the author's opinion this is the most likely case. The existence of an intrusive layer of Lower Carboniferous age underlying the area and extending to the south-west is suggested by the geological account and the pattern of the aeromagnetic anomalies.

The Chiefswood agglomerate neck is associated with the most predominant feature, a strong positive magnetic anomaly which

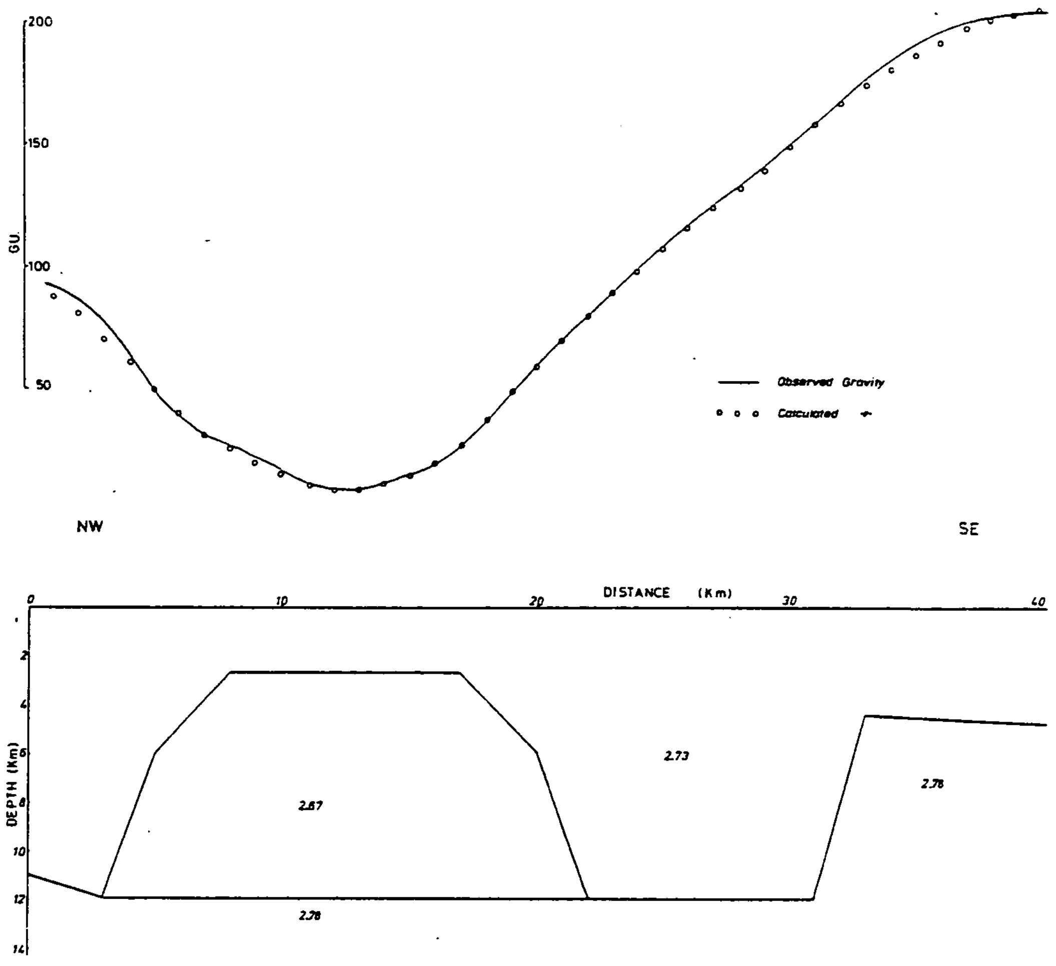

Fig. 5.14 Gravity profile AB. A possible interpretation of the gravity high at the south-eastern part in terms of basement uplift. Densities in g/cm^3.

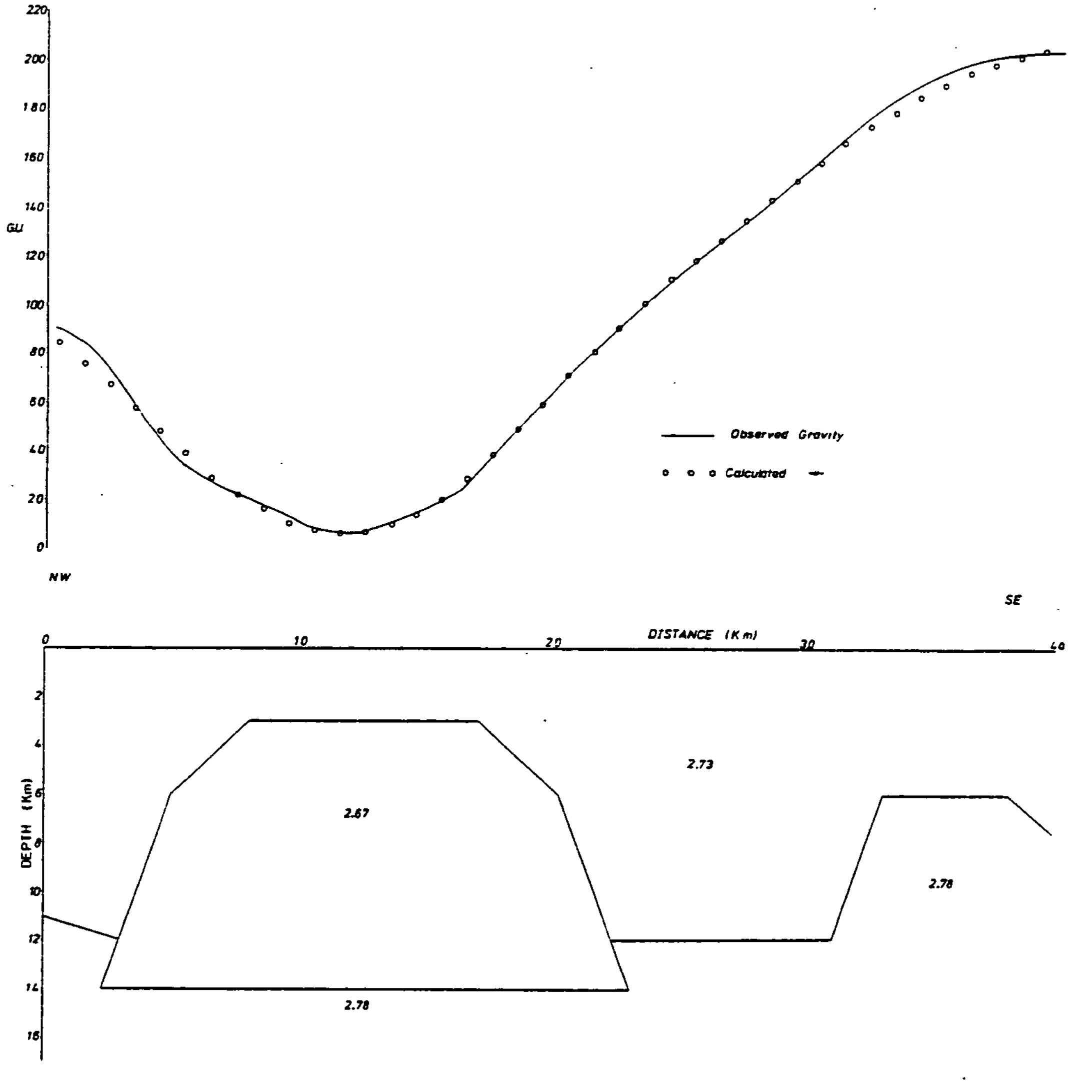

Fig. 5.15 Gravity profile AB. An alternative interpretation. Densities in g/cm^3.

has the shape characteristic of a stock-like source. Other minor magnetic highs are associated with local intrusive dykes and sills and the pattern suggests that there is an association or connection with the extrusive basaltic belt near Kelso.

While this is the situation to the north-east of the zero magnetic contour, to the south-west the pattern changes. The postulated intrusion associated with the south-east part of the profile AB does not show a clear magnetic expression and lies within a region of negative anomalies. Here, elongated magnetic features occur, trending north-west to south-east, which are associated with reversely magnetised Tertiary dykes (Bruckshaw and Robertson, 1949). These interrupt the major SW-NE magnetic high over the Southern Uplands.

Figures 5.16 and 5.17 show two representative models constructed to fit the gravity anomaly profile AB.

If the intrusion is at some depth below the surface as has been modelled in figure 5.16, then the picture of the magnetic field above the surface may be weak and untraceable. If it is near the surface, as in figure 5.17, then by being in an area where strongly magnetised dykes are predominant it may still be very difficult to trace. The whole aeromagnetic pattern is disturbed to the south-west of the zero magnetic contour.

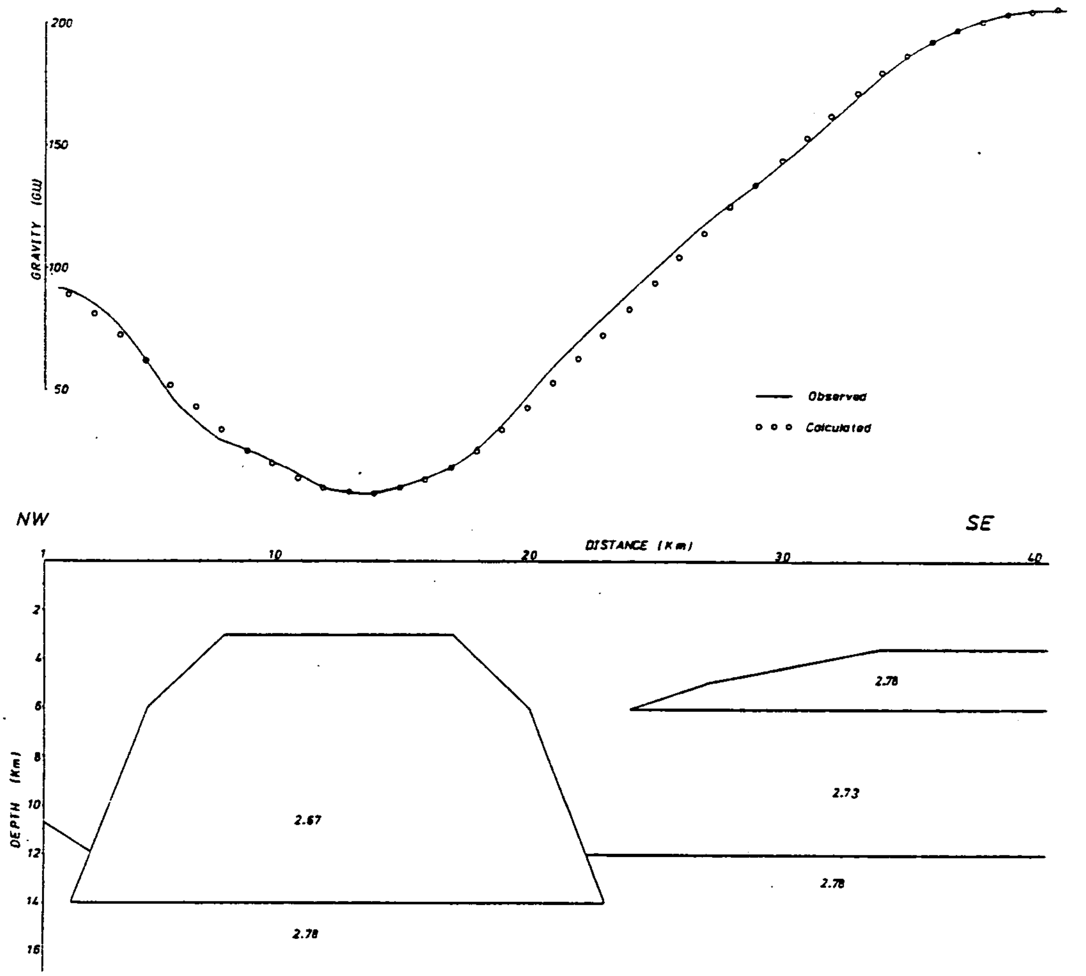

Fig. 5.16 Gravity profile AB. Alternative interpretation in terms of an intrusion at depth. Densities in g/cm^3.

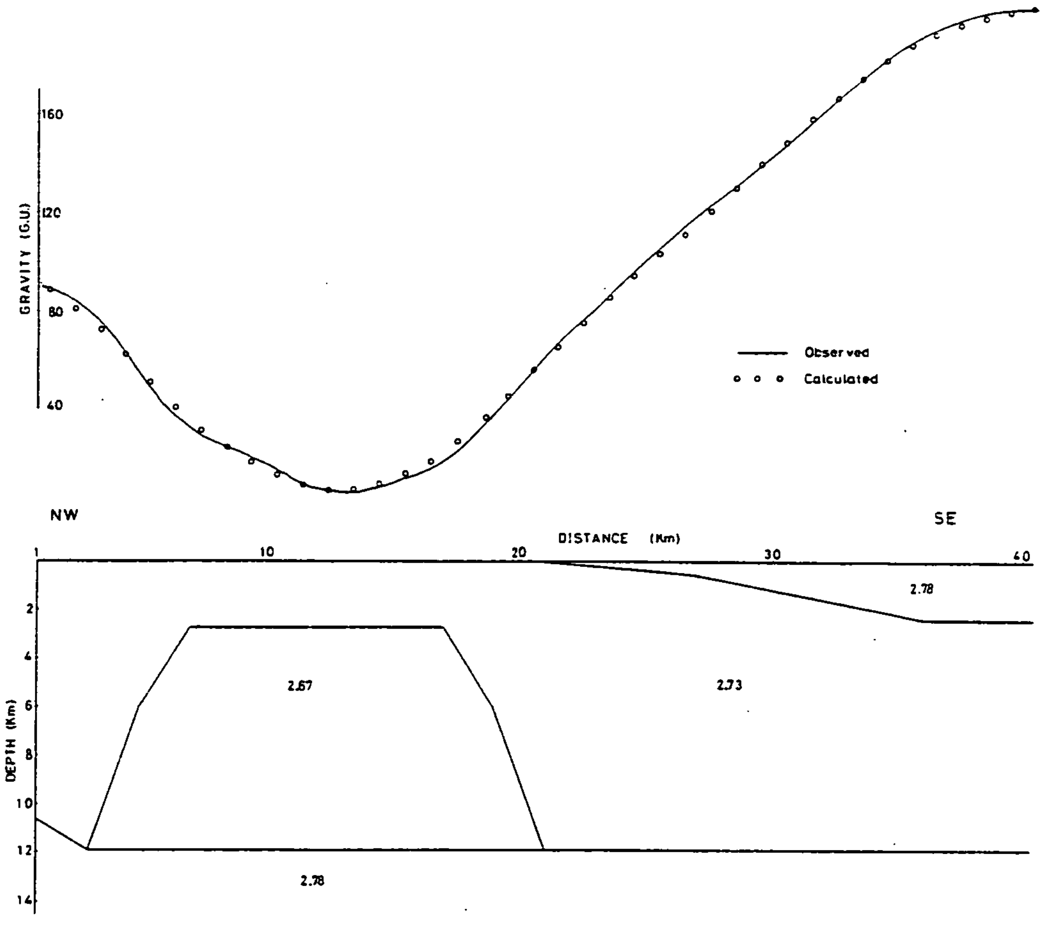

Fig. 5.17 Gravity profile AB. Alternative interpretation in terms of a near-surface intrusion. Densities in g/cm^3.

Finally, considering figures 5.15 and 5.16, a step on the south-eastern side of the granite at the basement was put in, in order to generate the correct trend to match with the observed profile. In figure 5.15, this was made more successfully than in the case represented by figure 5.16.

Although Gunn (1970) proposed a basement uplift like figure 5.14 on the basis of magnetic data, much of this anomaly is now interpreted as due to the granite. Moreover, this profile is not consistent with seismic evidence. However, the magnetic data tend to argue against a very shallow source of higher denser material. The small magnetic high shown on figure 5.13 at about 35 km along the profile is perhaps consistent with a source at intermediate depth, like figure 5.16, which is still consisted with a seismic refractor at 12 km depth.

5.4 North-eastern Southern Uplands

From the gravity data and the detailed model in the Tweeddale area it was obvious that the batholith extended at depth to the north-east, along the Caledonian trend, even though the axes in Tweeddale tend to swing E-W (see Fig.5.7 and the aeromagnetic anomalies, Fig. 5.12).

Before describing the attempt to model the gravity data over a larger area, the geological and aeromagnetic information will be outlined.

5.4.1 Geological evidence

From the beginning of this century, it was recognised that the Silurian strata of Midlothian, East Lothian and Berwickshire had been invaded by numerous igneous intrusions in early Devonian times, most of which are quartz-porphyrites, but a few have a granitic texture.

Considering the last category, the granitic masses of Priestlaw in East Lothian, Cockburnlaw and Lamberton Beach in Berwickshire and Broad Law in Midlothian were studied in detail by Walker (1924). Later on, a few more igneous bodies were incorporated in the study, notably the large Spango mass, the Polshill granite, the small Kirnie Law granitic exposure and the small dioritic-looking boss at Lyne Water (Walker, 1928) all of which can be seen in figure 5.18.

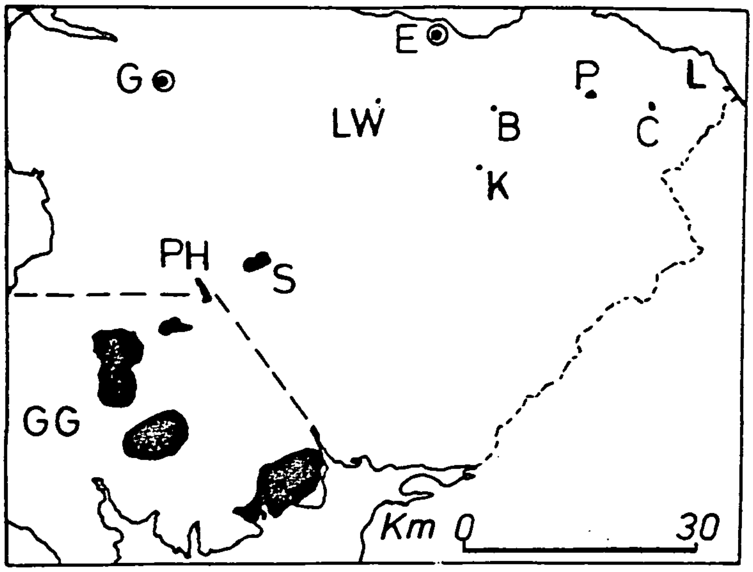

Fig. 5.18 Outcrops of granitic masses in the Southern Uplands (after Walker, 1928).

E: Edinburgh, G; Glasgow, GG: Galloway Granites,
P: Priestlaw Granite, C: Cockburnlaw Granite,
L: Lamberton Beach Granite, B: Broad Law Granite,
S: Spango Granite, PH: Polshill Granite,
LW: Lyne Water Granite, K: Kirnie Law Granite.
---- : Boundary separating the Galloway Granites

Their age is considered to be post-Silurian because they were intruded after the main Caledonian movements and show little or no Silurian foliation (Walker, 1928) and, from evidence of pebbles found in Upper Old Red Sandstone conglomerates, is restricted to the Lower and Middle Old Red Sandstone. Most of the above intrusions and particularly the masses of Priestlaw, Cockburnlaw, Broad Law and Lamberton Beach, are very similar petrographically and show a quartz-dioritic magma composition which is strongly allied to the granodiorites of Galloway (Walker, 1924, 1928). The tonalitic or granodioritic magma, prevalent over such a wide area is the most striking feature of that belt of the British Caledonides, and it is quite probable that the plutons are the underground expression of the Lower Devonian volcanic activity, forming a layer of similar magmatic composition and continuous at depth.

5.4.2 Aeromagnetic anomalies

All of the granitic masses in south-east Scotland are associated with strong magnetic anomalies. From the aeromagnetic map (in back-pocket), the Priestlaw granitic intrusion is associated with a positive magnetic expression of a total amplitude of 110 nT and from the form of the anomaly it is suggested that the intrusion is a steep-sided, stock-like body, normally magnetised in the earth's present magnetic field. From the smoothed version of the aeromagnetic map (Gunn, 1972), it is concluded that the body extends to a large depth. Modelling attempts (Bennett, 1969) have shown a value of $\sim$ 12 nT for the magnetisation contrast. The Cockburnlaw intrusion is also associated with a positive aeromagnetic anomaly of 100 nT and from the shape of the anomaly it is suggested that the body is elongated, with an east-west direction. The Lamberton Beach intrusion falls within the largest positive magnetic anomaly in Berwickshire, but this will be discussed later.

All these aeromagnetic anomalies are clearly associated with instrusions which are exposed. However, the aeromagnetic map reveals other features similar in shape to them.

A roughly circular positive magnetic anomaly to the west of the Priestlaw exposure occurs in the vicinity of Lammer Law (NT 5761), with a total amplitude of 60 nT. The shape of the anomaly reveals a stock-like intrusion, similar in form to that in the Priestlaw area. Since, as will be outlined farther on, it coincides with a small negative residual gravity anomaly, it is strongly believed that it is caused by another granitic boss coming near to the surface, something which Bennett has already suggested. He carried out detailed ground magnetic traverses in an attempt to delineate the boundaries of the intrusion.

According to his results, the top of the body may lie at about 170-330 metres below O.D. and the estimated magnetisation contrast between the intrusion and the country rock is close to the one estimated for Priestlaw, ie, 13-14 nT.

Thus the magnetization of both the Priestlaw and Lammer Law granites is very close to that found for Tweeddale.

Also from the aeromagnetic map (back-pocket) another smaller closure occurs south of Priestlaw intrusion with a positive amplitude of 60 nT near Byrecleugh (NT 6258) which, from ground magnetic surveys (Bennett, 1969) proved to be two distinct anomalies, suggesting the presence of two intrusions, one at Byrecleugh and the other farther north. The latter coincided with an unnamed hill at NT 637601, and is probably produced by a small stock-like body, normally magnetised, rather near to the surface.

5.4.3 The Berwick upon Tweed aeromagnetic anomaly

The Berwick upon Tweed aeromagnetic anomaly is the most prominent feature of the aeromagnetic map in the Berwickshire area (figure 5.20). The amplitude of the anomaly is more than 250 nT and shows a body which is elongated NW-SE, within a region of negative gravity anomalies. The anomaly is only 20km north of the Cheviot suite.

A profile (M2) was constructed and the shape of the anomaly is shown in figure 5.21. A rough interpretation was attempted from the shape and the amplitude of the anomaly (figure 5.21) by the method developed by Bruckshaw and Kunaratnam (1960).

Assuming a uniform magnetisation of the body, represented by a two-dimensional thick slab, the depth to the top of the slab, its width and its magnetisation can be obtained from this method. It was found that the depth to the top of the causative body is 1.5 ± 0.3km, with a width of 2.5km and an amplitude of magnetisation of 1700 nT corresponding to a susceptibility of about 0.034 .

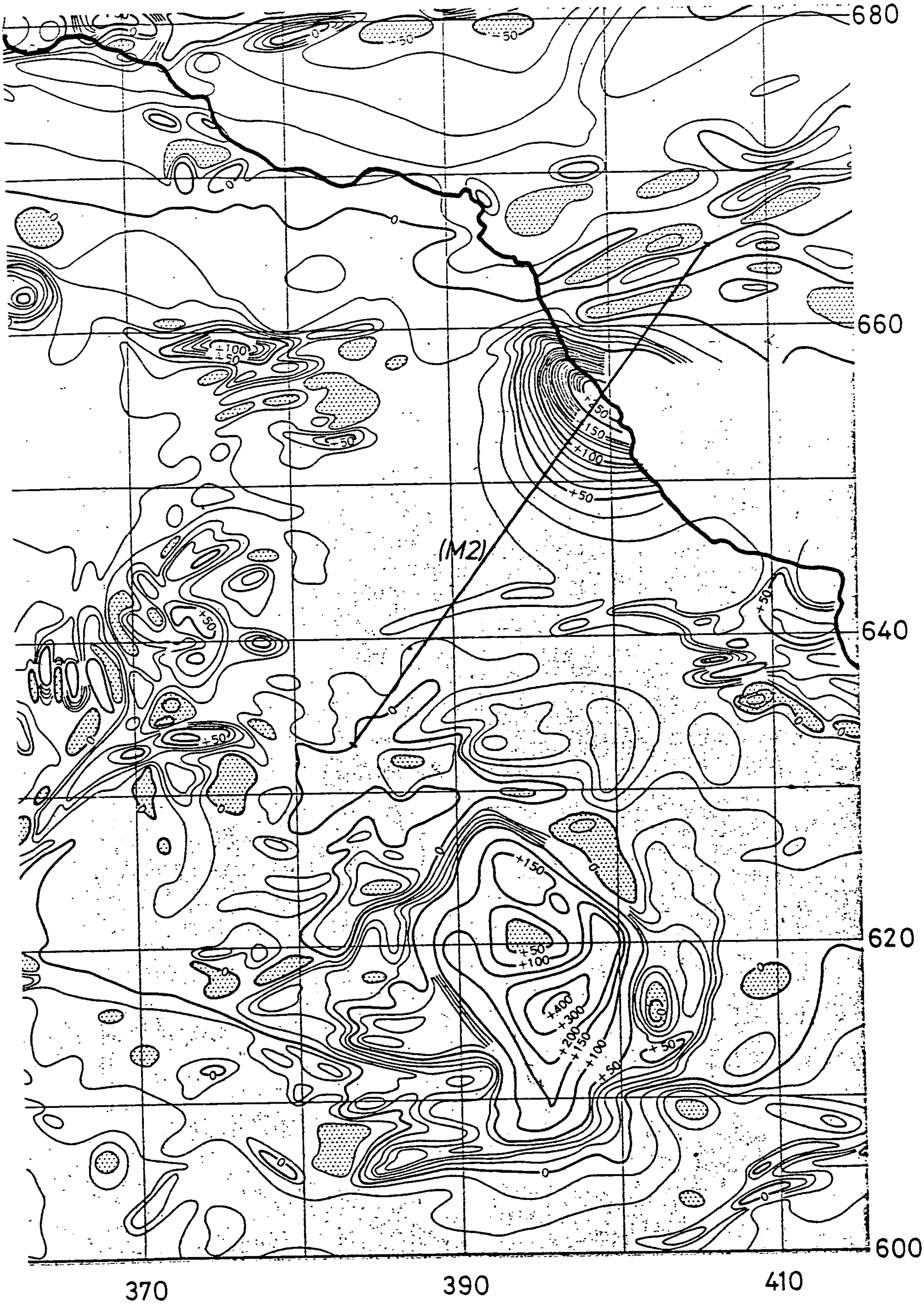

Fig. 5.20 Aeromagnetic map of part of Berwickshire (after Bullerwell, 1968), showing also direction of profile (M2). Contour interval 10nT.

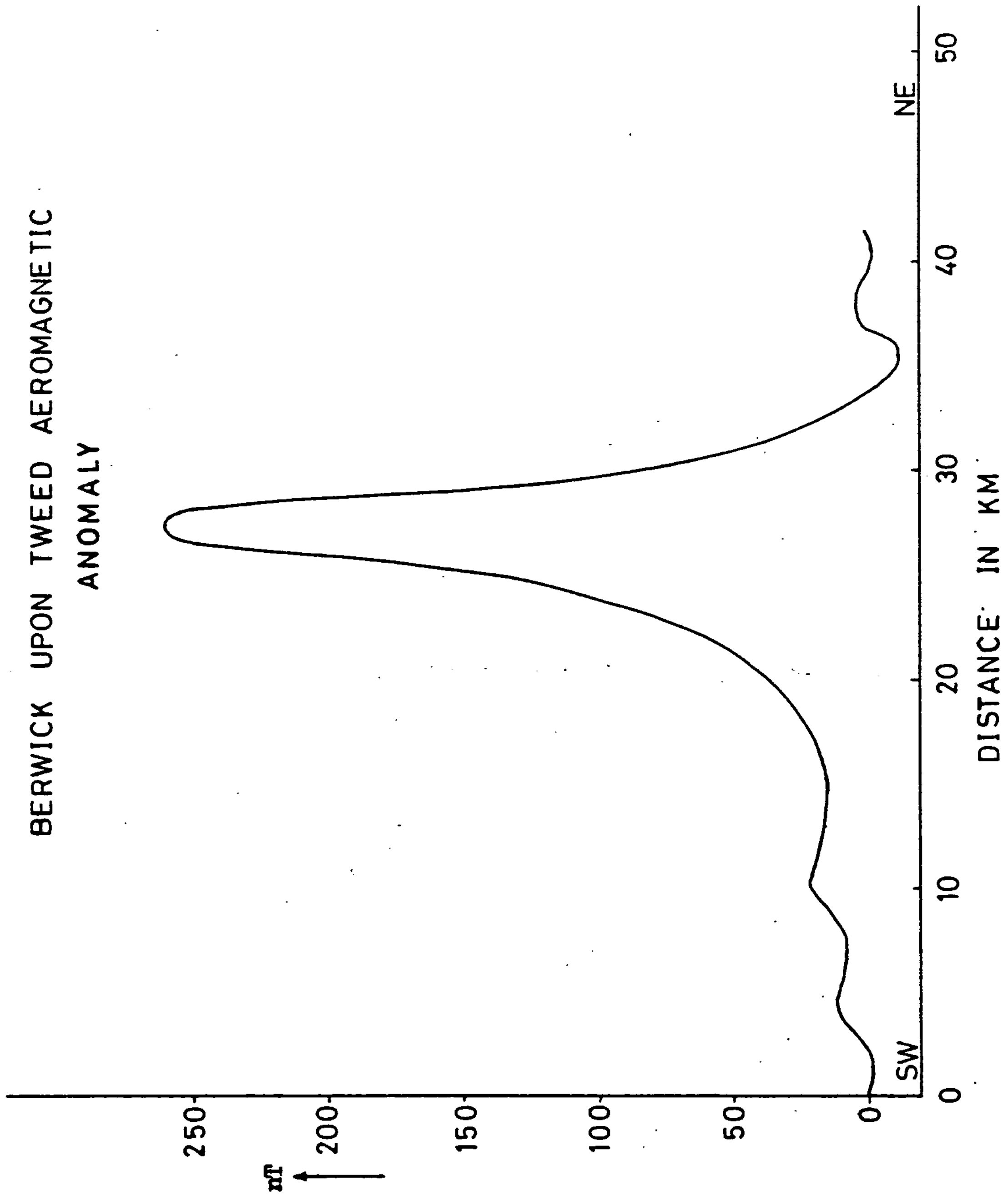

Fig. 5.21 Magnetic profile (M2) with coordinates NT 837332 and NUØ62652.

All of the above results must be considered carefully, because the assumptions of the method are not very realistic.

For the moment, the cause of the Berwick aeromagnetic anomaly is quite speculative, but there are indications that this intrusion might be a granitic one:-

(i) The Lamberton Beach acid intrusion is only 6-7km to the north-west of Berwick and definitely falls within the region of the strong positive magnetic anomaly. Also, all the other small bosses in East Lothian (Lammer Law, Priestlaw) are characterised by positive magnetic anomalies but with **smaller amplitude.**

(ii) The susceptibility of the intrusion falls within the limits of granites (with magnetite) variation (Parasnis, 1972).

(iii) The causative body falls in a region where negative gravity anomalies occur. To the north-east of Berwick upon Tweed a narrow negative gravity anomaly belt extends about 20km offshore (Tully and McQuillin, 1978). It is not clear if this gravity anomaly belt can be exclusively attributed to the succession of the Carboniferous sediments.

The postulated intrusion might have played an important role in the formation of the Shiell's (1963) Monocline (figure 5.21a), which resulted from E-W compression. It is suggested that the offshore granitic(?) intrusion should have given greater stability on the foreshore part of the monocline and during the Hercynian movements the uplift of the Southern Uplands block

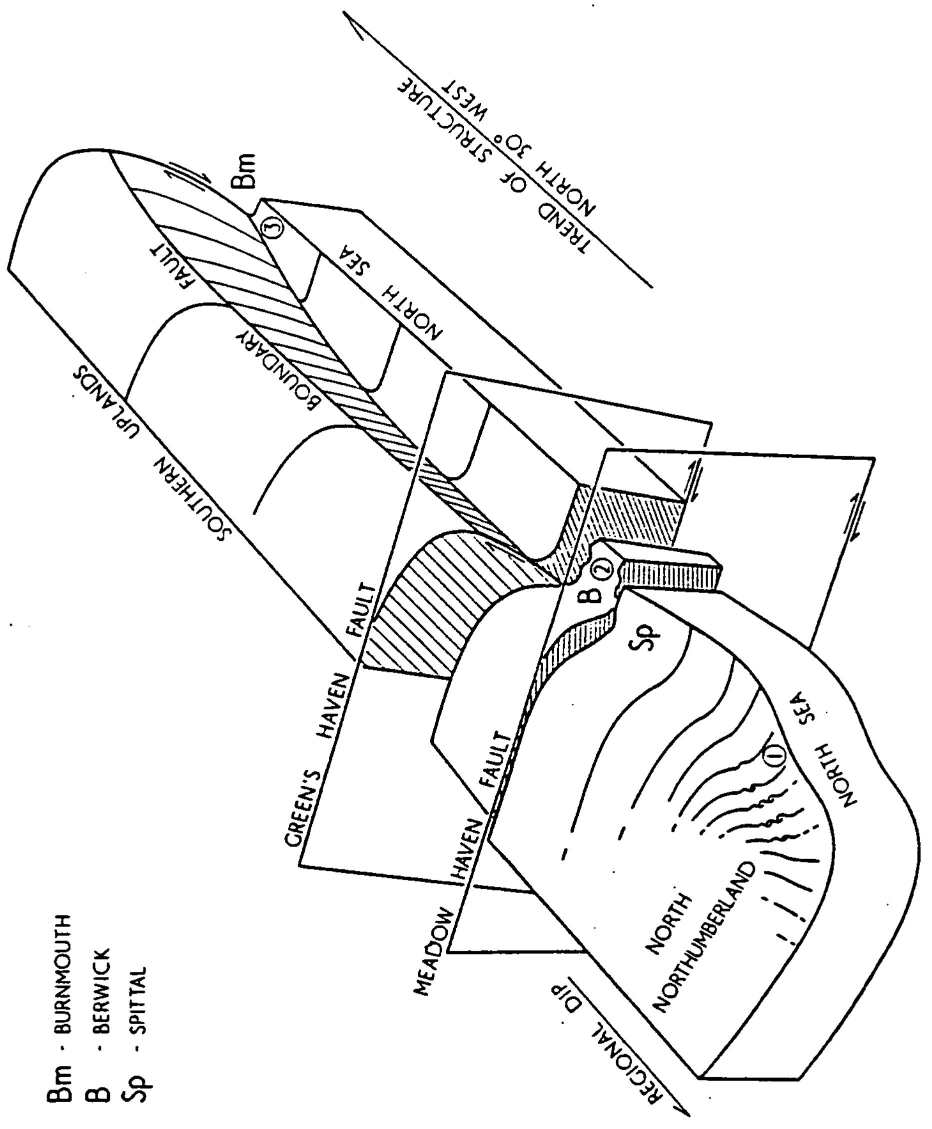

Fig. 5.21a Diagramatic representation of the Berwick Monocline (after Shiell, 1963). Length of the structure is about 14km.

took place along the plane of weakness forming the reverse Boundary Fault (figure 5.21a).

The interpretation of the aeromagnetic anomaly as due to the granite might be wrong: it might be due to associated lavas like parts of the Cheviot magnetic anomaly, but in this case hidden by the Carboniferous.

5.4.4 Gravity Modelling

Because the negative gravity anomaly in the Tweeddale is distinct and closed, this area was examined separately (section 5.2) and modelled in sections 5.2.4.1 (gravity) and 5.2.4.2 (magnetic). Section 5.4 is dealing with the less well-defined extension of the Tweeddale anomaly to the north-east, where it covers most of the eastern Southern Uplands. In this part, section 5.4.4, almost the whole of this negative anomaly will be modelled.

The gravity data were rotated 35° so that the upper (NW) margin of the Bouguer gravity anomaly map of the area where the granite batholith was going to be modelled was delineated by the Lammermuir Fault. The north-east edge of the gravity map was just before the beginning of the Upper Devonian sediments of the Oldhamstocks-Cockburnspath basin. Figure 5.22a shows the Bouguer gravity anomaly map which has dimensions of 18 x 60km.

In this area the Upper Old Red Sandstone sediments of the Lauderdale area have been stripped off (see detailed modelling of that area in Chapter VI). Figure 5.22b shows the residual Bouguer gravity anomaly map, where again, the calculated quadratic regional gravity field from the LISPB model (figure 5.3) has been removed.

Both maps in figure 5.22 were reduced with the standard Bouguer density 2.67 g/cc and the GPCP generated an array of 2km grid size. Subsequently, program MODG3D was used to construct a model of the interface with 2km side square blocks.

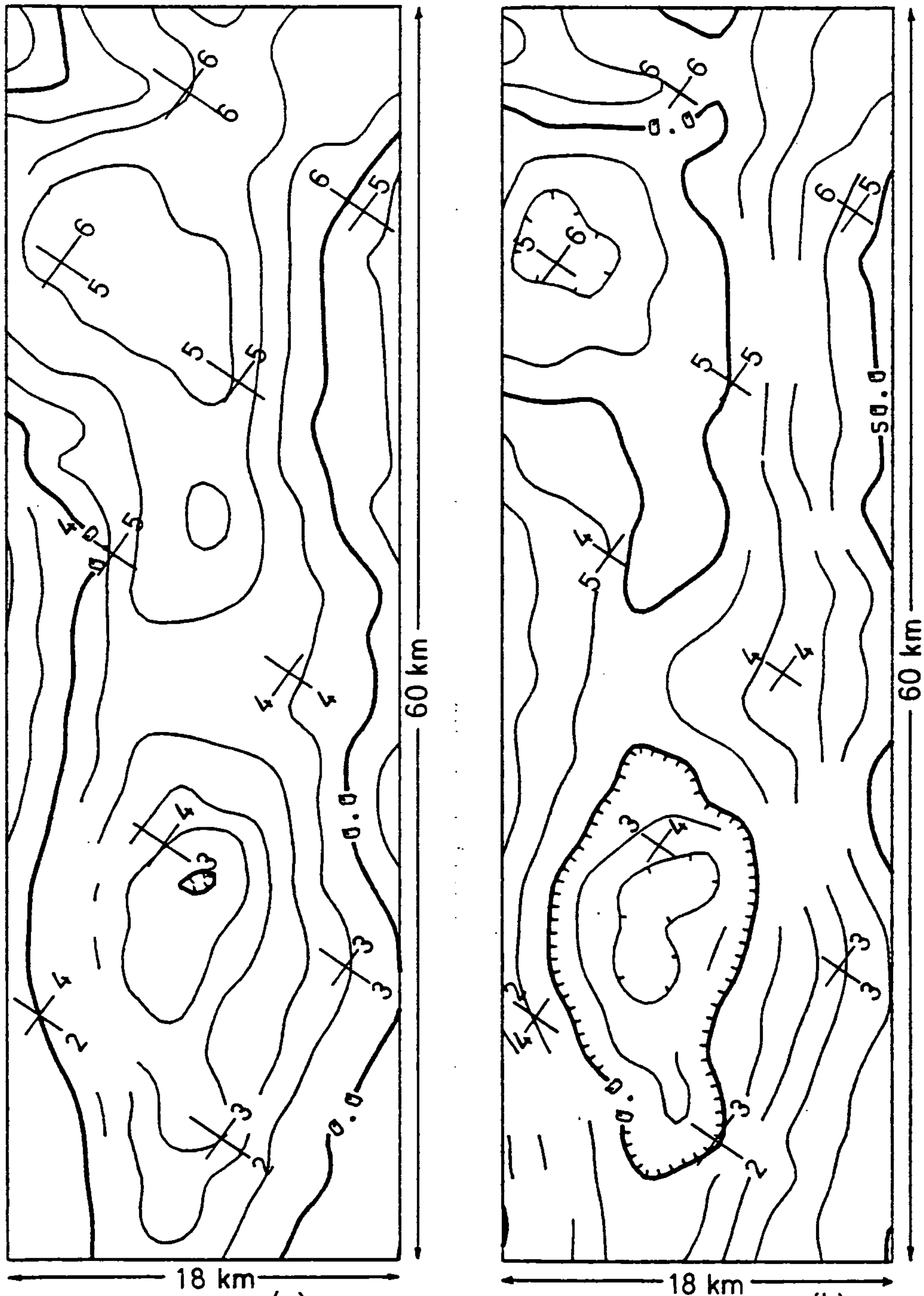

Fig. 5.22 (a) Bouguer gravity anomaly map.

(b) Residual gravity map.

Contour interval 10 gu. Intersections show 10km National Grid square lines.

Depth control was applied by fixing a point in the Tweeddale area at a depth of 2km. The resulting model is shown in figure 5.23, 5.23a, 5.23b where the density contrast is 0.06 g/cc. Any other density contrast with a value close to the one of 0.06 g/cc will not cause a significant change in the overall shape of the model, only a displacement in the vertical scale.

The general shape of the batholith over the Tweeddale area has not significantly changed, but as can be seen from the model, the granite appears to reach even shallower depths (less than 1km) around the Lammer Law area. This is actually expected looking at the residual gravity map. To the north-east of the Lammer Law the granite is dipping again. It appears that the boss under the Lammer Law area is a comparable feature to the Tweeddale granite. It extends to the north-west and is responsible for the offset to the north-west of the zero anomaly contour of the gravity map.

Therefore, it is quite probable that the steep gravity gradients observed over East Lothian are caused by the granite batholith, deepening steeply to the north-west after coming nearest to the surface under the Lammer Law region.

Because the Southern Uplands are characterised by high elevation, particularly the Tweeddale area, it was thought that the gravity map over that area might be topographically biased. For this purpose it was decided to compile a gravity map reduced with a more representative Bouguer density for the whole area of the Southern Uplands covered by the study area. The value of

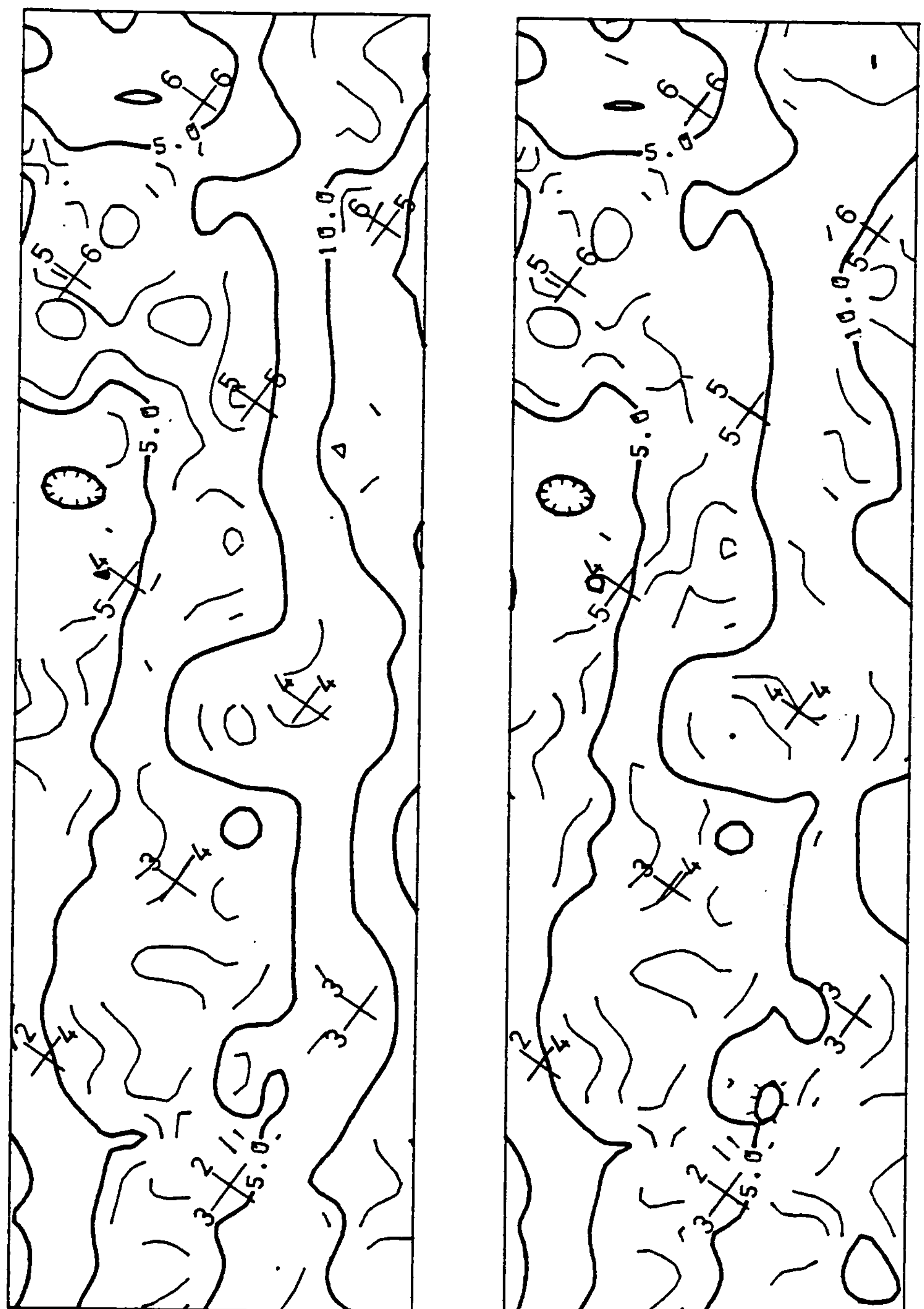

Fig. 5.23 Isodepth map of the Southern Uplands batholith at 1km contour interval. Intersections represent 10km National Grid square lines. (a)(b) modelling results subtracting a linear and quadratic trend (LISPB) respectively from the gravity map of figure 5.22(a).

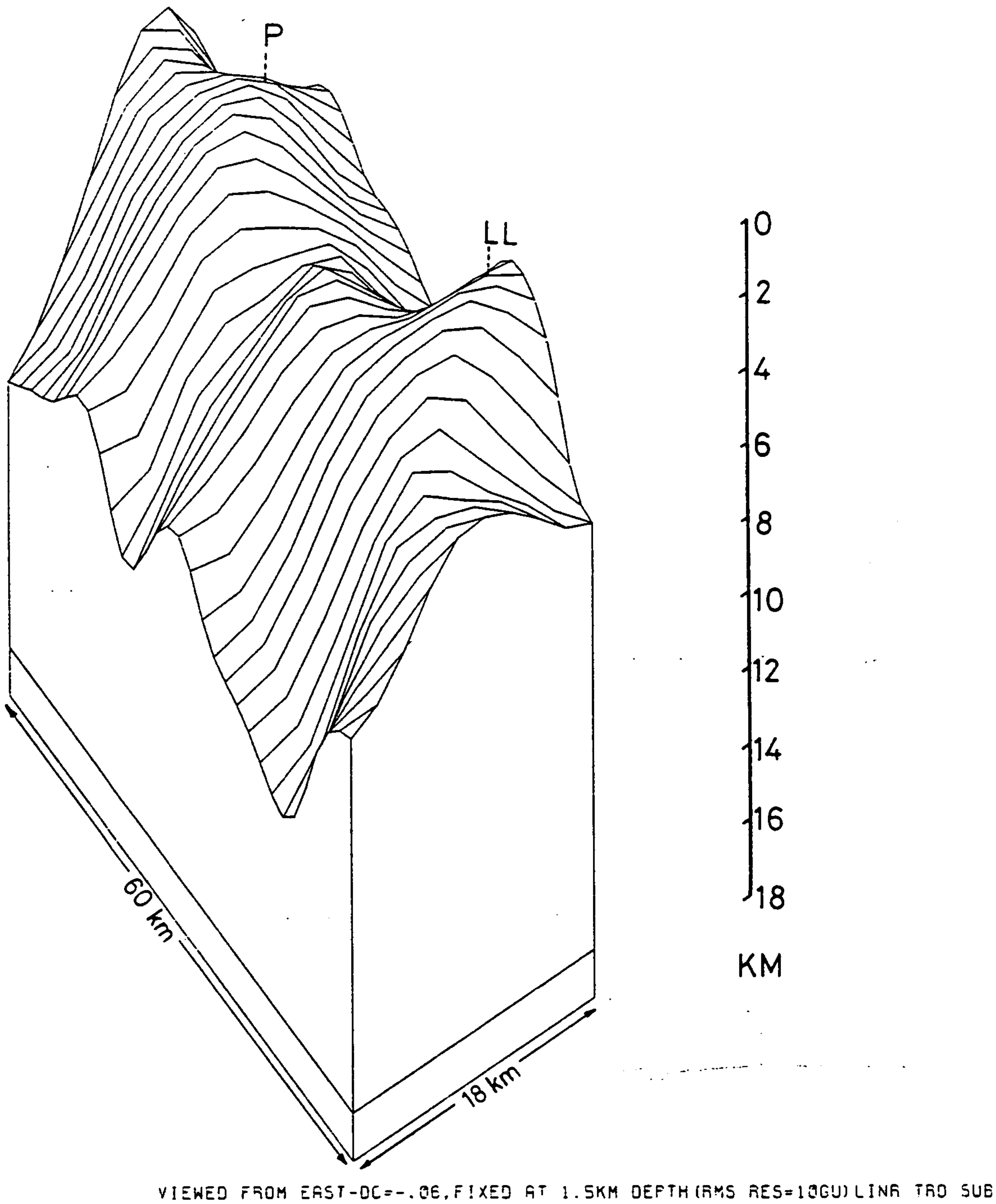

Fig. 5.23a Three-dimensional model of the Southern Uplands batholith viewed from the east. Density contrast 0.06 g/cm^3. Linear trend (LISPB) subtracted, LL: Lammer Law; P: Peebles.

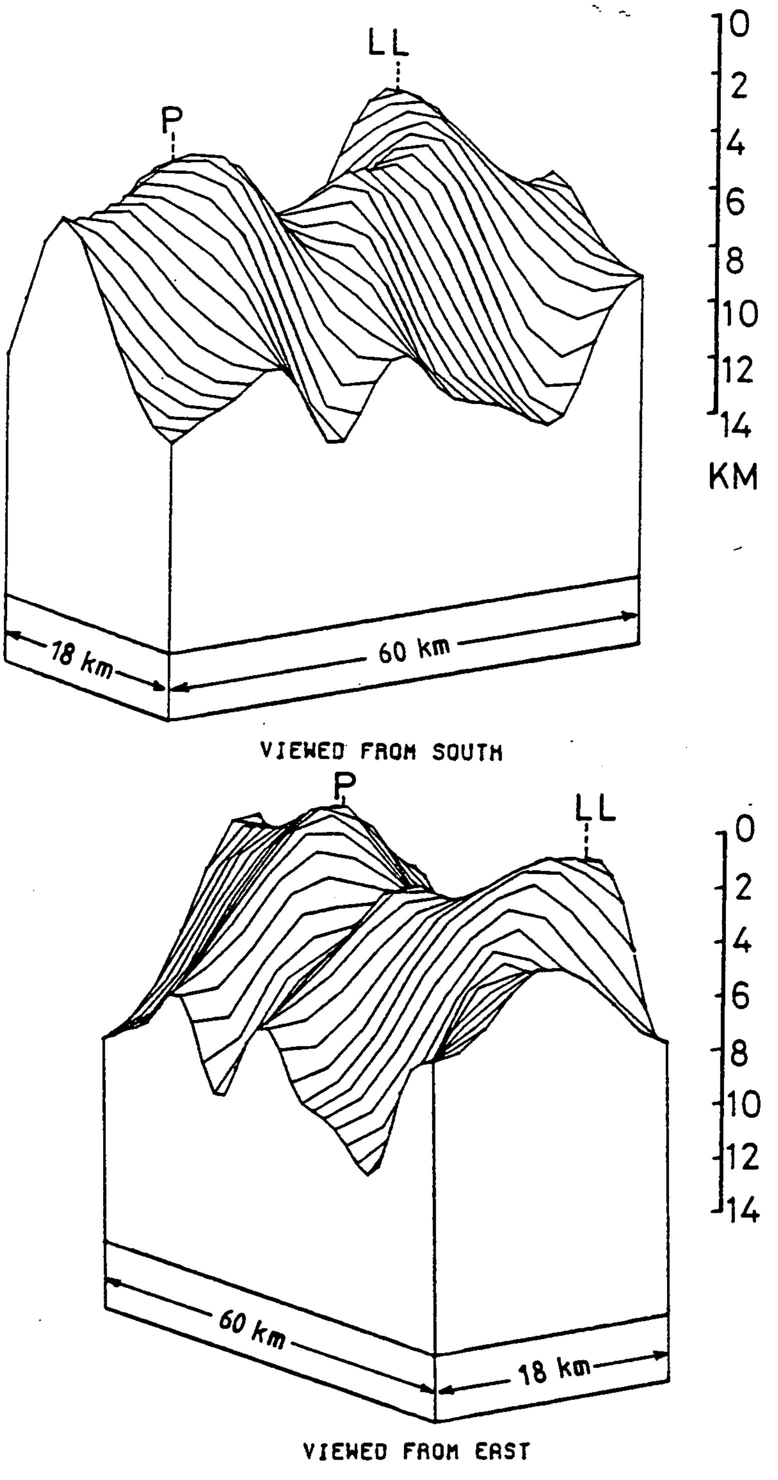

Fig. 5.23b Three-dimensional model of the Southern Uplands batholith (subtracting a quadratic trend (LISPB)). P: Peebles; LL: Lammer Law.

2.70 g/cc was chosen and the map is shown in figure 5.24.

The Tweeddale granite was, after that, remodelled, although no radical changes were expected in the model. From the gravity map (figure 5.25a), the residual map was constructed (figure 5.25b), subtracting as before the regional gravity field calculated from LISPB.

Again, MODG3D program was used to approximate the interface of the granite with a density contrast of 0.08 g/cc and square blocks of 2km side. The resulting model is shown in figure 5.26(a,b).

The gravity map of the north-east part of the Southern Uplands has hardly changed. The Lammer Law boss appears in a clearer manner than before now that the -40 gu closure has appeared there and, near the Priestlaw area and south of it, the batholith is expected to be at a slightly shallower depth than it was before (figure 5.23).

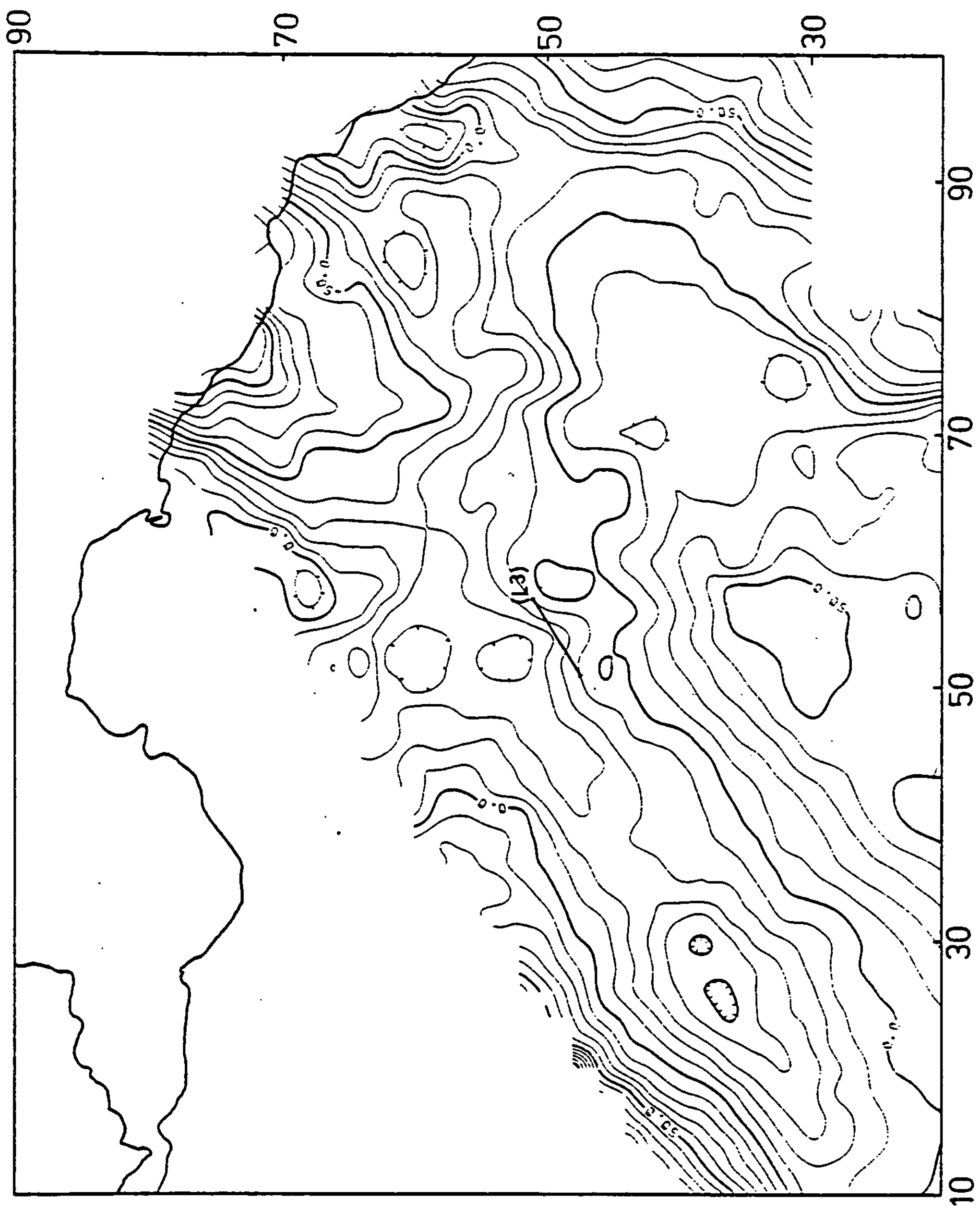

Fig. 5.24 Bouguer gravity anomaly map, compiled with Bouguer density 2.70 g/cm^3 and plotted at 10 gu contour interval (Grid size 2km).

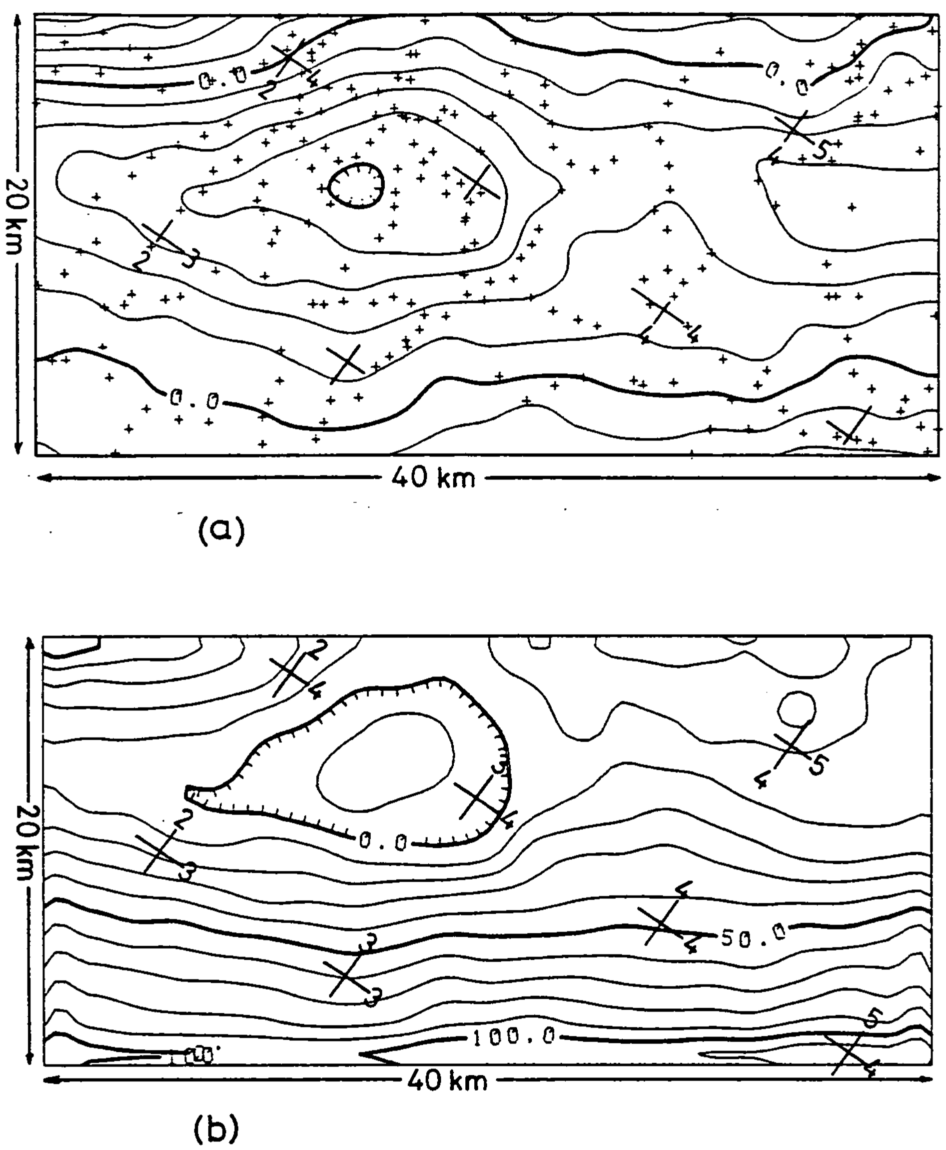

Fig. 5.25 (a) Bouguer gravity anomaly map compiled with 2.70 g/cm^3 Bouguer density. Contour interval 10 gu (crosses represent gravity stations).

(b) Residual gravity map at 10 gu contour interval. Both maps were plotted by GPCP at a 2km grid interval. Intersections show 10km National Grid square.

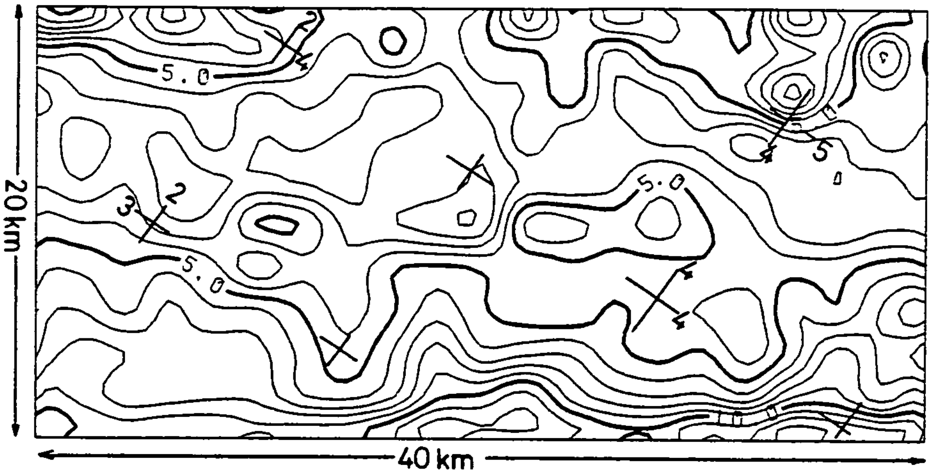

(a)

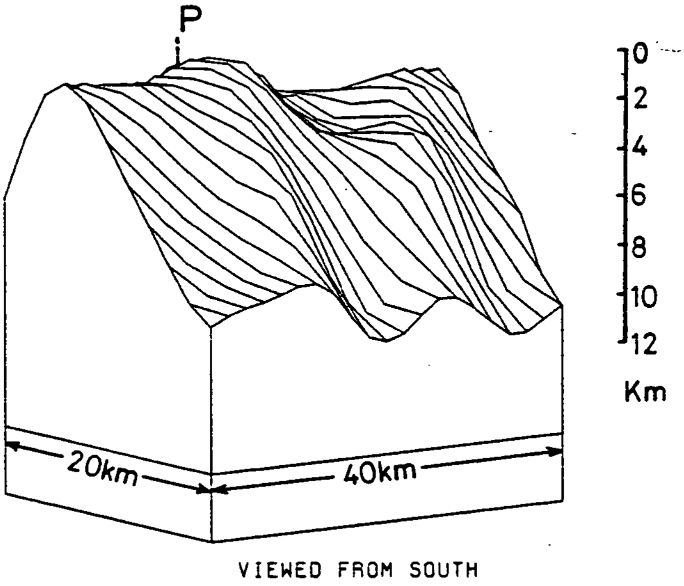

(b)

Fig. 5.26 (a) Isodepth of the Southern Uplands batholith covering the same area as the residual gravity map (figure 5.25b).

(b) Three dimensional model of the upper surface of the batholith covering the same area as map in figure 5.25b. P: Peebles.

CHAPTER VI

DEVONIAN BASINS AND THE EAST LOTHIAN AREA

6.1 Introduction

The scope of this chapter is the modelling of the Devonian basins of East Lothian and Eastern Berwickshire, the investigation of the north-eastern component of the Southern Uplands Fault System and the quantitative modelling of the East Lothian Lower Carboniferous lavas.

6.2 Devonian Basins of SE Scotland

6.2.1 Introduction

In East Lothian and Berwickshire, the outcrops of the Old Red Sandstone sediments are confined to the south-east of the Dunbar-Gifford Fault; they comprise of a belt which, starting from Gifford, stretches to the north-east, between the Dunbar-Gifford Fault and the Lammermuir Fault to Dunbar, and thereafter, to the south-east through the Monynut Edge towards the west of Duns. Two belts extend eastwards from Monynut Edge, one narrow belt reaching the coast at Cockburnspath and Siccar Point and the other, farther south, reaching St Abb's and the Eyemouth coast.

The same belt west of Duns extends to the south-west and joins with the sediments of the Lauderdale District to the north and, to the south, it extends beyond Jedburgh. To the north of the Lauderdale Basin there are two more patches of Old Red Sandstone which form almost a continuous belt to the north through Channelkirk, joining with the Fala and Soutra conglomerate on either side of the Lammermuir Fault. Except for the red feldspathic sandstones and conglomerates around Eyemouth and St Abbs which belong to the Lower Old Red Sandstone, all the other exposures appear to belong to the upper division. In this region it is probable that those sediments described as belonging to the Upper Devonian are in fact of Carboniferous age (Greig, 1971), as the division between these two facies can only be drawn with difficulty.

It is believed that the Upper Old Red Sandstone once covered a much larger area than today, extending over the Lammermuirs. By denudation and erosion the conglomerates now mark the margins of those hills, lying unconformably upon the Silurian greywackes. The Upper Old Red Sandstone subdivisions in East Lothian and Berwickshire are the Lower or Great Conglomerate and the later one, the Upper Red Sandstones and Marls with occasional pebbly beds (Howell, et al, 1866). Later, Clough et al (1910) and Greig (1971) considered the sandstones south-east of the Lammermuir Fault, near Gifford and Fala as the lowest division.

According to the original workers, the downward movement under which the deposition of these sediments took place brought the whole Lammermuir chain under shallow water and covered them with conglomerates and sandstones, but recent sedimentological work on the Upper Old Red Sandstone sediments of the Scottish Borders (Leeder, 1973) has shown a wholly fluviatile origin. Under the same fluviatile environment, deposition occurred in the Fife and Kinross area, controlled by an eastward dipping palaeoslope (Chisholm and Dean, 1974).

Generally in the northern part of the Midland Valley the deposition of the Old Red Sandstone took place along a SW to NE trending axis, south of, and parallel to, the Highland Boundary Fault, thinning south-westwards. The palaeoslope in the Lower Devonian had a south-west dipping direction (Bluck, 1978; Morton, 1979), during which a red-bed sedimentary sequence of probably alluvial origin (western Midland Valley) was developed in a fault controlled basin (Morton, 1979). During Upper Devonian times the palaeoslope changed and, generally, a SE dipping direction was shown (Bluck, 1978).

Although geologists seem to agree about the direction of the palaeocurrents near the northern margins of the Midland Valley, the same is not true in the Borders region. Paterson et al (1976) disagree with Leeder (1973), figure 6.1, suggesting the orthogonal direction of palaeocurrents (eastward or south-eastward dipping palaeoslope), and in a few places they disagree with Smith (1967).

The granite batholith under the north-eastern part of the Southern Uplands puts a constraint on the direction of the palaeocurrents. The SE direction of the palaeocurrents indicated by Paterson et al (1976) is more consistent with the uplift of the Lammermuirs caused by the batholith and the generally southerly direction of the drainage system in Upper Devonian times. Bluck's (1978) picture, figure 6.2,

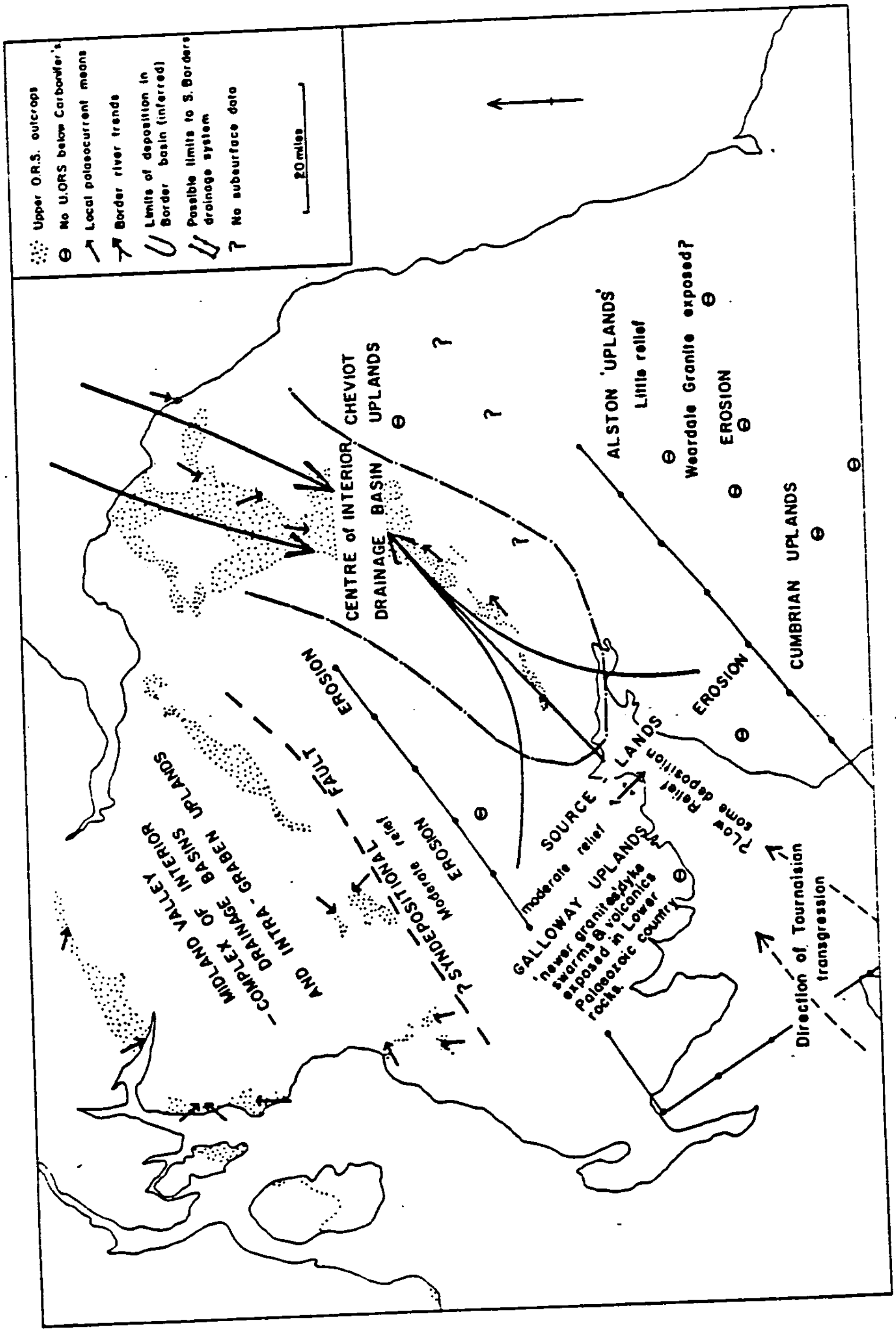

Fig. 6.1 Palaeogeography of South Scotland and northern England of Upper Old Red Sandstone, indicating the drainage system of that area (after Leeder, 1973).

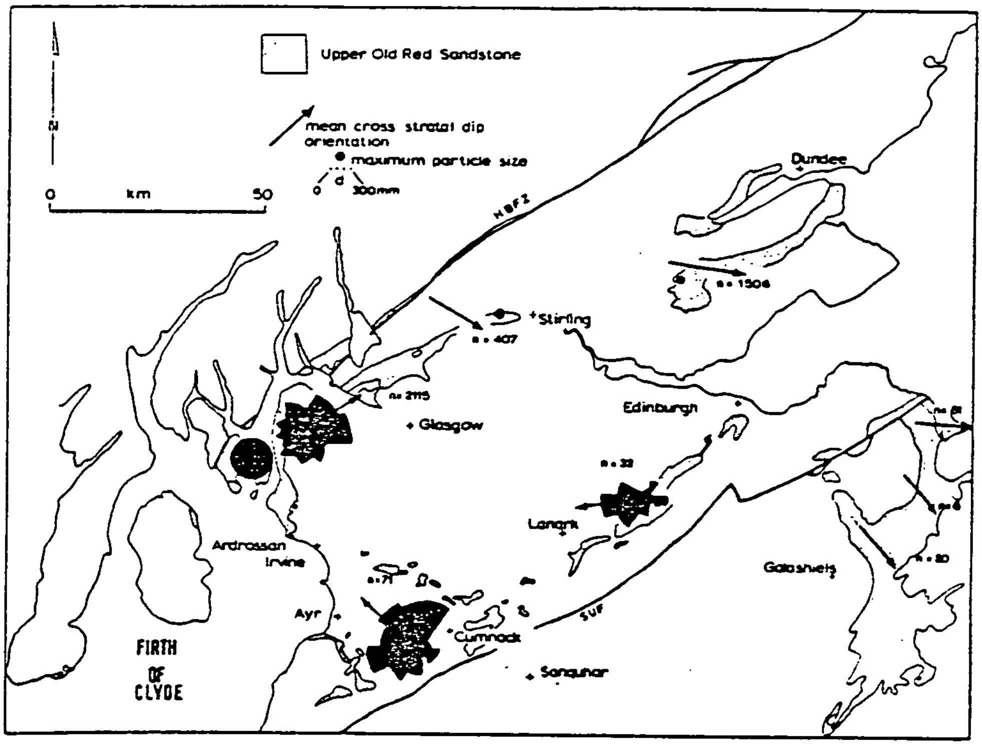

Fig. 6.2 Directional structures and an average maximum clast size for the basal part of Upper Old Red Sandstone (after Bluck, 1978 (fig. 11)).
SUF: Southern Uplands Fault; HBFZ: Highland Boundary Fault zone.

shows this even more clearly: the deposition of the Upper Old Red Sandstone has taken place in a peripheral manner around the uplifted zone of the NE termination of the Southern Uplands.

In the following, parallel to the geological account a geophysical picture based on gravity data will be given for the areas of Lauderdale, Eyemouth and Oldhamstocks.

6.2.2 Lauderdale Basin

The conglomerates of Lauderdale seem to mark the course of a deeply eroded valley which, as it drains to the south, today opens out southwards and flattens, particularly to the south-east. The ridge which separates the Soutra conglomerates with the ones at the head of the Lauder Basin seemed to exist before the deposition of the Upper Old Red Sandstone over that area (Clough et al, 1910), this is compatible with the granite emplacement and uplift after the end of Silurian times. At a later epoch when the local erosion greatly increased, the conglomerates gathered on the bottom of the valley and farther to the south along the gentler slopes, followed later on by the accumulation of red sandstones and marls of the local drainage system with a south-easterly direction.

The cross-sectional shape of the basin is suspected, especially from the northern part to about Lauder in the south, to have a V-shape, because of the configuration of the gravity contours. In order to avoid complications due to the regional gravity field, gravity profiles were traced across it parallel along the Caledonian trend.

Two profiles, located on figure 4.7 have been taken from a 5 gu contour gravity map, compiled with Bouguer density of 2.67 g/cc and plotted using the TRIANG routine. The observed profiles were digitised at 100m intervals and the MODG2D automatic inversion program was used. The density contrast used between the Silurian greywackes and the Upper Old Red Sandstone sediments was 0.20 g/cc.

This density contrast is rather too large for the contrast between greywacke and conglomerate. In the western part of Scotland, McLean (1961a) found 2.54 ($\pm$0.02)g/cc for fine quartz conglomerate. Tables II-2 and II-3 show a mean value of 2.62 g/cc for the Great Conglomerate. However, because this basin is not filled exclusively with conglomerates but also with sandstones, the density contrast 0.20 g/cc is probably realistic.

The resulting model from those two profiles, figure 6.3, 6.4 show a V-shaped valley with a depth of about 300m below ground level.

Because the Lauderdale Valley fluctuates in an altitude between 600 and 700ft and the surrounding hills between about 1250 and 1450ft (Hog's Law, NT 555 552), it was thought that the gravity map, from which those two profiles were traced, might be topographically biased. For this reason the gravity data were reduced with a 2.70 g/cc Bouguer density, which is

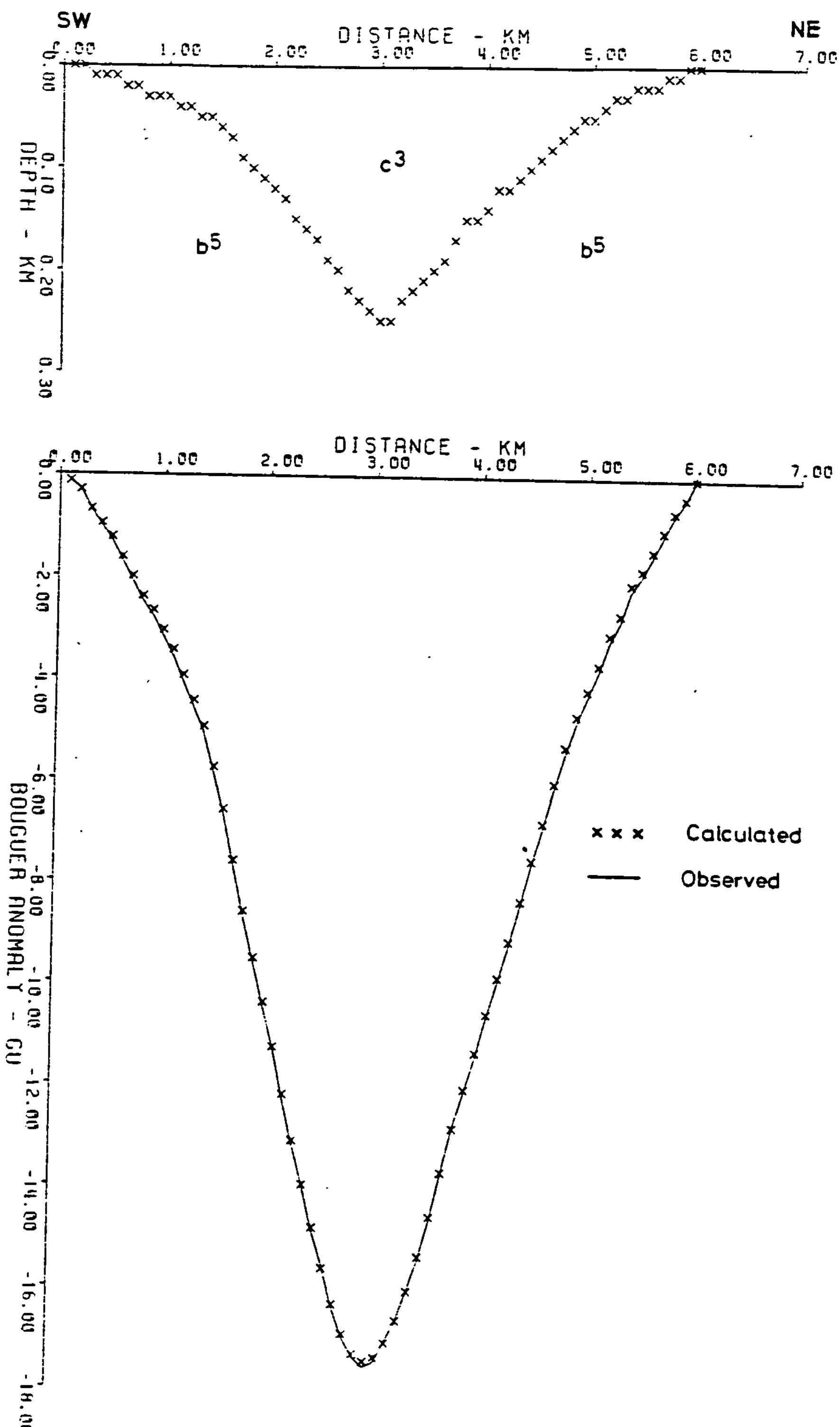

Fig. 6.3 Profile (L1). Interpretation of the Lauderdale Upper Old Red Sandstone basin. National Grid coordinates of the end points of the profile are NT 515 478 and NT 565 511. Density contrast -0.20 g/cm^3. c^3: Upper Old Red Sandstone; b^5: Silurian.

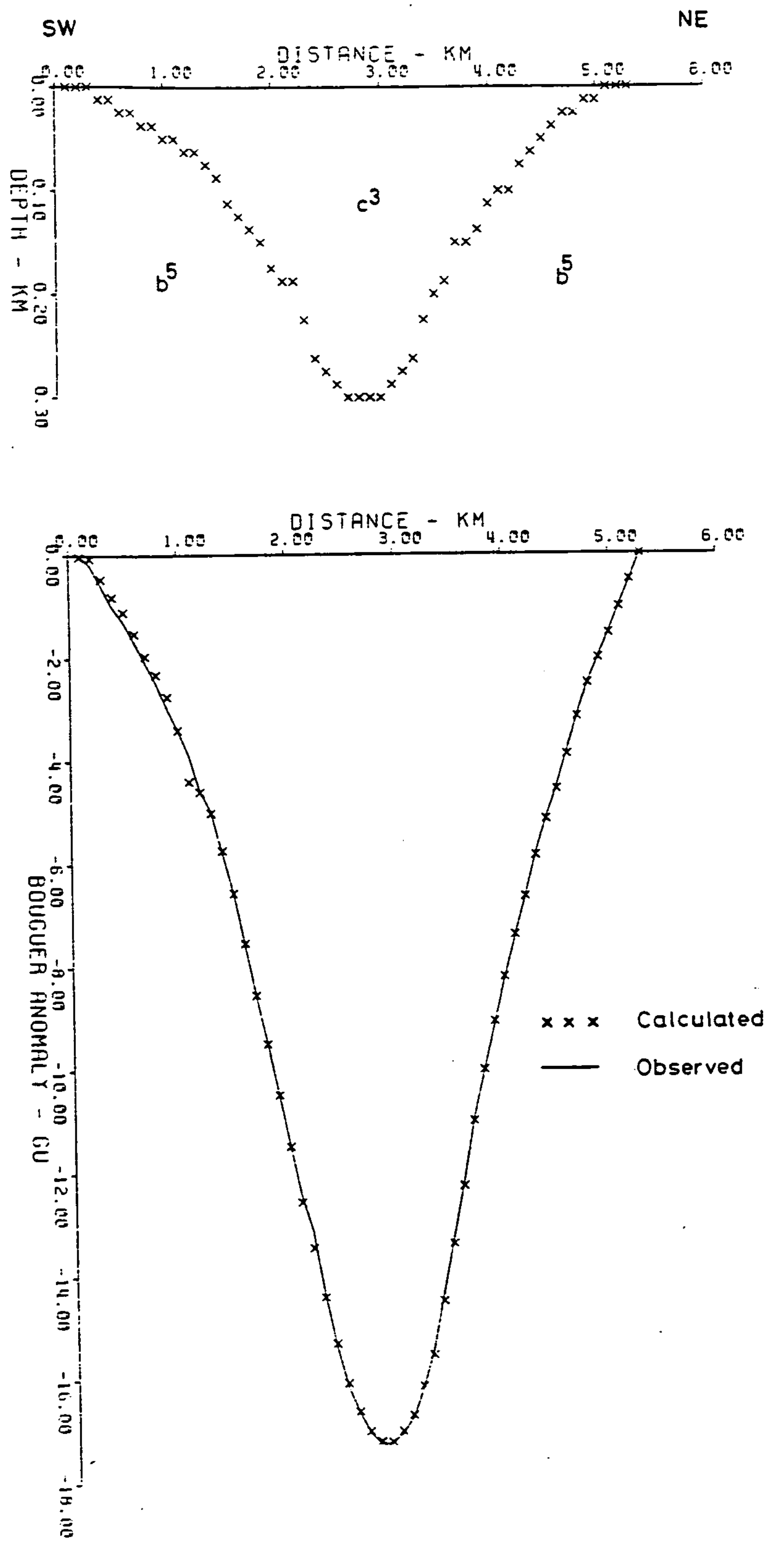

Fig. 6.4 Profile (L2). An interpretation of the Upper Old Red Sandstone, Lauderdale Basin. National Grid coordinates of the end points of the profile NT 522 6471 and NT 566 500. Density contrast $-0.20\ g/cm^3$. c^3: Upper Old Red Sandstone; b^5: Silurian.

representative of the Southern Uplands (Chapter II) and plotted with GPCP, with a grid interval of 1km. Subsequently, profile (L3) was traced; its position appears on figure 5.24.

Digitised values at 500m intervals were input to the MODG2D program. This time a density contrast of -0.10 g/cc was assumed for the Old Red Sandstone sediments, implying that the basin was filled exclusively with conglomerates.

The model shows (figure 6.5) that the maximum depth of the bottom of the basin in the region defined by the profile is about 550m.

A three-dimensional modelling attempt was also made in this area but it was very soon realised that the regional field was not suitable for the modelling programs. Although the result was a reasonably good model for the region south of Lauder, it was unacceptable for the area north of it.

As a conclusion, the Lauderdale Devonian Basin has a thickness near Lauder which is unlikely to exceed the value of 600m and probably is nearer to 300m; it becomes relatively thinner towards the north and the data are inadequate to show if its northern margin is fault bounded. South of Lauder the basin broadens and three-dimensional modelling suggests that the thickness of the sediments is similar to that to the north and certainly less than 1000m.

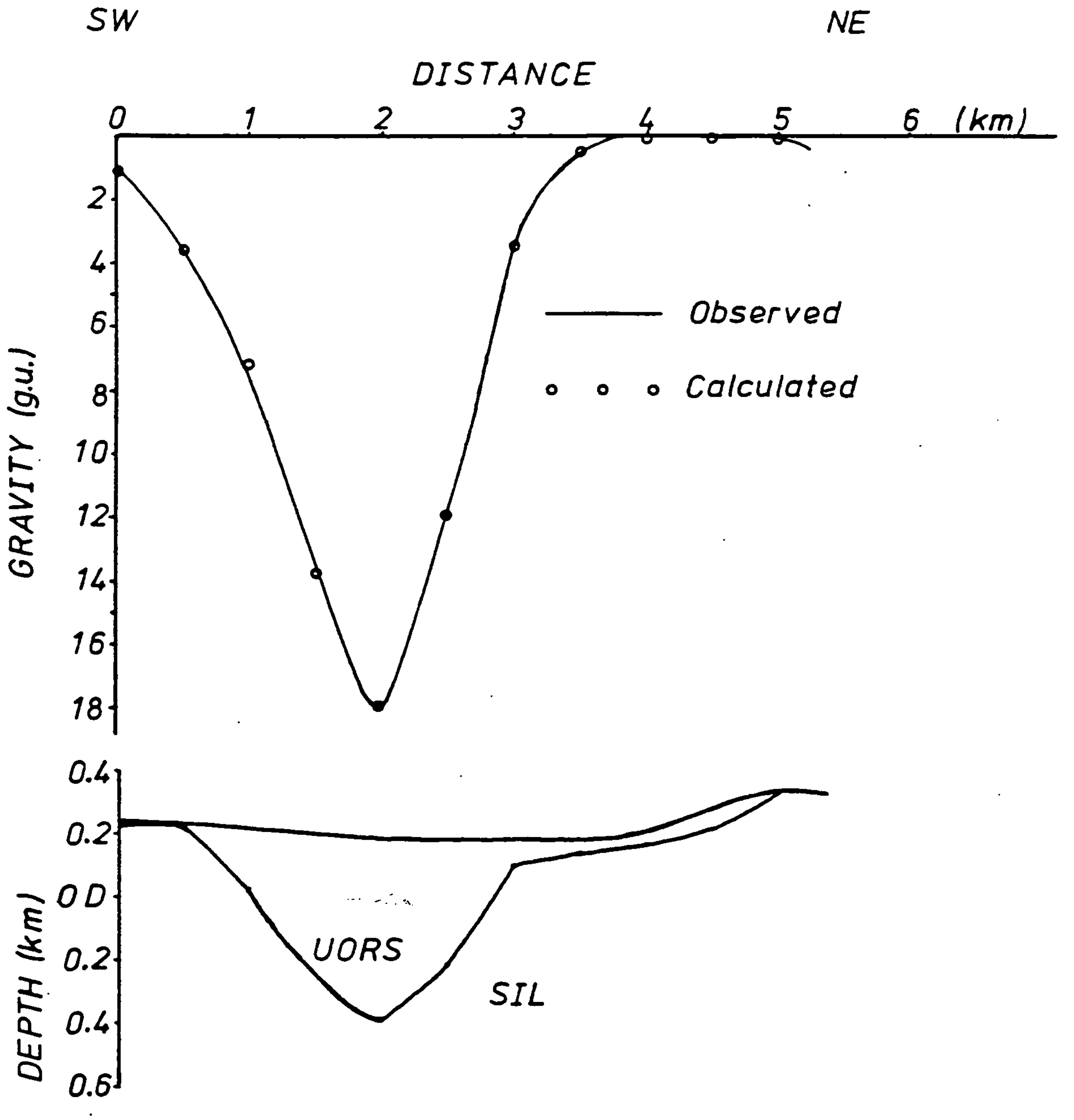

Fig. 6.5 Profile (L3). A possible interpretation of the Lauderdale sedimentary basin. Density contrast -0.10 g/cm^3. UORS: Upper Old Red Sandstones; SIL: Silurian. Coordinates of the end points of the profile are NT 5100 4744 and NT 5675 5088.

6.2.3 Oldhamstocks Basin

6.2.3.1 The Great Conglomerate

The eastern part of the Lammermuir chain in Berwickshire is crossed almost perpendicularly by the Great Conglomerate belt. In the north this commences south of Dunbar, extends south along the Monynut Edge and then passes through the narrow channel between Greenhope (NT 7361) and Cranshaws (NT 6962). Subsequently, it opens again with its western margin reaching Dirrington Law (NT 7055) west of Duns, where it attains a thickness of nearly 680m (Pringle, 1948). From this area, the western flank of the conglomerate swings to the SW, but with its texture becoming finer and more sandy, passing up into fine feldspathic sandstone (Clough et al, 1910), where it expands even more and is expected to reach a considerable thickness.

The conglomerate belt at Oldhamstocks and Innerwick is bounded to the west by the Silurian greywackes of the Lammermuir Hills, from which is believed to be formed (according to Geikie in Howell et al, 1866), and to the east by the Lower Carboniferous sediments with the Innerwick Fault being the physical boundary between these two formations.

According to Davies (person. commun.) the Great Conglomerate of Monynut Edge, west of the Innerwick Fault, is of Lower Old Red Sandstone age. The conglomerate probably lies under the Lower Carboniferous sediments on the eastern side of the fault.

About 200-300m to the south of the Cove Fault (which starts from Cove (NT 780717) and runs westwards to the Oldhamstocks area) and parallel to it, runs a narrow Old Red Sandstone belt, which extends from Oldhamstocks to the coast near Siccar Point. It consists, surprisingly, of sandstones and marls belonging to the top third division of the Upper Old Red Sandstone succession, and is thus of younger age than the Great Conglomerate.

Geikie (Howell et al, 1866) pointed out this sudden transition eastwards from the conglomerates at the eastern flank of the Lammermuirs to red sandstones and marls. He noticed that along the fault, which runs from near the Whiteadder south-eastward to the Borthwick Hill (NT 7656), conglomerates comprise the western side of this fault, while the eastern side is occupied mainly by red sandstones with red shales and marls. A somewhat similar case occurs farther north in the narrow belt between Oldhamstocks and Siccar Point. Geikie also tried to give an explanation to this phenomenon and suggested that the "effect of the fault (running SE of Whiteadder River) would thus be to depress the Silurian region on the north-east side, so as to let in, in a wedge shape, the sandstones and marls which were formed at a later time against a higher and of course newer margin, which still remains." He also proposed that the eastern end of the conglomerate round the Lammermuirs might mark the edge of the old Silurian land.

Considering the conglomerate zone of Monynut Edge, the Great Conglomerate of this region attains a greater height than the nearby Lammermuir Hills (about 400m). This is an indication that at one time it must have extended far more beyond the narrow belt it occupies today.

This strip was studied gravimetrically by two-dimensional models, derived by two profiles (I1) and (I2) over that area (see figures 6.6 and 6.7).

The first profile (I1), interpreted in figure 6.6, was digitised at 100m intervals and the automatic MODG2D inversion program was used. A density contrast of 0.20 g/cc was assigned between the Silurian greywackes and the Great Conglomerate, although this is rather too large and is more representative of the contrast between Silurian and Lower Carboniferous sediments. A linear regional field of -1.4 gu/km was subtracted from SW to NE in order to make the model outcrop in the south-western part.

The second profile (I2), figure 6.7, extends parallel to the Caledonian trend. A density contrast of 0.12 g/cc was used, which is more appropriate to the contrast between Silurian and Great Conglomerate, and the modelling program MODG2D was again used. In figure 6.7, the depth of the basin to the NE of the Innerwick Fault appears to be relatively large; this is due to the unrealistically low density contrast used for the Lower Carboniferous sediments of that area. Also, the throw of the Innerwick Fault appears to be large, but this feature will be discussed later.

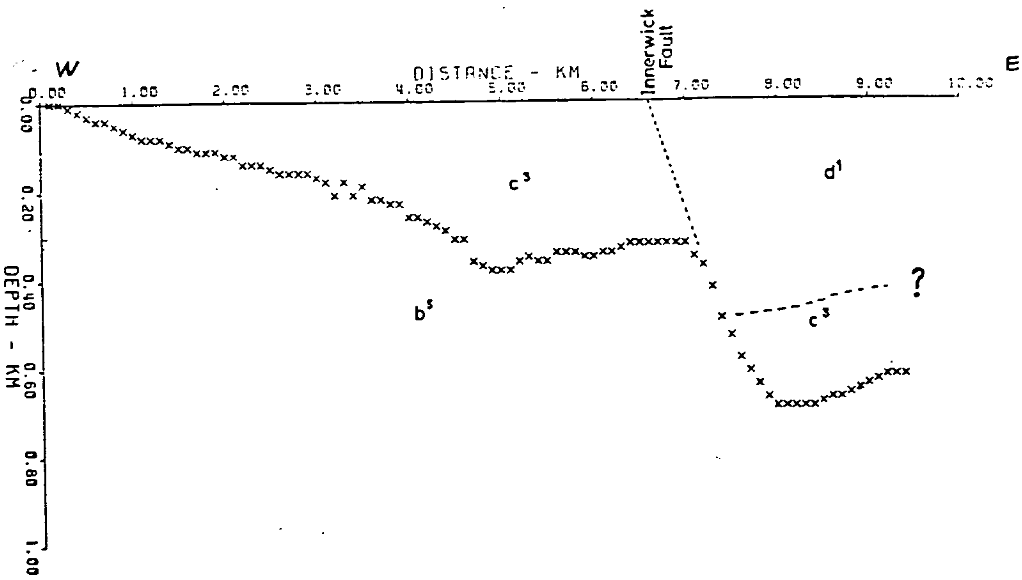

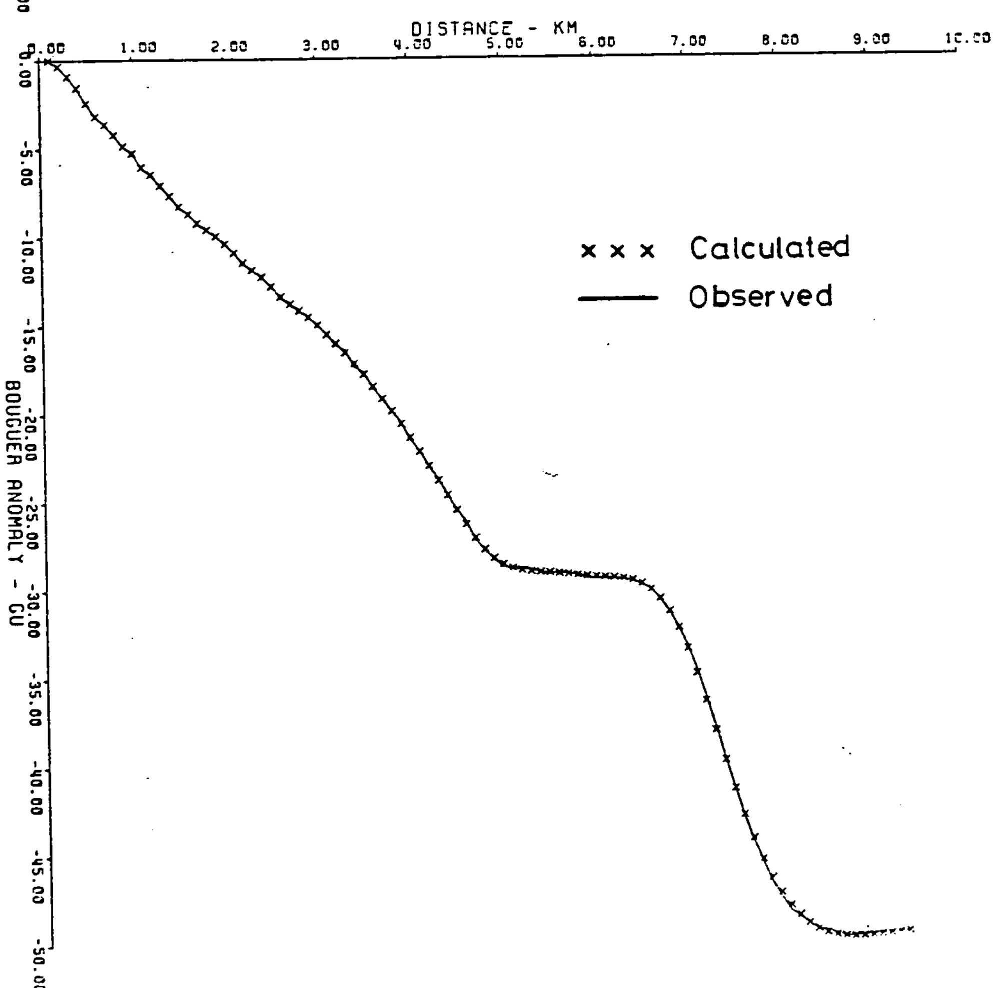

Fig. 6.6 Profile (I1) see fig. 4.7. A possible interpretation of the Oldhamstocks basin (density contrast -0.2 g/cm^3). b^5: Silurian; c^3: Upper Old Red Sandstone; d^1: Lower Carboniferous. Coordinates of the ends of the profile are NT 652 717 and NT 743 742.

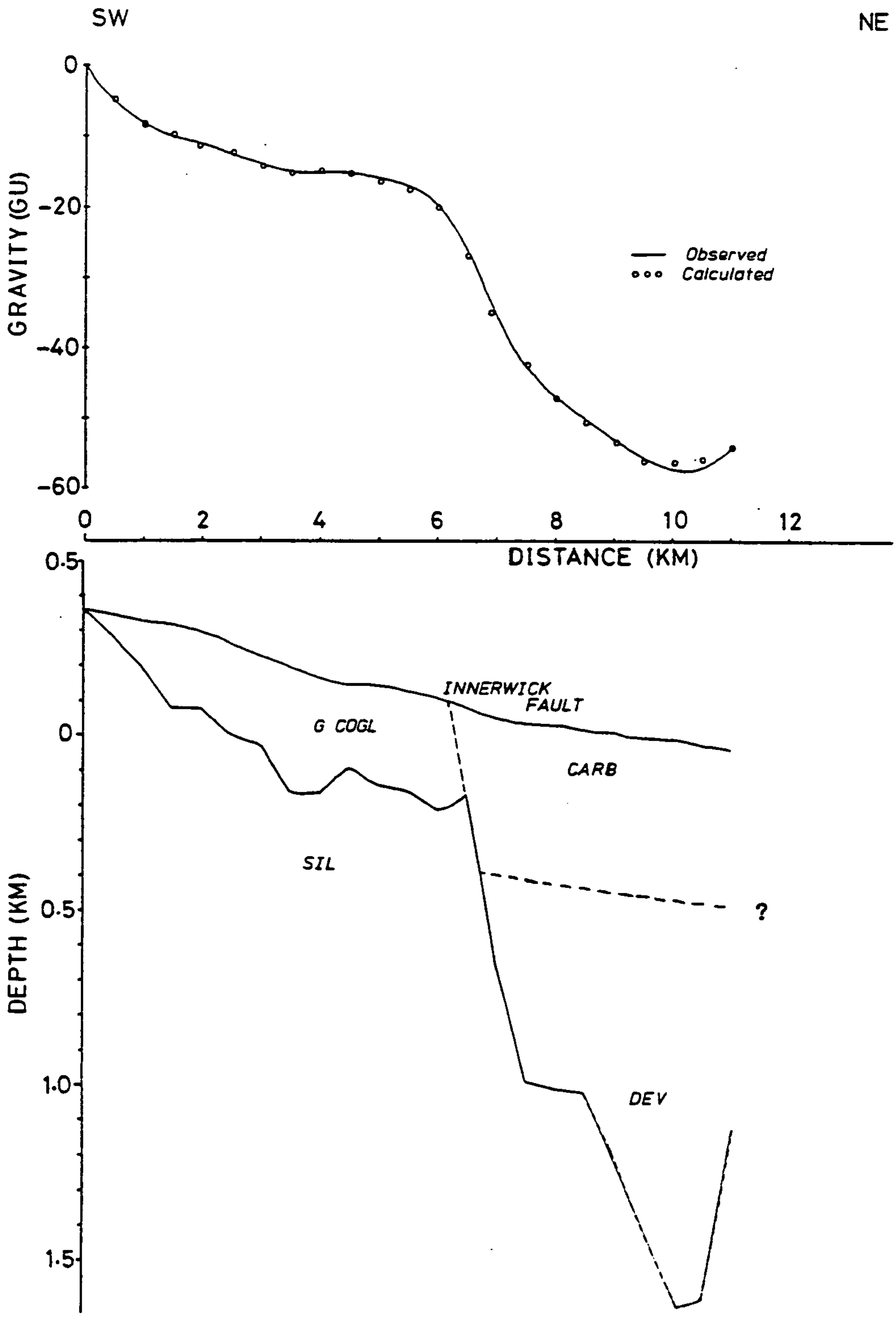

Fig. 6.7 Profile (I2) - see fig. 4.3. An interpretation of the Oldhamstocks basin (density contrast -0.12 g/cm^3). Coordinates of the end points of the profile are NT 670 700 and NT 756 770. **---? indicate approximate boundary between Devonian and Carboniferous sediments.**

Considering these two models, it appears that the floor of the Old Red Sandstone has a gentle slope towards the coast to the east, like the present topography of the Silurian in that area. As the density contrast 0.12 g/cc between the Silurian and the Great Gonglomerate is quite representative, it seems that the maximum thickness of the conglomerate is unlikely to exceed 400m. This value is in agreement with the one shown on the unpublished IGS geological map (figure 6.8) while Geikie's calculations (thickness of 540m with a maximum limit of 610m) were overestimated (Howell et al, 1866).

6.2.3.2 The Lower Carboniferous sediments

The Carboniferous sediments of the Oldhamstocks Basin were studied by two further gravity profiles. The following information was used for the construction of the models over that area:

1. Two boreholes were made in Skateraw (NT 734751) and Birnieknowes (NT 755724) by the Institute of Geological Sciences; the first one is Skateraw, pierced 29.44m of sediments of the Lower Limestone Group, overlying 260.22m of Calciferous Sandstone Measures (Dinantian), the base of which was not reached. The other, in Birnieknowes, pierced 438.76m of Calciferous Sandstone Measures (Dinantian) and 69.42m of Upper Old Red Sandstone sediments, with its base not reached.

2. The offshore information was from seismic reflection profiles carried out by IGS. They reveal a sequence of synclines and anticlines shown in figures 6.8 and 6.8a.

3. Density information: Bennett (1969) has found a density contrast of -0.12 g/cc between Old Red Sandstone and Silurian strata and 0.18 g/cc between Old Red Sandstone and Calciferous Sandstone Series, "based on laboratory measurements of the saturated density of rock specimens from those formations."

Therefore, it is clear that the Calciferous Sandstone series have a density which is relatively smaller than those shown by McLean (1961a) and the value of 2.54 g/cc which could generally be accepted as a representative value of the Lower Carboniferous sediments in South-West Scotland. This could be explained by the occurrence of oil-shales in the Calciferous Sandstone series, which can be seen on the coast between Dunbar and Cockburnspath. (Clough et al,(1910), believed they were indicative of an approach to the conditions which led to the formation of the great oil-shale group in Mid and West Lothian). McLean (1961a) reports a density of 2.27 $\pm$ 0.10 g/cc for the carbonaceous shales of the Central and Western Midland Valley.

Considering the above, it is not clear if the Upper Old Red Sandstone sediments underlying the Calciferous Sandstone series consist of conglomerate or red sandstones. In the following, considering the profile (OL1), an attempt was made

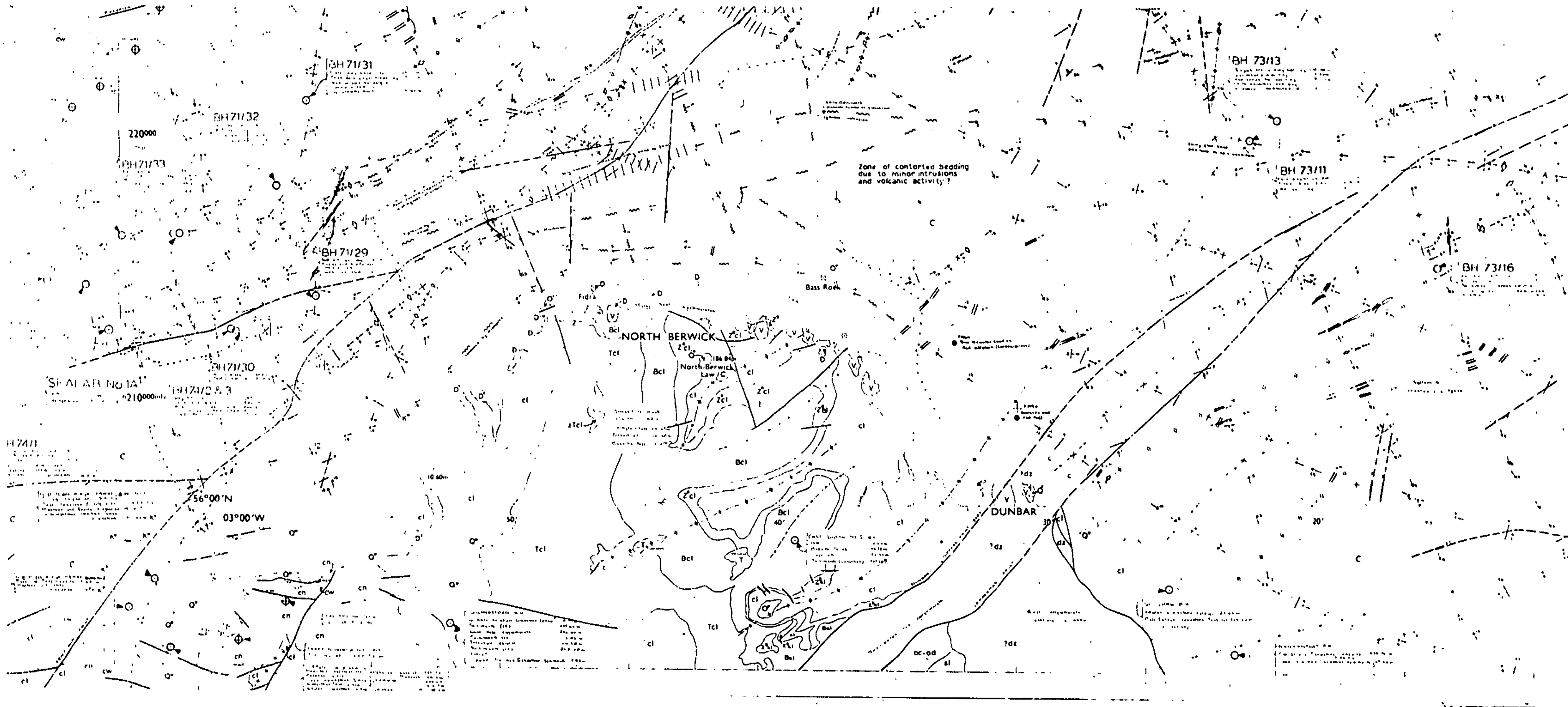

Fig. 6.8. **Open-file IGS geological map of East Lothian coast with offshore information deduced from geophysical data.**

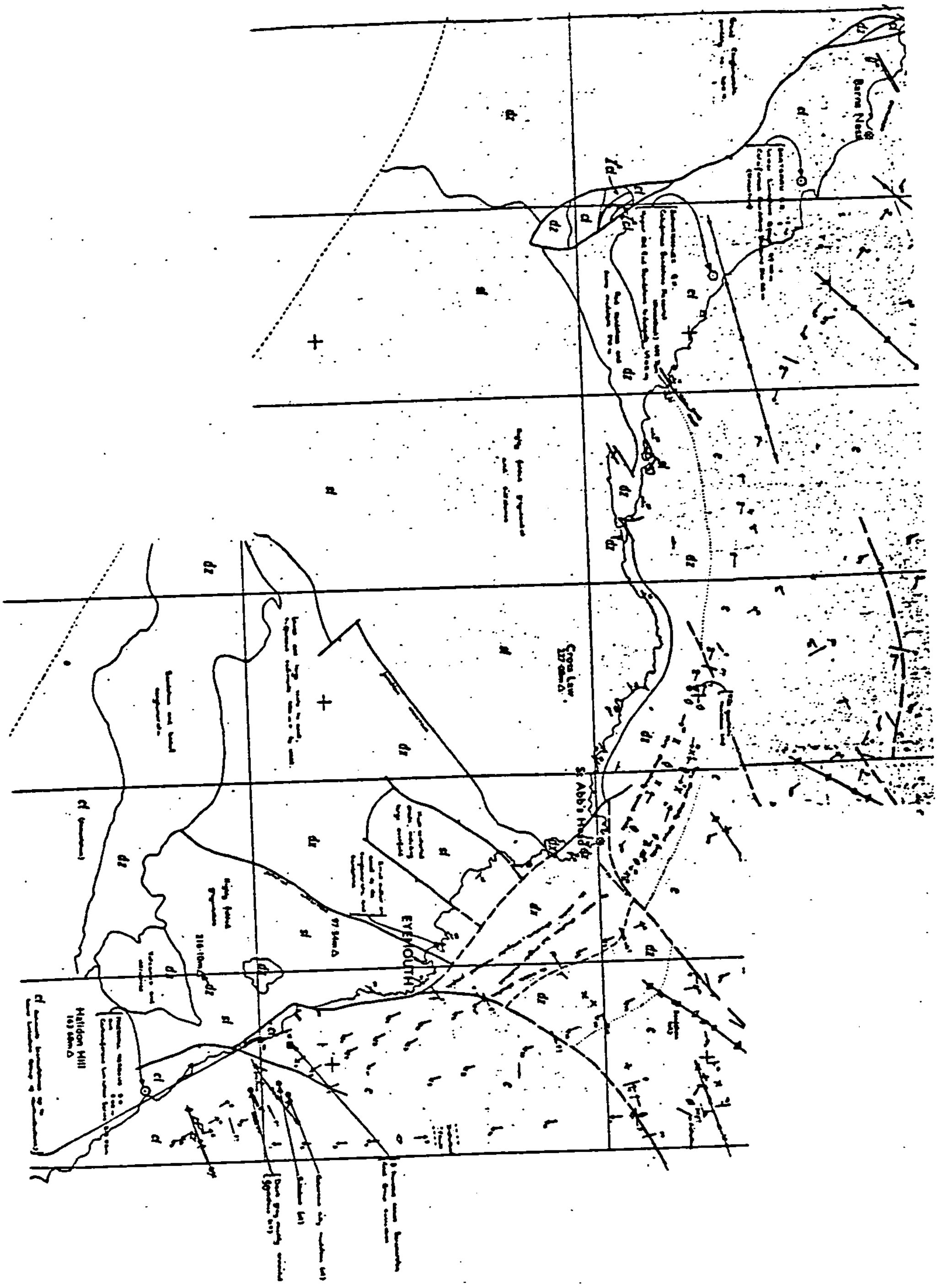

Fig. 6.8a. Open-file IGS geological map of the Berwickshire coast with offshore information deduced from geophysical data.

to trace the boundary between the Silurian and the combined overlying sediments. A density contrast of 0.20 g/cc was chosen. This is the contrast between the densities of the Silurian and the average of the conglomerate(2.60 g/cc (Bennett,1969) or approximately 2.62 g/cc (Table II-3)) and the Calciferous Sandstone series, and the shales of 2.42 g/cc (Bennett, 1969); also, 2.52 g/cc is close to the value for the sandstone at Siccar Point (Table II-3).

Because only a single interface is required, again the MODG2D inversion routine was used. A regional trend of -4 gu/km was subtracted from the observed values of gravity given at 100m intervals. The resulting model is shown in figure 6.9. The most surprising feature is the Cove Fault which appears to have a normal throw of 800 m and a dip of about 77°. The anticline, deduced from offshore seismic profiles has been picked up, which means that it reaches the coast and probably continues even farther westwards. The syncline marked near Birnieknowes (figure 6.8a) does not appear in the model, although the syncline north-west of Skateraw does, since the interface of the model deepens, especially after the eighth kilometre of the profile.

Figure 6.10 shows a more quantitative model of the same area. Again, the observed values of profile (OL1) were used, subtracting a regional trend of -4 gu/km. It was assumed that conglomerates are underlying the Lower Calciferous sediments and a density of 2.60 g/cc was assigned. For the Calciferous Sandstone series and shales, and the Carboniferous

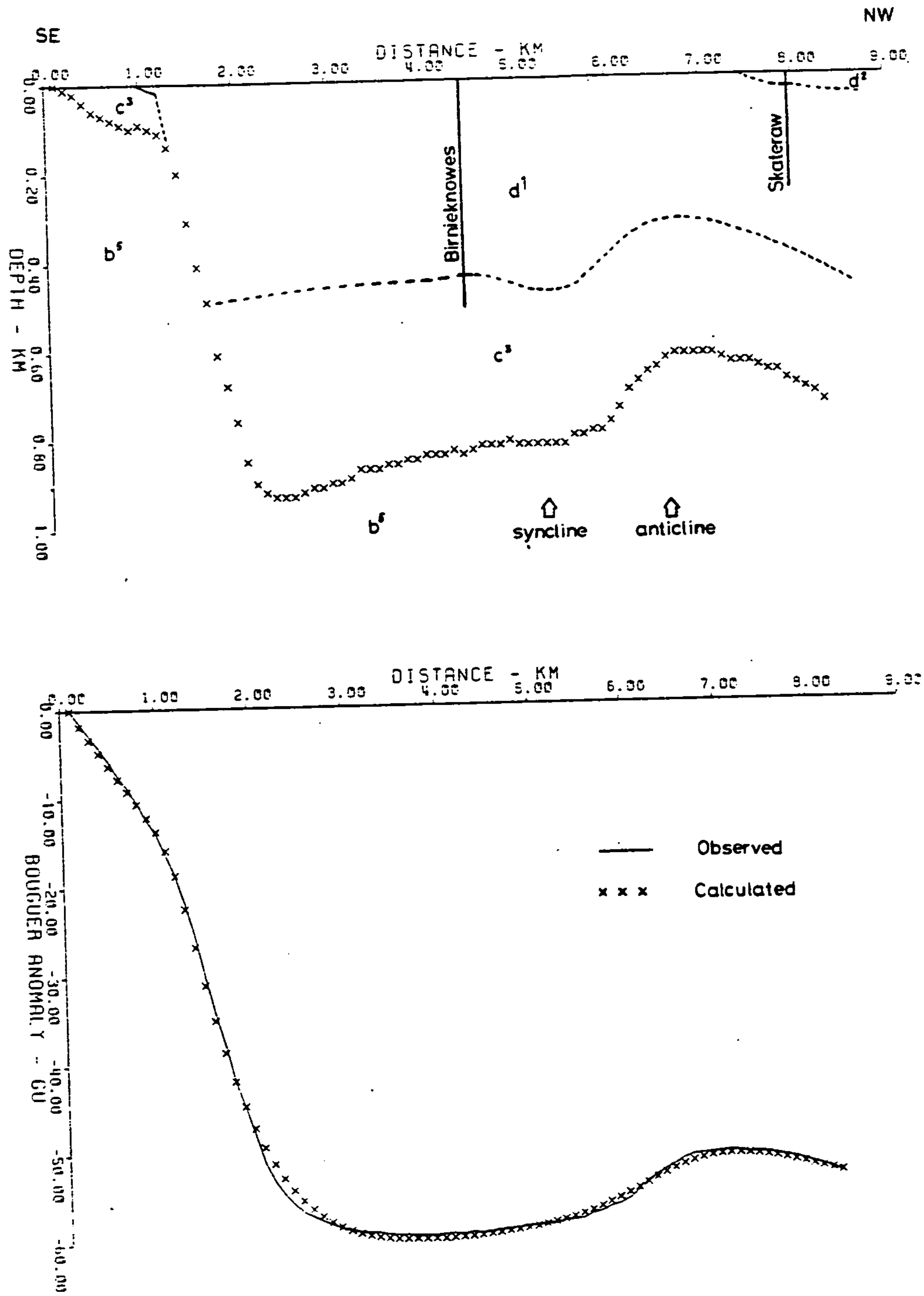

Fig. 6.9 Profile (OL1) - in figure 4.7. A possible interpretation of the Oldhamstocks basin with the borehole information. Coordinates of the profile ar NT 784 707, NT 755 724 and NT 720 753.

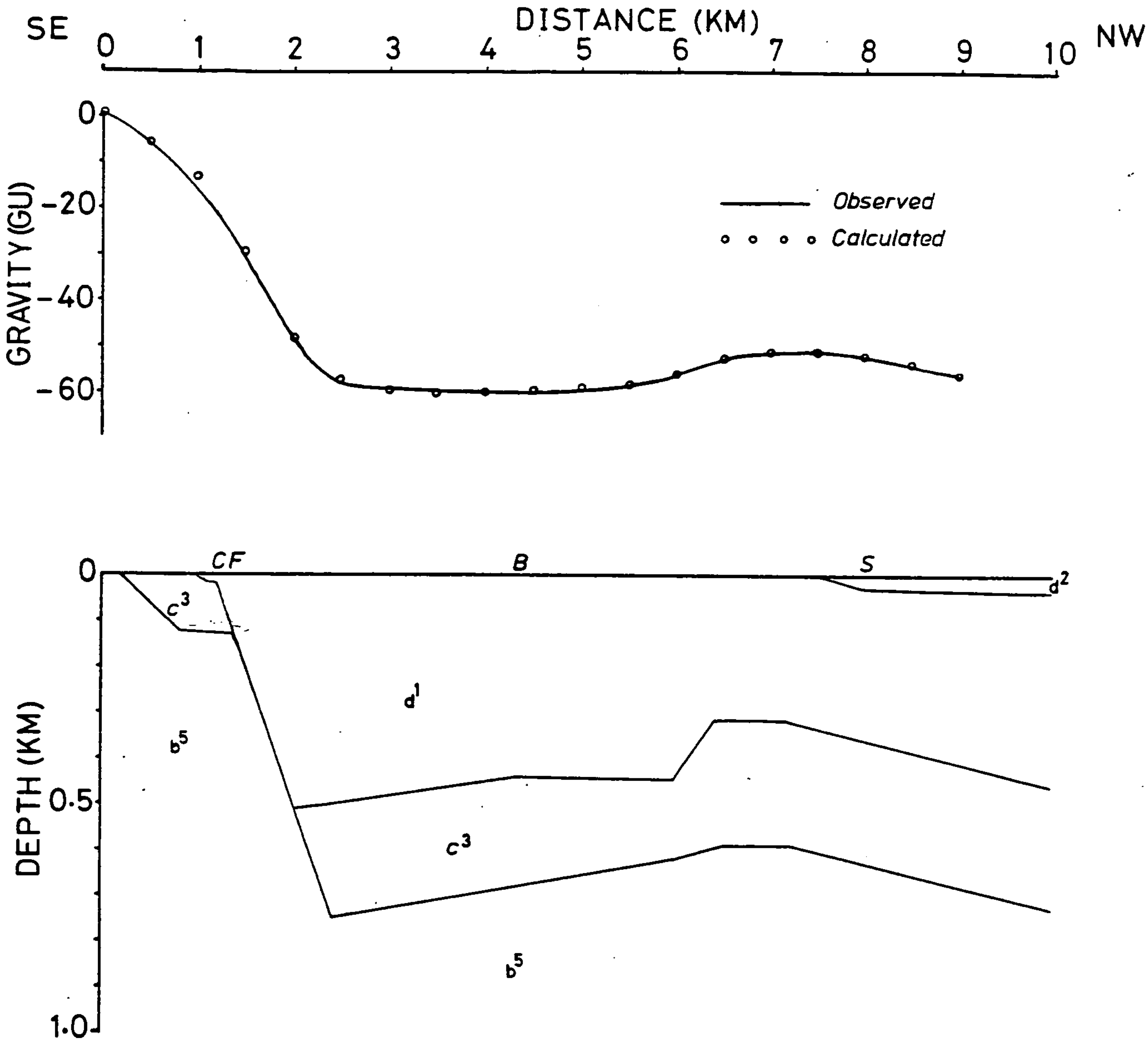

Fig. 6.10 An alternative model of the gravity profile (OL1). Density contrasts in text. CF: Cove Fault; B: Birnieknowes; S: Skateraw.

Limestone Group, densities of 2.42 g/cc and 2.55 g/cc were used. A value of 2.50 g/cc was assigned for the belt of red sandstones south of the Cove Fault. The TALG2D program was used. To control the interfaces of the upper two layers, the borehole and the offshore seismic information were used.

From this model it appears that the depth of the Carboniferous sediments is about 500m and as the density contrast of 0.18 g/cc seems to be the maximum one, then the depth of 500m for the Carboniferous sediments should be the minimum one. The underlying Devonian sediments fluctuate, in this case, between 200-250m. The small Devonian Basin south of the Cove Fault is very shallow, probably about 130m and is unlikely to be more than 200-250m. The Cove Fault still appears with the considerable throw of about 600m , but with a slightly smaller dip in this model, about 72°.

A qualitative attempt was also made to model the Oldhamstocks basin in a three-dimensional way. The boundaries of the area for this purpose are shown in figure 6.11a by the rotated Bouguer gravity anomaly map. After constructing the residual gravity map (figure 6.11b) by subtracting the estimated value calculated by LISPB, MODG3D was used to approximate the Silurian interface by 1km side vertical prisms with a density contrast of 0.12 g/cc between Silurian and post-Silurian sediments. This density contrast is rather small for the sediments east of the Innerwick Fault, but it is going only to generate a vertical scale displacement by overestimating the

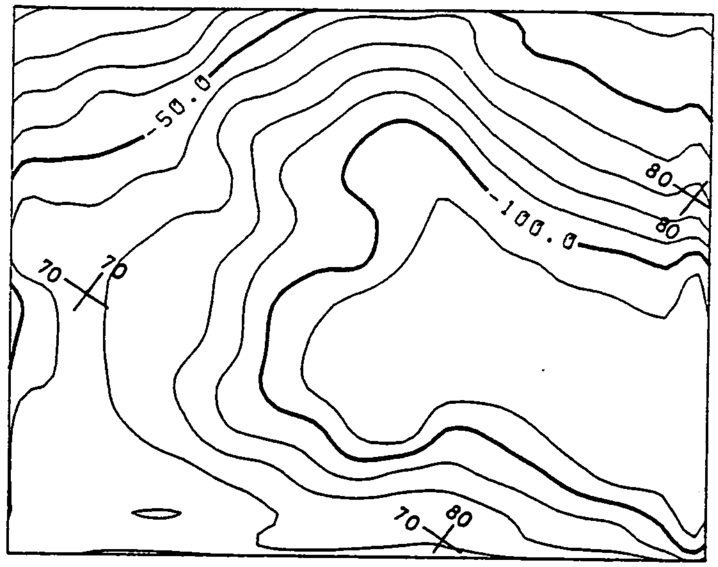

(a)

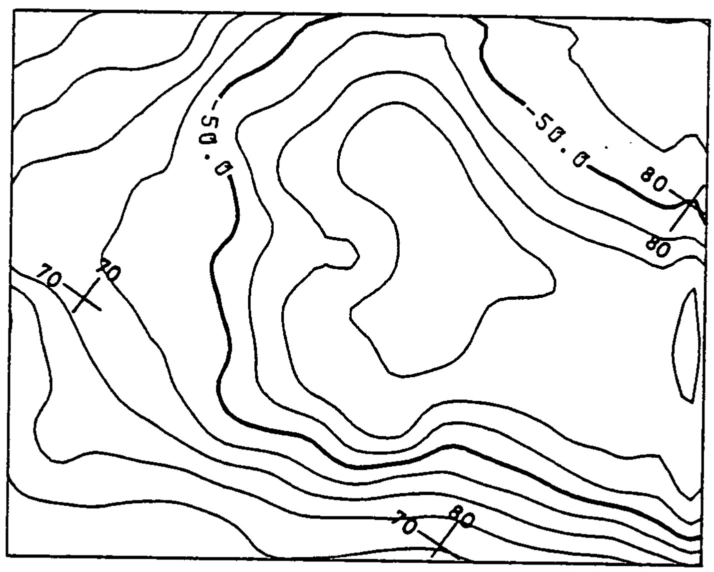

(b)

Fig. 6.11 (a) Bouguer gravity anomaly map of Oldhamstocks basin at 10 gu contour interval.

(b) Residual gravity anomaly map subtracting the LISPB regional field (figure 5.3).

In both maps intersections show the corners of 10km National Grid squares.

depth to the Silurian interface, accentuating as a consequence the faulting features of that area (Cove Fault, Innerwick Fault).

The SYMVU routine produced the three-dimensional picture (figure 6.12) of the array-depths generated by MODG3D. As can be seen from figure 6.12, the Oldhamstocks Basin comprises a trough which extends into the sea. The Devonian and Lower Carboniferous sediments are mostly bounded on the west by the Innerwick Fault and on the south by the Cove Fault which extends clearly into the sea. To the NW, approaching Dunbar, the basin becomes shallower. It is expected that the maximum thickness of the sediments occurs offshore, where the smallest gravity values (about -120 gu) are met (Tully and McQuillin, 1978).

The movements of the Innerwick Fault attain their maximum throw **(probably less than 500 m)** NW and SE of the Innerwick, which is at the western end of the axis of an anticline (figure 6.8a).

6.2.4 Eyemouth Basin

In eastern Berwickshire, SW of Eyemouth, there is a narrow northeasterly trending belt of Lower Old Red Sandstone, consisting of a series of sandstones and fine conglomerates of feldspathic character, associated with tuffaceous beds and

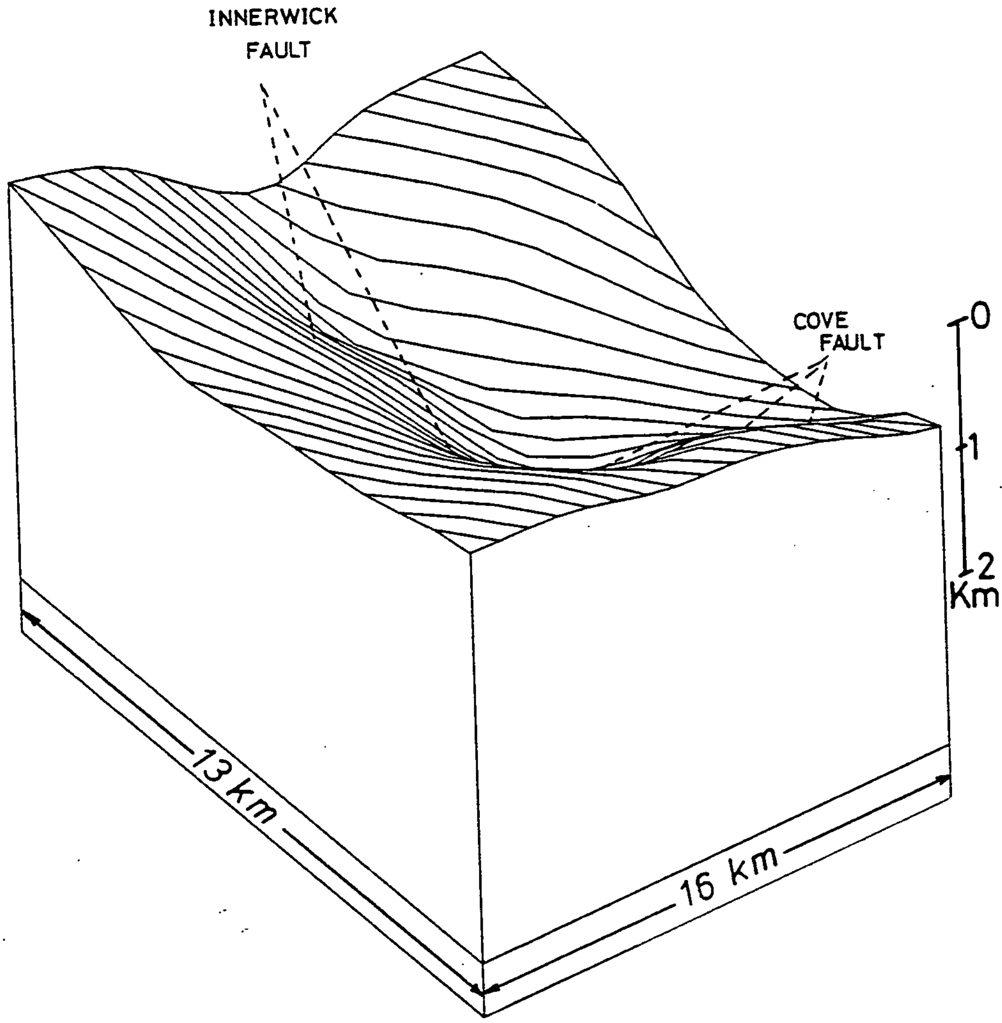

Fig. 6.12 Three-dimensional model of the Silurian interface of Oldhamstocks basin, viewed from the south and covering the same area as the maps in figure 6.11.

flows of andesitic lava. Geikie (1864) first described the geology of this area and the 1:63,360 geological map of this region indicates uncertain junctions between the Lower Silurian and Devonian sediments, except for the boundaries along the two fault lines: the Eyemouth Fault running from Edingtonhill (NT 9158) to the coast of Eyemouth, and the unnamed fault to the south of Coldingham running from north-east of Cairncross (NT 9064) to Coldingham Bay (NT 918665).

Again, in this region, an attempt was made to generate a quantitative picture of the thickness of the Lower Old Red Sandstone. The area which was chosen for modelling is outlined in figure 6.13, where the Bouguer gravity anomaly map is superimposed on a sketch geological map.

The Lower Silurian-Devonian interface was approximated by sixteen square blocks of 2km side, chosen so that the block boundaries approximately coincided with the fault-like trends on the gravity map. From the sixteen gravity values, digitised from the gravity map (figure 6.13), a linear trend of 2 gu/km was subtracted and program MODG3D worked out the vertical extent of each prism. The resulting model is shown in figure 6.14; a density contrast of -0.10 g/cc between the sediments of the basin and the Lower Silurian of this region was taken.

Considering figure 6.14, it can be seen immediately that the prism at the north-western side does not outcrop as it is

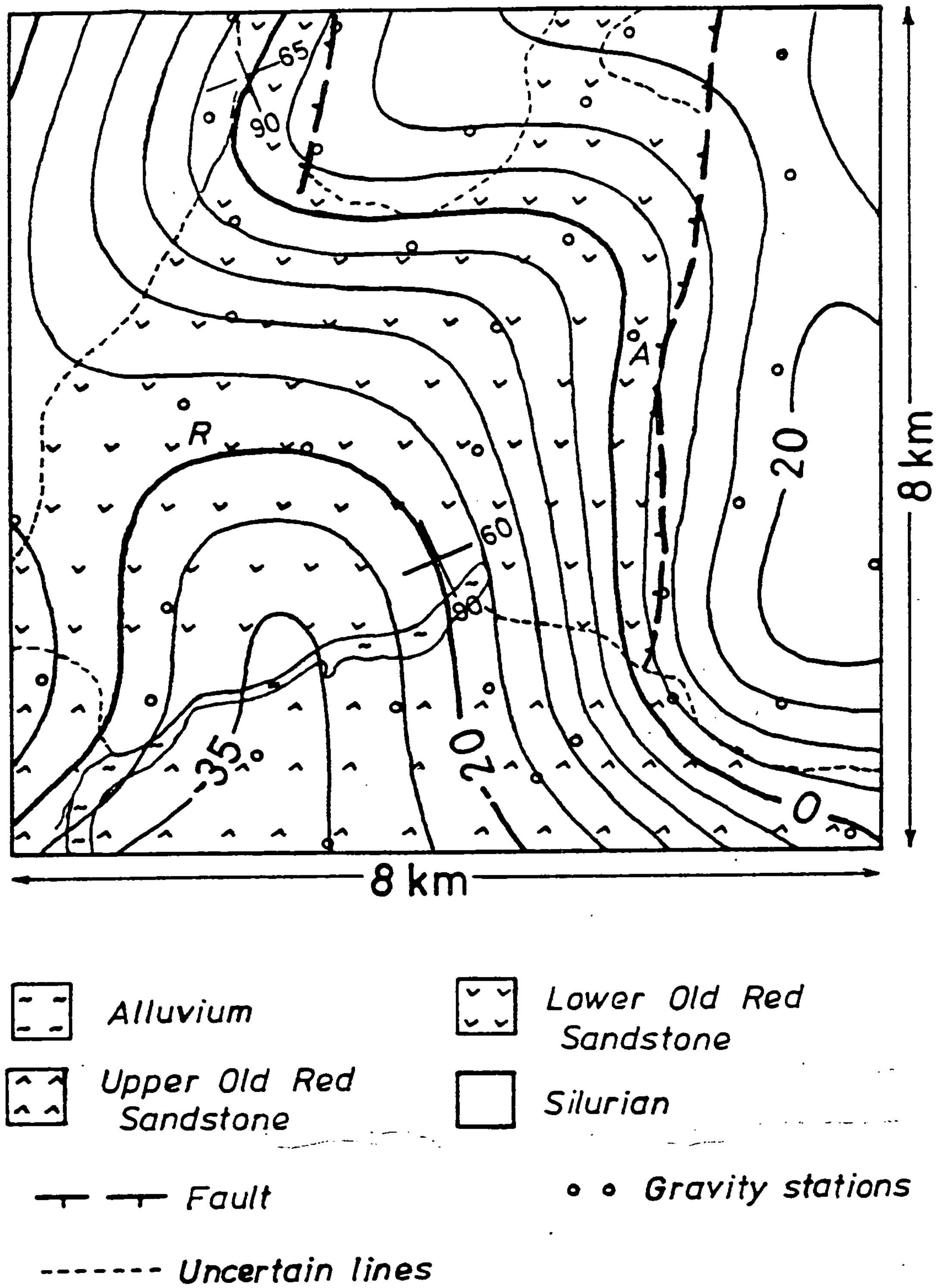

Fig. 6.13 Bouguer gravity anomaly map superimposed on a sketch geological map of the Eyemouth area. Contour interval 5 gu. Intersections represent corners of 5km National Grid squares. A: Ayton; R: Reston.

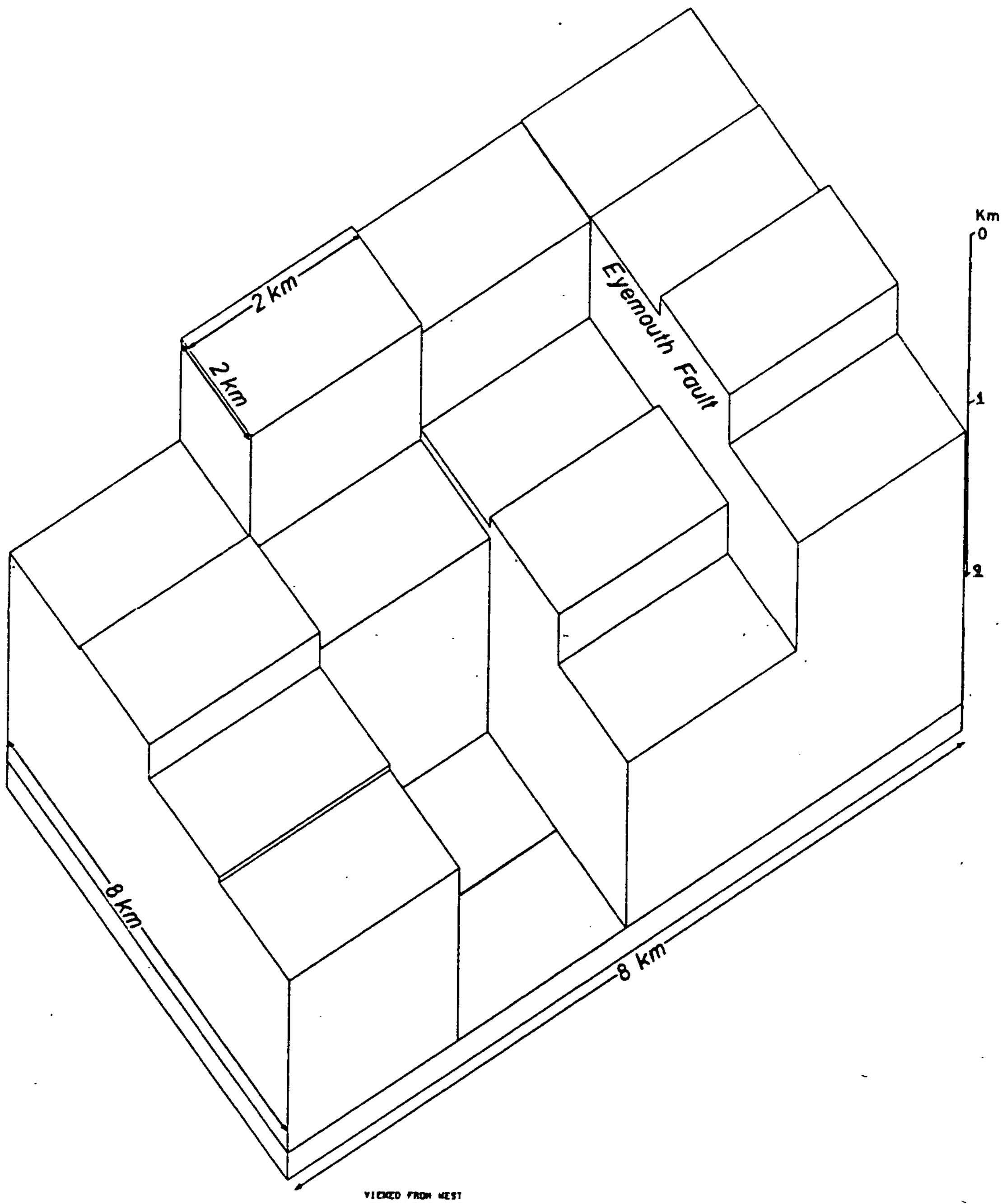

Fig. 6.14 Three-dimensional interpretation Silurian interface of the Eyemouth basin, approximated by 2km square prisms.

expected to from the geological map (figure 6.13). All the other prisms to the north-east and east outcrop at a relatively satisfactory level. However, in spite of the imperfections of this model, the following conclusions may be drawn:

1. The Silurian inlier north of Ayton is faulted not only on the north-western side, the Coldingham Bay Fault, but also on the south-western side. In the first case, the Coldingham Bay Fault appears with a throw of about 600m while in the second case the throw of the sediments to the SW appears confidently to be of the same magnitude (about 600m).

2. The Eyemouth Fault starts about 1km NE of Ayton by having a significant down-throw to the NW and thereafter it maintains its throw of about 600m, running along a south-westerly direction until approximately the boundary with the Upper Old Red Sandstone sediments. Thereafter, the whole structure is about 300 m deeper, but the calculated throw is virtually the same.

3. The Lower Old Red Sandstone sediments appear to be faulted under the Upper Devonian, attaining a maximum thickness of about 1900m (using the above density contrast).

4. The narrow belt of Lower Old Red Sandstone sediments which extends along the north-eastern side of the Silurian inlier until it reaches the Eyemouth coast has a relatively small thickness (about 120-130m) and the throw of the Eyemouth Fault, which runs partly along its north-eastern side, seems to be insignificant there.

5. The latter suggests that the inlying Silurian block which contains the Coldingham Bay beds is actually continuous with the Lower Silurian sediments south and west of Eyemouth; this would contradict Shiell's and Dearman's (1963, 1966) conclusions that the Silurian strata around that area, are in fact either of Arenig age - deformed initially by mid-Ordovician movements - or of Cambrian age deformed initially in pre-Arenig times.

6. The 1910 edition of the 1:63,360 geological map, Sheet 34, from which the sketch geological map of figure 6.13 was made, is actually better constructed in the north-eastern part than the IGS unpublished geological map (figure 6.8a).

Considering the age of the Eyemouth Fault, Geikie (1864) concluded that it must be pre-Upper Devonian as its throw continues at its south-western part under the Upper Devonian sediments of this area (Edingtonhill), but is not observed in them. This is in excellent agreement with figure 6.14.

6.3 Lammermuir and Dunbar-Gifford Faults

In this section the supposed north-eastern component of the Southern Uplands Fault System is investigated by examining its gravity expression, and its position as a tectonic boundary.

Although to the south-west, the Leadburn Fault component of the Southern Uplands Fault system is generally associated with either the Glen App Fault (Anderson, 1951; Greig, 1971) or the Straiton Fault (McGregor and McGregor, 1948), to the north-east, the picture is less clear: the Lammermuir Fault is mapped _en echelon_ with the Leadburn Fault, running from the southern termination of a minor north-south fault (the Cockmuir Fault) to the East Lothian coast south of Dunbar. Anderson (1951) considered that the Pentland Fault might take over from the Southern Uplands Fault System, while Max (1976), following Tulloch and Watson (1958) suggested that the Leadburn Fault might be continuous under or within the Midlothian Coalfield, perhaps reaching the Firth of Forth, near Prestonpans. However, according to detailed studies in the Midlothian Coalfield (Hipkin, 1977b), the Leadburn Fault component is not continuous under the Coalfield, but terminates at the Roslin-Vorgie Fault System. Thus, it never reaches the Firth of Forth coast.

Max (1976) also stated that the present line of the Southern Uplands Fault continuing north along the Lammermuir Fault, is unrealistic. These ideas are critically examined below, but first a closer look at the throw of the Lammermuir Fault and

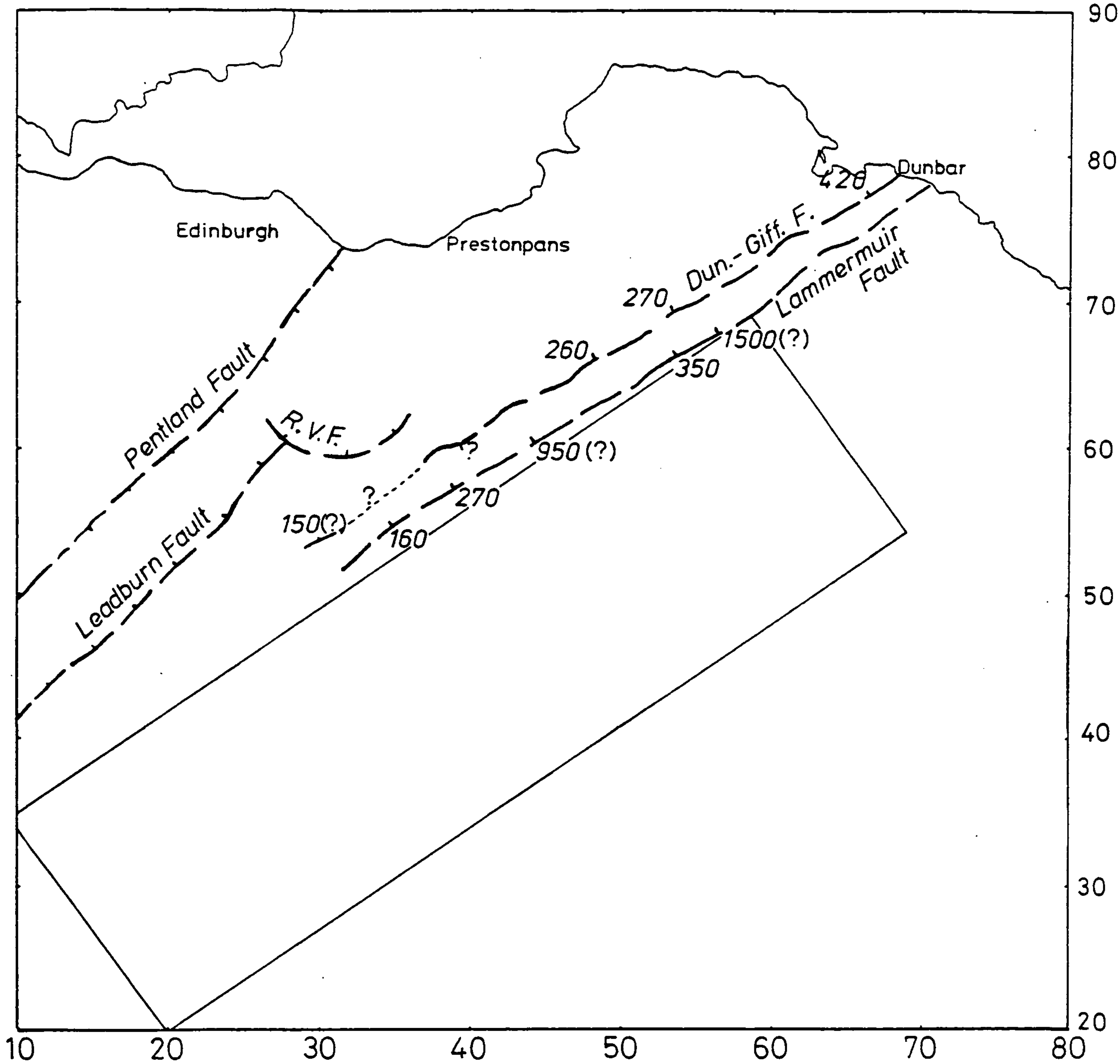

Fig. 6.15 Diagramatic representation of the throw of the Lammermuir and Dunbar-Gifford Fault in East Lothian.
R.V.F. : Component of the Roslin - Vogrie Fault System.
Rectagular represents the limits of the granite model (see figure 5.23a).

TABLE VI-1

LAMMERMUIR FAULT				
National Grid Reference	Hade (degrees)	Displacement (m)	Depth to first density interface (SE side) (m)	
NT 375 562	small	~160		Hipkin
NT 390 572	small	~270		Lagios (1978)
NT 436 609	10	945-1100	40-50	Bennett (1969)
NT 544 654	small	~350		Shearer
NT 561 681	25	1500-1700	30-40	Bennett (1969)
DUNBAR-GIFFORD FAULT				
NT 290 532	small	~150	small	Hipkin
NT 392 612	?	opposite throw	?	Lagios (1978)
NT 485 661	30	~260	~50	Bennett (1969)
NT 534 692	small	~270	small	Shearer
NT 658 786	25	420-460	170-180	Bennett (1969)

SUMMARY OF THROW OF THE LAMMERMUIR AND DUNBAR-GIFFORD FAULTS the other fault running parallel to the NW of it, the Dunbar-Gifford Fault, is necessary.

Table VI-1 summarises the results of detailed gravity profiles across the Lammermuir, Dunbar-Gifford Faults, obtained by Bennett (1969), the author and other members of Geophysics Department of Edinburgh University. The throw of the faults is displayed in figure 6.15.

Considering the latter figure, the calculated downthrows of the Lammermuir Fault by Bennett (1969) seem to be rather overestimated. Also, the detailed gravity profile across the Dunbar-Gifford Fault east of the A7 (NT 392 612) suggested a throw opposite from the one expected. It is not clear whether this result is true or whether it was affected by the south-westerly continuation (?) of a dolerite dyke to the NE of the profile.

The Southern Uplands are frequently considered as a distinct tectonic province, bounded to the north by the Southern Uplands Fault, of which the Lammermuir Fault is considered to be a part. This needs to be examined more clearly (as actually happens later). The characteristics which define the Southern Uplands as a tectonic unit are the following:

(i) Generally high elevation with relative stability after Silurian times.

(ii) Pre-Devonian trench and oceanic sediments at or near the surface.

(iii) Few post-Silurian sedimentary basins, with no major ones along the Caledonian trend.

Similarly the Midland Valley is characterized by the following:

(i) Generally lower elevation (compared to the Southern Uplands); occasional high elevation is due to more resistent igneous rocks.

(ii) Most outcropping rocks are post-Silurian and are not oceanic or trench sediments, but unmetamorphosed land or shallow marine sediments; there are also abundant Carboniferous volcanics.

(iii) Development of deep post-Silurian sedimentary basins along the Caledonian trend as well as in other directions and significant faulting and folding during the Permo-Carboniferous times.

A precise definition of these two tectonic units is difficult to make, because several marginal areas appear to be transitional, with some properties of both units.

Underlying granitic masses could be the cause of the long-standing stability of the Southern Uplands and the associated lack of sedimentary basins, as well as its high elevation.

Taking the Southern Uplands Fault System as a boundary marker between two distinct tectonic provinces, the Midland Valley and the Southern Uplands, the Pentland Fault is not an acceptable continuation from the Leadburn Fault for the following reasons:

1. Its position is north-west of the Midlothian Coalfield.

2. It changes its downthrow (Anderson, 1951) to the NW and SE as it runs to the Firth of Forth. This is a characteristic mostly met with in the (Western) Midland Valley faults.

3. It is the area immediately SE of the Leadburn Fault (and not the Pentland Fault) which is overlying the large granite batholith (Chapter V) extending in the Southern Uplands along the Caledonian trend. Hence, the Leadburn component, having the same trend, appears to be the most natural boundary between the Midland Valley and the Southern Uplands. In fact, it is suggested here that the Leadburn component of the Southern Uplands Fault was formed because of the uplift of the Southern Uplands during the emplacement of the granite batholith (since uplift of country rocks along faults was long ago proposed during the emplacement of some plutons (Noble, 1952)).

After excluding the Pentland Fault as the continuation of the Southern Uplands Fault, as a tectonic boundary , the question still remains as to its most probable location.

The Lammermuir Fault is unlikely to be a tectonic boundary because of its age, which is believed to be initiated in post-Devonian times (the Dunbar-Gifford Fault was formed at a later stage). Also, one would tend to consider as a north-easterly boundary of the Southern Uplands, the north-easterly termination of the underlying area batholith; in fact the north-western margin of the batholith in the East Lothian area extends farther to the NW than the Lammermuir and the Dunbar-Gifford Fault.

Therefore, it is suggested that the north-eastern continuation of the Southern Uplands boundary is (1) either along the edge of the granite batholith in East Lothian (farther NW of the Lammermuir and Dunbar-Gifford Faults) or (2) the monocline fold of the eastern side of the Midlothian Coalfield, running from the Roslin-Vorgie Fault System to the coast near Prestonpans. To the east of this fold, the Old Red Sandstone and to a lesser extent, the Carboniferous are absent or more thinly developed than to the west.

The north-easterly increase of the throw of the Lammermuir and the Dunbar-Gifford Fault, can be explained as the differential rate of subsidence along the underlying batholith in Carboniferous times (it should be noted (Chapter V) that the batholith to the NE of Lammer Law extends at progressively greater depths under the surface) which generally gives a better stability in that area (East Lothian) compared with the one of the Midlothian where the rate of subsidence was relatively higher and the deposition of sediments considerably greater.

6.4 East Lothian Area

Detailed geological accounts of the East Lothian and East Fife areas have been given by Geikie (1902), Clough et al (1910) and McGregor and McGregor (1948).

It is well known that intensive volcanicity broke out during the Lower Carboniferous times and the vast outpouring of lavas (calc-alkaline) started first in the eastern part of the Midland Valley, notably in the Burntisland area and the Garleton Hills, and then they spread to the western part, the lava beds becoming progressively younger from NE to SW.

In the upper part of the Dinantian, the lavas formed the Burntisland and Garleton Hills Group, which are believed to be in continuous sequence under the Firth of Forth and, also, may be continuous with the Clyde Plateau lavas, forming the Forth Volcanic Group (Francis, 1965). The continuation of the lavas at depth receives support from the aeromagnetic picture of these areas.

The lower part of the volcanic sequence in the East Lothian area (Garleton Hills) is basaltic, while the upper part is more acid (trachytes etc) compared with that of West Lothian and Eastern Fife. McGregor and McGregor (1948) estimated the whole sequence in Garleton Hills to be 600 m.

Apart from the basaltic lavas and the trachytes in the East Lothian area there are numerous intrusions and necks, which were the subject of study for many geologists, not only there, but also in the East Fife area (Francis(1961) and referred papers).

According to Francis (1968) there are two types of intrusions: (1) Alkaline, which are restricted to areas of Carboniferous sediments and take the form of dolerite sills up to 120m in thickness. In the East Lothian area they are confined mainly to the Traprain Law area, forming the Traprain Law phonolite intrusion, and in the area immediately south of Aberlady Bay. (2) Calc-alkaline, forming dykes and sills of quartz-dolerites and tholeiites. They have an E-W direction and although the sills are met with in the Carboniferous sediments, the dykes extend into older rocks. In East Lothian few of the dykes can be traced in the eastern part of this region. The age of these intrusions is late Carboniferous and, in the Midland Valley, they are related to the Midland Valley Sill (Francis, 1965), extending beneath the sediments and covering a large area of the eastern part of the Midland Valley.

The aeromagnetic picture suggests a complex pattern over the East Lothian area and the magnetic high (230nT) a few kilometres SW of Aberlady suggests rather a local thickening of the lavas at that point.

An attempt was made to estimate the thickness of those volcanic rocks in the East Lothian area and under the Firth of Forth from the aeromagnetics; subsequently, their gravitational attraction was calculated to find out its contribution to the observed steep gravity gradient across East Lothian.

For this, the aeromagnetic map (Bullerwell, 1968) was digitised at 2km intervals. The resulting values are contoured in figure 6.16. As was expected, these values present a smooth picture of the digitised area, simplifying its complexity.

Dr Powell's (Glasgow University) MAGRAV program was used. The upper surface of the lava beds was fixed at a shallow constant depth (about 20m) beneath the ground surface (350m) below the flight level (about 330m) of the aeromagnetic survey.

To start the iterative procedure of the program, an input array of base depths was given. In the south-eastern part of the digitised area, near Gifford, the lavas are exposed and their thickness is known (about 40m). Thus, the base depth of the input model was given at this point. A magnetisation contrast of 450nT was given as an input. The latter value was based on susceptibility measurements of a quartz-dolerite dyke near Musselburgh. After 30 iterations the RMS residual between the input digitised values and the calculated values, was 2.16 nT. The resulting base depths are shown in figure 6.17.

The maximum thickness of the lavas occurs a few kilometres SW of Aberlady Bay with a value of about 470m. It is clear

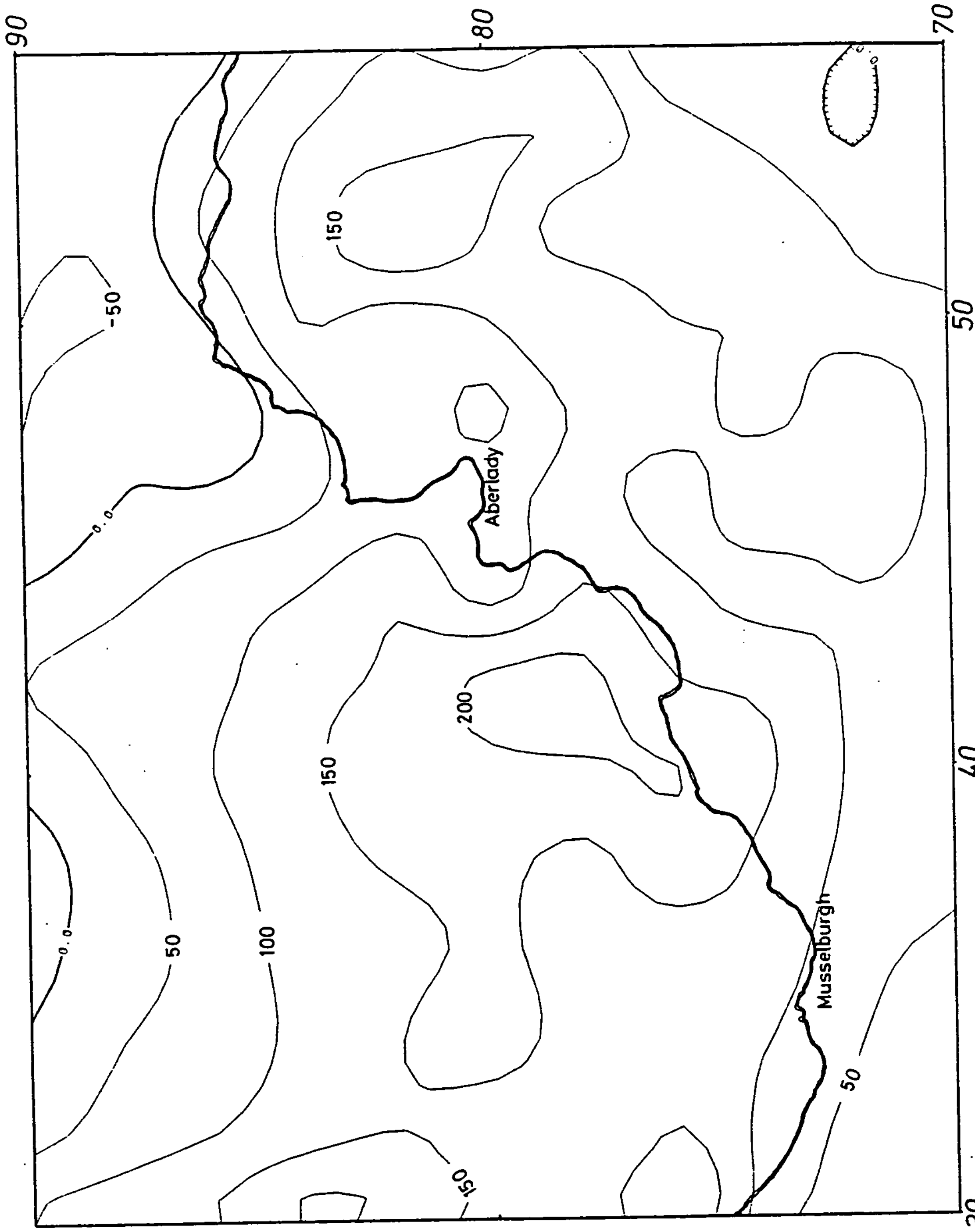

Fig. 6.16 Map showing the result of digitising the aeromagnetic map (Bullerwell, 1968) at 2km intervals. Contour interval 50 nT.

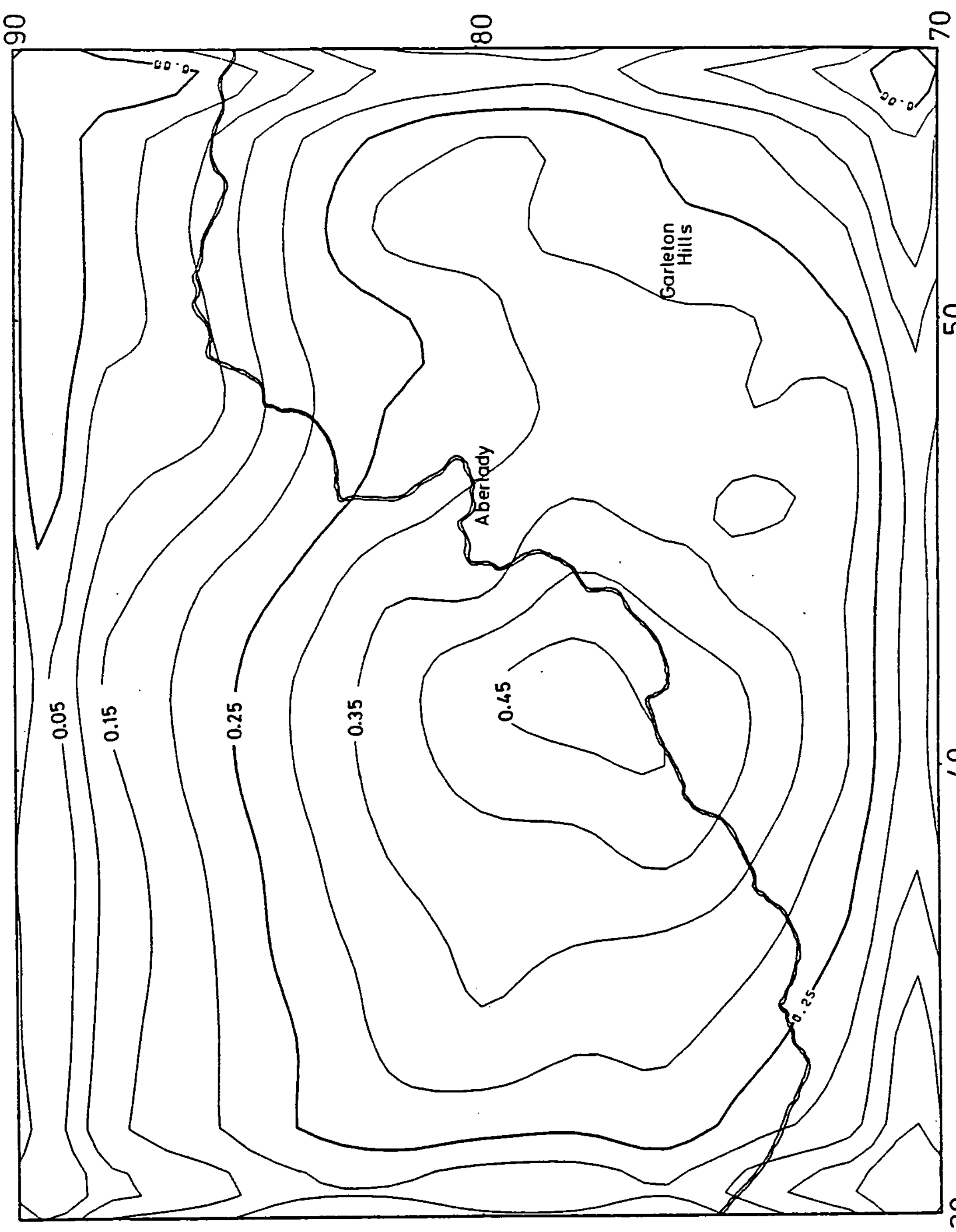

Fig. 6.17 Three-dimensional aeromagnetic interpretation of the volcanic rocks in the Firth of Forth and East Lothian. Contours at 0.050km interval.

that they are continuous under the Firth of Forth and definitely extend to the west. To the north, figure 6.17, the volcanic rocks are roughly bounded by the zero magnetic anomaly contour, with their thickness increasing southwards.

Having a quantitative estimate of the thickness of the East Lothian volcanic sequence, their gravitational attraction was calculated by postulating a density contrast between the Lower Carboniferous sediments and the basic Carboniferous rocks. A mean density of 2.80 g/cc was assigned for the basic rocks: basalts - late Carboniferous sills and dykes. Density measurements of basalt from Markle Quarry (Table II-2) have shown a value (about 2.722 g/cc), see Table II-3, similar to the one found for the Clyde Plateau lavas (McLean, 1961a), and a value of nearly 2.90 g/cc is representative for the more dense dykes and sills. The trachytes proved to be less dense than the basalts, as was actually expected. Hence, a density contrast of 0.25-0.30 g/cc between the Carboniferous basic rocks and the sediments is reasonable.

A slightly modified version of program MODG3D was used to calculate an approximate gravitational attraction of this basic sheet. The bottom depths-array was the lower termination of the prisms of MODG3D, while their upper part was fixed at a constant shallow depth (about 20m). The density contrast was 0.25 g/cc, which will probably yield a lower limit to the amplitude of the gravity expression of the lava beds.

Figure 6.18 shows the gravity map of the area, according to this procedure. The gravity maximum SW of Aberlady Bay has a value of 39 gu. Assigning a density contrast of 0.30 g/cc, then the maximum value will be 47 gu.

Independently of the maximum value, the interesting fact is that the observed maximum gradient at the south-eastern part of figure 6.18 is only about 3 gu/km. This implies that the presence of the lava beds contribute little (one fourth) to the observed gradient (13 gu/km) of the Bouguer anomaly in the Haddington area of East Lothian. As a consequence, the steep gradient must be caused by the edge of the granite batholith at this area, as suggested in 5.4.4. This supports the hypothesis that the granite is responsible for the relative stability of the whole East Lothian area compared to the Midlothian and East Fife Coalfield area in Carboniferous times, as reflected by the different rate of deposition and considerable different development of the sedimentary sequence.

By having a picture of the thickness of the lavas and removing their effect from the Bouguer anomaly map of the area, the monoclinal fold on the East-Midlothian boundary (perhaps formed because of the influence of the granite batholith) becomes even more clear as the eastern boundary of the Midland Valley.

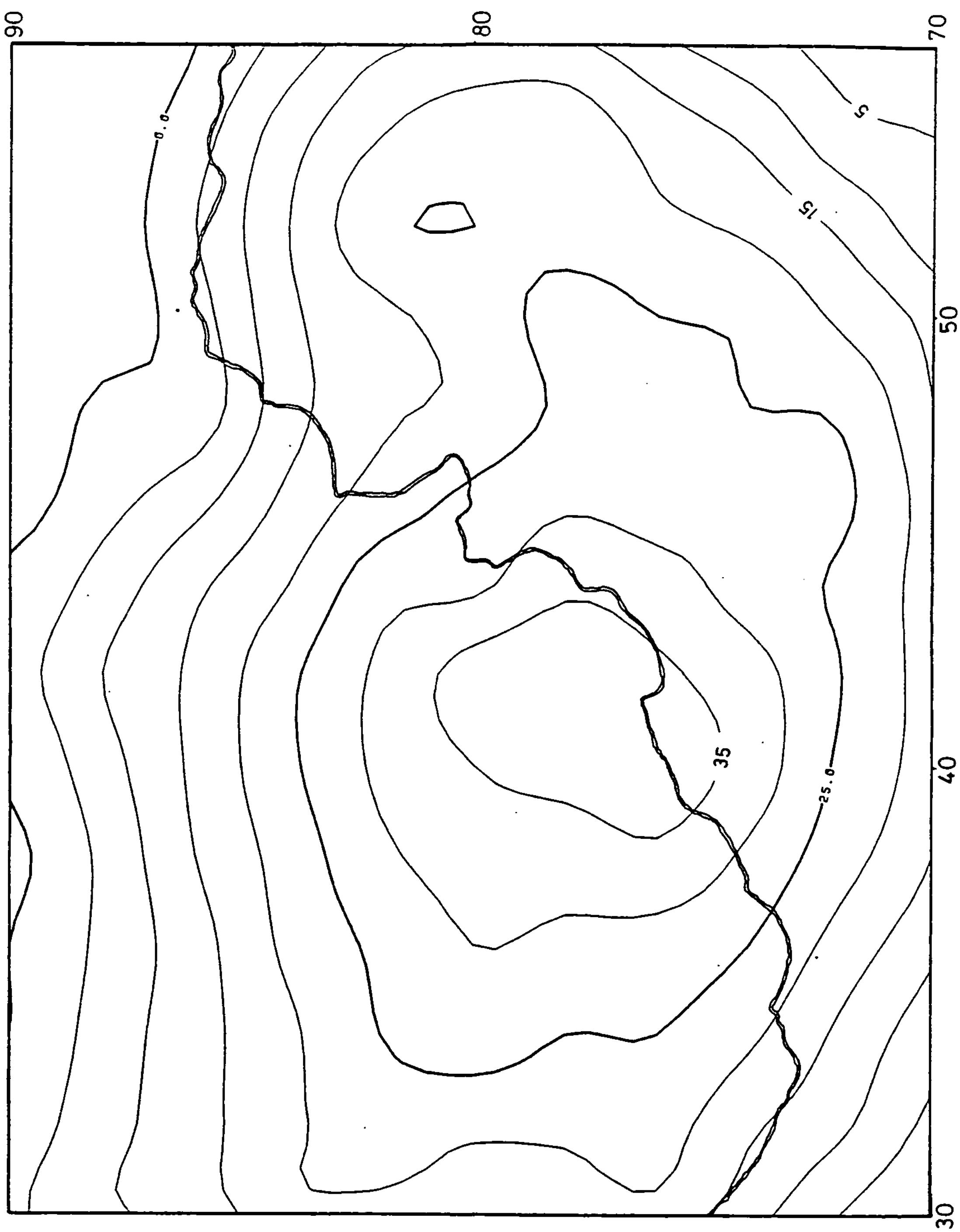

Fig. 6.18 Map showing the gravity effect of the volcanics in East Lothian and the Firth of Forth (figure 6.17). Contour interval 5 gu.

6.4.1 Continuation of the Southern Uplands Granite under East Lothian

In this section, the northerly continuation of the granite batholith under East Lothian is examined and discussed.

From the models of the Southern Uplands batholith discussed in section 5.4.4, it has already been inferred that the granite does extend to the north of the modelled area into East Lothian; earlier in this chapter it was also suggested that it is the underlying granite, rather than the Carboniferous volcanics, which causes the steep gravity gradients there. The continuation of the granite will now be shown explicitly by a two-dimensional gravity model.

The gravity profile KL was constructed, running at an angle of about 18^{o} to the LISPB line. The position of the profile is shown on the gravity anomaly map-in back pocket. Again a regional field from the LISPB model (Fig. 5.2 and 5.3) was calculated and removed. The residual gravity profile is shown in the upper part of figure 6.19.

The shallow structure of the model (Fig.6.19) was deduced from Sheet 33 of the 1" Geological Map of Scotland, dated 1894, as well as from a still unpublished one in preparation for the area (Tulloch, personal communication). The Spilmersford borehole (Davies, 1974), (at NT 4570 6902 and shown on figure 6.8) was found very useful as a control for the Lower Carboniferous sediments and volcanics: this was the reason for choosing the profile over Spilmersford. The following generalized succession was found in the bore (Davies, 1974):

(i) 21 m of Lower Limestone Group,

(ii) 259.64 m of Calciferous Sandstone sediments (Dinantian),

(iii) 256.64 m of lavas, tuffs and agglomerates (Dinantian),

(iv) 1.06 m of Calciferous Sandstone sediments,

(v) 114.5 m of intrusive dolerite (late Westphalian, McAdam, 1974),

(vi) 8.9 m of Upper Old Red Sandstone sediments, the base of which was not reached.

The rock densities used to construct the model (Fig.6.19) were deduced and based on density measurements made by the author (Chapter II), on values of density used in the western part of the Midland Valley (McLean and Qureshi, 1966) and on geophysical surveys at the Spilmersford borehole (Allsop, 1974); the following values were adopted:

(i) 2.55 g/cm^3 for Lower Limestone Group,

(ii) 2.54 g/cm^3 for Calciferous Sandstone sediments,

(iii) 2.54 g/cm^3 for Upper Old Red Sandstone (the same density with the Calciferous Sandstone Series was used here for the sake of simplicity of the model),

(iv) 2.72 g/cm^3 for Lower Palaeozoic sediments (Silurian and Ordovician),

(v) 2.73 g/cm^3 for the lavas and tuffs and agglomerates,

(vi) 2.90 g/cm^3 for the dolerite intrusion (sill),

(vii) 2.65 g/cm^3 for granite.

Using these densities, the TALG2D program was used to match the residual values of the profile KL. The results are shown in figure 6.19.

In this model, it is clearly shown that the granite extends northwards under East Lothian to about the coast, at one point coming within

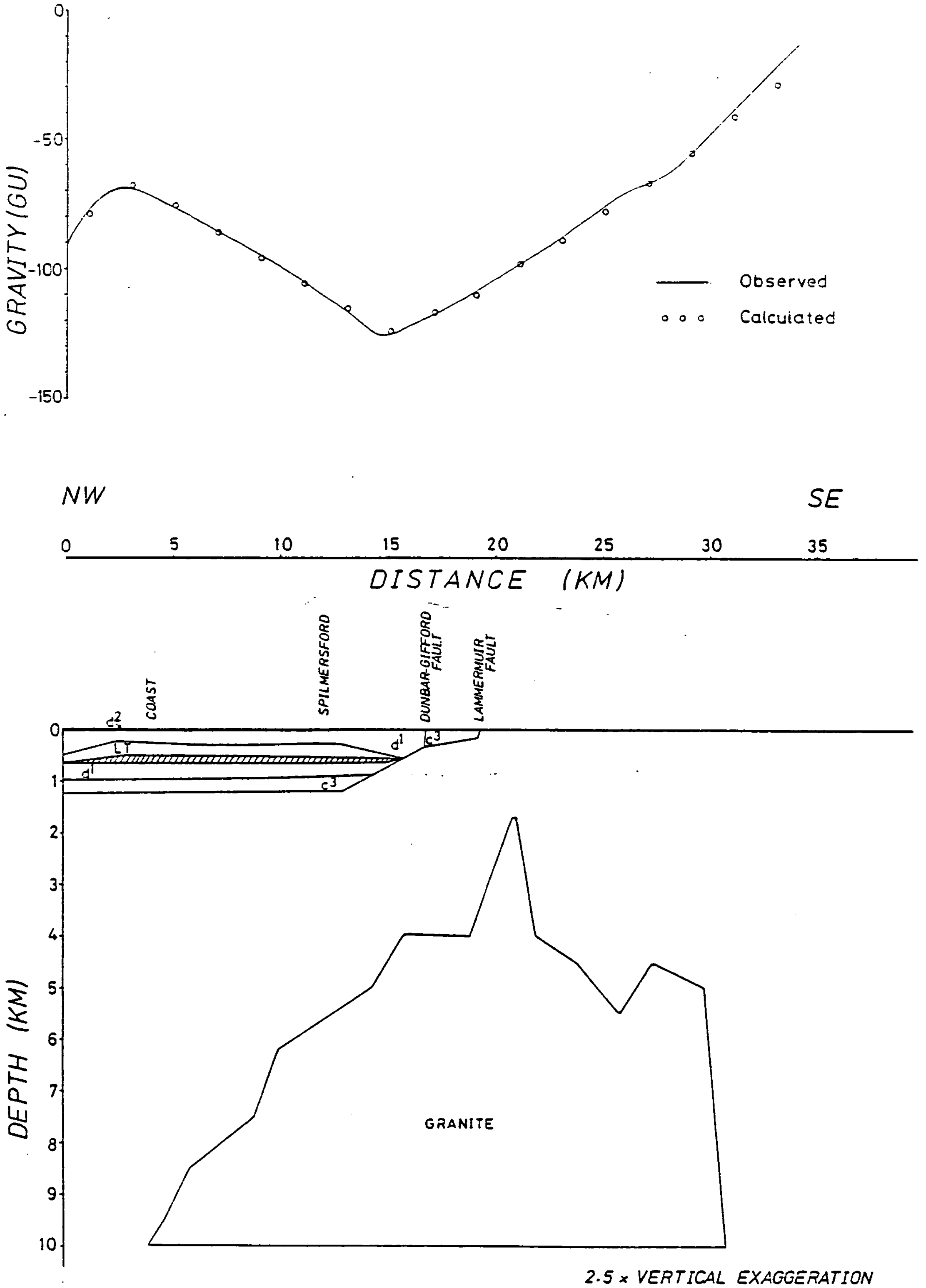

Fig. 6.19 An interpretation of profile KL (see gravity map, back pocket). Densities used in text. LT : Lavas, tuffs, agglomerates; shaded layer represents olivine-basalt. Coordinares: NT 385 795 and NT 567 512.

1700 m of the surface. This occurs just south-west of Lammer Law, at a point corresponding closely to the centre of the Lammer Law aeromagnetic anomaly, although the profile is 1.5 km to the south-west of the centre. This offset, together with the fact that it is a two- rather than three-dimensional model, probably explains the different depths obtained, 1700 m here and less than 330 m from the aeromagnetic anomaly (Bennett, 1969).

The total thickness of the volcanic rocks in figure 6.19 is also consistent with the model derived from aeromagnetic anomalies in section 6.4.

CHAPTER VII

CONCLUSIONS

7.1 Gravity Data Processing

A total of 2500 gravity stations have been observed in south-east Scotland, mainly by the author. This is a part of Britain for which no gravity anomaly observations had been reported in the literature before and for the first time a Bouguer anomaly map was prepared for it and published (Lagios and Hipkin, 1979 a,b). These data are now available to the public in catalogue form (Appendix C). All stages of their reduction and presentation (Chapter II) were handled adequately on a computer, including the contouring of the map (Chapter IV).

The base station network and other field measurements were observed with unusual accuracy: a least-squares network adjustment gave a root mean square residual of only 0.096 g.u. (9.6 microgal), which is much better than the National Gravity Reference Net (1973) - see Chapter III.

7.2 Geological Interpretations

In Chapter V it was strongly argued that a granite batholith underlies the north-eastern part of the Southern Uplands (Fig.5.23a and Fig. 5.23b) and it was also shown more specifically in Chapter VI that the batholith underlies almost the whole East Lothian area (Fig.6.19). This interpretation offers a significant key to explaining and understanding the structure and evolution of the upper crust there, which is noted for its high elevation and long-standing stability.

LISPB did not succeed in tracing the upper and mid-crustal refractor horizons under the Southern Uplands with much certainty. Now, in the light of the evidence of a granite underlying this area, this can be understood: the small width of the Southern Uplands and the presence of the granitic bodies would cause scatter and consequently, the "disappearance" of the seismic rays coming from greater depths towards the surface. This phenomenon has recently been demonstrated in a preliminary way in the region between the Highland Boundary Fault and the Great Glen Fault (Dimitropoulos, person. commun.).

The age of emplacement of the batholith is taken to be Lower or Middle Devonian because it appears to be related to the small granite outcrops in East Lothian and Berwickshire, which have this age (section 5.4.1). This coincides with the age for the main movements on the Leadburn Fault, deduced by Hipkin (1977 b) from the cutting out across the fault of Lower Devonian sediments underneath the Carboniferous and Upper Devonian.

Thus the Leadburn component of the Southern Uplands Fault System was initiated during the uplift which accompanied the emplacement of the granite, and the fault runs along its north-western flank (the Leadburn Fault is situated 1 km beyond the north-western margin of the area modelled in figures 5.7 to 5.10, and parallel to this edge). Relatively little (<90 m) post-Devonian movement on the Leadburn Fault is recorded (Tulloch and Watson, 1958), compared with about 2 km during the Devonian.

In areas where faulting features appear to be running along or little beyond the margins of the granite (e.g. Leadburn Fault), their throw develops with large dimensions, particularly when the granite comes closer to the surface. However, when faults are met in areas which are underlain by the batholith, their throw appears to be generally small (Lammermuir and Dunbar-Gifford Faults,(?)Southern Uplands Fault near New Cumnock).

Although the north-western boundary of the Southern Uplands is defined clearly in the central part by the Leadburn Fault, in the north-east, the boundary is more properly defined by the edge of the granite than by the Lammermuir Fault, which has been envisaged as the boundary by many geologists (Chapter VII). It was shown (Chapter VI) that the shape of the gravity field in East Lothian is probably not strongly affected by the Lower Carboniferous volcanics, and therefore is dominated by the edge effect of the granite, which extends at depth nearly to the coast.

Hence, the boundary of the Southern Uplands, as defined by the edge of the batholith, might be near the present coast-line from Prestonpans (the eastern boundary of the Midland Valley, section 6.4) to Dunbar.

The southern limits of the batholith are deduced from gravity models in section 5.3.4.1 and 5.4.4 to run in the central Southern Uplands approximately between St. Mary's Loch, via Galashiels, to Lauder, more or less parallel to the Caledonian trend.

The position of the remainder of the southern boundary and most of the eastern boundary is largely conjectural. Beyond Lauder, the southern limit becomes obscure because the superposition of the Upper Devonian and Lower Carboniferous sediments, and Carboniferous intrusive and extrusive volcanics creates a more confused gravity anomaly field.

Nevertheless, the gravity high, which in Selkirkshire clearly identifies the southern limit, is perhaps related to highs around Greenlaw and south of Eyemouth, which suggests a boundary roughly following the Rivers Blackadder, Whiteadder and Tweed between Greenlaw and Berwick upon Tweed. This broadly marks the boundary between the lower lying Merse, inferentially beyond the buoyant effect of the granite, and the more elevated Southern Uplands, underlain by it. Again, it is near the northern margin of the Carboniferous Borders Basin, the formation of a basin suggesting greater stability to the north.

Although such a southern boundary is speculative, it does include all the minor granite exposures of the eastern Southern Uplands and is consistent with the very few other means of inferring where the granite might be. However, it does exclude Cheviot. It would be difficult either to prove or disprove a connection at depth between Cheviot and the Southern Uplands batholith on the basis of the gravity anomalies, but the development of the Borders Basin between them makes a lack of connection not completely improbable.

The eastern boundary is again conjectural but Geikies's observation of a facies change in the Devonian to the west of the Innerwick Fault (section 6.2.3.1), and the development of a significant Devonian basin at Oldhamstocks suggest that the boundary between

Dunbar and Eyemouth is near the present coast-line, perhaps initially following the Innerwick and Cove Faults. The coastal boundary fault described by Shiell (1963) - see figure 5.21 a - might then close the eastern and southern boundaries but an extension seawards is perhaps suggested by the aeromagnetic anomalies.

In general, the picture of granite intrusion causing uplift along an axis between Tweeddale and Lammer Law, decreasing to the east and south-east fits very well with Bluck's (1978) Upper Old Red Sandstone depositional trends (figure 6.2).

The presence of the granite is generally consistent with recent plate tectonic models (Phillips _et al_, 1976). Because a granitic belt is not expected to overlie the region where subduction was taking place, the author prefers those tectonic models which put the suture of Iapetus along the Solway rather than in the Southern Uplands.

REFERENCES

AGGER, H.E. and CARPENTER, E.W. 1965. A crustal study in the vicinity of the Eskdalemuir seismological array station. Geophys. J.R. Astron. Soc., Vol. 9, pp. 69-83.

ALLSOP, J.M. 1974. Geophysical surveys at the Spilmersford Borehole, East Lothian, Scotland. Bull. geol. Surv. Gt. Br., Vol. 45, pp. 63-72.

ANDERSON, E.M. 1951. The dynamics of faulting and dyke formation with applications to Britain. Oliver and Boyd, Edinburgh.

ASSUMPCAO, M. and BAMFORD, D. 1978. LISPB-V studies of crustal shear waves. Geophys. J.R. Astron. Soc., Vol. 54, pp. 61-73.

BAMFORD, D., FABER, S., JACOB, B., KAMINSKI, W., NUNN, K., PRODEHL, C., FUCHS, K., KING, R. and WILLMORE P. 1976. A lithosphere seismic profile in Britain. I - preliminary results. Geophys. J.R. Astron. Soc., Vol. 44, pp. 145-160.

BAMFORD, D., NUNN, K., PRODEHL, G., JACOBS, B. 1977. LISPB-III. Upper crustal structure of N. Britain. J. Geol. Soc. Lond. Vol. 133, pp. 481-488.

BAMFORD, D., NUNN, K., PRODEHL, C., JACOB, B. 1978. LISPB-IV. Crustal structure of Northern Britain. Geophys. J.R. Astron. Soc., Vol. 54, pp. 43-60.

BENDAT, J.S. and PIERSOL, A.G. 1971. Random data: analysis and measurement procedures. Wiley-InterScience, New York.

BENNETT, J.R.P. 1969. Results of geophysical surveys in the Haddington area. Inst. Geol. Sci. Rep. GP/AG/70/13.

BEVINGTON, P.R. 1969. Data reduction and error analysis for the physical sciences. Edit. McGraw-Hill, New York.

BLAXLAND, A.B., AFTALION, M., VAN BREEMEN, O. 1979. Pb isotopic composition of feldspars from Scottish Caledonian granites and the nature of the underlying crust. Scott. J. Geol., Vol. 15, pp. 139-151.

BLUCK, B.J. 1978. Sedimentation in a late orogenic basin: the Old Red Sandstone of the Midland Valley of Scotland. Repr. Geol. Jour. Sp. Is No. 10.

BOTT, M.H.P. 1953. Negative gravity anomalies over acid "intrusions" and their relation to the structure of the earth's crust. Geol. Mag., Vol. 90, pp. 257-67.

BOTT, M.H.P. 1956. A geophysical study of the granite problem. Quart. J. Geol. Soc. Vol. 12, pp. 45-67.

BOTT, M.H.P. 1959. The use of electronic digital computers for the evaluation of gravimetric terrain corrections. Geophys. Prospect., Vol. 7, pp. 45-54.

BOTT, M.H.P. 1962. A simple criteria for interpreting negative gravity anomalies. Geophysics, Vol. 27, pp. 376-381.

BOTT, M.H.P. 1974. The geological interpretation of a gravity survey of the English Lake District and the Vale of Eden. J. Geol. Soc. Lond. , Vol. 130, pp. 309-331.

BOTT, M.H.P. and MASSON-SMITH, D. 1957. The geological interpretation of a gravity survey of the Alston Block and the Durham Coalfield. Quart. J. Geol. Soc., Vol. 113, pp. 93-116.

BOTT, M.H.P. and MASSON-SMITH, D. 1960. A gravity survey of the Criffell granodiorite and the New Red Sandstone deposits near Dumfries. Proc. Yorks. Geol. Soc., Vol. 32, pp. 317-332.

BOTT, M.H.P. and SMITH, R.A. 1958. The estimation of the limiting depth of gravitating bodies. Geophys. Prospect., Vol. 6, pp. 1-10.

BOTT, M.H.P. and SMITHSON, S.B. 1967. Gravity investigations of subsurface shape and mass distributions of granite batholiths. Bull. Geol. Soc. Amer., Vol. 78, pp. 869-885.

BOTT, M.H.P. , ROBINSON, J. and KOHNSTAMM, M.A. 1978. Granite beneath Market Weighton, East Yorkshire. J. Geol. Soc. Lond., Vol. 135, pp. 535-43.

BRIDEN, J.C., MORRIS, W.A., PIPER, J.D.A. 1973. Palaeomagnetic studies of the British Caledonides - IV. Regional and Global Implications. Geophys. J.R. Astron. Soc., Vol. 34, pp. 107-134.

BRIGGS, I.C. 1974. Machine contouring using minimum curvature. Geophysics, Vol. 39, pp. 39-48.

BROWN, G.C. and HENNESSY, J. 1978. The initiation and thermal diversity of granite magmatism. Phil. Trans. R. Soc. A.288, pp. 631-643.

BRUCKSHAW, J.M. and KUNARATNAM, K. 1960. The interpretation of magnetic anomalies due to dykes. Geophys. Prospect. Vol. 11, pp. 509-522.

BRUCKSHAW, J.M. and ROBERTSON, E.I. 1949. The magnetic properties of the tholeiite dykes of north England. Month. Not. of R.A.S. Geophys. Suppl., Vol. 5(8), pp. 308-320.

BULLARD, E.C. and JOLLY, H.L. 1936. Gravity measurements in Great Britain. Month. Not. of R.A.S. Geophys. Suppl. Vol. 3, No. 9, pp. 443-477.

BULLERWELL, W. 1968. Aeromagnetic map of part of Great Britain and Northern Ireland, Sheet 11. Inst. Geol. Sci., London.

CALCOMP - Applications software (1973) G.P.C.P. (A general purpose contouring program). Users' manual. California Computer Products, Inc. La Palma - USA.

CARTWRIGHT, D.E. and EDDEN, A.C. 1973. Corrected tables of tidal harmonics. Geophys. J.R. Astron. Soc., Vol. 33, pp. 253-264.

CARTWRIGHT, D.E. and TAYLER, R.J. 1971. New computation of the tide-generating potential. Geophys. J.R. Astron. Soc., Vol. 23, pp. 45-74.

CHISHOLM, J.I. and DEAN, J.M. 1974. The Upper Old Red Sandstone of Fife and Kinross: a fluviatile sequence with evidence of marine incursion. Scott. J. Geol., Vol. 10(1), pp. 1-30.

CHRISTIE, P.A.F. 1978. A report on the Cambridge North Sea experiment. Paper presented at 2nd UK Geophys. Assembly, Liverpool. Abstract in: Geophys. J.R. Astron. Soc., Vol. 53, pp.140.

CHURCH, W.R. and GAYER, R.A. 1973. The Ballantrae ophiolite. Geol. Mag., Vol. 110, pp. 497-510.

CLOUGH, C.T., BARROW, G., CRAMPTON, C.B., MAUFE, H.B., BAILEY, E.B. and ANDERSON, E.M. 1910. The Geology of East Lothian. Mem. Geol. Surv. Scotland. Edinburgh.

DAVIES, A. 1974. The Lower Carboniferous (Dinantian) sequence at Spilmersford, East Lothian, Scotland. Bull. geol. Surv. Gt. Br., Vol. 45, pp. 1-24.

DEWEY, J.F. 1969. Evolution of the Appalachian Caledonian orogeny. Nature, Vol. 222, p. 124 - 129.

DEWEY, J.F. 1971. A model for the Lower Palaeozoic evolution of the southern margin of the Early Caledonides of Scotland and Ireland. Scott. J. Geol., Vol. 7, p. 219-235.

DEWEY, J.F. and PANKHURST, R.J. 1970. The evolution of the Scottish Caledonides in relation to their isotopic age pattern. Trans. Roy. Soc. Edin., Vol. 68, pp. 361-387.

DIMITROPOULOS, K. and DONATO, J. 1979. A geophysical interpretation of the Inner Moray Firth sedimentary basin. In press. Abstract in Geophys. J.R. Astron. Soc., Vol. 57, p 260.

EL-BATROUKH, S.I. 1975. Geophysical investigations on Loch Doon granite, south-west Scotland. PhD. Thesis, University of Glasgow.

FITTON, J.G., HUGHES, D.J. 1970. Volcanism and plate tectonics in the British Ordovician. Earth and Planetary Sci. Letters, Vol. 8, pp. 223-228.

FRANCIS, E.H. 1961. Thin beds of graben keolinized tuff and tuffaceous siltstone in the Carboniferous of Fife. Bull. geol. Surv. Gt. Br., Vol. 17, pp. 191-215.

FRANCIS, E.H. 1965. Carboniferous-Permian igneous rocks, In: the Geology of Scotland (Ed. G.Y. Craig). Edinburgh.

FRANCIS, E.H. 1968. Review of Carboniferous Permian volcanism in Scotland. Geol. Rdsch., Vol. 57, pp. 219-246.

GARSON, M.S. and PLANT, J. 1973. Alpine type ultramafic rocks and episodic mountain building in the Scottish Highlands. Nature Phys. Sci., Vol. 242, pp. 34-38.

GEIKIE, A. 1864. The geology of Eastern Berwickshire. Mem. Geol. Surv. Scotland, London.

GEIKIE, A. 1902. The geology of Eastern Fife. Mem. Geol. Surv. Scotland, Glasgow.

GEORGE, T.N. 1960. The stratigraphic evolution of the Midland Valley. Trans. Geol. Soc. Glasg., Vol. 24, p. 32.

GIBSON, M.O. 1937. Network adjustment by least squares - alternative formulations and solution by iterations. Geophysics, Vol. 6, pp. 168-79.

GRANT, F.S. 1972. Review of data processing and interpretation methods in gravity and magnetics. Geophysics, Vol. 37, pp. 647-661.

GREIG, D.C. 1971. The south of Scotland. HMSO, Edinburgh.

GUNN, P.J. 1972. Wiener filter transformations of gravity and magnetic fields and a regional interpretation of the Midland Valley of Scotland and Northern Ireland. PhD Thesis, University of Durham.

GUNN, P.J. 1973. Location of the Proto-Atlantic suture in the British Isles. Nature, Vol. 242, pp. 11-112.

GUNN, P.J. 1975. Interpretation of the Bathgate magnetic anomaly, Midland Valley, Scotland. Scott. J. Geol., Vol. 11(3), pp. 263-267.

HALL, J. 1970. The correlation of seismic velocities with formations in the SW of Scotland. Geophys. Prospect., Vol. 18, pp. 134-148.

HALL, J. 1971. A preliminary seismic survey adjacent to the Rashiehill borehole near Slamannan, Stirlingshire. Scott. J. Geol., Vol. 7, pp. 170-174.

HALL, J. 1974. A seismic reflection survey of the Clyde Plateau lavas in North Ayrshire and Renfrewshire. Scott. J. Geol., Vol. 9, pp. 253-279.

HALL, D.H. and DANGLEY, M.A. 1970. Regional magnetic anomalies IGS Report No. 70/10.

HAMMER, S. 1939. Terrain correction tables for gravity. Geophysics. Vol. 4, pp. 184-194.

HARDY, J. 1892. Report of meetings for 1891: History of the Berwickshire Naturalist Club, Vol. IX, p. 481.

HARLAND, W.B. and GAYER, R.A. 1972. The Arctic Caledonides and earlier oceans. Geol. Mag., Vol. 109, pp. 289-314.

HIPKIN, R.G. 1977a. A gravity survey over the Midlothian Coalfield. Contr. Paper in Southern Uplands Workshop, Edinburgh.

HIPKIN, R.G. 1977b. A gravity survey of the South Midlothian Coalfield and the Southern Uplands Fault System. Contr. paper in the 1st UKGA, Edinburgh. Abstr. in Geophys. J. R. Astron. Soc., Vol. 49, p. 289.

HIPKIN, R.G. 1978a. A microgravimetric network for secular gravity studies in Scotland. Geophys. J.R. Astron. Soc., Vol. 52, pp. 383-46.

HIPKIN, R.G. 1978b. A microgravimetric network for secular gravity studies in Scotland. Paper pres. at the Intern. Gravity Commission, Paris.

HIPKIN, R.G. and LAGIOS, E. 1978. A gravity survey of SE Scotland: the Southern Uplands. Paper pres. at the 2nd UKGA, Liverpool. Abstract in: Geophys. J.R. Astron. Soc., Vol. 52, p. 160.

HOLDER, A.P. and BOTT, M.H.P. 1971. Crustal structure in the vicinity of south-west England. Geophys. J.R. Astron. Soc., Vol. 23, pp. 465-468.

HOSSAIN, M.A. 1976. Analysis of the major gravity and magnetic anomalies centred about Bathgate, central Scotland. MSc Thesis, University of Glasgow.

HOWELL, H.H., GEIKIE, A. and YOUNG, J. 1866. The geology of East Lothian. Mem. Geol. Surv. Gt. Britain, London.

IBM. 1969. System/360 scientific subroutine package (PL/I) (360A-CM-Ø7X). Program description and operations manual, New York.

JACOB, A.W.B. 1969. Crustal phase velocities observed at the Eskdalemuir Seismic Array. Geophys. J.R. Astron. Soc., Vol. 18, pp. 189-197.

JAIN, S. and WILSON, C.D.V. 1967. Magneto-telluric investigations in the Irish Sea and Southern Scotland. Geophys. J.R. Astron. Soc., Vol. 12, pp. 165-180.

JEANS, P.J.F. 1973. Plate tectonic reconstruction of the Southern Caledonides of Great Britain. Nature Phys. Sci., Vol. 245, pp. 120-122.

JONES, A.G. 1977. Geomagnetic induction studies in Southern Scotland, PhD. Thesis, University of Edinburgh.

JONES, A.G. and HUTTON, R. 1979a. A multi-station magnetotelluric study in Southern Scotland - I. Fieldwork, data analysis and results. Geophys. J.R. Astron. Soc., Vol. 56, pp. 329-350.

JONES, A.G. and HUTTON, R. 1979b. A multi-station magnetotelluric study in southern Scotland - II. Monte-Carlo inversion of the data and its geophysical and tectonic implications. Geophys. J.R. Astron. Soc., Vol. 56, pp. 351-368.

KANE, M.F. 1962. Comprehensive system of terrain corrections using a digital computer. Geophysics, Vol. 27, pp. 455-62.

KELLING, G. 1962. The petrology and sedimentology of Upper Ordovician rocks in the Rhinns of Galloway, south-west Scotland. Trans. R. Soc. Edinburgh, Vol. 65, pp. 107-137.

KENNEDY, W.Q. 1958. The tectonic evolution of the Midland Valley of Scotland. Trans. geol. Soc. Glasgow, Vol. 23, p. 106.

KRIGE, D.G. 1966. Two-dimensional weighted moving average trend surfaces for ore evluations. Proc. Symposium on mathematical statistics and computer applications in ore evaluation, Johannesburgh, pp. 13-79.

KROHN, D. 1976. Gravity terrain corrections using multiquadratic equations. Geophysics, Vol. 41, pp. 266-275.

LAGIOS, E. 1978. A gravity survey of SE Scotland: East Lothian, the Lammermuir Fault, and the Old Red Sandstone Basins. Paper presented at the 2nd UKGA 1978, Liverpool. Abstract in: Geophys. J.R. Astron. Soc., Vol. 52, p. 160.

LAGIOS, E. and HIPKIN, R.G. 1979a. More on the Tweeddale granite. Paper presented at 3rd UKGA, Southampton. Abstr. in: Geophysi. J.R. Astron. Soc., Vol. 57, p. 275.

LAGIOS, E. and HIPKIN, R.G. 1979b. The Tweeddale granite - a newly discovered betholith in the Southern Uplands. Nature, Vol. 280, pp. 672-675.

LEEDER, M.R. 1973. Sedimentology and palaeogeography of the Upper Old Red Sandstones in the Scottish Border basin. Scott. J. Geol., Vol. 9, pp. 118-144.

LONGMAN, C.D., BLUCK, B.J. and VAN BREEMEN, O. 1979. Ordovician conglomerates and the evolution of the Midland Valley. Nature, Vol. 280, pp. 578-581.

MASSON-SMITH, D., HOWELL, P.M. and ABERNETHY-CLARK, A.B.D.E. 1974. The National Gravity Reference Net, 1973. Ord. Surv. prof. Pap., Vol. 26, 22 pages.

MAX, M.D. 1976. The pre-Palaeozoic basement in SE Scotland and the Southern Uplands Fault. Nature, Vol. 264, pp. 485-486.

McADAM, A.D. 1974. The petrography of the igneous rocks in the Lower Carboniferous (Dinantian) at Spilmersford, East Lothian, Scotland. Bull. geol. Surv. Gt. Br., Vol. 45, pp. 39-46.

McGREGOR, M. and McGREGOR, A.G. 1948. The Midland Valley of Scotland (2nd Ed.). British Regional Geology, Geol. Surv., UK. HMSO, Edinburgh.

McKERROW, W.S., LEGGETT, J.K. and EALES, M.H. 1977. Impricate thrust model of the Southern Uplands of Scotland. Nature, Vol. 267, pp. 237-239.

McLEAN, A.C. 1961. Gravity survey of the Sanquhar Coalfield. Proc. Roy. Soc. Edin. B, Vol. 68, pp. 112-127.

McLEAN, A.C. 1961a. Density measurements of rocks in SW Scotland. Proc. Roy. Soc., Edin., Vol. 68, pp. 103-111.

McLEAN, A.C. 1966. A gravity survey in Ayrshire and its geological interpretation. Trans. Roy. Soc. Edin., Vol. 66, pp. 239-265.

McLEAN, A.C. and DEEGAN, C.E. 1978. The solid geology of the Clyde Sheet (55°N/6°W). Inst. Geol. Sci. Rep. 78/9.

McLEAN, A.C. and QURESHI, I.R. 1966. Regional gravity anomalies in the western Midland Valley of Scotland. Trans. Roy. Soc. Edin., Vol. 66, pp. 267-83.

McROBERT, W.R. 1914. Acid and intermediate intrusions and associated ash necks in the neighbourhood of Melrose. Quart. J. Geol. Soc., IXX, pp. 303-14.

MITCHELL, A.H.G. and McKERROW, W.S. 1975. Analogous evolution of the Burma Orogen and Scottish Caledonides. Geol. Soc. America Bull., Vol. 86, pp. 305-15.

MORELLI, C. 1976. Modern standards for gravity surveys. Geophys. J.R. Astron. Soc., Vol. 45, p. 199.

MORTON, D.J. 1979. Palaeogeographical evolution of the Lower Old Red Sandstone basin in the western Midland Valley. Scott. J. Geol., Vol. 15(2), pp. 97-116.

MOSELEY, F. 1977. Caledonian plate tectonics and the plane of English Lake District. Geol. Soc. America Bull., Vol. 88, pp. 764-788.

NAFE, J.E. and DRAKE, C.L. 1963. Physical properties of marine sediments, in: "The Sea," Vol. 3, Ed. M.N. Hill (Interscience) pp. 794-815. New York.

NAGY, D. 1966. The prism method of terrain corrections using digital computers. Pure and Applied Geophysics, Vol. 63, pp. 31-39.

NETTLETON, L.L. 1939. Determination of density for reduction of gravimeter observations. Geophysics, Vol. 4, pp. 176-83.

NICOL, J. 1843. On the geology of Peeblesshire. Trans. Highl. Soc. of Scotland, vol. XIV, New Ser., Vol. VIII, pp. 149-206.

NOBLE, J.A. 1952. Evaluation of criteria for the forcible intrusion of magma. Jour. Geology, Vol. 60, pp. 34-57.

OLEA, R.A. 1975. Optimum mapping techniques using Regionalised Variable Theory. Kansas Geol. Survey, Univ. of Kansas.

PARASNIS, D.S. 1952. A study of rock densities in the English Midlands. Mon. Not. Roy. Astr. Soc. Geophys. Suppl., Vol. 6, pp. 252-71.

PARASNIS, D.P. 1972. Principles of applied geophysics. Ed. Chapman and Hall, London.

PARKER, R.L. 1972. The rapid calculation of potential anomalies. Geophys. J.R. Astron. Soc., Vol. 31, pp. 447-455.

PARSLOW, G.R. 1968. The physical and structural features of the Cairnsmore Fleet granite and its aureole. Scott. J. Geol., Vol. 4, pp. 91-108.

PARSLOW, G.R. and RANDALL, B.A.O. 1973. A gravity survey of the Cairnsmore of Fleet granite and its environs. Scott. J. Geol., Vol. 9, pp. 219-231.

PATERSON, I.B., BROWNE, M.A.E. and ARMSTRONG, M. 1976. Upper Old Red Sandstone palaeogeography. Scott. J. Geol., Vol. 12, pp. 89-91.

PEACH, B.N. and HORNE, J. 1899. The Silurian rocks of Britain, I. Scotland. Mem. Geol. Surv., Glasgow.

PENTZ, H.H. 1952. A least square method for gravity meter base stations. Geophysics, Vol. 18, pp. 314-400.

PHILLIPS, W.E.A. 1973. The pre-Silurian rocks of Clare Island, Co. Mayo, and the age of metamorphism of the Dalradian in Ireland. J. geol. Soc. Lond., Vol. 129, pp. 585-606.

PHILLIPS, W.E.A., STILLMAN, C.J. and MURPHY, T. 1976. A Caledonian plate tectonic model. J. geol. Soc. Lond., Vol. 132, pp. 576-609.

PIPER, J.D.A. 1978. Palaeomagnetism and palaeogeography of the Southern Uplands block in Ordovician times. Scott. J. Geol., Vol. 14(2), pp. 93-107.

POWELL, D.W. 1970. Magnetised rocks within the Lewisian of Western Scotland and under the Southern Uplands. Scott. J. Geol., Vol. 6, pp. 353-371.

POWELL, D.W. 1971. A model for the Lower Palaeozoic evolution of the south margin of the early Caledonides of Scotland and Ireland. Scott. J. Geol., Vol. 7, pp. 369-372.

POWELL, D.W. 1977a. Gravity and magnetic interpretations of Ballantrae ophiolites. Contributed paper: S.U. Workshop held in Edinburgh, 11 March 1977.

POWELL, D.W. 1977b. Gravity and magnetic interpretations of Southern Uplands granites. Contributed paper: S.U. Workshop held in Edinburgh, 11 March 1977.

PRINGLE, J. 1948. The South of Scotland. Brit. Reg. Geology, Geological Survey and Museum, Edinburgh, HMSO.

QURESHI, I.R. 1961. A gravity survey of the regions of the Highland Boundary Fault between Callander and Cowal. PhD Thesis, University of Glasgow.

QURESHI, I.R. 1970. A gravity survey of a region of the Highland Boundary Fault in Scotland. Quart. J. geol. Soc., Vol. 125, pp. 481-502.

RITCHIE, M. and ECKFORD, R.J.A. 1931. The lavas of Tweeddale and their position in the Caradocian sequence. Summ. Prog. for 1930. Mem. Geol. Surv., pp. 46-57.

ROBSON, D.A. 1977. The structural history of the Cheviot and adjacent regions. Scott. J. Geol., Vol. 13, pp. 255-262.

SAMPSON, R.J. 1975. Surface-II graphic system. Number 1 series on special analysis. Kansas Geological Survey.

SCRUTTON, R.A. and DINGLE, R.V. Basement control over sedimentation on the continental margin west of Southern Africa. Trans. Geol. Soc.Afr., Vol. 77, pp. 253-260.

SEARLE, R.C. 1969. Barometric hypsometry and a geophysical study of part of the Gregory Rift Valley. PhD Thesis, University of Newcastle upon Tyne.

SHIELLS, K.A.G 1963. The geological structure of north-east Northumberland. Trans. R. Soc. Edinb., Vol. 65, pp. 449-481.

SHIELLS, K.A.G. and DEARMAN, W.R. 1963. Tectonics of the Coldingham Bay area of Berwickshire, in the SW of Scotland. Proc. Yorks. Geol. Soc., Vol. 34, p. 209.

SHIELLS, K.A.G. and DEARMAN, W.R. 1966. On the possible occurrence of Dalradian rocks in the SW of Scotland. Scott. J. Geol., Vol. 2, pp. 231-242.

SMITH, A.E. 1950. Graphic adjustment by least squares, Geophysics, Vol. 16, pp. 222-227.

SMITH, T.E. 1967. A preliminary study of sandstone sedimentation in the Lower Carboniferous of the Tweed Basin. Scott. J. Geol., Vol. 3, pp. 282-305.

STROGEN, P. 1974. The sub-Palaeozoic basement in Central Ireland. Nature, Vol. 250, pp. 562-563.

SWAIN, C.J. 1976. A Fortran IV program for interpolating irregularly spaced data using the difference equations for minimum curvature. Computers and Geosciences, Vol. 1, pp. 231-240.

SWAIN, C.J. and KHAN, M.A. 1977. A catalogue of gravity data in Kenya. Leicester University Publications.

SWAIN, C.J. and KHAN, M.A. 1978. Gravity measurements in Kenya. Geophys. J.R. Astron. Soc., Vol. 53, pp. 427-429.

SYMAP. 1975. User's reference manual. Laboratory of Computer Graphics and Spatial Analysis, Graduate School of Design, Harvard University.

SYMVU. 1977. A user's guide. Edinburgh Catalogue No. 18.900.102 (Ed. D.T. Muxworthy). Program Library Unit, Edinburgh.

TALWANI, M., WORZEL, J.L. and LANDISMAN, M. 1959. Rapid gravity computations for two-dimensional bodies, with application to the Mendocino submarine fracture zone. J. Geophys. Res., Vol. 64, pp. 49-59.

TOBLER, W. 1977. Corrections to C J Swain's program for interpolating irregularly spaced data. Computers and Geosciences, Vol. 3, p. 181.

TULLOCH, W. and WATSON, H.S. 1958. The geology of the Midlothian Coalfield. Mem. Geol. Surv. Scot., Edinburgh.

TULLY, M.C. and McQUILLIN, R. 1978. A gravity survey of the UK sector of the North Sea. Paper pres. at 2nd UKGA, Liverpool. Abstr. in: Geophys. J.R. Astron. Soc., Vol. 52, p. 140.

UPTON, B.G.J., ASPEN, P. and GRAHAM, A. 1976. Pre-Palaeozoic basement of the Scottish Midland Valley. Nature, Vol. 260, pp. 517-518.

WALKER, F. 1924. Four granitic intrusions in SE Scotland. Trans. Edinb. Geol. Soc., Vol. 11, p. 357.

WALKER, F. 1928. Plutonic intrusions of the Southern Uplands, East of Nith Valley. Geol. Mag., Vol. 65, pp. 153-162.

WALKER, P. 1977. An automatic data reduction and analysis of a gravity survey of the Kavirondo Rift Valley, Kenya. MPh Thesis, University of Leeds.

WALTON, E.K. 1955. Silurian greywackes in Peeblesshire. Proc. Roy. Soc. Edinb. B., Vol. 65, pp. 327-357.

WALTON, E.K. 1965. In "The geology of Scotland" (ed. G.Y. Craig). pp. 161-227. Edinburgh.

WATSON, J. 1964. Conditions in the metamorphic Caledonides during the period of late orogenic cooling. Geol. Mag., Vol. 101, pp. 457-465.

WATSON, S.W. 1976. The sedimentary geochemistry of the Moffat shales: a carbonaceous sequence in the Southern Uplands of Scotland. PhD Thesis (unpubl.) University of St Andrews.

WHITTEN, E.H. 1974. Orthogonal polynomial contoured trend surface maps for irregularly spaced data. Computer Applications, Vol. 1, pp. 171-192.

WILLIAMS, A. 1969. Ordovician of the British Isles, in Kay, M. ed. North Atlantic geology and continental drift. Am. Assoc. Petroleum Geologists Mem. 12.

WILLIAMS, A. 1972. Distribution of brachiopod assemblages in relation to Ordovician palaeogeography in Organisms and continents through time (ed. N.F. Hughes) Spec. Pap. Palaeont., Vol. 12, pp. 241-269.

WILLIAMS, A. 1975. Plate tectonics and biofacies evolution as factors in Ordovician correlation, in The Ordovician system: proceeding of a Palaeodological Association Symposium Cardiff, University of Wales Press and Nat. Mus. Wales, (ed. M.G. Bassett). pp. 18-53.

WILSON, G.V. 1918. Preliminary notes on volcanic necks in north-west Ayrshire. Trans. Geol. Soc. Glasgow, Vol. 16, pp. 86-99.

WILSON, J.T. 1966. Did the Atlantic close and re-open? Nature, Vol. 211, pp. 676-681.

WILSON, G.V. and FLETT, J.S. 1921. Memoirs of the Geological Survey, Scotland. Special reports on the mineral resources of Great Britain. The lead, zinc, copper and nickel ores of Scotland. Edinburgh.

WOOLLARD, G.P. 1962. The relation of gravity anomalies to surface elevations, crustal structure and geology. Res. Rep. Series No. 62-9. Univ. of Wisconsin, Dept. Geology.

WRIGHT, A.E. 1976. Alternating subdiction direction and the evolution of the Atlantic Caledonides. Nature, Vol. 264, pp. 156-160.

YOUNG, H.D. 1962. Statistical treatment of experimental data. McGraw-Hill, New York.

ZIEGLER, A.M. 1970. Geosynclinal development of the British Isles during Silurian period. J.Geol., Vol. 78, p. 445.

APPENDIX A

DATA INPUT TO PROGRAM NETWORK

	Reference Number	Observed Gravity -9814000.00	Time in Gregorian Day Number -27000.00000
9	1	1849.16	1147.44375
	4	1329.40	1147.46875
	5	2004.61	1147.48958
	6	1960.55	1147.51875
	8	1957.38	1147.54375
	9	1929.56	1147.56250
	10	1359.61	1147.58750
	4	1329.39	1147.67639
	1	1849.16	1147.69444
3			
	1	1849.16	710.52083
	7	1786.32	710.57083
	7	1786.09	710.70486
4			
	16	1111.60	1317.43403
	18	1393.58	1317.46528
	18	1393.49	1317.69236
	16	1111.60	1317.75903
3			
	15	1333.98	1297.45694
	16	1111.60	1297.64375
	15	1333.98	1297.81111
3			
	15	1333.98	1298.47222
	16	1111.40	1298.63611
	15	1333.98	1298.73611
3			
	16	1111.60	1312.43611
	17	1447.85	1312.58403
	17	1447.85	1312.78472
3			
	16	1111.60	1313.45486
	17	1448.05	1313.63611
	17	1447.85	1313.71597
3			
	16	1111.50	1315.43333
	17	1447.85	1315.60625
	17	1447.85	1315.81111
3			
	18	1392.64	1323.46319
	14	1548.65	1323.61944
	14	1548.65	1323.79306
5			
	1	1849.16	1325.38958
	19	1372.81	1325.45208
	18	1393.97	1325.58958
	18	1393.09	1325.72083
	1	1849.16	1325.79653
3			
	15	1333.98	1295.44792
	16	1111.83	1295.62639
	15	1333.98	1295.80903

3			
	4	1828.95	1257.42639
	15	1333.98	1257.60278
	4	1829.40	1257.70347
4			
	4	1829.40	1255.42708
	15	1334.02	1255.60069
	15	1333.94	1255.78611
	4	1829.40	1255.86389
3			
	12	1663.61	1253.43819
	14	1548.65	1253.61528
	12	1663.61	1253.74306
4			
	12	1663.61	1250.45556
	14	1548.54	1250.61319
	14	1548.54	1250.79931
	12	1663.61	1250.85069
4			
	4	1829.40	1248.43333
	13	1230.93	1248.53056
	13	1230.93	1248.61806
	13	1230.93	1248.76042
3			
	11	1768.80	1239.49792
	12	1663.69	1239.68403
	10	1859.61	1239.81181
3			
	11	1768.80	1238.47361
	11	1768.80	1238.66458
	10	1859.61	1238.83056
3			
	20	1485.27	1243.46875
	12	1663.61	1243.62222
	20	1485.27	1243.79722
4			
	11	1768.59	1229.47083
	10	1859.61	1229.55417
	11	1769.01	1229.68819
	10	1859.61	1229.75000
3			
	5	2004.61	1222.45417
	6	1960.61	1222.58611
	8	1957.38	1222.75208
4			
	4	1829.40	1219.41111
	9	1929.59	1219.55625
	9	1929.56	1219.69514
	8	1957.38	1219.79097
3			
	4	1829.40	1186.44236
	5	2004.25	1186.67708
	4	1829.40	1186.73819
3			
	4	1829.40	1199.43125
	5	2004.89	1199.58194
	4	1829.40	1199.75139

3			
	4	1829.40	1204.40625
	5	2004.53	1204.59931
	4	1829.40	1204.75486
3			
	4	1829.40	1210.48472
	5	2004.91	1210.63819
	4	1829.40	1210.78681
3			
	4	1829.40	1212.41389
	5	2004.75	1212.59375
	4	1829.40	1212.72778
4			
	1	1849.16	1154.47292
	4	1829.13	1154.49375
	5	2004.41	1154.64583
	6	1960.45	1154.68333
5			
	1	1849.16	1164.43889
	6	1960.93	1164.47778
	8	1957.32	1164.53403
	9	1929.69	1164.61944
	1	1849.16	1164.65903
4			
	4	1829.40	1179.44097
	9	1929.78	1179.52708
	10	1859.80	1179.65556
	4	1829.40	1179.73333
4			
	4	1829.40	1408.41667
	7	1786.02	1408.43542
	7	1786.17	1408.74167
	4	1829.40	1408.76042
4			
	4	1829.40	1416.42361
	20	1485.57	1416.45347
	20	1485.67	1416.70347
	4	1829.40	1416.74653
3			
	3	1787.79	1471.39931
	15	1333.94	1471.42778
	3	1787.79	1471.73889
3			
	3	1787.79	1472.40625
	15	1334.02	1472.60833
	3	1787.79	1472.63681
9			
	3	1787.79	1444.44097
	3	1787.81	1444.45486
	3	1787.82	1444.46528
	3	1787.76	1444.47222
	30	1230.78	1444.54583
	31	983.40	1444.59375
	32	1049.65	1444.64722
	29	1404.39	1444.70139
	3	1787.79	1444.74514

12			
	3	1787.79	1451.36250
	30	1230.72	1451.43889
	33	977.09	1451.46528
	32	1049.46	1451.52014
	54	997.62	1451.57292
	16	1111.55	1451.62847
	17	1447.94	1451.64583
	13	1393.17	1451.65694
	19	1372.84	1451.67917
	14	1548.65	1451.69306
	4	1829.37	1451.74306
	3	1787.79	1451.76319
16			
	3	1787.79	1458.43889
	3	1787.78	1458.44583
	2	1689.51	1458.46389
	1	1848.91	1458.48194
	1	1848.87	1458.48611
	3	1787.89	1458.49931
	2	1689.73	1458.50972
	2	1689.73	1458.51181
	1	1849.15	1458.52917
	1	1849.12	1458.53194
	3	1787.84	1458.54514
	3	1787.76	1458.54792
	2	1689.49	1458.55694
	2	1689.50	1458.56042
	3	1787.83	1458.57153
	3	1787.79	1458.57431
5			
	3	1787.95	1445.41528
	1	1849.16	1445.43889
	3	1787.79	1445.45417
	1	1849.16	1445.47361
	3	1787.62	1445.49236
7			
	3	1787.79	1624.35833
	7	1785.97	1624.40000
	13	1230.71	1624.42500
	18	1393.28	1624.45833
	17	1447.72	1624.76875
	15	1333.96	1624.79861
	3	1787.79	1624.82847
5			
	3	1787.79	1625.35417
	13	1230.55	1625.41667
	17	1447.62	1625.45000
	15	1333.63	1625.82847
	3	1787.79	1625.86250
6			
	3	1787.79	1627.34583
	16	1111.54	1627.40694
	19	1372.58	1627.82431
	20	1485.29	1627.84653
	11	1768.65	1627.87500
	3	1787.79	1627.91597

6		
3	1787.79	1635.35556
15	1333.85	1635.39514
25	1335.90	1635.44236
26	1220.22	1635.66111
15	1333.71	1635.90208
3	1787.79	1635.83194
8		
3	1787.79	1634.35069
25	1335.74	1634.49583
26	1220.26	1634.71736
19	1372.90	1634.76944
12	1663.46	1634.79514
9	1929.29	1634.81667
7	1785.82	1634.83819
3	1787.79	1634.86806
3		
16	1111.60	1637.39583
21	1093.31	1637.52292
15	1333.98	1637.71181
4		
15	1333.98	1638.40139
21	1093.24	1638.61389
25	1335.96	1638.69306
16	1111.60	1638.76181
4		
26	1220.22	1641.43889
26	1220.22	1641.64792
24	1477.26	1641.73958
18	1393.10	1641.77083
3		
26	1220.22	1642.43681
24	1477.26	1642.60069
19	1372.46	1642.73403
3		
19	1372.46	1644.42847
24	1477.08	1644.58958
19	1372.46	1644.76806
3		
21	1093.24	1647.44583
54	997.43	1647.55069
25	1335.74	1647.58958
7		
5	2004.61	1651.41597
7	1786.06	1651.43264
11	1769.01	1651.45417
9	1929.53	1651.46875
6	1969.69	1651.49028
7	1786.03	1651.50833
5	2004.61	1651.52361
3		
3	1787.79	1652.35139
22	1721.11	1652.49931
3	1787.79	1652.74931
4		
3	1787.79	1654.35417
22	1721.30	1654.48194
23	1379.91	1654.71528
3	1787.79	1654.76389

3			
	3	1787.79	1655.36528
	23	1879.67	1655.60972
	3	1787.79	1655.77431
5			
	3	1787.79	1660.34444
	27	2016.43	1660.55903
	28	1941.89	1660.59167
	23	1879.93	1660.62361
	3	1787.79	1660.68611
3			
	22	1721.11	1665.40000
	27	2016.37	1665.53750
	23	1879.91	1665.72222
4			
	22	1721.11	1666.39931
	28	1941.65	1666.44236
	28	1941.62	1666.67014
	22	1721.11	1666.71111
3			
	13	1230.93	1676.42569
	20	1485.58	1676.77639
	7	1796.09	1676.30347
3			
	34	1288.90	355.59028
	53	1217.27	355.67708
	34	1288.90	355.70139
3			
	34	1288.90	362.56597
	37	1215.06	362.63681
	34	1288.90	362.68889
4			
	35	1670.17	369.39583
	38	1560.96	369.64306
	34	1289.15	369.68264
	35	1670.17	369.69861
4			
	36	1808.23	344.58056
	39	1639.51	344.60069
	1	1849.16	344.68056
	36	1808.23	344.69097
3			
	36	1808.23	708.59722
	39	1639.55	708.62500
	36	1808.23	708.70069
3			
	34	1288.90	429.42361
	52	1163.91	429.44792
	41	1456.40	429.69444
6			
	29	1404.39	930.42569
	42	1270.32	930.43958
	43	1316.50	930.46597
	44	1311.17	930.47847
	45	1231.67	930.66111
	46	1801.07	930.30208

3			
	47	1246.79	932.41875
	47	1246.95	932.56528
	43	1316.40	932.69097
4			
	47	1246.79	933.38542
	44	1310.77	933.45833
	43	1316.54	933.52083
	43	1316.40	933.66944
4			
	29	1404.39	893.39653
	52	1163.89	893.66736
	37	1214.90	893.75764
	29	1404.39	893.32639
3			
	29	1404.39	902.78403
	34	1288.97	902.80694
	29	1404.39	902.86181
3			
	29	1404.39	918.38194
	51	1292.42	918.31181
	29	1404.39	918.35764
3			
	34	1288.90	937.36597
	53	1217.31	937.38958
	34	1288.90	937.70694
4			
	43	1316.40	940.37292
	31	983.31	940.44583
	32	1049.97	940.48681
	46	1801.07	940.54306
4			
	43	1316.40	941.37153
	31	983.37	941.43681
	32	1049.84	941.68611
	43	1316.40	941.72222
5			
	34	1288.90	944.36597
	45	1231.12	944.39444
	32	1049.89	944.62222
	45	1231.80	944.71528
	34	1288.90	944.76736
3			
	34	1288.90	947.38542
	47	1246.61	947.66181
	34	1288.90	947.68958
15			
	34	1288.90	954.35833
	41	1456.44	954.39444
	46	1801.26	954.43542
	1	1849.29	954.45833
	46	1801.15	954.47222
	40	1415.41	954.49931
	51	1292.54	954.50694
	42	1270.20	954.51736
	49	1419.97	954.53403
	34	1288.97	954.54097
	1	1848.93	954.59236

	39	1639.54	954.60764
	50	1354.08	954.63958
	48	1459.63	954.65833
	34	1288.85	954.66736
3			
	34	1288.90	683.42014
	38	1560.89	683.60069
	34	1288.90	683.63889
4			
	1	1849.16	690.41667
	34	1288.99	690.44444
	50	1353.85	690.63889
	34	1288.63	690.65278
3			
	46	1801.07	804.49861
	41	1457.24	804.68056
	46	1801.07	804.75000
06			
	34	1288.90	1675.36458
	47	1247.07	1675.41667
	55	1214.38	1675.48056
	45	1231.70	1675.49931
	32	1049.72	1675.58750
	34	1288.90	1675.77708
19			
	3	1787.79	1681.35278
	34	1288.95	1681.38542
	45	1231.77	1681.41042
	32	1049.72	1681.42361
	21	1093.10	1681.55764
	32	1049.57	1681.66736
	15	1334.05	1681.78125
	34	1288.83	1681.80833
	29	1404.34	1681.81736
	3	1787.79	1681.84583
5			
	46	1801.07	723.49583
	1	1849.80	723.51875
	1	1849.80	723.57708
	1	1850.14	723.62708
	46	1801.07	723.68264
09			
	03	1787.79	1989.32361
	30	1230.92	1989.36944
	33	977.02	1989.39236
	56	938.28	1989.50000
	57	703.26	1989.55694
	54	997.64	1989.62292
	19	1372.65	1989.69097
	3	1787.79	1989.76667

APPENDIX B

NETWORK COMPUTER PROGRAM

1. Description

Network is a Fortran-IV computer program which performs a least-square adjustment of gravity base station network.

With the first READ statement, the total number of traverses (K), bases (M), observations (NOBS) and the datum of the network (Gl), are read from channel 7. A serial reference number (NBASE) must be assigned to each of the base stations, beginning at 1 for the site of the network datum Gl.

With the second and third READ statements the rest of the required data are read from channel 8, as presented in Appendix A; that is, the reference number of a base (NBASE), the observation of its gravity value before adjustment (GRAV) reduced by 9814000 g.u. and the time of observation (TIME) given in days and decimals of a day. Traverses values may optionally have been corrected prior to the adjustment by any linear drift function; traverses need not be closed loops, but if not, the same set of trial base station values must have been used in the initial reduction.

Subsequently the arrays A and B of the (M + 2K) normal equations are constructed: AX = B, corresponding to equations 3.3, 3.4 and 3.5. The solution of the latter set of simultaneous equations is executed by subroutine SOLVE, which is a modified version of the SIMQ subroutine (IBM Scientific Subroutine Package, 1969), using the method of Gauss elimination. This routine returns the unknowns X in the array B, with the first M elements as the adjusted base values and the remaindering K elements as estimates of, or corrections to, the drift rate during each traverse.

The standard deviation (DGRAV) and the standard error (STEER) of each base as well as the RMS residual of the network adjustment (SIGMA) are calculated according to the analysis presented in section 3.3.7 of Chapter III. Also, the lower and upper limits of the adjusted values of the gravity bases and their standard deviations, with a 95% confidence interval - applying Student's "t" test - is calculated according to equations 3.10 and 3.11 (Chapter III); all those results are output to channel 6.

The residuals after adjustment (ERROR) from all the observational equations are prepared for display as a histogram on a line printer and output to channel 6. For this, the IBM S.S.P., (1969) subroutine HIST was modified so that the class interval was one standard deviation (SIGMA). Class frequencies predicted by a normal distribution are also shown.

After the main program, the listing of the subroutines SOLVE and HIST is presented.

2. Listing

```
C                          PROGRAM NETWORK
C          PERFORMS LEAST-SQUARE ADJUSTMENT OF A GRAVITY BASE STATION
C                              NETWORK

      REAL*8 ERROR(364),ERRSQ,SERSQ,TIME2,GT,A(221,221),B(221),SIGMA
     1,ERSQM(57),DGRAV(57),STERR(57),CNIN(57),GUL(57),GLL(57),VUL(57),VL
     1L(57),GPR(364),GAUSPR
      DIMENSION NBASE(364),GRAV(364),TIME(364),FREQ(20),NBST(57),T(50),
     1X025(50),X975(50)
      COMMON A,ERROR,B,ERSQM,DGRAV,STERR,GRAV,TIME,NBASE,CNIN,GUL,GLL,
     1VUL,VLL,GPR
C              PERCENTAGE POINTS OF T DISTRIBUTION
C                       FOR 95% CONFIDENCE
      DATA T/12.706,4.303,3.182,2.776,2.571,2.447,2.365,2.306,2.262,2.2
     128,2.201,2.179,2.160,2.145,2.131,2.120,2.110,2.101,2.093,2.086,2.0
     180,2.074,2.069,2.064,2.060,2.056,2.052,2.048,2.045,2.042,2.040,2.0
     138,2.036,2.034,2.034,2.032,2.030,2.028,2.026,2.021,2.020,2.019,2.0
     118,2.017,2.016,2.015,2.014,2.013,2.012,2.011/
C            PERCENTAGE POINTS FOR CHI-SQUARE DISTRIBUTION
C                          FOR 95%CONFIDENCE
      DATA X975/.000982,.0506356,0.216,0.484,0.831,1.237,1.689,2.179,2.7
     100,3.247,3.816,4.403,5.008,5.628,6.262,6.907,7.564,8.230,8.906,9.
     1590,10.282,10.982,11.688,12.401,13.197,13.843,14.573,15.308,16.04
     17,16.790,17.5,18.35,19.1,19.9,20.7,21.5,22.3,23.1,23.8,24.4331,25.
     12,26.0,26.8,27.5,28.3,29.1,29.9,30.7,31.5,32.3574/
      DATA X025/5.0238,7.377,9.348,11.143,12.832,14.449,16.012,17.534,1
     19.022,20.483,21.920,23.336,24.735,26.119,27.488,28.845,30.191,31.
     1526,32.852,34.169,35.478,36.780,38.075,39.364,40.646,41.923,43.19
     14,44.460,45.722,46.979,48.1,49.3,50.5,51.7,52.9,54.1,55.3,56.5,57
     1.9,59.341,60.5,61.7,62.9,64.3,65.6,66.9,68.2,69.4,70.5,71.42/

C       K=NO OF TRAVERCES,M=TOTAL NUMBER OF OBSERVATIONS
C               G1=ABSOLUTE VALUE OF GRAVITY
        READ(7,100)K,M,NOBS,G1
100     FORMAT(2I3,I4,F10.2)
      NN=M+2*K
      NS=NN*NN
      NFREE=NOBS-NN
      DO 2 I=1,NN
      DO 2 J=1,NN
      B(J)=0.
    2 A(I,J)=0.

       N=0

      DO 1 I=1,K
       L=M+I
      LN=M+K+I
      READ(8,200) IK
200     FORMAT(I2)
      A(L,L)=-IK

      DO 1 NP=1,IK
       N=N+1
```

```
 READ(8,300) NBASE(N),GRAV(N),TIME(N)
300     FORMAT(I7,5X,F10.2,7X,F10.5)
        TIMEN=TIME(N)
        J=NBASE(N)

          GRAVN=GRAV(N)
        TIME2=TIMEN*TIMEN
       GT=GRAVN*TIMEN

       A(L,J)=A(L,J)+1
       A(J,L)=A(J,L)-1
       A(J,J)=A(J,J)+1
       A(J,LN)=A(J,LN)+TIMEN
       A(LN,J)=A(LN,J)+TIMEN
       A(L,LN)=A(L,LN)+TIMEN
       A(LN,LN)=A(LN,LN)+TIME2
       A(LN,L)=A(LN,L)+TIMEN

       B(J)=B(J)+GRAVN
       B(L)=B(L)+GRAVN
       B(LN)=B(LN)+GT

     1 CONTINUE

       DO 3 J=1,NN
3       A(1,J)=0.
       A(1,1)=1.
       B(1)=G1

C     SOLUTION OF SIMULTANEOUS EQUATIONS
          CALL SOLVE(A,B,NN,IER)
C        IF IER=0 ACCEPTABLE SOLUTION
         WRITE(6,888) IER
888     FORMAT('IER=',I2)
C          WRITE(6,999) (I,B(I),I=1,NN)

       ERSUM=0.
       SERSQ=0.
       MK=M+K

       DO 51 N=1,M
       ERSQM(N)=0.
        STERR(N)=0.
       NBST(N)=0
    51 DGRAV(N)=0.

        DO 55 N=1,NOBS
   55   ERROR(N)=0.

       N=0
       REWIND 8
       DO 11 KK=1,K
       L1=M+KK
       L2=MK+KK
       READ(8,200) IK
       DO 11 NP=1,IK
```

```
      N=N+1
       READ(8,300) J,GRAVN,TIMEN
      NBST(J)=NBST(J)+1
      ERROR(N)=ERROR(N)+GRAVN-B(J)+B(L1)-TIMEN*B(L2)
      ERSUM=ERSUM+ERROR(N)
      ERRSQ=ERROR(N)*ERROR(N)
      ERSQM(J)=ERSQM(J)+ERRSQ
      SERSQ=SERSQ+ERRSQ
   11 CONTINUE

      DO 52 N=1,M
C       IF(NBST(N).EQ.1)GO TO 133
C       GO TO 134
C  133  DGRAV(N)=0.
C       STERR(N)=0.
C          GO TO 52

C     CALCULATION OF STANDARD DEVIATION & STANDARD ERROR
C                      OF EACH BASE
134     DGRAV(N)=DGRAV(N)+DSQRT(ERSQM(N)/NBST(N))
        STERR(N)=STERR(N)+DGRAV(N)/SQRT(FLOAT(NBST(N)))
  52       CONTINUE
      DO 93 I=1,M
  93  B(I)=B(I)+9814000.
C     EVALUATION OF UPPER & LOWER LIMIT OF GRAVITY & ITS STANDARD
C             DEVIATION ACCORDING TO STUDENT 'T' TEST
      DO 94 I=1,M
      L=NBST(I)-1
      IF(L) 95,95,96
96    CNIN(I)=DGRAV(I)*T(L)/SQRT(FLOAT(NBST(I)))
      GUL(I)=B(I)+CNIN(I)
      GLL(I)=B(I)-CNIN(I)

       VLL(I)=DGRAV(I)*SQRT(FLOAT(L)/X025(L))
       VUL(I)=DGRAV(I)*SQRT(FLOAT(L)/X975(L))
      GO TO 94
95    GUL(I)=0.
      GLL(I)=0.
        VLL(I)=0.
       VUL(I)=0.
  94  CONTINUE

      WRITE(6,997)
      WRITE(6,999)(I,B(I),DGRAV(I),STERR(I),I=1,M)
      WRITE(6,718)
718   FORMAT(9X,'BASE',3X,'LOWER  LIMIT',2X,'ABS. GRAVITY',2X,'UPPER  LI
     1MIT')
      WRITE(6,719)(I,GLL(I),B(I),GUL(I),I=1,M)
719   FORMAT(10X,I2,5X,F10.2,4X,F10.2,4X,F10.2/)

      WRITE(6,494)
494   FORMAT(9X,'BASE',3X,'LOWER  LIMIT',2X,'ST DEVIATION',2X,'UPPER  LI
     1MIT')
```

```
      WRITE(6,729) (I,NBST(I),VLL(I),DGRAV(I),VUL(I),I=1,M)
729    FORMAT(10X,I2,'(',I2,')',1X,F10.2,4X,F10.2,4X,F10.2/)
997    FORMAT(10X,'BASE STATION',2X,'ADJUSTED VALUE',2X,'STAND. DEVIATIO
     1N',2X,'STAND. ERROR')
C     WRITE(6,702) (J,ERROR(J),J=1,NOBS)
C998   FORMAT(I3,5X,F10.5)
        WRITE(6,568) SERSQ
568     FORMAT('SERSQ=',F10.5)
C     CALCULATION OF MEAN & RMS ERROR OF NETWORK

      EMEAN=ERSUM/FLOAT(NOBS)
      SIGMA=DSQRT(SERSQ/FLOAT(NOBS-1))

      WRITE(6,704) EMEAN
      WRITE(6,703) SIGMA
  704 FORMAT(20X,'EMEAN=',F10.5)
C702   FORMAT(20X,I2,5X,F10.5)
703   FORMAT('0',20X,'SIGMA',F10.5)
  999  FORMAT(14X,I3,9X,F10.2,9X,F5.2,12X,F5.2/)


C                   HISTOGRAM

C           FIND MINIMUM,MAXIMUM VALUE OF ERROR
      ERMAX=-10000000.0
      ERMIN=-ERMAX
      DO 24 I=1,NOBS
      XI=ERROR(I)
      IF(XI.GT.ERMAX) ERMAX=XI
      IF(XI.LT.ERMIN) ERMIN=XI
   24 CONTINUE
C      DETERMINATION OF NUMBER OF INTERVALS
       I=1
       INC=0
5981   INC=INC+2*I
       HL=INC*SIGMA/2.
        IF(HL.LT.ABS(ERMIN).AND.HL.LT.ERMAX) GO TO 5981

       INC=INC+1
       X1=-HL-HL/2.
       X2=HL+HL/2.
C      WRITE UPPER & LOWER LIMIT NUMBERS FOR THE HISTOGRAM
      WRITE(6,15206) X1,X2,SIGMA
15206  FORMAT('  X1 = ',F15.9,'  X2 = ',F15.9,' HISTOGRAM INTERVAL = ',F
     15.3)
C            EVALUATION OF THE FREQUENCY NUMBER
        DO 71 J=1,INC
71       FREQ(J)=0.
      X12=X2-X1
      DO 26 I=1,NOBS
      J=IDINT((ERROR(I)-X1/X12)*INC)+1
      FREQ(J)=FREQ(J)+1.
   26 CONTINUE
      CALL HIST(1,FREQ,INC)
      STOP
      END
```

```
C     SUBROUTINE SOLVE FOR SOLUTION OF A SET OF NORMAL
C     EQUATIONS BY THE METHOD OF GAUSS ELIMINATION
C        MODIFIED VERSION OF SIMQ ROUTINE(IBM,1969)

      SUBROUTINE SOLVE(A,B,N,KS)
      REAL*8 A(48841),B(221),BIGA,SAVE

      TOL=0.0
      KS=0
      JJ=-N
     DO 65 J=1,N
      JY=J+1
      JJ=JJ+N+1
      BIGA=0.
      IT=JJ-J
      DO 30 I=J,N

      IJ=IT+I
      IF(DABS(BIGA)-DABS(A(IJ))) 20,30,30
 20    BIGA=A(IJ)
      IMAX=I
 30   CONTINUE

      IF(DABS(BIGA)-TOL) 35,35,40
 35   KS=1
      RETURN

 40   I1=J+N*(J-2)
      IT=IMAX-J

       DO 50 K=J,N
       I1=I1+N
       I2=I1+IT
       SAVE=A(I1)
       A(I1)=A(I2)
       A(I2)=SAVE

 50    A(I1)=A(I1)/BIGA
       SAVE=B(IMAX)
       B(IMAX)=B(J)
       B(J)=SAVE/BIGA

       IF(J-N) 55,70,55
 55    IQS=N*(J-1)
       DO 65 IX=JY,N
       IXJ=IQS+IX
       IT=J-IX
       DO 60 JX=JY,N

      IXJX=N*(JX-1)+IX
      JJX=IXJX+IT
 60   A(IXJX)=A(IXJX)-(A(IXJ)*A(JJX))
 65   B(IX)=B(IX)-(B(J)*A(IXJ))
```

```
70    NY=N-1
      IT=N*N
           DO 80 J=1,NY
              IA=IT-J
       IB=N-J
       IC=N
       DO 80 K=1,J
       B(IB)=B(IB)-A(IA)*B(IC)
       IA=IA-N
80     IC=IC-1
       RETURN
       END
C     SUBROUTINE HIST FOR PRINTING HISTOGRAM IN A
C      LINE PRINTER. MODIFIED VERSION OF HIST(IBM,1969)

      SUBROUTINE HIST(NU,FREQ,IN)
      DIMENSION JOUT(20),FREQ(20)
       DATA K/'*'/,NOTH/' '/
1     FORMAT('EACH ',A1,'EQALS ',I2,' POINTS',/)
2     FORMAT(I6,4X,20(4X,A1))
3     FORMAT('INTERVAL',4X,19(I2,3X),I2)
4     FORMAT(1H1,47X,' HISTOGRAM ',I3)
5     FORMAT('FREQUENCY',20I5)
6     FORMAT(' CLASS')
7     FORMAT(113('-'))
      WRITE(6,4) NU
      DO 12 I=1,IN
12    JOUT(I)=FREQ(I)
           WRITE(6,5)(JOUT(I),I=1,IN)
       WRITE(6,7)
      FMAX=0.0
      DO 20 I=1,IN
      IF(FREQ(I)-FMAX) 20,20,15
15    FMAX=FREQ(I)
20    CONTINUE

      JSCAL=1
      IF(FMAX-50.) 40,40,30
30    JSCAL=(FMAX+49.0)/50.0
      WRITE(6,1) K,JSCAL

40     DO 50 I=1,IN
50     JOUT(I)=NOTH

       MAX=FMAX/FLOAT(JSCAL)
       DO 80 I=1,MAX
       X=MAX-(I-1)
       DO 70 J=1,IN
       IF(FREQ(J)/FLOAT(JSCAL)-X) 70,60,60
60     JOUT(J)=K
70     CONTINUE
       IX=X*FLOAT(JSCAL)

80     WRITE(6,2) IX,(JOUT(J),J=1,IN)
```

```
      DO 90 I=1,IN
90    JOUT(I)=I
      WRITE(6,7)
      WRITE(6,3)(JOUT(J),J=1,IN)
      WRITE(6,6)
      RETURN
      END
```

APPENDIX C

CATALOGUE OF GRAVITY DATA OF SOUTH-EAST SCOTLAND

PART I

CLASSIFIED BY 10km NATIONAL GRID SQUARE

Stations with reference number from 1 to 57 are base stations which have been involved in the least-squares adjustment of the gravity base network.

Easting, Northing and Elevation are in metres; Bouguer anomaly and Terrain Coefficient in gu and gu/density unit (gr/cm^3), respectively.

REFERENCE NUMBER	EASTING	NORTHING	ELEVATION	BOUGUER ANOMALY	TERRAIN COEFFICIENT
1	328150.	673950.	-		-
2	325875.	670550.	-		-
3	326500.	672475.	-		-
4	336875.	672450.	31.060	29.90	0.62
5	346275.	679400.	11.942	112.97	0.22
6	349837.	683440.	35.303	85.16	0.18
7	351750.	673280.	54.290	24.80	0.74
8	356050.	684762.	35.045	70.87	0.60
9	360470.	680917.	13.241	28.26	0.36
10	365913.	673947.	24.713	-3.54	0.79
11	362250.	675850.	57.072	-5.88	1.22
12	376200.	672740.	43.358	-114.09	1.67
13	364182.	664385.	271.920	-33.06	1.83
14	389120.	653588.	123.061	-5.83	0.79
15	345875.	651110.	213.605	-19.54	1.44
16	357955.	645738.	281.145	6.13	1.34
17	377445.	648195.	120.255	3.83	0.43
18	379025.	654925.	161.950	-16.85	1.62
19	395180.	658525.	196.210	4.61	2.36
20	375850.	668837.	137.709	-75.33	2.43
21	351250.	628638.	250.850	54.96	0.59
22	316525.	687175.	135.971	20.29	0.92
23	329275.	695825.	71.049	-17.18	0.32
24	392700.	636475.	39.000	-36.96	0.75
25	361663.	624760.	101.803	33.05	0.66
26	381835.	633150.	173.431	-3.27	1.09
27	330663.	707375.	49.439	-8.79	0.89
28	340175.	704540.	64.343	-34.42	0.65
29	323550.	660000.	-		-
30	297187.	637374.	-		-
31	309837.	624270.	253.860		-
32	330763.	624890.	228.240		-
33	295990.	619320.	-		-
34	324570.	658870.	248.700	22.17	0.85
35	330950.	668900.	70.570		0.63
36	326000.	673000.	-		-
37	322720.	651780.	290.190	83.63	0.59
38	331440.	662840.	100.750	-27.02	1.10
39	329751.	669490.	100.006		0.71
40	323120.	662620.	211.960	51.15	1.96
41	325790.	663462.	173.210	6.41	0.83
42	318560.	658380.	277.690	67.77	1.90
43	316080.	648010.	211.640	62.34	1.58
44	316410.	643085.	192.244	63.93	4.52
45	333063.	634650.	158.434	-18.83	5.08
46	325455.	671293.	-		-
47	323163.	639363.	165.030	-26.65	4.50
48	325980.	663400.	169.150	1.80	0.80
49	323540.	659820.	183.170	18.68	1.38
50	329270.	655560.	228.340	47.97	0.76
51	322290.	661660.	273.310	58.32	2.73
52	322260.	649890.	301.280	68.89	0.85
53	325660.	651600.	280.200	68.16	1.13

54	348930.	612470.	-		-
55	326020.	639190.	176.500	-39.47	3.01
56	346025.	553525.	-		-
57	395975.	557105.	-		-
		NT 03			
3063001	305625.	639375.	239.878	90.94	0.97
3063002	307937.	637125.	207.874	100.62	1.70
		NT 04			
3064001	307625.	642813.	264.567	69.89	1.48
		NT 12			
3162001	319920.	629089.	310.600	-26.90	13.92
3162002	315070.	620290.	452.000	3.61	5.33
3162003	311262.	629553.	219.800	-14.56	8.19
3162004	310925.	628180.	225.100	-11.78	7.88
3162005	311130.	626440.	227.700	-6.48	9.50
3162006	310400.	625200.	246.555	6.21	10.00
3162007	310375.	623360.	266.320	1.08	7.64
3162008	312050.	621570.	292.510	-0.91	17.51
3162009	313488.	620450.	294.300	5.60	19.90
3162010	314800.	620140.	441.635	2.98	6.60
3162011	315437.	620500.	414.770	2.70	7.02
3162012	316625.	621150.	361.540	4.86	11.29
3162013	318025.	621630.	312.340	3.22	11.01
3162014	319312.	622290.	295.590	2.46	10.50
3162015	319785.	622660.	300.600	5.54	9.11
3162016	319800.	625630.	542.500	-2.26	12.54
3162017	314450.	621600.	717.190	4.88	15.71
3162018	314638.	623537.	840.000	1.05	22.77
3162019	316850.	624737.	829.660	-0.97	20.25
3162020	317475.	625850.	766.990	-1.53	18.99
3162021	317512.	627075.	808.530	-14.68	22.00
3162022	317825.	627837.	816.860	-9.03	25.54
3162023	316663.	629512.	793.480	-23.41	14.24
		NT 13			
3163001	319720.	639860.	188.270	1.32	2.53
3163002	319210.	638750.	181.400	5.42	3.55
3163003	318330.	637680.	176.720	3.50	4.28
3163004	317790.	635810.	180.900	3.45	4.89
3163005	316240.	635200.	181.700	-1.81	7.07
3163006	313580.	634210.	203.750	8.51	5.24
3163007	311480.	634430.	202.260	25.22	3.24
3163008	311270.	636140.	201.420	50.79	2.63
3163009	310330.	639080.	245.630	87.09	2.77
3163010	311050.	637240.	212.283	54.93	3.52
3163011	311920.	633125.	223.100	12.57	4.60
3163012	312070.	631460.	205.100	-9.74	8.55
3163013	317375.	631225.	736.090	-21.05	18.59
3163014	317612.	632425.	715.060	-22.97	21.56
3163015	318250.	633525.	574.850	-23.50	13.26
3163016	318950.	634550.	484.930	-12.32	9.86
3163017	319525.	635575.	476.400	-21.07	9.40
3163018	314900.	636075.	229.820	19.39	5.42
3163019	311800.	636350.	215.580	38.63	3.35
3163020	312625.	635788.	220.870	25.41	3.50
3163021	313975.	635900.	246.280	24.91	6.20
		NT 14			
3164001	313188.	649500.	226.467	54.03	1.41

3164002	310375.	646563.	235.306	63.74	1.38
3164003	319510.	640530.	181.660	7.34	3.04
3164004	318580.	640850.	185.600	13.96	5.07
3164005	317250.	641800.	189.860	35.01	5.15
3164006	317020.	642380.	194.030	42.38	5.33
3164007	316260.	644240.	204.420	78.12	4.92
3164008	316050.	646600.	207.540	89.11	3.70
3164009	316120.	647500.	214.700	69.18	1.91
3164010	315430.	647440.	223.780	64.48	1.02
3164011	314940.	646740.	245.260	68.43	0.96
3164012	315320.	646440.	241.420	74.42	1.13
3164013	315390.	646160.	263.600	85.58	1.07
3164014	315680.	645940.	254.290	93.29	1.19
3164015	315750.	643010.	197.830	71.11	4.04
3164016	315060.	643220.	200.950	78.92	3.90
3164017	314330.	643520.	201.627	90.08	4.10
3164018	314030.	644010.	206.730	98.65	3.32
3164019	313710.	644610.	219.260	88.23	1.90
3164020	312930.	644580.	236.100	84.08	1.85
3164021	312440.	644350.	258.150	81.97	1.43
3164022	316530.	648490.	220.400	58.31	1.71
3164023	316920.	648360.	249.560	65.38	2.04
3164024	317400.	648180.	301.570	79.42	2.12
3164025	317430.	647880.	318.200	89.33	2.26
3164026	317980.	647560.	344.480	85.54	2.50
3164027	318360.	646950.	286.640	78.18	3.30
3164028	318510.	646680.	280.300	75.84	4.39
3164029	318640.	646190.	285.900	62.63	1.73
3164030	318840.	649910.	302.700	74.53	2.40
3164031	319050.	649890.	319.400	81.93	2.44
3164032	319210.	649910.	331.300	86.66	1.93
3164033	319410.	649930.	342.000	79.53	1.62
3164034	314120.	645890.	232.000	67.72	1.11
3164035	311080.	643000.	259.400	89.51	2.47
3164036	312390.	641550.	557.480	92.96	15.80
3164037	313460.	641300.	535.535	71.96	17.17
3164038	312300.	641100.	570.890	83.85	18.53
		NT 15			
3165001	318350.	651400.	259.690	34.44	1.74
3165002	319400.	656400.	277.970	24.96	0.72
3165003	318420.	655620.	281.080	33.44	0.62
3165004	317620.	653000.	247.560	28.61	0.98
3165005	318450.	652690.	274.930	13.33	0.49
3165006	318450.	651950.	271.220	19.79	0.65
3165007	318800.	651700.	265.050	21.82	0.81
3165008	316410.	650080.	225.990	47.82	1.03
3165009	316270.	650460.	244.420	47.10	1.13
3165010	315970.	650590.	238.050	48.53	0.97
3165011	315380.	651080.	226.270	47.28	0.94
3165012	315100.	651350.	230.270	48.05	1.08
3165013	314970.	651600.	235.930	57.95	1.03
3165014	314970.	651960.	256.600	53.62	2.76
3165015	314380.	652100.	267.300	54.22	1.82
3165016	314080.	652210.	273.100	57.14	1.64
3165017	313990.	652270.	270.380	52.10	0.90
3165018	312500.	655570.	350.550	99.44	1.89
3165019	312590.	655370.	340.510	100.81	2.64

3165020	312650.	654900.	306.070	98.85	2.87
3165021	312830.	654040.	316.130	89.21	2.04
3165022	312870.	653850.	314.650	90.92	1.91
3165023	312950.	653780.	313.380	87.74	1.57
3165024	313030.	653740.	314.280	86.71	1.41
3165025	313850.	652430.	277.140	55.05	0.91
3165026	313780.	652540.	280.240	55.12	0.91
3165027	313720.	652620.	282.540	55.13	0.91
3165028	313650.	652720.	283.960	56.85	0.94
3165029	313580.	652800.	284.980	59.48	0.99
3165030	313530.	652870.	285.460	60.09	1.02
3165031	313480.	652970.	287.900	61.58	1.09
3165032	313420.	653070.	292.970	63.86	1.07
3165033	313250.	653350.	302.300	77.08	1.18
3165034	313170.	653610.	309.310	79.20	1.31
3165035	316100.	655738.	260.848	61.28	2.26
3165036	315738.	655975.	321.000	80.53	2.64
3165037	315450.	656725.	347.300	96.04	2.44
3165038	315463.	656950.	366.700	97.37	2.34
3165039	315488.	657063.	372.116	100.17	2.49
3165040	315400.	657825.	346.543	110.79	3.24
3165041	316950.	656820.	295.700	60.27	2.37
3165042	317790.	657525.	276.600	63.08	2.04
3165043	319950.	658870.	254.460	45.39	1.36
3165044	319520.	658590.	257.000	47.85	1.34
3165045	319000.	658400.	263.260	54.15	1.67
3165046	318760.	658310.	269.900	56.68	1.75
3165047	319320.	659200.	272.790	71.21	2.14
3165048	318860.	658720.	272.200	67.93	1.90
3165049	319350.	651400.	260.330	33.22	1.74
3165050	319210.	651250.	258.600	35.58	1.66
3165051	318940.	651050.	258.200	36.19	1.34
3165052	318790.	650860.	260.300	41.67	1.35
3165053	318640.	650440.	249.560	50.50	1.99
3165054	318500.	650240.	246.300	55.86	3.26
3165055	318320.	650100.	240.800	55.12	2.61
3165056	318370.	650090.	245.010	55.47	2.44
3165057	318400.	650100.	251.500	58.46	2.29
3165058	319910.	650230.	360.100	80.53	1.65
3165059	319950.	656920.	276.800	24.98	0.75
3165060	319670.	656720.	278.900	28.14	0.83
3165061	319560.	656610.	279.800	27.73	0.86
3165062	319250.	656240.	281.000	27.54	0.72
3165063	318960.	655990.	284.400	29.44	0.71
3165064	318560.	655520.	282.500	31.70	0.57
3165065	318470.	655350.	280.370	32.70	0.53
3165066	318320.	655130.	278.600	32.05	0.53
3165067	318130.	654680.	280.600	32.02	0.48
3165068	317930.	654450.	279.180	34.67	0.49
3165069	317610.	654050.	279.850	35.05	0.51
3165070	317160.	654390.	281.040	41.26	0.68
3165071	316670.	654950.	285.300	46.96	0.79
3165072	319680.	652750.	277.700	17.60	0.54
3165073	319360.	652670.	275.800	15.71	0.48
3165074	318320.	652770.	273.100	18.12	0.51
3165075	318120.	652800.	267.580	22.32	0.50
3165076	317390.	653210.	270.400	28.46	0.71
3165077	317380.	653340.	273.150	31.20	0.73

3165078	316920.	653170.	243.200	36.07	1.02
3165079	316400.	652820.	233.450	39.91	1.41
3165080	315800.	652350.	234.100	42.09	1.44
		NT 16			
3166001	316680.	669460.	80.800	78.39	1.01
3166002	317580.	668320.	105.800	93.40	1.53
3166003	318450.	667310.	169.800	98.24	2.14
3166004	318900.	666070.	244.400	107.47	1.70
		NT 17			
3167001	319950.	670960.	65.000	81.82	0.84
3167002	319310.	672940.	49.000	68.92	0.68
3167003	318900.	674790.	51.000	70.70	0.48
3167004	317760.	675580.	31.000	62.52	0.42
3167005	315300.	677670.	58.500	70.78	0.62
3167006	314210.	677950.	46.300	76.05	0.40
3167007	312990.	678380.	5.000	77.66	1.22
3167008	311550.	678010.	48.200	93.04	0.50
3167009	310610.	677130.	72.200	106.09	0.36
3167010	310110.	676040.	75.000	109.03	0.29
3167011	310710.	675070.	63.400	108.43	0.33
3167012	312630.	674360.	41.000	97.24	0.53
3167013	314350.	674050.	28.000	70.06	0.49
3167014	313210.	672400.	36.600	80.11	0.98
3167015	314170.	670010.	70.400	43.71	1.09
		NT 18			
3168001	312175.	683038.	44.501	74.89	0.50
3168002	312363.	685975.	83.100	43.61	0.39
3168003	313375.	684325.	17.374	50.57	0.92
3168004	315025.	683850.	38.100	49.64	0.43
3168005	316775.	684600.	35.357	45.17	0.55
3168006	318163.	686088.	54.254	50.27	1.16
3168007	313475.	689450.	131.100	-0.62	0.72
3168008	317275.	689038.	145.390	12.69	0.57
3168009	311200.	689125.	129.100	11.78	0.73
		NT 19			
3169001	312788.	692363.	131.978	-2.11	0.55
3169002	312500.	690175.	162.458	-1.40	0.68
3169003	314613.	691350.	179.527	-11.00	0.86
3169004	317400.	690525.	143.866	-1.54	0.33
3169005	317775.	692850.	133.100	-5.25	0.27
3169006	317975.	695250.	82.540	-1.25	0.51
3169007	318013.	697825.	111.587	11.78	1.22
3169008	319475.	699125.	112.806	19.36	0.55
3169009	315825.	698925.	115.550	8.69	3.85
3169010	313113.	698350.	117.988	16.89	0.67
3169011	312475.	699725.	117.378	21.25	0.40
3169012	313295.	697100.	128.351	12.00	0.90
3169013	314525.	695450.	104.577	0.30	0.86
3169014	314700.	693145.	119.817	-10.56	0.57
3169015	315250.	696663.	156.698	14.60	2.57
		NO 10			
3170001	312088.	700450.	121.040	22.07	0.37
3170002	311600.	702675.	119.100	14.79	0.40
3170003	312950.	704575.	116.080	14.42	0.50
3170004	312925.	706513.	153.040	23.37	0.72
3170005	312150.	707725.	230.154	30.49	1.59
3170006	314050.	707800.	176.205	20.45	0.68

3170007	315238.	707850.	106.100	20.63	1.14
3170008	318658.	708300.	130.485	12.29	1.80
3170009	316997.	706500.	162.090	5.66	1.13
3170010	316875.	704870.	173.736	-0.86	1.77
3170011	315513.	705500.	127.100	13.36	0.72
3170012	314725.	704325.	116.464	11.45	0.55
3170013	317725.	702625.	137.100	1.39	4.24
3170014	319365.	701500.	118.598	7.79	5.56
		NT 21			
3261001	325440.	619000.	408.737	39.91	2.88
3261002	327030.	619940.	371.551	27.98	4.65
		NT 22			
3262001	321800.	623120.	281.530	6.04	7.49
3262003	323975.	622920.	249.300	2.54	8.37
3262004	323975.	620470.	248.290	9.54	7.76
3262005	325430.	623350.	251.350	6.02	7.16
3262006	325585.	623990.	252.450	5.73	4.95
3262007	329100.	624530.	242.210	6.02	4.19
3262008	328000.	620000.	350.145	20.61	3.57
3262009	328370.	625550.	264.900	3.24	7.53
3262010	328230.	626230.	280.400	4.32	7.37
3262011	328070.	627340.	296.310	-3.17	6.56
3262012	327320.	628520.	360.000	-3.20	4.20
3262013	323840.	621720.	250.546	11.11	11.74
3262014	324750.	620020.	296.266	14.65	6.49
3262015	320460.	626220.	498.400	-8.74	3.39
3262016	320440.	626800.	578.200	-7.33	7.36
3262017	321820.	627450.	695.800	-3.06	13.65
3262018	322270.	627940.	697.400	-7.53	12.73
3262019	322200.	628960.	593.600	31.61	14.37
3262020	322900.	629790.	610.800	-19.22	7.98
3262021	320760.	624080.	464.200	6.70	4.46
		NT 23			
3263001	326750.	639552.	156.831	-45.95	3.82
3263002	327900.	638422.	178.909	-43.50	4.62
3263003	329215.	638499.	156.971	-44.55	6.32
3263004	322560.	638412.	197.710	-22.34	2.94
3263005	321775.	637825.	191.400	-26.81	3.99
3263006	321320.	636535.	208.560	-28.85	4.96
3263007	321350.	635863.	214.450	-32.74	5.39
3263008	320800.	634500.	234.130	-33.78	7.62
3263009	320200.	633455.	252.580	-35.32	8.86
3263010	320365.	632420.	253.940	-37.80	10.03
3263011	320050.	631163.	266.350	-33.87	13.37
3263012	327650.	639725.	161.544	-43.95	4.54
3263013	328738.	639175.	174.955	-44.63	3.94
3263014	329488.	639250.	154.767	-49.33	5.65
3263015	325230.	639340.	188.060	-35.50	2.72
3263016	326820.	638210.	315.500	-45.76	5.14
3263017	327360.	637290.	384.400	-44.21	7.52
3263018	327680.	636710.	429.500	-44.65	10.59
3263019	328120.	636010.	483.100	-40.78	11.93
3263020	327960.	635170.	535.500	-37.54	14.08
3263021	327495.	633180.	562.000	-26.64	21.16
3263022	322220.	639510.	178.910	-21.38	2.28
3263023	324630.	639660.	186.900	-34.26	2.88
3263024	323440.	639830.	250.200	-26.91	3.21
3263025	321390.	638400.	250.200	-17.47	3.00

3263026	320830.	639340.	206.300	-9.42	2.28
3263027	321840.	637120.	208.500	-29.11	5.24
3263028	322680.	636880.	229.590	-34.82	7.67
3263029	323660.	637180.	212.100	-43.00	5.80
3263030	324470.	637000.	196.300	-47.52	7.16
3263031	324580.	637600.	189.500	-45.86	6.34
3263032	325140.	638510.	187.800	-43.22	4.12
3263033	327580.	639110.	161.800	-44.48	4.20
3263034	329440.	632600.	266.570	-23.40	4.51
3263035	328310.	631890.	353.600	-23.15	5.92
3263036	327690.	631290.	364.400	-21.34	5.63
3263037	327270.	631040.	376.780	-18.29	7.27
3263038	324790.	630860.	710.800	-23.48	14.90
3263039	322550.	635025.	529.440	-24.44	24.99
3263040	322330.	634264.	571.125	-35.23	18.90
3263041	322552.	633475.	625.140	-36.53	19.36
3263042	323050.	633275.	674.100	-27.51	25.97
3263043	324050.	632850.	718.110	-25.38	24.66
3263044	324175.	632250.	730.000	-24.02	24.12
3263045	325013.	633950.	683.560	-29.72	18.98
3263046	325325.	635200.	581.860	-36.69	16.59
3263047	324575.	635550.	493.170	-42.51	14.67
3263048	323700.	636065.	309.070	-46.44	7.01
		NT 24			
3264001	322940.	649609.	281.100	60.42	0.87
3264002	323580.	649482.	257.990	50.23	1.35
3264003	324405.	648515.	204.740	37.88	4.10
3264004	324475.	648030.	200.580	30.37	3.97
3264005	324185.	647013.	194.180	18.40	4.13
3264006	324480.	642950.	176.800	-10.49	4.80
3264007	324960.	641862.	169.590	-21.83	4.69
3264008	325100.	640392.	166.900	-37.74	3.04
3264009	324100.	640583.	183.180	-27.86	3.23
3264010	320675.	640386.	179.660	-2.79	2.80
3264011	320835.	640988.	198.030	-1.78	3.06
3264012	321000.	641697.	204.360	6.00	7.49
3264013	321600.	643722.	249.320	9.78	2.07
3264014	322260.	644355.	278.070	8.15	1.10
3264015	323360.	645702.	233.730	15.27	2.39
3264016	320675.	640370.	179.258	-2.99	2.80
3264017	320880.	640090.	171.130	-2.90	3.04
3264018	320180.	646280.	345.000	52.68	2.04
3264019	321720.	646090.	306.540	37.47	1.60
3264020	322110.	645880.	297.700	30.77	1.21
3264021	322570.	649710.	292.330	64.36	0.86
3264022	323140.	649710.	275.800	58.62	0.94
3264023	323040.	649980.	269.100	65.97	0.98
3264024	324475.	649263.	230.369	44.90	3.25
3264025	324785.	649230.	282.245	45.18	2.25
3264026	324937.	649375.	291.846	47.82	1.88
3264027	325075.	649490.	307.535	48.93	2.00
3264028	325250.	649550.	309.982	48.85	1.87
3264029	323834.	645675.	189.506	7.96	5.20
3264030	323925.	644425.	188.630	2.74	5.70
3264031	324295.	642800.	170.837	-8.03	6.14
3264032	324455.	641620.	177.275	-20.99	4.06
3264033	325575.	640313.	161.009	-35.89	3.85
3264034	327470.	649090.	622.400	32.33	17.63

3264035	327310.	648360.	600.200	27.29	16.20
3264036	328140.	648040.	457.100	18.12	5.57
3264037	327540.	647070.	517.200	18.50	8.69
3264038	327710.	645920.	553.500	4.51	11.49
3264039	328190.	644440.	567.200	-4.21	11.26
3264040	328910.	643770.	601.100	-14.26	12.91
3264041	328850.	642560.	550.800	-21.11	13.84
3264042	329340.	640940.	410.000	-34.28	9.88
3264043	325800.	640330.	161.100	-35.88	4.19
3264044	326270.	640570.	168.910	-37.04	5.07
3264045	326950.	641580.	247.800	-34.02	4.15
3264046	327460.	641660.	332.030	-26.24	4.12
3264047	327810.	641000.	342.000	-44.08	8.20
3264048	327000.	641020.	359.400	-22.57	11.48
3264049	325800.	640330.	161.510	-34.87	4.19
3264050	323700.	646660.	205.400	21.61	3.63
3264051	322750.	645200.	253.200	11.92	1.55
3264052	321240.	642560.	217.000	3.61	5.45
3264053	323020.	640030.	192.000	-22.34	4.38
3264054	329930.	645020.	307.800	-5.66	15.89
		NT 25			
3265001	323050.	658590.	231.100	16.53	0.81
3265002	327680.	656770.	262.300	72.12	0.57
3265003	324830.	658220.	242.490	24.03	0.69
3265004	326180.	658680.	249.373	34.29	0.76
3265005	327080.	657000.	265.590	71.67	0.55
3265006	328370.	656270.	259.110	66.24	0.69
3265007	329700.	656380.	263.690	50.21	0.78
3265008	326630.	655630.	260.170	79.95	0.69
3265009	326900.	655870.	268.090	78.25	0.54
3265010	324370.	650150.	214.590	56.29	3.67
3265011	323220.	651850.	245.340	71.97	2.12
3265012	323225.	651550.	272.770	81.34	0.80
3265013	322450.	651920.	282.340	82.37	0.61
3265014	321600.	653120.	288.340	28.40	0.62
3265015	320020.	652150.	291.400	33.03	1.12
3265016	320900.	652870.	290.000	26.89	0.61
3265017	322500.	658220.	236.300	19.79	0.74
3265018	321770.	653670.	278.750	18.56	0.54
3265019	322370.	654450.	264.450	11.39	0.56
3265020	324750.	657540.	262.650	30.14	0.70
3265021	324250.	656680.	270.390	35.90	0.82
3265022	327650.	652550.	284.790	53.87	1.37
3265023	328600.	653270.	270.760	42.49	1.19
3265024	328880.	653800.	270.500	40.14	0.98
3265025	329230.	655000.	282.050	48.11	0.71
3265026	327150.	658180.	268.690	54.40	0.67
3265027	323880.	656915.	251.663	22.56	0.61
3265028	321475.	657700.	263.151	8.77	0.66
3265029	323680.	659570.	166.350	24.20	2.19
3265030	323800.	659580.	178.200	21.27	1.67
3265031	323950.	659550.	194.230	20.66	1.35
3265032	324210.	659470.	225.410	21.68	1.15
3265033	324310.	659190.	229.860	23.55	0.94
3265034	324770.	658850.	251.500	20.48	0.80
3265035	325770.	658210.	262.100	36.23	0.70
3265036	326190.	658690.	248.800	34.26	0.76
3265037	326270.	659250.	239.500	25.95	0.74

3265038	326330.	659590.	236.110	22.88	0.75
3265039	326440.	659930.	231.300	20.69	0.75
3265040	324160.	654700.	279.500	58.33	0.59
3265041	324940.	655540.	276.020	79.94	0.62
3265042	325100.	655440.	267.900	81.61	0.63
3265043	325440.	655250.	273.210	85.92	0.47
3265044	325830.	655000.	264.900	87.18	0.54
3265045	326040.	654870.	266.100	82.85	0.55
3265046	326020.	654470.	271.600	84.20	0.52
3265047	326320.	654910.	271.600	84.35	0.51
3265048	326430.	655090.	269.750	83.62	0.51
3265049	326600.	655030.	274.600	80.34	0.53
3265050	326780.	655050.	270.480	78.14	0.56
3265051	327100.	655020.	254.280	80.53	0.80
3265052	327240.	654870.	259.830	72.18	0.69
3265053	328040.	654100.	259.430	51.61	0.95
3265054	328880.	653810.	270.890	40.18	0.98
3265055	329130.	654660.	282.460	43.04	0.73
3265056	329230.	655710.	282.530	50.26	0.79
3265057	329880.	657840.	232.200	53.76	0.84
3265058	329420.	658110.	203.050	60.56	1.14
3265059	323420.	659820.	185.830	19.55	1.37
3265060	323630.	659340.	185.040	18.76	1.60
3265061	323240.	658920.	216.760	14.78	0.92
3265062	323200.	658720.	221.900	11.86	0.90
3265063	323070.	658100.	237.400	16.14	0.65
3265064	323110.	657870.	236.460	17.35	0.60
3265065	323320.	657520.	232.890	19.00	0.67
3265066	323370.	657310.	242.900	19.62	0.55
3265067	323400.	656980.	248.010	17.01	0.53
3265068	323120.	656810.	252.700	14.56	0.50
3265069	322970.	656500.	258.200	11.13	0.48
3265070	322610.	656460.	261.500	11.73	0.50
3265071	322470.	656370.	265.840	10.66	0.51
3265072	322230.	655910.	269.400	5.37	0.44
3265073	322340.	655680.	265.290	6.85	0.43
3265074	321990.	655240.	275.720	3.26	0.47
3265075	322230.	655040.	271.590	4.80	0.49
3265076	322670.	655420.	261.000	6.88	0.46
3265077	322910.	655650.	259.660	10.19	0.47
3265078	323490.	655650.	259.700	18.22	0.66
3265079	323520.	656460.	254.200	13.32	0.56
3265080	322780.	651680.	283.920	83.64	0.61
3265081	322720.	651780.	289.990	82.84	0.59
3265082	322630.	651850.	285.700	83.48	0.55
3265083	322550.	651910.	283.250	83.74	0.55
3265084	322470.	651940.	280.450	77.34	0.65
3265085	322380.	652000.	282.980	79.77	0.72
3265086	322320.	652090.	288.160	76.49	0.56
3265087	322200.	652120.	287.880	73.64	0.65
3265088	322120.	652170.	290.900	71.84	0.59
3265089	322060.	652280.	294.980	75.06	0.58
3265090	321950.	652310.	297.960	69.59	0.64
3265091	321870.	652370.	303.240	70.43	0.63
3265092	321790.	652440.	309.350	56.43	0.67
3265093	321710.	652500.	315.920	64.36	0.90
3265094	321670.	652530.	319.410	56.59	0.77
3265095	321710.	652720.	324.060	57.59	0.97

3265096	321630.	652870.	309.700	49.36	0.72
3265097	321580.	652970.	304.440	43.86	0.69
3265098	324590.	651380.	244.320	64.71	1.54
3265099	324990.	651375.	271.900	64.13	1.17
3265100	325230.	651370.	280.960	67.27	1.13
3265101	325710.	651340.	285.300	65.98	1.29
3265102	326110.	650560.	306.900	53.86	2.30
3265103	326300.	650320.	308.800	49.51	3.11
3265104	326310.	650100.	307.360	48.48	4.61
3265105	321970.	659940.	233.070	26.95	1.37
3265106	321440.	659910.	242.500	32.41	1.51
3265107	320990.	659670.	253.100	37.81	1.49
3265108	320680.	659380.	256.580	41.36	1.43
3265109	320360.	659210.	250.230	43.07	1.49
3265110	320070.	650130.	352.000	83.20	1.27
3265111	320200.	650050.	349.600	85.15	1.18
3265112	320490.	650050.	337.420	86.22	0.99
3265113	320780.	650010.	328.500	83.19	0.92
3265114	321000.	650080.	322.590	83.79	0.86
3265115	321310.	650240.	320.600	81.88	0.75
3265116	321850.	650080.	302.700	77.38	0.90
3265117	322030.	650040.	304.800	74.43	0.85
3265118	323020.	650070.	270.700	65.65	0.93
3265119	322960.	650220.	277.400	70.44	0.89
3265120	322880.	650440.	283.300	71.70	0.81
3265121	322720.	650760.	272.620	77.27	0.81
3265122	322640.	650910.	277.400	76.24	0.75
3265123	322550.	651350.	296.820	80.45	0.73
3265124	324420.	652570.	244.400	78.86	1.36
3265125	324550.	653030.	268.000	79.59	0.71
3265126	325010.	658740.	254.500	24.11	0.70
3265127	325380.	658440.	253.900	25.76	0.64
3265128	323420.	655370.	263.000	19.02	0.77
3265129	323620.	655700.	267.300	23.61	0.86
3265130	323710.	655780.	266.300	28.11	0.91
3265131	323820.	655940.	265.500	30.76	0.92
3265132	323940.	656120.	265.200	32.36	0.96
3265133	324100.	656360.	273.400	35.23	0.92
3265134	324320.	656850.	271.300	41.92	0.77
3265135	324680.	657430.	263.300	30.06	0.74
3265136	324820.	657980.	244.990	25.73	0.79
3265137	325200.	658060.	248.930	28.59	0.79
3265138	325860.	658080.	260.300	42.22	0.72
3265139	326130.	657720.	271.900	57.98	0.60
3265140	325580.	658330.	261.800	28.75	0.71
3265141	322920.	658390.	234.100	15.45	0.71
3265142	322740.	658240.	234.700	16.34	0.69
3265143	322530.	658230.	235.500	18.44	0.71
3265144	322220.	658080.	245.000	23.48	0.69
3265145	322020.	657940.	253.100	19.54	0.64
3265146	321550.	657710.	263.180	8.00	0.66
3265147	320990.	657450.	271.900	20.81	0.62
3265148	320650.	657280.	274.000	23.63	0.63
3265149	320300.	657100.	272.500	23.96	0.65
3265150	323220.	655080.	266.100	18.18	0.70
3265151	322980.	654780.	271.000	18.09	0.63
3265152	322710.	654470.	272.800	14.90	0.62
3265153	322510.	654390.	270.100	13.01	0.64

3265154	322260.	654180.	279.700	14.05	0.61
3265155	322125.	654050.	272.940	14.40	0.59
3265156	321700.	654540.	277.150	7.25	0.45
3265157	321520.	654750.	287.400	1.89	0.50
3265158	321360.	654730.	289.370	4.89	0.53
3265159	321090.	654500.	285.560	5.58	0.45
3265160	320760.	654350.	291.700	5.75	0.44
3265161	320550.	654280.	297.200	4.99	0.50
3265162	320390.	654160.	294.920	7.84	0.40
3265163	320450.	654030.	285.300	6.64	0.37
3265164	320650.	653450.	285.000	12.08	0.41
3265165	320920.	652860.	290.190	27.58	0.61
3265166	320520.	652500.	292.000	30.95	0.76
3265167	320530.	652820.	285.600	22.55	0.56
3265168	320310.	652890.	289.450	22.64	0.50
3265169	320100.	652890.	281.100	19.18	0.53
3265170	326225.	652110.	283.200	68.39	1.27
3265171	327450.	652625.	288.000	54.16	1.14
3265172	327900.	652700.	283.770	51.27	1.32
3265173	328563.	653120.	276.450	42.21	1.16
3265174	328775.	653000.	280.050	39.99	1.23
3265175	329275.	652550.	273.770	37.43	1.95
3265176	329750.	652415.	284.070	31.21	2.11
3265177	329887.	652650.	276.900	33.78	1.99
3265178	329525.	654050.	273.746	37.02	0.91
3265179	329775.	654105.	273.690	35.33	0.93
3265180	326263.	657613.	275.342	62.69	0.64
3265181	326575.	657375.	269.735	68.92	0.55
3265182	326650.	657225.	267.128	70.39	0.57
3265183	326763.	657175.	266.222	71.29	0.57
3265184	327200.	656963.	262.400	71.25	0.53
3265185	327975.	656500.	251.111	68.95	0.58
3265186	328700.	656050.	265.006	59.90	0.68
3265187	324820.	659900.	220.527	23.33	1.07
3265188	321970.	659940.	233.070	26.79	1.37
3265189	323490.	655930.	254.388	16.36	0.63
3265190	323490.	655690.	257.998	18.27	0.65
3265191	323490.	655590.	262.113	18.87	0.69
3265192	323490.	655490.	264.489	20.65	0.74
3265193	323480.	655390.	266.595	22.65	0.78
3265194	323540.	655270.	270.213	27.25	0.83
3265195	323580.	655190.	274.793	30.59	0.75
3265196	323610.	655100.	279.290	38.55	0.72
3265197	323630.	655010.	282.969	44.02	0.67
3265198	323660.	654920.	283.678	47.26	0.61
3265199	323670.	654820.	284.199	49.52	0.57
3265200	323640.	654720.	284.251	51.37	0.56
3265201	323630.	654620.	283.413	53.52	0.53
3265202	323640.	654520.	281.817	56.71	0.51
3265203	323650.	654420.	281.013	59.29	0.50
3265204	323700.	654350.	280.015	62.02	0.50
3265205	323790.	654290.	278.491	65.39	0.51
3265206	323880.	654250.	277.163	68.02	0.51
3265207	323960.	654210.	274.911	70.68	0.54
3265208	324020.	654160.	272.005	72.70	0.58
3265209	324040.	654080.	268.297	74.89	0.56
3265210	324060.	653990.	267.505	80.84	0.56
3265211	324110.	653900.	263.239	79.30	0.58

3265212	324140.	653810.	260.375	78.04	0.62
3265213	324180.	653720.	259.068	77.08	0.65
3265214	324200.	653610.	257.307	75.87	0.69
3265215	324240.	653530.	255.819	77.42	0.71
3265216	324280.	653440.	257.230	74.59	0.79
3265217	324290.	653360.	254.937	74.26	0.73
3265218	324280.	653270.	252.256	76.97	0.79
3265219	324300.	653180.	249.510	77.51	0.88
3265220	324310.	653080.	247.147	76.73	1.01
3265221	324310.	652990.	246.475	78.27	1.04
3265222	324320.	652890.	247.132	77.91	1.02
3265223	324330.	652800.	247.097	75.20	1.04
3265224	324330.	652710.	246.260	76.05	1.08
3265225	324340.	652620.	244.509	77.43	1.16
3265226	324350.	652500.	243.824	75.69	1.22
3265227	324360.	652490.	241.449	73.71	1.33
3265228	324350.	652310.	239.773	73.17	1.43
3265229	324380.	652210.	239.753	72.17	1.45
3265230	324370.	652110.	239.130	72.38	1.53
3265231	324380.	651980.	238.680	73.03	1.54
3265232	324210.	651870.	245.215	72.45	2.12
3265233	327200.	659140.	260.830	36.26	0.97
3265234	327190.	658890.	268.356	42.00	0.95
3265235	327160.	658400.	270.700	49.84	0.74
3265236	326770.	658580.	288.688	39.74	1.42
3265237	328720.	658880.	222.047	45.04	0.83
3265238	329230.	658900.	227.286	43.37	0.75
3265239	329330.	659060.	223.093	41.41	0.77
3265240	329420.	659200.	218.520	39.09	0.79
3265241	329560.	659390.	212.693	34.74	0.81
3265242	329680.	659590.	208.537	30.23	0.82
3265243	329830.	659820.	202.084	23.03	0.85
3265244	329910.	659930.	197.251	19.91	0.88
3265245	327010.	650100.	475.500	40.68	9.16
		NT 25			
3266001	329320.	668570.	121.380	-2.64	0.81
3266002	327780.	668230.	120.000	26.52	0.77
3266003	324610.	668300.	181.000	103.09	1.60
3266004	323470.	668560.	156.000	97.12	1.79
3266005	322080.	668920.	116.000	96.36	1.67
3266006	320560.	659050.	127.000	93.59	1.64
3266007	328020.	661370.	191.170	-12.60	0.93
3266008	327150.	662220.	159.330	-5.95	0.94
3266009	329339.	669740.	70.540	12.84	0.84
3266010	329680.	669560.	94.010	0.38	0.73
3266011	329620.	669640.	90.140	4.98	0.73
3266012	329550.	669700.	86.220	9.86	0.75
3266013	329480.	669770.	82.800	7.18	0.81
3266014	329410.	669840.	78.180	10.05	0.75
3266015	323080.	662600.	213.560	51.60	2.11
3266016	323070.	662650.	211.020	53.71	2.10
3266017	323050.	662690.	207.540	55.88	2.26
3266018	323020.	662730.	205.080	56.93	2.31
3266019	323000.	662770.	203.820	59.74	2.70
3266020	322980.	662820.	203.490	62.36	2.60
3266021	322960.	662870.	205.380	64.25	2.55
3266022	323410.	663030.	181.980	58.78	2.38
3266023	322260.	663560.	227.250	86.34	4.58

3266024	321900.	663940.	226.200	81.34	5.70
3266025	321620.	664070.	225.880	89.75	5.42
3266026	323000.	663070.	185.580	71.60	3.98
3266027	322930.	662940.	206.760	66.24	2.50
3266028	322910.	662970.	207.120	66.87	2.54
3266029	322990.	662380.	225.640	52.59	2.23
3266030	323030.	662410.	227.390	49.54	2.01
3266031	323070.	662380.	227.980	47.34	1.91
3266032	323110.	662350.	226.700	45.17	1.87
3266033	323160.	662320.	224.700	43.07	1.80
3266034	323170.	662270.	225.430	41.82	1.77
3266035	323200.	662230.	224.480	41.06	1.74
3266036	323230.	662180.	223.120	39.76	1.66
3266037	323250.	662140.	222.080	38.90	1.57
3266038	323280.	662100.	221.720	38.12	1.61
3266039	323310.	662060.	222.410	36.79	1.59
3266040	323310.	662060.	223.600	35.92	1.59
3266041	328550.	661700.	159.293	-21.32	0.99
3266042	328780.	662220.	152.226	-20.98	0.81
3266043	329250.	663100.	148.786	-29.66	0.70
3266044	329090.	663990.	143.952	-28.51	0.90
3266045	329440.	664510.	131.916	-25.29	0.82
3266046	323490.	660176.	186.750	21.92	1.30
3266047	324305.	661565.	172.530	21.50	1.33
3266048	323312.	661110.	205.600	24.87	1.45
3266049	323562.	660980.	182.840	24.23	1.42
3266050	323750.	661100.	177.010	24.48	1.47
3266051	323450.	661890.	223.000	34.26	1.57
3266052	323287.	662105.	221.800	37.76	1.59
3266053	323337.	662290.	213.640	38.45	1.59
3266054	323890.	662240.	205.130	28.56	1.20
3266055	324405.	662325.	187.700	22.24	1.08
3266056	324845.	662090.	168.820	15.98	1.22
3266057	324020.	660805.	182.040	19.01	1.10
3266058	324125.	660735.	181.350	17.83	1.08
3266059	324190.	660430.	184.290	18.28	1.07
3266060	324650.	660710.	175.950	16.08	1.19
3266061	324970.	661180.	168.140	13.98	1.18
3266062	325050.	661400.	154.500	17.04	1.47
3266063	325130.	661780.	140.700	15.35	1.80
3266064	325430.	661960.	142.100	14.35	1.64
3266065	325090.	663600.	178.090	25.01	1.01
3266066	324760.	663870.	187.210	33.30	1.20
3266067	324250.	664510.	198.540	65.06	2.50
3266068	324150.	664130.	206.980	55.88	1.94
3266069	324060.	663780.	194.250	51.30	1.82
3266070	323830.	663570.	194.520	58.35	1.94
3266071	323010.	663070.	186.050	72.30	3.98
3266072	323350.	662820.	200.970	50.31	1.78
3266073	322890.	662310.	232.650	43.44	2.40
3266074	322510.	661910.	266.800	59.39	2.49
3266075	323440.	660590.	181.540	24.53	1.44
3266076	323480.	660170.	186.770	21.77	1.30
3266077	326130.	660240.	226.680	19.03	0.89
3266078	325880.	660500.	206.880	17.04	0.98
3266079	325800.	660820.	195.060	13.12	1.04
3266080	325700.	661070.	183.280	9.70	1.05
3266081	325700.	661520.	129.480	13.37	2.66

3266082	325650.	663070.	175.130	-0.07	0.82
3266083	324880.	662420.	165.190	17.61	1.38
3266084	326740.	663000.	158.730	-7.58	0.80
3266085	326840.	663080.	157.300	-11.94	0.80
3266086	327230.	663250.	156.250	-16.50	0.76
3266087	327120.	663390.	154.200	-15.42	0.73
3266088	327370.	663450.	156.070	-19.09	0.71
3266089	327810.	663860.	151.550	-24.87	0.89
3266090	328150.	664670.	137.160	-25.21	1.14
3266091	326950.	663560.	157.900	-13.20	0.73
3266092	326900.	663820.	148.150	-11.32	0.89
3266093	326760.	664180.	168.490	-11.34	0.84
3266094	323260.	660470.	185.520	25.43	1.46
3266095	323130.	660380.	187.760	25.06	1.47
3266096	323010.	660260.	190.200	24.85	1.52
3266097	323200.	660140.	187.830	24.01	1.41
3266098	322180.	661190.	257.310	44.04	1.98
3266099	321910.	660630.	257.440	36.79	1.69
3266100	321930.	660250.	232.720	32.48	1.52
3266101	322120.	661580.	279.260	61.01	2.66
3266102	321440.	661110.	281.800	67.70	2.59
3266103	321080.	660830.	281.150	67.10	2.37
3266104	320190.	660610.	285.500	85.78	8.87
3266105	320600.	660450.	288.600	70.85	2.51
3266106	320300.	660250.	289.010	72.66	3.02
3266107	320090.	660330.	290.800	73.45	3.19
3266108	324810.	660180.	204.586	22.29	1.08
3266109	324820.	660500.	189.065	10.95	1.22
3266110	324970.	661180.	168.140	13.92	1.18
3266111	325870.	664150.	167.000	15.72	0.90
3266112	325540.	664840.	171.934	31.06	1.17
3266113	325580.	665430.	175.031	36.75	1.35
3266114	325490.	665820.	166.208	43.00	1.89
3266115	324780.	665450.	201.867	65.80	3.88
3266116	324440.	665030.	200.315	65.28	3.40
3266117	323750.	661100.	177.010	24.32	1.47
3266118	327300.	661750.	181.795	-2.22	0.80
3266119	327480.	660110.	228.828	18.16	0.85
3266120	327670.	660380.	216.621	14.38	0.89
3266121	327820.	660710.	204.699	8.94	0.87
3266122	328220.	661230.	181.200	-11.28	0.85
3266123	328540.	661060.	183.030	-7.46	0.81
3266124	329490.	661010.	185.290	-9.20	0.86
3266125	329430.	661660.	162.019	-16.57	0.88
3266126	329920.	660080.	197.965	15.64	0.92
3266127	329920.	660170.	195.430	12.69	0.92
3266128	329960.	660280.	195.445	8.66	0.93
3266129	326750.	662700.	112.877	5.83	3.81
3266130	327130.	662030.	168.598	-3.22	0.86
3266131	327300.	661750.	181.795	-2.01	0.80
3266132	326930.	661670.	186.199	0.81	0.93
3266133	326770.	661600.	186.839	1.18	0.92
3266134	326570.	661480.	183.483	6.73	0.94
3266135	326280.	661150.	183.594	12.14	0.99
3266136	327238.	665573.	143.526	16.69	0.76
3266137	326783.	665645.	158.348	14.17	0.80
3266138	326513.	665218.	163.434	10.79	0.81

3266139	326700.	665230.	161.576	9.84	0.79
3266140	327400.	665350.	155.768	-1.80	0.73
3266141	327800.	665400.	151.368	-12.86	0.75
3266142	327880.	666050.	145.546	-2.05	0.69
3266143	327690.	666280.	140.613	3.08	0.68
3266144	327450.	666620.	145.806	11.63	0.76
3266145	327238.	666373.	143.526	17.59	0.76
3266146	326990.	668000.	129.850	50.90	0.72
3266147	328080.	665760.	148.283	-12.32	0.77
3266148	328480.	665530.	137.921	-26.73	0.82
3266149	329480.	665930.	105.782	-27.83	0.77
3266150	329550.	666560.	101.168	-23.20	0.73
3266151	329970.	665170.	116.587	-31.99	0.96
3266152	329350.	664190.	139.156	-25.91	0.80
3266153	329000.	663620.	148.613	-24.09	0.89
3266154	329000.	663380.	146.777	-25.32	0.70
3266155	329240.	663100.	149.029	-29.34	0.70
3266156	329480.	663500.	141.005	-31.15	0.71
3266157	329860.	664000.	131.632	-34.17	0.77
3266158	328800.	662140.	153.661	-21.68	0.83
3266159	329200.	662100.	139.110	-21.06	1.19
3266160	328860.	662430.	151.761	-24.23	0.76
3266161	328880.	662600.	154.053	-24.79	0.73
3266162	329050.	662800.	147.816	-26.66	0.74
3266163	328670.	662930.	149.352	-23.83	0.69
3266164	329880.	664790.	71.438	-15.91	5.60
3266165	328480.	665120.	132.419	-28.47	0.91
3266166	328420.	665300.	144.857	-25.47	1.20
3266167	329500.	666910.	109.146	-18.56	0.78
3266168	328950.	667510.	130.979	-9.64	0.78
		NT 27			
3267001	323525.	674625.	21.340	82.32	0.76
3267002	322025.	675575.	48.770	86.16	0.37
3267003	320975.	675450.	57.320	83.02	0.48
3267004	321512.	674375.	52.320	80.06	0.66
3267005	323600.	675838.	39.040	81.93	0.34
3267006	324862.	675675.	23.480	86.79	0.35
3267007	327550.	671300.	48.900	90.55	0.71
3267008	329012.	671650.	48.900	66.09	0.52
3267009	326650.	670775.	78.940	98.85	0.90
3267010	321310.	672012.	48.479	71.26	0.73
3267011	321630.	672202.	49.058	70.94	0.69
3267012	321805.	672215.	47.463	72.13	0.70
3267013	322360.	672307.	44.710	72.59	0.71
3267014	322597.	672285.	45.073	73.88	0.71
3267015	322847.	672198.	47.221	76.08	0.74
3267016	323173.	672300.	49.985	78.84	0.71
3267017	323532.	672475.	52.181	81.08	0.69
3267018	323845.	672498.	70.119	87.29	0.63
3267019	324115.	672663.	68.496	93.42	0.57
3267020	324448.	672665.	73.085	97.68	0.57
3267021	324705.	672693.	74.770	99.47	0.56
3267022	325073.	672670.	74.475	99.73	0.52
3267023	325385.	672450.	79.595	101.26	0.50
3267024	325635.	672475.	73.785	102.32	0.49
3267025	325833.	672447.	73.200	102.56	0.49
3267026	326240.	672452.	74.760	103.03	0.52
3267027	326607.	672575.	84.071	100.80	0.72

3267028	329216.	675175.	14.449	92.26	0.44
3267029	328905.	675652.	7.397	97.53	0.37
3267030	328302.	675935.	5.163	106.74	0.42
3267031	327725.	676272.	4.078	100.66	0.34
3267032	327267.	676452.	4.463	98.22	0.32
3267033	327050.	676560.	5.154	98.36	0.31
3267034	326408.	676772.	5.898	96.57	0.31
3267035	326180.	676845.	8.397	97.59	0.29
3267036	325873.	676947.	7.690	93.42	0.33
3267037	325673.	677007.	7.094	92.65	0.29
3267038	324938.	676935.	7.310	90.82	0.40
3267039	324580.	677007.	8.357	91.69	0.40
3267040	324250.	677010.	7.924	91.70	0.42
3267041	323853.	677055.	5.793	90.91	0.47
3267042	323410.	677222.	5.553	90.03	0.43
3267043	322710.	677335.	7.088	94.81	0.40
3267044	321745.	676910.	28.578	95.38	0.61
3267045	321000.	676875.	13.808	96.19	0.57
3267046	320275.	677044.	5.182	90.36	0.58
3267047	320685.	676150.	43.586	87.39	0.47
3267048	327080.	671940.	66.035	96.38	0.67
3267049	327180.	671850.	60.381	95.99	0.68
3267050	327280.	671680.	54.359	93.75	0.68
3267051	327380.	671540.	52.229	91.78	0.68
3267052	327470.	671390.	48.748	90.50	0.72
3267053	327510.	671300.	47.771	88.73	0.73
3267054	328130.	670760.	52.017	75.96	0.86
3267055	328320.	670540.	63.222	67.71	0.68
3267056	328460.	670380.	65.459	60.25	0.66
3267057	328950.	670230.	53.968	26.76	0.87
3267058	329210.	670000.	60.955	16.26	0.83
3267059	328660.	670350.	58.032	43.60	0.79
3267060	328750.	670300.	54.547	31.47	0.90
3267061	328980.	670200.	54.857	25.28	0.89
3267062	329070.	673790.	30.729	84.76	0.67
3267063	329010.	674280.	28.561	89.32	0.51
3267064	329790.	674960.	5.071	80.30	0.46
3267065	325512.	671262.	75.761	105.11	0.89
3267066	325603.	671275.	74.212	105.27	0.93
3267067	325762.	671287.	71.841	106.94	1.01
3267068	326050.	671362.	66.581	107.80	0.83
3267069	326162.	671400.	65.040	107.54	0.80
3267070	326262.	671475.	63.399	104.06	0.74
3267071	326362.	671525.	62.592	101.83	0.69
3267072	326550.	671600.	60.554	100.44	0.66
3267073	326775.	671712.	60.249	99.04	0.63
		NT 28			
3268001	320100.	689950.	143.866	36.94	0.64
3268002	320363.	688525.	143.561	40.24	0.82
3268003	322300.	689150.	96.317	54.24	1.20
3268004	324625.	689288.	64.125	67.73	1.08
3268005	326875.	689325.	61.570	61.62	0.63
3268006	326038.	687963.	98.146	65.34	1.11
3268007	324025.	686875.	51.511	60.10	2.87
3268008	323500.	685775.	10.973	70.50	0.92
3268009	320450.	686450.	145.694	52.17	3.07
3268010	321888.	687300.	167.030	39.17	3.16

3268011	323600.	698025.	159.106	48.60	1.79
3268012	325525.	686525.	36.881	51.03	1.07
		NT 29			
3269001	322275.	697850.	77.754	3.58	0.54
3269002	323838.	699450.	127.437	16.58	0.94
3269003	325200.	691038.	71.354	72.81	0.67
3269004	322775.	690750.	79.553	45.35	0.44
3269005	320545.	690363.	155.753	35.13	1.26
3269006	320913.	692100.	131.399	21.40	0.46
3269007	320350.	693525.	123.170	2.76	0.30
3269008	322013.	693150.	119.177	20.82	0.36
3269009	323875.	693075.	150.906	27.26	1.19
3269010	325550.	692825.	94.100	18.71	0.63
3269011	324825.	694550.	100.919	21.80	0.32
3269012	321750.	695425.	65.562	0.07	0.54
3269013	320800.	696850.	96.957	2.63	0.38
3269014	324400.	696950.	78.974	8.58	0.41
3269015	326200.	697738.	70.104	2.73	0.28
3269016	327438.	697325.	57.942	-0.26	0.25
3269017	327825.	695188.	95.738	7.00	0.40
3269018	329750.	692850.	40.264	-3.62	0.91
3269019	328100.	691588.	8.900	39.53	0.66
3269020	328975.	698488.	51.846	-15.32	0.28
		NO 20			
3270001	321932.	701190.	107.930	10.52	1.96
3270002	322950.	702070.	155.174	16.90	0.97
3270003	325488.	701940.	122.865	12.20	0.74
3270004	324645.	703960.	204.856	12.44	1.64
3270005	323850.	705080.	271.100	12.38	2.82
3270006	322805.	706300.	274.100	-21.01	3.61
3270007	324925.	700075.	141.458	6.51	1.08
3270008	328600.	700950.	71.994	8.98	0.34
3270009	328338.	702700.	95.128	17.30	0.45
3270010	328100.	705425.	102.138	-3.47	0.92
3270011	326920.	706425.	103.060	-8.03	2.24
3270012	325388.	707725.	57.040	2.53	2.34
3270013	322250.	708238.	94.050	1.47	3.12
3270014	328475.	707488.	43.040	-8.02	0.71
3270015	328400.	708975.	41.060	-3.22	0.47
		NT 31			
3361001	333601.	614696.	306.850	70.99	0.92
3361002	339589.	614998.	273.406	39.78	0.76
3361003	330563.	618450.	227.570	32.96	4.57
3361004	332040.	619650.	233.782	32.77	4.20
		NT 32			
3362001	331350.	628700.	353.725	-1.98	4.50
3362002	330425.	627900.	327.980	-3.17	5.31
3362003	330750.	626913.	299.055	0.90	5.24
3362004	330900.	626075.	277.756	6.28	5.68
3362005	331280.	625280.	264.500	10.29	3.94
3362006	332530.	620480.	222.504	27.46	4.54
3362007	333450.	621200.	220.576	32.19	5.06
3362008	334180.	621740.	210.892	32.53	5.26
3362009	335310.	621670.	208.483	35.62	4.76
3362010	336470.	621480.	195.378	40.49	3.58
3362011	337200.	622510.	187.147	43.55	5.28
3362012	337970.	623700.	190.366	43.47	3.08
3362013	338800.	624270.	171.907	45.15	3.93

3362014	339930.	629650.	164.038	22.70	9.83
3362015	338930.	629350.	199.340	21.05	4.49
3362016	337450.	628600.	195.682	20.42	5.05
3362017	335830.	627750.	194.767	21.01	5.78
3362018	336630.	626380.	310.240	31.94	5.21
3362019	337160.	625020.	260.180	32.39	3.18
3362020	336980.	625800.	363.682	31.61	3.73
3362021	334530.	627170.	218.846	16.16	3.89
3362022	334260.	626210.	215.525	19.15	4.25
3362023	333320.	625420.	237.440	17.34	3.81
3362024	332260.	625320.	239.573	12.14	3.84
		NT 33			
3363001	330300.	638795.	152.299	-43.90	6.14
3363002	330605.	637950.	148.557	-49.25	6.96
3363003	331315.	636885.	147.223	-31.19	9.21
3363004	331970.	635950.	161.916	-24.71	5.05
3363005	332580.	635275.	165.660	-26.33	4.17
3363006	333080.	636335.	142.416	-23.06	4.97
3363007	333570.	637999.	162.289	-21.29	10.30
3363008	333625.	638763.	173.070	-20.50	11.54
3363009	332400.	633937.	169.561	-12.68	4.90
3363010	331575.	633450.	180.405	-22.41	6.32
3363011	330800.	633537.	190.187	-14.92	10.28
3363012	331775.	632775.	195.925	-14.00	7.13
3363013	331800.	631825.	216.856	-4.20	10.89
3363014	331413.	631025.	244.227	-10.14	8.08
3363015	331175.	630300.	269.780	-8.72	6.22
3363016	330425.	639388.	151.486	-42.70	7.68
3363017	331500.	637375.	157.517	-41.04	5.63
3363018	333820.	637040.	139.577	-28.19	8.22
3363019	336100.	636820.	133.154	-15.95	8.23
3363020	330010.	633350.	227.700	-23.28	6.00
3363021	331570.	632030.	213.400	-12.41	8.03
3363022	333370.	635490.	151.800	-18.43	5.77
3363023	334960.	636760.	136.900	-17.25	11.67
3363024	337240.	637140.	141.700	-13.12	8.43
3363025	338080.	637380.	135.600	-7.33	8.58
3363026	333470.	639510.	189.080	-24.19	9.83
3363027	330550.	638125.	150.572	-48.97	6.49
3363028	339425.	639525.	504.750	-2.67	13.45
3363029	335875.	633050.	566.620	3.81	16.40
3363030	337502.	632825.	509.010	16.45	9.98
3363031	338112.	634100.	527.300	5.70	12.82
3363032	338925.	635107.	522.730	6.82	15.09
		NT 34			
3364001	333270.	641550.	209.851	-26.01	10.84
3364002	333930.	643120.	257.306	-24.46	9.95
3364003	334850.	648750.	335.593	3.50	7.94
3364004	334860.	647450.	342.600	-11.33	10.46
3364005	334750.	646100.	356.818	-14.95	9.53
3364006	334380.	643970.	285.757	-19.82	9.72
3364007	331200.	643770.	258.330	-13.87	13.23
3364008	330450.	644280.	303.600	-14.41	9.39
3364009	331850.	642920.	236.500	-20.35	15.49
3364010	332930.	642740.	229.200	-28.08	11.51
3364011	335550.	645875.	591.312	-14.98	9.43
3364012	336513.	645150.	573.635	-19.99	5.67
3364013	337175.	644275.	590.400	-13.65	6.18

3364014	337150.	643125.	559.280	-11.20	14.01
3364015	338125.	642725.	562.050	-10.43	7.62
3364016	339160.	641265.	502.010	-12.83	7.24
3364017	338550.	640300.	541.630	-4.95	19.39
		NT	35		
3365001	337175.	658470.	229.499	24.79	0.98
3365002	337285.	658430.	236.304	27.71	1.01
3365003	337633.	658380.	249.991	26.83	0.99
3365004	337970.	658250.	255.745	24.47	0.82
3365005	338075.	658205.	256.138	22.44	0.82
3365006	338300.	658050.	257.449	21.90	0.77
3365007	339250.	659875.	238.091	6.84	0.84
3365008	339550.	656325.	276.879	14.53	1.06
3365009	339512.	656465.	277.020	14.31	1.05
3365010	339480.	656550.	274.377	15.41	1.13
3365011	339400.	656763.	273.257	15.93	1.29
3365012	339275.	656890.	271.797	13.56	1.35
3365013	339155.	656950.	264.976	15.34	1.34
3365014	339075.	657050.	267.419	16.76	1.12
3365015	339013.	657200.	270.308	16.75	0.99
3365016	338863.	657350.	271.494	16.99	0.86
3365017	338715.	657540.	271.671	16.25	0.83
3365018	338665.	657608.	268.406	15.97	0.78
3365019	338550.	657722.	265.716	15.48	0.77
3365020	338475.	657812.	262.569	16.29	0.76
3365021	339600.	655610.	270.100	14.58	1.32
3365022	339450.	656210.	275.000	14.73	1.11
3365023	339200.	657380.	272.330	18.85	0.99
3365024	337530.	658110.	256.300	21.60	0.94
3365025	338080.	658290.	256.000	23.91	0.82
3365026	336480.	658440.	219.500	21.82	1.05
3365027	336000.	659110.	203.400	19.82	1.20
3365028	336450.	659420.	195.100	18.41	1.44
3365029	336680.	659770.	151.700	20.63	2.25
3365030	330080.	657100.	249.430	52.89	0.78
3365031	331620.	656150.	260.760	32.29	1.01
3365032	331300.	655370.	280.340	29.82	1.17
3365033	330870.	654150.	273.610	27.03	1.22
3365034	339900.	653000.	245.280	13.58	6.08
3365035	339000.	652560.	253.940	3.71	4.76
3365036	335420.	650680.	299.000	7.03	5.30
3365037	334870.	652320.	362.610	13.79	1.26
3365038	336320.	655650.	310.270	27.19	2.37
3365039	336920.	656840.	264.200	21.71	1.01
3365040	334980.	657660.	256.970	20.78	1.18
3365041	332620.	656660.	235.620	30.27	1.24
3365042	331780.	658400.	196.250	43.40	0.99
3365043	332200.	659980.	153.710	20.61	1.10
3365044	330290.	657450.	237.510	50.93	0.84
3365045	330120.	652655.	285.210	32.87	1.93
3365046	330680.	652425.	306.500	28.93	2.56
3365047	330675.	652613.	298.264	29.66	2.34
3365048	330338.	654530.	271.480	33.49	0.96
3365049	330788.	654075.	273.402	28.13	1.21
3365050	330755.	653750.	279.800	27.26	1.28
3365051	330910.	653100.	285.300	27.88	2.10
3365052	332945.	656375.	240.266	32.33	1.59

3365053	334533.	657623.	253.237	22.75	1.10
3365054	335180.	658800.	204.500	23.63	1.62
3365055	335500.	658520.	204.112	24.90	1.52
3365056	335815.	658500.	217.770	29.95	1.27
3365057	336030.	658200.	229.783	24.87	1.28
3365058	336270.	658020.	239.613	15.26	1.12
3365059	336560.	657725.	230.775	25.20	1.24
3365060	336700.	657475.	240.800	27.18	1.07
3365061	336800.	657300.	251.400	22.48	0.98
3365062	336890.	656965.	262.338	22.92	0.97
3365063	337010.	656630.	264.132	20.29	1.24
3365064	337100.	656513.	271.138	18.40	1.25
3365065	337250.	656339.	280.324	18.18	1.37
3365066	337343.	656188.	284.581	22.73	2.05
3365067	337515.	656160.	298.962	22.64	1.55
3365068	337705.	656110.	310.086	23.75	1.65
3365069	337800.	656040.	318.278	23.84	1.64
3365070	337960.	655945.	323.319	21.41	1.25
3365071	338195.	655805.	325.985	19.18	1.06
3365072	338338.	655735.	322.772	18.88	0.98
3365073	338530.	655650.	314.059	17.08	0.90
3365074	337100.	656513.	271.138	18.36	1.25
3365075	332140.	657970.	212.899	39.48	1.04
3365076	336560.	655830.	302.516	24.66	2.09
3365077	336020.	655410.	331.569	24.81	2.59
3365078	334990.	654080.	399.200	22.20	2.30
3365079	334830.	653350.	403.600	22.83	1.80
3365080	334640.	652740.	378.000	17.30	1.49
3365081	332510.	659050.	161.200	38.73	1.51
3365082	335140.	659710.	171.900	28.34	1.24
3365083	335620.	659260.	190.800	21.57	1.23
3365084	336820.	658450.	228.900	17.81	0.93
3365085	337620.	659360.	250.200	27.52	0.97
3365086	338100.	659400.	232.380	15.18	1.26
3365087	338640.	659650.	239.832	6.84	1.01
3365088	339260.	659880.	237.700	5.58	0.84
3365089	339420.	659230.	236.307	9.61	0.85
3365090	339230.	658430.	254.566	11.18	0.85
3365091	339170.	657920.	261.100	11.03	0.87
3365092	334490.	653670.	449.885	30.51	5.53
3365093	333990.	653500.	420.929	35.13	4.30
3365094	333630.	653250.	460.553	32.82	5.60

NT 36

3366001	334060.	667330.	50.989	-19.05	1.08
3366002	334530.	666660.	78.720	-16.76	1.31
3366003	335270.	665560.	123.980	-0.13	1.38
3366004	336080.	666020.	186.980	4.57	1.69
3366005	337170.	665280.	204.862	14.29	1.30
3366006	337760.	664840.	169.109	15.34	1.06
3366007	338580.	664480.	128.384	20.27	1.06
3366008	339420.	664330.	145.919	15.73	0.85
3366009	339880.	663730.	172.974	9.65	0.79
3366010	338450.	665340.	140.583	18.77	0.89
3366011	338670.	666340.	120.548	21.62	0.83
3366012	339520.	667080.	100.961	25.06	0.75
3366013	338870.	667690.	117.293	27.18	0.84
3366014	334060.	657330.	50.989	-19.05	1.08
3366015	334060.	667330.	50.989	-19.05	1.08

3366016	334490.	665690.	107.819	-13.61	1.53
3366017	334990.	664590.	151.211	4.35	1.56
3366018	334980.	663850.	187.064	4.51	1.83
3366019	336470.	662440.	200.043	16.70	0.77
3366020	337510.	663170.	176.707	16.25	0.81
3366021	336330.	663980.	245.769	11.72	2.12
3366022	334020.	663010.	149.540	-12.41	1.50
3366023	334930.	662030.	209.526	5.50	1.38
3366024	334070.	661000.	142.256	7.18	1.22
3366025	333490.	662030.	127.001	-12.25	1.15
3366026	333000.	664320.	86.294	-27.17	1.25
3366027	333140.	665690.	45.577	-26.88	1.67
3366028	332510.	666570.	68.412	-30.72	0.87
3366029	334060.	667330.	50.989	-19.05	1.08
3366030	334060.	667330.	50.989	-19.05	1.08
3366031	337790.	666810.	169.234	25.60	1.08
3366032	336990.	668080.	117.427	22.52	0.96
3366033	338070.	668490.	152.665	32.00	1.12
3366034	339660.	669120.	106.594	36.27	0.56
3366035	337530.	669520.	149.720	26.24	1.76
3366036	338630.	669930.	146.526	32.48	1.09
3366037	336540.	669070.	84.143	12.88	1.14
3366038	335860.	669960.	53.026	5.00	0.86
3366039	335820.	667890.	94.869	3.45	0.99
3366040	334690.	668970.	43.747	-8.64	0.76
3366041	338880.	663710.	145.987	15.27	0.92
3366042	338630.	662860.	161.077	13.48	1.04
3366043	338650.	661990.	192.888	7.52	1.00
3366044	339090.	661390.	233.364	4.11	1.04
3366045	334060.	667330.	50.989	-19.05	1.08
3366046	339100.	661390.	233.400	4.17	1.09
3366047	339150.	661238.	239.817	2.17	1.09
3366048	339222.	661100.	247.002	-2.53	1.12
3366049	339185.	660900.	243.632	-2.50	1.04
3366050	339125.	660750.	237.209	0.11	0.88
3366051	339160.	660624.	236.562	1.30	0.86
3366052	339200.	660390.	233.777	3.67	0.92
3366053	339220.	660175.	223.178	5.31	0.87
3366054	339055.	661475.	231.891	3.37	1.14
3366055	338975.	661575.	224.881	3.33	1.15
3366056	338862.	661675.	212.047	5.77	1.07
3366057	333250.	665350.	67.110	-27.78	1.22
3366058	333450.	662570.	120.700	-17.22	1.27
3366059	333820.	661120.	129.530	5.66	1.29
3366060	335420.	661670.	210.560	13.50	1.04
3366061	336850.	662670.	191.460	16.76	0.77
3366062	335850.	660400.	213.950	14.82	1.44
3366063	332520.	661080.	130.450	-4.67	0.97
3366064	330620.	669220.	78.029	-13.91	0.58
3366065	331460.	668420.	64.891	-24.91	0.58
3366066	332160.	667930.	63.800	-29.36	0.64
3366067	331790.	665860.	78.312	-35.00	0.83
3366068	331080.	665330.	98.279	-37.99	0.75
3366069	330690.	664940.	107.240	-34.48	0.74
3366070	332930.	663340.	96.654	-23.74	1.12
3366071	333490.	662030.	127.271	-12.34	1.15
3366072	333450.	662580.	121.197	-17.28	1.27

3366073	333000.	664260.	87.285	-27.33	1.24
3366074	332430.	665250.	56.425	-31.25	1.27
3366075	332490.	665560.	68.242	-30.93	0.79
3366076	334890.	669530.	33.690	-3.22	0.85
3366077	333420.	667520.	57.490	-15.43	0.96
3366078	334650.	660300.	157.900	19.13	1.14
3366079	330950.	668900.	70.570	-24.17	0.63
3366080	331870.	653860.	83.049	-33.81	1.01
3366081	330120.	660520.	172.920	5.49	0.90
3366082	330280.	660940.	169.310	-5.32	0.90
3366083	330580.	661330.	157.840	-14.69	0.83
3366084	330760.	661590.	149.080	-17.25	0.87
3366085	330990.	661930.	134.110	-25.13	1.04
3366086	331210.	662290.	125.580	-23.42	0.98
3366087	331860.	660560.	148.160	7.73	0.99
3366088	331180.	660860.	157.890	-7.15	0.91
3366089	330030.	660380.	188.948	7.48	0.94
3366090	330120.	660520.	172.875	4.98	0.90
3366091	330160.	660630.	169.921	2.94	0.93
3366092	330220.	660770.	170.482	-0.88	0.87
3366093	330280.	660940.	169.235	-5.61	0.90
3366094	330370.	661060.	164.208	-8.22	0.88
3366095	330520.	661220.	153.051	-12.93	0.87
3366096	330580.	661330.	157.837	-15.15	0.83
3366097	330650.	661400.	154.597	-16.29	0.82
3366098	330760.	661590.	149.065	-18.34	0.87
3366099	330820.	661690.	143.668	-19.81	0.92
3366100	330940.	661850.	136.600	-22.82	1.03
3366101	330990.	661930.	134.649	-24.19	1.03
3366102	331070.	662180.	131.171	-26.84	1.00
3366103	331210.	662290.	125.580	-24.11	0.98
3366104	330170.	666200.	71.061	-27.12	1.47
3366105	330320.	666080.	59.905	-22.95	2.33
3366106	330930.	666300.	104.847	-35.89	0.90
3366107	331300.	666570.	85.550	-31.18	0.81
3366108	332170.	666260.	66.832	-32.69	0.87
3366109	331840.	666720.	76.032	-33.86	0.73
3366110	331210.	665580.	95.573	-34.80	0.71
3366111	330440.	665300.	108.977	-27.84	0.68
3366112	330240.	665380.	111.182	-32.09	0.72
3366113	331150.	664320.	89.143	-37.45	0.93
3366114	332300.	667000.	58.942	-31.14	0.83
3366115	331810.	667360.	69.508	-30.85	0.70
3366116	331300.	667590.	75.583	-30.52	0.60
3366117	330810.	667800.	70.873	-25.03	0.71
3366118	330420.	668030.	86.330	-22.80	0.65
3366119	334060.	667330.	50.989	-19.05	1.08
3366120	334530.	665660.	78.720	-16.76	1.31
3366121	335270.	666560.	123.980	-0.05	1.41
3366122	336080.	665020.	186.980	4.65	1.72
3366123	337170.	665280.	204.862	14.35	1.32
3366124	337760.	664840.	169.109	15.37	1.07
3366125	338580.	664480.	128.384	20.27	1.06
3366126	339420.	664330.	145.919	15.73	0.85
3366127	339880.	663730.	172.974	9.65	0.79
3366128	338450.	665340.	140.683	18.77	0.89
3366129	338670.	666340.	120.548	21.62	0.83
3366130	339520.	667080.	100.961	25.04	0.74

3366131	338870.	657690.	117.293	27.18	0.64
3366132	334060.	667330.	50.989	-19.05	1.08
3366133	334060.	667330.	50.989	-19.05	1.08
3366134	334490.	665690.	107.819	-13.61	1.53
3366135	334990.	664590.	151.211	4.35	1.56
3366136	334980.	663850.	187.064	4.51	1.83
3366137	336470.	662440.	200.043	16.75	0.79
3366138	337510.	663170.	176.707	16.27	0.82
3366139	336330.	663980.	245.769	11.83	2.16
3366140	334020.	663010.	149.540	-12.41	1.50
3366141	334930.	662030.	209.626	5.50	1.38
3366142	334070.	661000.	142.256	7.18	1.22
3366143	333490.	662030.	127.001	-12.25	1.15
3366144	333000.	664320.	86.294	-27.17	1.25
3366145	333140.	665690.	45.677	-26.88	1.67
3366146	332510.	665670.	68.412	-30.94	0.79
3366147	334060.	667330.	50.989	-19.05	1.08
3366148	334060.	667330.	50.989	-19.05	1.08
3366149	337790.	666810.	169.234	25.60	1.08
3366150	336990.	668080.	117.427	22.52	0.96
3366151	338070.	668490.	152.665	32.03	1.13
3366152	339660.	669120.	106.594	36.24	0.55
3366153	337530.	669520.	149.720	26.29	1.78
3366154	338630.	669930.	146.526	32.48	1.09
3366155	335540.	669070.	84.143	12.88	1.14
3366156	335860.	669960.	53.026	5.00	0.86
3366157	335820.	667890.	94.869	3.51	1.01
3366158	334690.	668970.	43.747	-8.64	0.76
3366159	338880.	663710.	145.987	15.27	0.92
3366160	338630.	662860.	161.077	13.48	1.04
3366161	338650.	661990.	192.888	7.55	1.01
3366162	339090.	661390.	233.364	4.14	1.05
3366163	334060.	667330.	50.989	-19.05	1.08
		NT 37			
3367001	338092.	672830.	36.713	49.87	0.85
3367002	337135.	672105.	50.281	26.92	0.83
3367003	336250.	671200.	37.471	13.60	0.78
3367004	335645.	670300.	31.833	7.86	0.98
3367005	338300.	670725.	127.202	32.52	0.83
3367006	338035.	671165.	143.005	35.57	2.09
3367007	338675.	671820.	119.539	44.82	1.32
3367008	339262.	672490.	103.501	49.39	1.09
3367009	338615.	672775.	53.826	61.09	1.08
3367010	337700.	672750.	32.084	43.88	0.76
3367011	338910.	670063.	149.538	33.11	1.16
3367012	339925.	670890.	122.212	38.74	0.63
3367013	337537.	673175.	28.027	41.00	0.59
3367014	338955.	673963.	26.879	71.43	0.55
3367015	339600.	673930.	34.928	68.10	0.60
3367016	330502.	671488.	47.950	6.90	0.46
3367017	331625.	671150.	55.780	-13.24	0.53
3367018	333512.	670550.	29.260	-12.27	0.54
3367019	333775.	671750.	21.350	-11.25	0.49
3367020	330260.	674470.	4.945	59.43	0.43
3367021	330380.	674320.	4.857	62.63	0.44
3367022	330740.	674080.	4.323	49.86	0.44
3367023	330970.	673920.	4.787	43.58	0.47
3367024	331100.	673830.	4.573	40.73	0.50

3367025	331220.	673760.	4.446	37.70	0.53
3367026	331340.	673660.	4.509	31.09	0.56
3367027	331480.	673560.	4.509	26.18	0.61
3367028	331720.	673410.	6.276	19.28	0.58
3367029	331960.	673370.	7.949	16.04	0.56
3367030	332160.	673380.	7.121	13.63	0.54
3367031	332410.	673320.	8.182	4.58	0.47
3367032	332630.	673150.	8.003	4.61	0.43
3367033	332950.	673040.	5.660	3.18	0.49
3367034	333540.	672840.	6.501	2.92	0.45
3367035	334060.	672740.	6.564	1.46	0.45
3367036	334510.	672730.	4.304	3.43	0.48
3367037	334660.	672040.	21.037	-3.57	0.55
3367038	335210.	671630.	22.834	-0.67	0.68
3367039	335450.	670330.	29.712	4.74	0.85
		NT 39			
3369001	331300.	696588.	52.456	-39.58	0.20
3369002	334175.	698075.	35.692	-64.07	0.31
3369003	336600.	699975.	28.346	-69.48	0.28
3369004	332650.	695963.	50.627	-55.90	0.40
3369005	330850.	694050.	55.199	-30.53	0.78
3370001	330538.	700025.	67.666	-23.26	0.30
3370002	335425.	700975.	36.271	-56.16	0.43
3370003	338363.	700550.	6.126	-65.11	0.35
3370004	338100.	702850.	49.682	-45.87	0.65
3370005	337850.	704600.	97.231	-25.42	0.67
3370006	338250.	706375.	170.718	-7.77	1.03
3370007	338250.	708050.	140.543	-3.30	0.44
3370008	336200.	708800.	154.259	0.34	1.27
3370009	334750.	707875.	184.434	-2.89	1.55
3370010	334200.	705850.	176.814	-5.55	1.38
3370011	333975.	704525.	165.232	-2.49	1.51
		NO 30			
3370012	334450.	702975.	88.422	-19.44	0.58
3370013	332005.	702560.	111.892	-12.10	0.64
3370014	332475.	705150.	125.608	2.39	0.45
3370015	330550.	705820.	143.286	9.63	1.35
3370016	332725.	706810.	133.533	-2.20	0.81
		NT 42			
3462001	348625.	627677.	260.604	50.26	1.11
3462002	349313.	624775.	242.621	47.84	0.81
3462003	349400.	623850.	183.185	43.09	1.05
3462004	347282.	622513.	171.602	43.07	2.07
3462005	348813.	621450.	211.531	45.56	1.32
3462006	349763.	622450.	225.552	46.86	1.14
3462007	345425.	621100.	180.442	42.89	1.98
3462008	345463.	622575.	252.370	50.21	0.86
3462009	344250.	623555.	338.407	50.77	1.87
3462010	343188.	624700.	262.128	50.48	1.96
3462011	340838.	624557.	181.356	47.85	2.69
3462012	343700.	626300.	159.106	43.58	2.65
3462013	341700.	629895.	158.410	26.36	6.91
3462014	345063.	627875.	123.749	43.85	2.63
3462015	346265.	629100.	117.043	48.21	3.75
3462016	346970.	629925.	136.246	48.39	3.13
		NT 43			
3463001	349538.	635650.	122.259	36.29	3.15
3463002	348050.	636950.	144.562	20.70	4.01

3463003	346275.	637400.	166.920	15.62	5.62
3463004	344850.	636425.	155.197	12.76	3.59
3463005	341275.	636350.	138.450	2.25	6.86
3463006	342310.	637215.	229.819	-1.34	1.77
3463007	343500.	639350.	271.577	-1.82	1.85
3463008	344850.	635000.	119.191	14.26	4.34
3463009	344875.	638075.	249.326	2.10	1.55
3463010	345450.	639275.	208.483	-5.03	1.73
3463011	347050.	639005.	164.304	9.53	4.73
3463012	348375.	638650.	202.742	20.02	2.84
3463013	349700.	639405.	239.573	19.00	1.39
3463014	340822.	636285.	144.480	-1.96	5.72
3463015	341375.	639688.	359.670	-9.64	2.48
3463016	347410.	631375.	145.085	47.18	1.87
3463017	348900.	631100.	143.866	55.94	1.87
3463018	348450.	633650.	144.539	38.87	2.16
3463019	345825.	632525.	112.650	31.55	8.40
3463020	345450.	639280.	208.500	-4.87	1.72
3463021	344880.	638060.	249.300	2.60	1.56
3463022	344850.	636380.	151.357	13.45	3.74
		NT 44			
3464001	346850.	645175.	288.950	-14.75	1.98
3464002	346017.	644600.	183.483	-13.06	5.14
3464003	347540.	643325.	355.397	-3.83	1.80
3464004	348650.	642195.	340.296	8.74	1.60
3464005	349725.	642075.	287.961	10.80	1.18
3464006	340088.	640438.	329.200	-10.94	4.36
3464007	340075.	641200.	340.770	-14.10	4.56
3464008	340395.	642213.	341.990	-14.49	5.61
3464009	340325.	643005.	360.270	-15.51	5.18
3464010	342338.	649500.	260.300	-24.28	1.70
3464011	341200.	648825.	292.300	-25.27	2.58
3464012	340150.	646895.	371.250	-24.89	3.35
3464013	341450.	645425.	260.600	-17.96	4.82
3464014	349950.	649525.	302.970	-24.60	1.64
3464015	349150.	648700.	331.930	-22.01	1.55
3464016	344280.	648310.	217.066	-29.85	2.91
3464017	344830.	645550.	191.870	-26.86	4.96
3464018	345760.	644400.	176.833	-10.79	4.30
3464019	345420.	640070.	159.606	-4.49	3.85
		NT 45			
3465001	345250.	658410.	371.347	-20.26	2.12
3465002	344868.	657625.	345.813	-16.29	1.31
3465003	344505.	657300.	322.550	-10.91	1.05
3465004	343545.	655085.	271.809	-7.34	3.29
3465005	343125.	654445.	253.029	-4.93	4.57
3465006	342570.	653575.	278.739	-10.81	2.74
3465007	342700.	652345.	294.210	-10.30	1.43
3465008	341155.	653315.	241.342	-3.64	4.97
3465009	340890.	653795.	250.247	-0.40	3.22
3465010	340370.	654625.	256.483	1.91	2.54
3465011	340385.	654025.	263.356	1.36	2.02
3465012	342245.	651675.	228.337	-10.92	2.65
3465013	349700.	653505.	222.455	-33.91	1.35
3465014	349495.	653875.	231.120	-31.89	1.28
3465015	349360.	654550.	220.857	-30.69	2.16
3465016	348750.	654905.	240.182	-32.82	2.13
3465017	348150.	655275.	265.078	-28.51	1.80

3465018	345260.	659465.	283.327	-18.04	1.60
3465019	348200.	651999.	341.075	-27.90	1.97
3465020	345300.	652150.	354.178	-23.10	0.96
3465021	345312.	654162.	323.090	-16.06	1.15
3465022	344787.	654287.	467.870	-12.47	8.47
3465023	344970.	653842.	384.962	-19.44	2.25
3465024	347600.	656900.	342.595	-25.58	1.49
3465025	347200.	658200.	339.242	-17.22	1.12
3465026	343300.	659475.	306.934	-3.63	1.57
3465027	342450.	658520.	330.100	-2.33	1.27
3465028	342612.	656925.	295.350	2.52	1.33
3465029	341100.	656100.	344.004	7.08	1.06
3465030	340350.	654620.	256.360	2.56	2.59
3465031	340870.	653770.	251.580	3.09	3.19
3465032	342150.	651870.	231.600	-17.05	2.62
3465033	340910.	652960.	237.490	-3.44	2.72
3465034	342120.	650330.	229.806	-24.98	2.56
		NT 46			
3466001	346925.	668687.	103.556	6.68	0.76
3466002	348210.	669815.	79.542	10.85	0.81
3466003	348245.	668950.	99.859	0.83	0.92
3466004	347465.	667850.	133.816	-7.92	0.94
3466005	349675.	665260.	208.437	-22.34	1.55
3466006	349290.	666900.	162.420	-17.71	0.88
3466007	348150.	665050.	147.101	-21.71	1.34
3466008	347175.	663950.	174.047	-29.03	1.15
3466009	348538.	663580.	192.761	-22.68	1.52
3466010	349198.	663460.	203.535	-32.77	2.03
3466011	346800.	661400.	220.458	-21.83	1.68
3466012	346120.	667405.	94.467	-4.15	1.14
3466013	345400.	666125.	107.971	-14.68	1.04
3466014	344975.	667500.	111.785	3.08	0.74
3466015	341710.	668600.	99.282	28.43	0.57
3466016	341625.	669600.	84.145	34.67	0.47
3466017	340600.	667550.	106.383	28.12	0.64
3466018	340075.	665912.	134.657	21.29	0.61
3466019	342720.	667635.	136.987	15.12	1.05
3466020	343425.	664950.	167.335	-13.02	0.66
3466021	344260.	664412.	169.752	-24.90	0.77
3466022	345905.	662970.	167.374	-31.96	1.21
3466023	345405.	662175.	199.620	-34.30	1.08
3466024	344440.	660263.	251.447	-9.17	1.27
3466025	343650.	660875.	236.835	-10.54	1.09
3466026	341475.	662138.	192.132	-14.44	0.99
3466027	340750.	662770.	202.482	-4.61	0.76
3466028	340825.	663510.	203.753	-0.64	0.90
3466029	340195.	664400.	169.015	10.56	0.80
3466030	342315.	662725.	185.512	-17.10	1.01
3466031	342725.	661965.	208.483	-24.14	0.75
3466032	343350.	662645.	184.216	-25.80	0.93
3466033	343450.	663900.	187.709	-21.33	0.78
3466034	344075.	665565.	159.106	-19.43	0.74
3466035	344410.	666462.	130.247	-7.82	0.70
3466036	344563.	661350.	215.358	-15.86	1.07
3466037	341400.	660750.	236.429	-15.23	0.76
3466038	340788.	660063.	239.967	-4.66	0.80
3466039	344825.	669200.	90.309	24.42	0.54

NT 47

3467001	340273.	672925.	62.351	51.74	0.70
3467002	341625.	671700.	93.098	46.89	0.39
3467003	342850.	670787.	86.400	42.97	0.43
3467004	343475.	670063.	101.408	32.18	0.43
3467005	346063.	670375.	91.712	29.36	0.55
3467006	347675.	671550.	87.478	32.62	0.49
3467007	349350.	672625.	61.431	31.77	0.61
3467008	349150.	676663.	78.326	77.06	0.96
3467009	348238.	677837.	32.262	94.93	0.48
3467010	347637.	678337.	19.043	98.67	0.39
3467011	347048.	679412.	12.130	111.14	0.25
3467012	348200.	679738.	10.543	106.14	0.27
3467013	343125.	672912.	84.525	57.15	0.42
3467014	343725.	672575.	91.937	53.27	0.51
3467015	343912.	671988.	124.790	47.66	0.72
3467016	344575.	672258.	115.159	49.52	0.50
3467017	344483.	673800.	79.370	60.77	0.47
3467018	344663.	674975.	57.435	75.04	0.44
3467019	345550.	675812.	61.902	77.20	0.55
3467020	346150.	674700.	78.341	74.27	0.41
3467021	346950.	673875.	96.713	65.00	0.41
3467022	348025.	673705.	96.344	57.08	0.42
3467023	345925.	673275.	107.020	56.92	0.52
3467024	345350.	671225.	118.511	37.04	0.48
3467025	344675.	670112.	105.561	29.87	0.45
3467026	340200.	674163.	35.701	67.11	0.58
3467027	340875.	674400.	32.115	71.52	0.55
3467028	341375.	674738.	28.651	75.76	0.53
3467029	342275.	675020.	31.121	80.69	0.51
3467030	344137.	675938.	25.220	86.17	0.52
3467031	344490.	675438.	43.112	84.75	0.45
3467032	344450.	676787.	13.690	107.70	0.42
3467033	346525.	677125.	33.498	93.08	0.54
3467034	347162.	677300.	37.936	91.13	0.70
3467035	347462.	676888.	70.161	81.55	0.68
3467036	342375.	671225.	86.776	48.27	0.39
3467037	346850.	671025.	91.381	31.95	0.52
3467038	348380.	671988.	78.163	33.62	0.50
3467039	348641.	673550.	81.014	49.78	0.48
3467040	348475.	674370.	95.058	60.44	0.45
3467041	348438.	674975.	100.713	67.39	0.61
3467042	346403.	678835.	11.418	111.61	0.27
3467043	340705.	670950.	104.376	40.98	0.44
3467044	341525.	670540.	91.924	40.80	0.40
3467045	348550.	670975.	62.161	20.08	0.70
3467046	349895.	671460.	52.549	18.44	0.80
3467047	340287.	675687.	8.159	83.81	0.37
3467048	341462.	675850.	4.952	85.07	0.43
3467049	342395.	675912.	4.908	85.87	0.52
3467050	343705.	676657.	4.113	96.59	0.45
3467051	344160.	677435.	4.727	101.95	0.35
3467052	344930.	678707.	6.392	112.67	0.25
3467053	345460.	679312.	8.708	116.41	0.21

NT 48

3468001	348695.	680925.	7.027	102.23	0.21
3468002	349325.	681117.	8.307	106.14	0.21
3468003	349838.	681725.	14.388	93.96	0.17

3468004	346650.	680135.	5.130	117.17	0.21
3468005	347750.	681112.	7.594	103.49	0.23
3468006	348088.	682675.	25.667	96.01	0.32
3468007	344970.	680075.	10.223	119.55	0.17
3468008	345650.	680475.	0.000	121.37	0.19
3468009	345350.	680512.	0.020	123.00	0.18
3468010	345050.	680450.	0.020	123.07	0.17
3468011	347487.	682787.	64.102	96.22	1.46
		NO 40			
3470001	340113.	708213.	182.040	-3.40	1.32
3470002	342613.	707938.	178.050	-5.06	0.73
3470003	344563.	707900.	207.060	-7.02	1.03
3470004	346375.	707775.	185.554	-0.61	0.78
3470005	346813.	706065.	144.841	-1.80	0.67
3470006	346150.	704625.	145.755	-2.71	1.86
3470007	348800.	704750.	73.518	12.16	0.75
3470008	346875.	703288.	39.075	3.33	1.12
3470009	347388.	701310.	13.137	5.09	0.28
3470010	344838.	703095.	49.040	-14.41	1.16
3470011	342365.	703140.	29.527	-30.87	1.72
3470012	341700.	704975.	81.412	-31.35	1.26
3470013	342063.	706300.	84.040	-9.81	1.59
3470014	344513.	705125.	167.040	-13.90	1.31
3470015	340325.	702575.	19.568	-44.09	0.60
3470016	349850.	708200.	174.060	17.84	0.68
3470017	348825.	702100.	17.070	18.20	0.31
		NT 52			
3562001	354255.	629450.	171.907	55.15	0.63
3562002	353850.	626213.	139.598	46.77	0.68
3562003	350125.	628100.	260.909	53.43	0.68
3562004	355675.	628325.	142.646	54.30	0.52
3562005	354850.	627263.	139.598	52.46	0.51
3562006	356050.	625875.	122.834	48.79	0.42
3562007	354800.	625138.	145.999	46.79	0.42
3562008	355675.	623625.	148.133	44.83	0.39
3562009	356600.	622375.	187.452	63.11	0.66
3562010	356450.	621157.	169.469	36.13	0.93
3562011	354625.	620300.	131.978	46.21	0.63
3562012	354038.	621775.	160.630	44.20	0.46
3562013	353390.	623100.	193.548	48.75	0.45
3562014	352775.	624650.	138.379	45.48	1.08
3562015	351282.	623138.	193.243	48.36	1.27
3562016	350075.	624775.	216.408	49.19	0.60
3562017	352900.	627600.	189.586	55.76	0.97
3562018	356950.	629300.	119.177	55.84	0.67
3562019	358910.	628155.	136.246	42.50	0.31
3562020	357567.	626975.	128.016	47.03	0.31
3562021	356975.	625050.	114.300	58.61	0.60
3562022	359575.	626650.	198.814	37.89	0.50
3562023	359338.	625257.	116.738	34.14	0.68
3562024	358500.	624100.	172.822	41.46	0.75
3562025	359638.	629525.	285.902	54.83	1.44
		NT 53			
3563001	359313.	639275.	126.797	35.00	0.74
3563002	357275.	638620.	109.156	38.74	1.94
3563003	357000.	637500.	136.550	39.93	1.78
3563004	356075.	638725.	166.726	31.06	1.40

3563005	355975.	639738.	164.592	25.92	1.79
3563006	354163.	639750.	268.224	29.95	1.29
3563007	354050.	638538.	235.001	37.33	0.76
3563008	353025.	639620.	278.282	26.65	1.27
3563009	350525.	639775.	242.082	19.82	1.13
3563010	351600.	639375.	176.175	27.41	1.80
3563011	351850.	638250.	177.698	30.39	1.82
3563012	351500.	637010.	177.598	35.71	1.87
3563013	351845.	635750.	120.108	41.95	1.75
3563014	358300.	636042.	142.342	52.16	1.20
3563015	359325.	634900.	154.338	49.30	0.83
3563016	359550.	633588.	174.041	39.10	1.23
3563017	359275.	631900.	77.419	48.46	1.04
3563018	359800.	630738.	81.686	45.59	0.58
3563019	357065.	630225.	137.770	54.98	0.54
3563020	356263.	631475.	172.822	51.58	1.02
3563021	357713.	632838.	120.701	57.52	0.81
3563022	356345.	633638.	143.256	53.07	1.63
3563023	354375.	633175.	155.143	54.72	2.47
3563024	353800.	631800.	251.765	56.76	1.56
3563025	354500.	630213.	178.918	56.02	0.78
3563026	353025.	633930.	103.632	46.36	1.88
3563027	350910.	632800.	208.483	48.36	1.35
3563028	350280.	634875.	137.770	41.00	1.90
3563029	354500.	635075.	98.146	53.28	3.38
3563030	356445.	634925.	119.482	56.21	3.09
		NT 54			
3564001	354445.	647200.	176.784	-11.29	1.30
3564002	354125.	646675.	159.129	-5.09	1.40
3564003	354288.	645725.	162.225	-3.91	1.47
3564004	354540.	644775.	187.452	-2.86	0.86
3564005	354745.	643775.	184.792	3.16	0.99
3564006	354995.	643185.	169.764	3.99	1.14
3564007	355090.	642375.	171.086	9.08	1.10
3564008	355200.	641545.	193.360	12.78	1.01
3564009	353735.	642525.	247.990	13.88	1.05
3564010	352500.	641925.	233.060	18.34	0.87
3564011	351375.	641975.	255.868	10.39	0.71
3564012	353410.	641170.	277.573	22.89	1.26
3564013	357350.	645610.	214.981	1.02	2.26
3564014	355435.	645800.	158.526	-4.05	1.24
3564015	353895.	643925.	229.956	7.34	0.94
3564016	353425.	643200.	271.577	14.13	1.28
3564017	353210.	642275.	279.806	16.29	1.40
3564018	351175.	640100.	201.473	18.93	1.30
3564019	351235.	642550.	250.925	9.28	0.62
3564020	351800.	643563.	255.422	3.27	0.62
3564021	353050.	645865.	242.150	4.47	1.23
3564022	353155.	645960.	182.445	-8.32	1.29
3564023	351970.	649600.	179.527	-22.47	1.42
3564024	352185.	648675.	185.318	-16.95	1.28
3564025	357300.	645070.	252.374	-1.15	1.28
3564026	353475.	647325.	172.004	-8.65	1.15
3564027	352538.	648025.	181.069	-9.74	1.29
3564028	351775.	647425.	233.271	-7.76	1.18
3564029	350150.	646425.	294.741	-1.03	1.07
3564030	351150.	647313.	256.337	-7.23	0.95
3564031	359025.	647600.	208.831	1.51	0.62

3564032	359175.	648650.	215.018	4.90	0.75
3564033	359825.	649760.	240.855	4.03	0.88
3564034	353420.	649825.	209.086	-30.16	1.22
3564035	354100.	648880.	184.319	-19.85	1.46
3564036	354500.	648325.	196.901	-20.30	1.46
3564037	355475.	647250.	217.933	-8.88	0.85
3564038	356705.	647850.	207.337	0.45	1.20
3564039	358140.	648050.	191.095	10.62	1.26
3564040	358120.	647550.	227.727	8.47	0.74
3564041	358335.	646800.	235.306	3.00	0.73
3564042	358195.	644675.	270.357	-2.30	1.25
3564043	358560.	644025.	214.629	10.92	0.90
3564044	358695.	643300.	182.751	19.57	0.77
3564045	359357.	643475.	209.550	17.65	0.93
3564046	359500.	642415.	193.853	22.83	0.64
3564047	359850.	641625.	180.746	23.66	0.69
3564048	359850.	640125.	149.962	31.25	0.51
3564049	358325.	641000.	231.343	24.28	1.29
3564050	357750.	641438.	230.429	18.71	0.91
3564051	356960.	642085.	176.169	9.85	1.20
3564052	356400.	642485.	144.585	8.25	1.52
3564053	356400.	649455.	263.348	-2.71	1.62
		NT 55			
3565001	350530.	654975.	252.374	-29.48	1.43
3565002	351650.	657175.	255.118	-41.90	4.64
3565003	352045.	658150.	359.054	-36.60	1.59
3565004	351300.	655490.	234.391	-31.87	4.21
3565005	351300.	651650.	189.890	-39.55	1.39
3565006	350725.	651335.	202.592	-36.50	1.38
3565007	350295.	652200.	205.435	-34.16	1.41
3565008	351600.	650900.	187.411	-32.84	1.35
3565009	350810.	653400.	202.681	-40.53	2.34
3565010	351625.	652725.	213.970	-43.91	1.50
3565011	352430.	651650.	212.141	-44.13	1.68
3565012	352640.	651175.	191.326	-39.94	1.76
3565013	353100.	650375.	198.461	-33.91	1.38
3565014	358275.	651880.	363.017	-5.19	2.39
3565015	356750.	653050.	367.285	-15.36	1.64
3565016	357392.	654601.	409.650	-21.86	2.25
3565017	355605.	655125.	448.056	-28.79	3.58
3565018	354525.	654413.	413.514	-30.92	3.28
3565019	354750.	651225.	382.829	-23.26	7.36
3565020	353775.	652975.	388.925	-34.20	4.47
3565021	352525.	655800.	509.020	-34.59	10.10
3565022	353750.	656375.	387.400	-32.71	3.97
3565023	356025.	656750.	445.000	-24.26	2.40
		NT 56			
3566001	353850.	665050.	200.860	-12.17	1.93
3566002	353415.	664880.	207.160	-12.18	2.02
3566003	353150.	664805.	209.850	-11.59	2.10
3566004	352480.	664720.	210.660	-12.41	2.20
3566005	351550.	664750.	211.730	-13.61	2.20
3566006	350975.	664270.	222.200	-15.56	2.92
3566007	351115.	665275.	194.700	-25.39	1.56
3566008	351470.	665585.	182.910	-27.54	1.52
3566009	350890.	665585.	186.430	-29.77	1.33
3566010	350020.	664905.	191.910	-22.40	1.48
3566011	350065.	666375.	155.470	-22.30	1.20

3566012	350640.	665820.	177.270	-28.93	1.34
3566013	351920.	666605.	148.970	-27.39	1.40
3566014	353210.	667300.	127.860	-19.33	1.64
3566015	353370.	667010.	134.110	-22.46	1.64
3566016	353650.	666690.	146.200	-25.13	1.68
3566017	353660.	665980.	174.960	-26.99	1.72
3566018	354270.	665670.	185.630	-10.19	2.02
3566019	354610.	665280.	205.010	-8.64	1.81
3566020	354370.	664700.	217.960	-11.24	2.02
3566021	354060.	664020.	253.320	-21.73	1.81
3566022	353500.	663210.	305.810	-24.76	2.95
3566023	353900.	663690.	277.060	-22.21	2.60
3566024	353685.	668115.	123.910	-12.66	1.51
3566025	354020.	668180.	134.460	-11.17	1.62
3566026	354175.	668410.	146.300	-12.85	1.67
3566027	354775.	668290.	173.120	-9.97	1.70
3566028	355000.	668180.	187.520	-7.32	1.82
3566029	355990.	667525.	189.500	8.53	2.35
3566030	356520.	667605.	198.170	12.08	2.57
3566031	356810.	667230.	213.680	13.97	2.90
3566032	357440.	667075.	220.450	12.04	2.98
3566033	358070.	666730.	262.330	6.04	2.98
3566034	358700.	666425.	270.120	3.60	2.90
3566035	359490.	665780.	352.040	-10.27	3.00
3566036	357440.	667075.	220.450	12.39	2.98
3566037	358070.	666730.	262.330	6.26	2.98
3566038	355000.	667260.	157.620	-5.75	3.13
3566039	357085.	667070.	202.510	13.69	2.88
3566040	356965.	666510.	206.280	8.05	2.71
3566041	356260.	665860.	195.620	2.70	2.70
3566042	355920.	665760.	186.340	-1.86	2.47
3566043	355540.	665820.	180.390	-3.47	2.21
3566044	355525.	666225.	178.650	-1.15	2.04
3566045	355170.	665605.	193.940	-5.43	1.87
3566046	354975.	665500.	204.220	-7.35	1.90
3566047	353540.	669725.	128.530	-4.20	1.11
3566048	353530.	669520.	129.540	-7.32	1.13
3566049	353415.	668790.	107.290	-12.58	1.44
3566050	353430.	668330.	109.730	-13.68	1.55
3566051	353900.	665920.	178.310	-18.35	1.71
3566052	354120.	665820.	171.300	-7.80	2.01
3566053	352575.	667070.	144.090	-22.14	1.35
3566054	351415.	668180.	128.710	-17.99	0.99
3566055	351775.	667980.	110.350	-18.66	1.38
3566056	351290.	668715.	116.780	-13.61	1.08
3566057	353720.	669860.	130.000	-6.00	1.13
3566058	353390.	669180.	124.260	-10.47	1.19
3566059	353420.	669000.	116.920	-2.57	1.24
3566060	353410.	668650.	104.410	-13.87	1.57
3566061	353470.	668100.	113.200	-13.51	1.54
3566062	353260.	667890.	108.070	-15.52	1.81
3566063	353040.	667630.	123.933	-15.76	1.46
3566064	358950.	665130.	422.757	-6.03	5.99
3566065	358250.	664325.	410.565	1.21	3.98
3566066	359975.	664885.	390.449	-9.67	2.20
3566067	352850.	661850.	487.320	-39.86	7.15
3566068	355500.	660562.	481.600	-28.26	3.51

3566069	358188.	667338.	268.834	13.84	4.48

NT 57

3567001	351830.	673120.	62.510	21.70	0.68
3567002	351890.	672940.	62.650	18.97	0.68
3567003	351980.	672710.	70.430	15.95	0.67
3567004	352060.	672520.	67.010	14.42	0.68
3567005	352220.	672150.	59.560	9.73	0.82
3567006	352360.	671680.	62.850	1.68	0.91
3567007	353170.	671720.	65.650	-0.17	1.12
3567008	353270.	671450.	82.110	-1.62	1.17
3567009	353490.	670690.	109.940	-6.64	1.12
3567010	357485.	670675.	149.608	-0.82	4.35
3567011	359100.	670580.	154.668	8.71	5.03
3567012	353175.	671710.	65.670	0.50	1.13
3567013	354083.	670575.	126.396	-5.57	1.28
3567014	354992.	670018.	147.291	-2.76	2.27
3567015	355645.	672562.	70.702	4.23	1.42
3567016	357700.	673670.	89.078	-3.27	1.28
3567017	359693.	674715.	95.566	-2.94	1.10
3567018	359230.	675600.	97.256	0.84	1.04
3567019	359250.	676850.	37.803	15.79	1.37
3567020	359430.	677965.	14.981	26.70	0.79
3567021	357715.	678505.	17.347	45.26	0.59
3567022	356938.	679590.	16.725	57.08	0.41
3567023	357485.	677850.	27.898	35.06	0.70
3567024	356602.	677990.	16.771	49.83	0.63
3567025	355240.	677625.	28.143	59.90	0.56
3567026	351575.	673850.	44.110	32.26	0.86
3567027	350525.	674863.	111.643	52.94	0.95
3567028	350175.	675638.	135.468	60.20	1.12
3567029	350962.	679413.	24.035	93.12	0.47
3567030	350400.	678775.	45.670	96.89	0.58
3567031	350312.	677972.	73.633	87.37	0.97
3567032	350555.	677162.	94.890	77.91	0.82
3567033	351087.	676010.	154.915	54.36	1.86
3567034	351500.	674900.	77.338	45.03	1.15
3567035	350700.	673875.	59.975	43.43	0.78
3567036	352075.	678250.	57.846	79.91	0.68
3567037	352200.	677625.	92.811	71.55	0.85
3567038	352338.	677250.	78.345	72.82	0.57
3567039	353100.	677225.	80.368	67.00	0.59
3567040	354338.	678400.	45.758	69.01	0.41
3567041	353275.	679788.	17.590	83.67	0.40
3567042	352500.	679745.	17.239	85.07	0.45
3567043	351138.	679700.	17.413	95.06	0.40
3567044	350160.	674250.	77.519	48.31	0.66
3567045	353140.	674967.	47.913	35.53	0.88
3567046	353375.	674375.	44.294	25.96	0.77
3567047	354475.	674238.	49.136	19.56	0.79
3567048	355275.	674700.	39.066	19.87	0.94
3567049	356125.	674800.	47.344	16.40	0.97
3567050	357100.	674813.	74.266	5.34	1.25
3567051	355515.	673526.	62.835	7.88	1.04
3567052	356090.	673175.	80.206	5.60	1.17
3567053	357075.	672525.	104.272	3.69	1.50
3567054	357828.	672998.	141.295	-5.90	2.34
3567055	359085.	672440.	116.880	4.03	1.79
3567056	359425.	671932.	134.987	1.99	1.98

3567057	358568.	671575.	135.413	-4.88	2.44
3567058	358905.	671093.	146.384	-2.99	3.36
3567059	355300.	671812.	99.939	2.26	1.33
3567060	356903.	676380.	90.378	24.33	1.26
3567061	357530.	676600.	90.725	22.96	1.44
3567062	358292.	676812.	57.685	23.06	0.81
3567063	358645.	676925.	39.840	22.87	0.93
3567064	350850.	671187.	64.561	9.25	0.84
3567065	350780.	670180.	77.999	0.72	0.89
3567066	351400.	671350.	58.289	7.26	0.90
3567067	352220.	672150.	59.566	9.92	0.82
3567068	351840.	673100.	62.709	21.69	0.65
3567069	350950.	672410.	55.248	22.05	0.75
3567070	354075.	676112.	79.553	42.63	0.75
3567071	354162.	677600.	48.692	65.03	0.48
3567072	354137.	679087.	34.506	76.75	0.42
		NT 58			
3568001	350340.	681858.	22.765	92.44	0.30
3568002	351240.	682195.	32.840	86.88	0.45
3568003	351300.	681725.	30.100	91.37	0.43
3568004	351095.	680585.	9.338	94.79	0.30
3568005	351158.	681162.	15.274	91.51	0.22
3568006	350685.	683432.	37.146	83.33	0.19
3568007	351050.	682575.	25.044	80.01	0.15
3568008	352875.	682355.	35.604	85.97	0.18
3568009	354220.	682300.	75.343	90.51	2.21
3568010	354100.	681400.	46.833	80.48	0.42
3568011	355740.	683050.	63.014	68.17	0.33
3568012	354885.	683307.	59.654	73.75	0.31
3568013	355135.	683975.	56.048	70.24	0.40
3568014	354610.	685287.	14.088	68.99	0.31
3568015	351590.	685615.	5.927	72.78	0.09
3568016	359665.	681426.	25.575	46.63	0.62
3568017	358820.	680810.	49.310	49.61	0.69
3568018	359300.	680100.	11.274	32.81	0.46
3568019	357612.	681765.	52.952	58.46	0.30
3568020	357120.	682775.	40.449	61.29	0.51
3568021	357960.	683020.	35.974	57.29	0.30
3568022	356725.	683475.	59.421	60.84	0.29
3568023	351455.	683962.	26.208	84.78	0.20
3568024	352337.	684512.	17.586	83.26	0.14
3568025	353962.	685112.	22.272	72.46	0.20
3568026	357887.	685137.	45.036	62.98	0.56
3568027	359075.	684762.	30.828	52.88	0.27
3568028	359937.	683512.	19.780	51.89	0.42
3568029	354325.	680325.	19.108	79.59	0.33
3568030	356300.	681013.	48.703	70.07	0.44
3568031	358275.	681475.	53.392	60.19	0.35
		NO 50			
3570001	352700.	702575.	22.030	17.30	0.20
3570002	354375.	702675.	27.050	13.24	0.22
3570003	354025.	704250.	35.387	21.72	0.24
3570004	354550.	706063.	55.199	24.32	0.34
3570005	354575.	708513.	113.447	19.15	0.39
3570006	352725.	708100.	134.030	15.95	0.53
3570007	353075.	706550.	92.060	24.08	0.68
3570008	352063.	704800.	52.050	22.20	0.50

3570009	351010.	706520.	128.060	13.67	0.87
3570010	356825.	708900.	98.050	17.99	0.40
3570011	357200.	707563.	71.384	16.30	0.28
3570012	359925.	708363.	64.040	22.87	0.29
3570013	357900.	705115.	32.040	22.95	0.24
3570014	355850.	703500.	19.050	17.74	0.17
3570015	351125.	701300.	19.842	18.54	0.18
3570016	350875.	703650.	33.100	18.73	0.37
		NT 62			
3662001	360650.	628700.	134.112	34.32	0.49
3662002	362738.	625600.	110.033	36.12	0.59
3662003	361075.	625863.	148.000	33.19	0.72
3662004	364325.	626675.	145.694	28.19	0.46
3662005	363250.	628200.	154.534	26.31	0.44
3662006	365063.	628325.	116.129	25.53	0.46
3662007	364830.	625090.	93.878	31.17	1.19
3662008	360995.	622900.	86.258	33.58	1.34
3662009	361675.	621335.	129.000	33.28	1.67
3662010	363690.	621030.	216.408	32.04	1.59
3662011	365695.	620475.	122.225	39.38	0.90
3662012	367415.	620313.	195.072	26.14	0.78
3662013	368985.	621738.	119.000	33.51	0.94
3662014	369500.	620595.	95.707	28.61	1.30
3662015	369020.	624700.	59.741	36.20	2.09
3662016	367660.	622800.	141.000	31.49	0.98
3662017	365038.	622225.	121.006	34.12	1.01
3662018	365425.	623613.	90.221	29.81	1.12
3662019	367125.	625760.	65.532	35.47	1.31
3662020	368342.	626675.	87.478	35.65	0.61
3662021	369105.	628115.	85.344	27.80	0.62
		NT 63			
3663001	368138.	639925.	177.394	15.80	0.64
3663002	368288.	638500.	135.331	16.03	0.78
3663003	368625.	637163.	94.183	15.10	0.46
3663004	369575.	636425.	78.334	13.32	0.45
3663005	369375.	634465.	65.837	21.42	0.48
3663006	368538.	633650.	63.094	21.25	0.61
3663007	366975.	632738.	85.954	25.06	0.58
3663008	366888.	634350.	131.674	19.65	0.42
3663009	365875.	635800.	147.218	17.37	0.31
3663010	363425.	635930.	143.256	23.85	0.36
3663011	361500.	634838.	135.331	29.47	0.83
3663012	360160.	633850.	170.383	34.09	0.94
3663013	360300.	635925.	232.258	24.77	1.73
3663014	362010.	632438.	84.734	37.33	0.60
3663015	360750.	631788.	65.227	42.66	0.85
3663016	360675.	630185.	78.638	39.86	0.55
3663017	362875.	630525.	80.772	36.60	0.49
3663018	364088.	631050.	76.810	32.89	0.73
3663019	365600.	630575.	109.118	22.89	0.62
3663020	369025.	632413.	67.666	20.23	0.34
3663021	367585.	630900.	80.162	19.12	0.47
3663022	369800.	631015.	73.152	18.92	0.40
3663023	363625.	633405.	108.509	28.65	0.63
3663024	365425.	632800.	114.605	27.78	0.58
3663025	366450.	638625.	185.318	13.58	1.47
3663026	364925.	639550.	162.763	19.75	0.38
3663027	363150.	638225.	151.486	28.49	0.23

3663028	363775.	637275.	131.978	27.95	0.37
3663029	360750.	639550.	135.941	34.32	0.52
		NT 64			
3664001	360900.	648300.	226.152	-3.91	0.55
3664002	361975.	648950.	215.363	-2.70	0.45
3664003	363025.	649625.	206.912	-4.53	0.54
3664004	363315.	648525.	213.722	-5.96	0.36
3664005	363100.	647575.	220.066	-3.91	0.37
3664006	365532.	646920.	185.318	3.32	0.38
3664007	365330.	646750.	197.572	2.29	0.41
3664008	367307.	646425.	208.483	3.78	0.55
3664009	368925.	646250.	181.661	10.07	0.39
3664010	367725.	645400.	206.554	2.01	0.78
3664011	366865.	644870.	172.517	4.75	0.41
3664012	365950.	644800.	163.893	0.71	0.32
3664013	364800.	644950.	179.567	0.87	0.39
3664014	360525.	647505.	237.584	-3.37	0.57
3664015	363100.	646300.	207.633	1.96	0.46
3664016	362295.	645445.	190.195	6.83	0.50
3664017	361700.	644950.	177.808	10.22	0.77
3664018	360610.	644200.	192.591	13.48	0.49
3664019	363075.	645030.	178.513	1.62	0.43
3664020	361750.	643200.	191.822	10.74	0.63
3664021	360125.	640725.	158.513	28.15	0.47
3664022	362763.	643155.	177.598	7.24	0.67
3664023	363625.	642875.	140.575	10.32	0.47
3664024	361325.	646170.	207.501	4.42	0.43
3664025	364740.	643125.	167.941	8.56	0.30
3664026	366900.	643925.	191.989	0.33	0.77
3664027	367975.	644140.	167.030	7.14	0.29
3664028	369288.	644650.	161.239	18.63	0.31
3664029	369905.	644990.	164.742	23.30	0.35
3664030	367575.	643425.	162.154	4.74	0.34
3664031	366700.	642850.	152.559	11.56	0.42
3664032	365950.	642275.	136.183	16.96	0.33
3664033	365863.	641270.	145.092	21.50	0.32
3664034	364425.	641313.	157.182	17.34	0.38
3664035	363525.	640900.	170.883	21.59	0.36
3664036	361325.	640363.	198.778	27.80	0.87
3664037	360275.	646645.	236.220	2.44	0.42
3664038	364500.	644045.	173.736	0.72	0.29
3664039	369525.	646625.	184.800	15.15	0.36
3664040	368580.	647200.	195.582	6.93	0.32
3664041	367750.	647780.	177.846	6.91	1.14
3664042	367275.	648557.	195.986	1.04	0.42
3664043	366988.	640425.	147.523	22.94	0.27
3664044	368225.	640010.	176.630	15.65	0.53
3664045	368325.	641038.	161.950	22.49	0.42
3664046	369340.	642663.	143.009	27.27	0.38
		NT 65			
3665001	369375.	657088.	215.356	-27.31	1.12
3665002	366775.	655975.	309.067	-16.94	1.12
3665003	368950.	657850.	241.097	-29.55	1.09
3665004	368330.	658685.	293.438	-29.09	1.69
3665005	360275.	650663.	266.395	0.88	0.91
3665006	361450.	650825.	255.923	-2.75	1.02
3665007	362500.	651275.	233.458	-9.80	1.13

3665008	363175.	650610.	217.322	-4.23	0.70
3665009	364175.	650175.	208.712	-4.77	0.55
3665010	364375.	651625.	226.940	-8.77	0.78
3665011	365850.	650825.	203.572	-7.63	0.62
3665012	366900.	651288.	234.696	-8.66	0.48
3665013	368200.	651688.	232.823	-9.77	0.58
3665014	369300.	651775.	222.515	-10.61	0.65
3665015	366530.	653765.	310.896	-12.94	1.58
3665016	365415.	654825.	340.157	-13.84	1.35
3665017	364330.	654525.	331.013	-15.99	1.28
3665018	363475.	653875.	319.430	-18.27	1.58
3665019	362405.	654775.	446.837	-12.32	4.41
3665020	361300.	655495.	436.473	-22.78	2.31
3665021	360600.	656475.	464.210	-25.99	2.86
3665022	363075.	656875.	436.473	-20.79	3.69
3665023	365335.	657095.	361.188	-18.11	2.28
3665024	364675.	656180.	300.228	-14.39	1.48
3665025	366775.	655975.	309.067	-17.05	1.12
3665026	366625.	658575.	273.101	-21.53	1.43
3665027	367375.	659538.	336.225	-29.94	1.59
3665028	367320.	657405.	316.382	-18.69	2.46
3665029	361700.	652525.	349.300	-5.55	1.91
		NT 66			
3666001	360175.	659418.	245.914	6.71	4.04
3666002	361620.	668275.	344.807	-17.56	2.91
3666003	362137.	667475.	314.488	-22.69	1.83
3666004	362435.	666965.	287.644	-20.70	3.27
3666005	363335.	665960.	287.448	-26.36	1.90
3666006	364008.	665150.	280.544	-33.25	1.94
3666007	365575.	663825.	250.295	-40.42	2.96
3666008	368525.	663135.	200.396	-41.33	4.10
3666009	369690.	661225.	187.190	-45.41	2.32
3666010	368870.	662625.	193.852	-44.03	3.13
3666011	363655.	664675.	284.178	-30.42	1.61
3666012	362560.	664655.	312.265	-15.21	1.49
3666013	360650.	654200.	433.437	-13.27	3.57
3666014	361315.	663605.	400.527	-20.18	2.46
3666015	362475.	662175.	301.752	-20.45	4.25
3666016	363425.	661105.	307.543	-30.11	2.76
3666017	365175.	661588.	420.014	-38.98	4.48
3666018	366150.	660275.	413.918	-27.50	3.99
3666019	368425.	664540.	212.141	-44.76	5.30
3666020	368313.	665725.	251.155	-40.66	4.58
3666021	369625.	664700.	358.750	-58.69	4.95
3666022	369320.	665888.	344.424	-51.10	7.15
3666023	368600.	666825.	359.054	-40.34	11.01
3666024	368770.	668563.	310.896	-40.86	14.51
3666025	368513.	669620.	354.482	-62.61	5.65
3666026	365775.	663675.	247.802	-44.16	2.69
3666027	366088.	667950.	267.615	-43.90	3.01
3666028	366040.	668958.	330.404	-39.21	3.31
3666029	365875.	667425.	261.519	-40.39	4.18
3666030	365015.	663275.	252.070	-36.45	3.10
3666031	367275.	666215.	242.012	-46.69	7.52
		NT 67			
3667001	365625.	674875.	104.024	-11.80	1.67
3667002	366300.	674925.	76.711	-16.70	2.69
3667003	367075.	675360.	78.393	-21.12	2.26

3667004	369788.	677032.	24.427	-50.62	1.21
3667005	368675.	678395.	12.725	-18.87	0.72
3667006	361700.	672888.	119.235	4.94	2.53
3667007	361837.	671962.	164.962	8.12	3.13
3667008	361435.	671275.	164.214	6.92	2.76
3667009	360942.	671337.	159.090	5.70	2.55
3667010	360362.	671125.	157.992	4.42	2.75
3667011	360075.	671387.	161.470	4.00	2.33
3667012	360300.	672470.	137.118	6.17	1.82
3667013	360962.	672790.	112.719	4.71	2.13
3667014	361750.	673825.	102.875	4.57	1.80
3667015	360375.	673960.	87.811	3.94	1.41
3667016	360062.	673610.	92.942	6.55	1.45
3667017	360758.	674337.	75.519	11.89	1.37
3667018	368575.	673940.	143.528	-43.45	2.71
3667019	369805.	673515.	135.484	-62.57	1.95
3667020	369725.	672150.	161.903	-64.16	4.66
3667021	362595.	675275.	60.542	1.37	1.54
3667022	362825.	674825.	88.008	5.45	1.76
3667023	364998.	675325.	79.805	-6.78	1.59
3667024	365575.	675690.	80.290	-11.58	1.47
3667025	366125.	676300.	51.855	-10.51	1.37
3667026	366800.	677050.	31.118	-11.49	1.09
3667027	366800.	677900.	18.304	-10.09	0.84
3667028	368255.	677800.	18.180	-20.77	0.89
3667029	367745.	676492.	53.131	-15.00	1.33
3667030	367500.	675720.	70.101	-20.42	1.86
3667031	365775.	674310.	117.876	-14.43	2.22
3667032	365217.	673310.	147.885	-15.31	2.20
3667033	365210.	672838.	158.550	-18.97	2.48
3667034	365675.	672700.	134.834	-26.00	4.00
3667035	365812.	673350.	107.987	-24.59	4.20
3667036	362600.	677532.	20.168	-10.01	0.91
3667037	364012.	677552.	11.237	-12.41	0.91
3667038	367725.	678850.	13.344	-12.13	0.62
3667039	360900.	679637.	31.025	21.78	0.53
3667040	361150.	678950.	6.741	18.84	0.65
3667041	361537.	677900.	12.851	4.75	0.83
3667042	360125.	677137.	33.566	2.99	1.27
3667043	360525.	676075.	56.075	-3.57	1.05
3667044	361325.	675050.	50.840	-1.41	1.52
3667045	362087.	674075.	98.513	5.92	1.93
3667046	364112.	675225.	80.780	-2.09	1.65
3667047	366625.	676162.	70.134	-12.86	1.43
3667048	366850.	677400.	23.774	-12.37	1.00
3667049	364650.	671358.	337.414	-25.96	5.00
3667050	367562.	674300.	148.743	-38.69	1.75
3667051	365850.	670488.	353.568	-37.02	4.17
3667052	367675.	670025.	396.545	-59.60	7.12
		NT 68			
3668001	360122.	682162.	30.454	42.90	0.79
		NO 60			
3670001	361950.	708725.	29.050	18.66	0.16
3670002	360313.	705725.	29.060	11.74	0.28
		NT 72			
3762001	370400.	625735.	51.206	27.01	1.18
3762002	370190.	624165.	133.502	33.04	1.03
3762003	371200.	629700.	93.269	18.54	0.48

3762004	370895.	628125.	79.000	19.72	0.96
3762005	373105.	629525.	159.410	14.37	0.87
3762006	372663.	628050.	116.738	11.90	0.91
3762007	372675.	626405.	88.392	1.69	0.80
3762008	374540.	625545.	66.000	-10.83	1.22
3762009	373400.	623375.	125.578	-14.04	0.94
3762010	373050.	622325.	129.000	-7.92	2.28
3762011	371125.	621463.	162.154	35.71	0.85
3762012	376100.	624875.	77.724	-26.02	1.56
3762013	376365.	623675.	143.561	-32.10	1.37
3762014	375907.	622275.	178.003	-30.71	1.58
3762015	378200.	625250.	86.868	-28.54	2.64
3762016	379995.	625675.	97.536	-15.23	11.99
3762017	378142.	629555.	171.602	-11.87	0.77
3762018	376650.	628430.	108.509	-9.60	1.04
3762019	375175.	628575.	113.995	11.77	0.73
3762020	375110.	626525.	101.498	-15.93	0.99
3762021	377242.	626800.	106.985	-21.63	1.42
3762022	378130.	623010.	115.824	-38.88	3.72
3762023	378125.	621475.	120.091	-33.91	5.15
		NT 73			
3763001	370800.	639750.	136.855	14.36	0.48
3763002	371320.	638450.	115.824	14.72	0.65
3763003	372400.	637713.	51.816	12.28	0.73
3763004	370850.	636475.	64.008	16.15	0.43
3763005	370063.	634900.	67.666	16.77	0.36
3763006	371775.	635100.	62.179	9.75	0.42
3763007	370450.	633013.	45.415	21.34	0.56
3763008	370250.	630963.	43.586	23.75	0.91
3763009	372325.	632538.	84.430	17.21	0.54
3763010	372220.	630600.	108.814	18.48	0.40
3763011	373925.	630300.	150.571	22.10	0.68
3763012	374800.	631500.	117.958	23.83	0.54
3763013	375825.	630950.	116.129	22.09	0.55
3763014	378150.	630225.	171.000	-7.51	0.63
3763015	379950.	631488.	199.000	-8.79	0.94
3763016	378375.	632550.	202.000	6.73	1.65
3763017	376425.	632663.	137.000	25.73	0.59
3763018	375475.	634600.	58.217	13.40	0.79
3763019	378650.	637390.	41.758	19.43	0.63
3763020	379465.	635450.	133.807	11.54	0.84
3763021	378525.	633975.	155.448	10.62	0.93
3763022	374240.	633238.	82.296	18.48	0.60
3763023	373240.	634192.	34.747	21.54	0.68
3763024	373250.	635950.	51.206	8.53	0.37
3763025	373913.	637225.	38.710	15.85	0.61
3763026	373605.	639105.	76.810	12.30	0.34
3763027	374975.	639225.	60.046	17.51	0.42
3763028	375675.	636850.	33.223	15.89	0.57
3763029	376775.	637813.	28.000	16.16	0.63
3763030	377825.	638575.	28.000	13.85	0.54
3763031	378475.	639700.	35.000	17.78	0.42
		NT 74			
3764001	372875.	649150.	217.322	7.09	1.00
3764002	371575.	647675.	229.210	15.33	0.89
3764003	370455.	646300.	173.906	22.81	0.48
3764004	371150.	646040.	148.411	22.33	0.67

3764005	372600.	645520.	163.331	12.63	0.46
3764006	374025.	645645.	152.586	12.35	0.60
3764007	375135.	645425.	114.000	11.53	0.47
3764008	375475.	646700.	133.800	12.43	0.46
3764009	376350.	647700.	128.016	4.22	0.40
3764010	378450.	648475.	106.500	4.82	0.37
3764011	379600.	649325.	100.916	2.06	0.35
3764012	377195.	649650.	115.076	-4.61	0.44
3764013	375230.	648925.	106.316	-5.14	1.34
3764014	375900.	649875.	135.869	-13.41	0.68
3764015	374305.	648545.	163.156	-6.88	0.82
3764016	373270.	647140.	165.500	6.59	0.69
3764017	370445.	644850.	161.040	24.34	0.40
3764018	371720.	644200.	176.589	15.61	0.53
3764019	372725.	642892.	137.907	14.17	0.62
3764020	373142.	643607.	141.494	13.49	0.56
3764021	373850.	644452.	129.268	14.93	0.69
3764022	377057.	646525.	97.780	9.58	0.36
3764023	370270.	643400.	181.077	20.35	0.48
3764024	370542.	641545.	192.043	24.13	1.17
3764025	371700.	641800.	151.813	19.80	0.73
3764026	371630.	640705.	125.882	18.25	0.43
3764027	372910.	641300.	113.212	20.39	0.39
3764028	374325.	640575.	82.884	12.11	0.32
3764029	374105.	641755.	87.121	15.13	0.42
3764030	374415.	643020.	91.367	12.17	0.48
3764031	376425.	643480.	75.895	12.45	0.32
3764032	376325.	642425.	73.704	12.31	0.29
3764033	376350.	641445.	74.362	14.80	0.27
3764034	377638.	640610.	65.377	16.12	0.28
3764035	378775.	640775.	42.672	14.23	0.34
3764036	377495.	642542.	71.330	16.07	0.25
3764037	377685.	645370.	76.312	11.55	0.33
3764038	379530.	644600.	68.350	9.70	0.23
3764039	378625.	643925.	60.960	14.99	0.27
3764040	379635.	642595.	52.426	12.22	0.25
3764041	377325.	644250.	64.519	11.99	0.39
		NT 75			
3765001	379825.	655750.	101.604	-25.11	0.73
3765002	378625.	655925.	129.108	-18.97	0.84
3765003	378825.	657200.	87.700	-45.24	1.63
3765004	379600.	658550.	145.100	-25.55	1.25
3765005	379500.	659750.	196.901	-25.72	1.27
3765006	376500.	658125.	133.502	-36.33	2.27
3765007	377175.	656950.	129.845	-22.92	2.27
3765008	375475.	659480.	237.134	-40.94	1.12
3765009	375200.	658355.	144.170	-35.96	3.84
3765010	373888.	658850.	201.168	-50.63	3.38
3765011	373050.	659875.	166.116	-53.08	3.16
3765012	371413.	658455.	262.433	-54.42	1.78
3765013	371500.	654875.	222.199	-28.33	1.40
3765014	374875.	651413.	174.700	-29.40	0.88
3765015	370607.	651917.	218.542	-10.61	0.45
3765016	372500.	651575.	235.610	-6.65	0.66
3765017	374050.	650957.	188.366	-16.12	0.90
3765018	374482.	650350.	172.008	-19.62	0.84
3765019	379575.	650525.	95.691	-5.43	0.37
3765020	378175.	650025.	96.300	-2.50	0.44

3765021	377225.	650705.	116.500	-13.53	0.52
3765022	376738.	652063.	119.740	-28.30	0.69
3765023	377705.	652150.	110.500	-19.80	0.58
3765024	378825.	651775.	98.037	-10.60	0.46
3765025	378875.	652850.	118.772	-11.93	0.55
3765026	378700.	653725.	125.544	-13.67	0.75
3765027	379863.	652930.	100.755	-9.83	0.45
3765028	377190.	653225.	121.700	-24.24	0.93
3765029	376225.	653850.	152.283	-31.25	1.65
3765030	374900.	653763.	244.400	-32.68	2.89
3765031	373600.	654155.	322.783	-28.05	3.11
3765032	370513.	656050.	195.206	-32.97	1.30
		NT 76			
3766001	378600.	669475.	117.189	-69.79	2.34
3766002	379710.	667580.	116.890	-66.15	5.08
3766003	378908.	666775.	157.207	-68.05	2.11
3766004	377625.	666585.	228.030	-67.21	1.51
3766005	376087.	667262.	271.108	-60.98	2.84
3766006	376850.	665660.	188.620	-66.47	1.62
3766007	376600.	664725.	233.590	-61.93	1.13
3766008	378425.	663040.	215.213	-52.80	1.31
3766009	378800.	663712.	153.775	-59.35	1.52
3766010	379355.	664315.	180.145	-61.40	1.15
3766011	379762.	665050.	165.919	-63.28	1.74
3766012	375050.	667132.	237.257	-60.46	1.56
3766013	374435.	666700.	240.853	-60.01	1.79
3766014	373275.	665500.	245.915	-58.08	2.83
3766015	372745.	664500.	234.153	-63.49	2.20
3766016	375525.	662325.	150.110	-54.56	3.11
3766017	376075.	664287.	213.090	-62.34	1.00
3766018	377875.	662337.	233.879	-50.08	1.19
3766019	375262.	669525.	161.713	-95.33	1.63
3766020	373268.	666125.	317.602	-63.02	3.03
3766021	371594.	666550.	391.060	-70.14	7.01
3766022	371175.	668175.	412.390	-63.62	9.37
3766023	371950.	668750.	353.873	-73.29	6.52
3766024	372888.	667962.	349.606	-69.99	6.28
3766025	377725.	668775.	249.326	-71.32	5.13
		NT 77			
3767001	372012.	674035.	79.549	-74.47	2.57
3767002	373075.	673775.	80.898	-90.06	2.25
3767003	373910.	673200.	73.655	-97.28	2.54
3767004	373625.	672537.	133.380	-99.86	2.76
3767005	373300.	671185.	193.024	-82.22	5.47
3767006	373680.	670800.	133.160	-96.71	3.99
3767007	374740.	672200.	100.459	-110.09	1.96
3767008	375610.	672365.	73.049	-111.71	1.72
3767009	378925.	670850.	47.695	-81.95	2.54
3767010	379575.	670205.	90.586	-70.05	3.77
3767011	377615.	6712[illegible]7.	64.730	-118.04	1.71
3767012	370450.	672812.	151.281	-68.93	2.28
3767013	370438.	673690.	138.410	-62.13	2.05
3767014	371437.	673825.	94.497	-68.00	2.47
3767015	371835.	674930.	46.936	-90.01	1.83
3767016	372723.	675471.	26.213	-95.22	1.27
3767017	371396.	676509.	22.902	-72.77	1.12
3767018	370471.	676786.	27.503	-61.27	1.18

3767019	370283.	676849.	25.592	-58.54	1.21
3767020	372723.	675471.	26.213	-95.22	1.27
3767021	376825.	670750.	106.139	-110.15	1.48
3767022	375850.	670150.	134.570	-87.54	1.57
3767023	374250.	670550.	139.482	-98.01	2.21
3767024	370650.	675613.	71.774	-79.62	1.79
3767025	375280.	671325.	115.520	-112.47	1.69
3767026	374387.	674337.	24.590	-93.53	1.58
		NT 83			
3863001	380700.	634575.	112.166	1.31	0.62
3863002	382088.	635850.	74.371	-2.34	0.59
3863003	383825.	637200.	48.158	-4.16	0.54
3863004	383342.	634525.	146.509	-3.34	1.63
3863005	384913.	633663.	87.000	0.12	0.85
3863006	384045.	631975.	108.000	-4.07	1.30
3863007	385975.	632675.	89.306	-3.98	3.65
3863008	387115.	633115.	71.018	-23.74	2.09
3863009	388600.	632575.	72.542	-24.88	3.04
3863010	389775.	631650.	99.000	-32.55	4.03
3863011	388813.	635038.	159.000	-13.90	1.29
3863012	388100.	636200.	97.231	-4.28	1.61
3863013	385750.	639250.	28.000	0.70	0.50
3863014	385250.	637313.	36.271	-3.78	0.70
3863015	386200.	635425.	66.000	-4.94	1.18
3863016	380838.	632350.	195.377	-6.03	1.18
3863017	380725.	637975.	83.000	8.05	0.86
3863018	382375.	638525.	21.641	10.05	0.75
3863019	383825.	639463.	21.000	5.51	0.47
3863020	380075.	639463.	43.891	17.62	0.37
3863021	389430.	637575.	66.000	-10.71	0.71
3863022	388075.	638255.	53.645	-13.20	0.44
		NT 84			
3864001	380625.	649700.	85.954	0.83	0.25
3864002	382513.	648313.	63.703	4.38	0.19
3864003	384575.	647175.	72.847	5.42	0.18
3864004	385250.	645400.	60.960	3.54	0.26
3864005	387000.	646213.	42.977	1.50	0.16
3864006	387775.	648155.	54.864	-2.66	0.13
3864007	389600.	647125.	14.326	-7.34	0.44
3864008	389713.	649925.	48.463	-13.19	0.14
3864009	385600.	648588.	66.446	0.18	0.13
3864010	383913.	649713.	59.436	0.77	0.18
3864011	385088.	643863.	45.720	4.19	0.17
3864012	387188.	643825.	34.138	-1.60	0.21
3864013	385513.	642775.	36.881	2.11	0.21
3864014	388875.	643750.	35.052	-1.42	0.21
3864015	388875.	641038.	66.446	-4.45	0.22
3864016	389150.	642225.	39.929	-6.60	0.26
3864017	387650.	642113.	55.169	-0.56	0.28
3864018	386425.	640175.	46.634	0.96	0.23
3864019	383350.	641135.	53.645	8.74	0.29
3864020	382910.	642250.	58.522	9.25	0.35
3864021	380625.	641525.	60.350	11.20	0.18
3864022	381500.	640710.	37.490	9.96	0.34
3864023	382488.	643415.	77.724	12.36	0.30
3864024	382075.	644588.	72.847	12.39	0.27
3864025	383450.	645025.	68.885	8.28	0.16
3864026	381313.	646125.	49.378	10.80	0.19

3864027	380713.	647825.	73.762	8.21	0.26
NT 85					
3865001	380095.	652527.	90.851	-10.01	0.46
3865002	380975.	653455.	93.300	-14.42	0.35
3865003	380745.	654585.	110.982	-22.26	0.45
3865004	381750.	655475.	81.523	-31.45	0.43
3865005	383670.	656775.	77.644	-34.78	0.87
3865006	380725.	655925.	85.555	-31.97	0.64
3865007	384782.	654875.	67.606	-26.19	0.25
3865008	383275.	654650.	69.616	-25.23	0.34
3865009	383575.	653525.	65.081	-15.09	0.28
3865010	382755.	652725.	74.200	-11.73	0.27
3865011	380925.	651560.	73.296	-8.39	0.39
3865012	383500.	657107.	77.992	-34.73	0.41
3865013	385030.	657080.	66.348	-33.81	0.38
3865014	389715.	657625.	115.500	-23.18	0.42
3865015	387688.	657750.	113.814	-33.79	1.12
3865016	387400.	658775.	100.279	-39.03	0.44
3865017	388750.	658725.	94.043	-32.19	0.40
3865018	389625.	658575.	93.900	-23.52	0.41
3865019	386675.	659635.	92.700	-30.19	0.51
3865020	382575.	659250.	97.841	-16.43	0.90
3865021	382017.	657200.	90.526	-33.75	0.57
3865022	382050.	650850.	81.682	-4.52	0.22
3865023	384985.	650688.	60.404	-1.96	0.24
3865024	386250.	650575.	86.798	-4.79	0.33
3865025	387350.	650150.	78.462	-6.38	0.21
3865026	389590.	651190.	52.560	-13.68	0.14
3865027	388017.	650775.	83.800	-11.04	0.38
3865028	386910.	651630.	77.419	-10.22	0.14
3865029	386795.	652525.	69.900	-9.49	0.14
3865030	388250.	652570.	64.870	-15.86	0.13
3865031	389880.	652600.	61.399	-16.37	0.14
3865032	388763.	653700.	58.900	-21.68	0.17
3865033	388525.	654675.	54.100	-21.33	0.23
3865034	389563.	656275.	76.050	-26.56	0.42
3865035	388325.	656370.	79.298	-28.84	0.81
3865036	386913.	655950.	78.773	-27.36	0.53
3865037	386613.	654975.	47.151	-25.59	0.47
3865038	386725.	653475.	67.000	-13.91	0.16
3865039	383175.	651725.	72.500	8.28	0.21
3865040	383720.	650450.	66.500	0.28	0.18
3865041	385130.	652150.	78.470	-5.74	0.17
3865042	387738.	653525.	67.045	-18.84	0.16
3865043	385450.	653400.	72.790	-13.89	0.19
NT 86					
3866001	380875.	665560.	116.765	-57.02	5.31
3866002	381200.	664400.	149.747	-54.13	2.79
3866003	380687.	663865.	181.018	-53.64	1.61
3866004	381855.	661092.	231.111	-23.55	2.19
3866005	381755.	665715.	112.297	-40.54	10.61
3866006	382385.	665965.	161.040	-36.00	10.14
3866007	382800.	666900.	189.574	-44.23	8.06
3866008	383170.	668075.	228.300	-62.34	3.59
3866009	388382.	667700.	178.918	-35.52	1.81
3866010	387350.	668450.	219.403	-47.93	3.47
3866011	385360.	662800.	95.489	-23.69	1.50
3866012	384650.	663587.	89.954	-30.85	2.95

3866013	384100.	663925.	92.415	-33.74	3.39
3866014	383550.	664712.	180.822	-43.08	2.05
3866015	382340.	664563.	106.567	-49.88	3.50
3866016	381650.	669400.	175.847	-64.10	4.89
3866017	384400.	667875.	211.283	-60.12	2.07
3866018	385325.	667133.	193.941	-55.94	1.37
3866019	386082.	666355.	180.756	-44.85	1.12
3866020	386920.	666475.	177.068	-36.72	1.27
3866021	389750.	666225.	97.421	-10.57	0.93
3866022	389850.	665485.	99.953	-10.74	0.78
3866023	389280.	664580.	109.575	-8.58	0.63
3866024	388750.	662755.	96.426	-17.70	0.68
3866025	388930.	661325.	81.239	-27.36	0.40
3866026	387145.	660400.	128.180	-32.65	1.04
3866027	385820.	660180.	93.200	-18.83	0.49
3866028	384025.	660758.	126.653	-11.16	1.49
3866029	382575.	660370.	155.245	-14.51	1.54
3866030	381300.	660120.	158.735	-20.17	1.85
3866031	385400.	661495.	135.540	-15.26	0.92
3866032	384300.	662195.	192.877	-16.31	2.27
3866033	386125.	661712.	133.970	-20.79	0.91
3866034	388025.	662145.	74.278	-21.88	0.57
3866035	387200.	665240.	133.004	-24.55	1.19

NT 93

3963001	391125.	638250.	42.000	-19.28	0.61
3963002	390755.	634525.	111.252	-25.33	1.11
3963003	393288.	634250.	42.367	-47.87	1.47
3963004	393300.	632713.	66.000	-53.75	1.83
3963005	392625.	631225.	56.000	-58.81	3.39
3963006	394700.	631600.	51.000	-77.97	1.54
3963007	396675.	631538.	42.977	-77.10	1.20
3963008	395175.	632900.	46.000	-76.82	0.98
3963009	394825.	634040.	41.148	-71.44	0.82
3963010	397175.	633925.	41.758	-66.09	0.75
3963011	398400.	633775.	48.768	-69.39	0.72
3963012	397525.	635425.	92.659	-69.41	0.66
3963013	395925.	636185.	58.826	-52.29	0.76
3963014	396225.	637535.	117.000	-61.59	0.80
3963015	394200.	637188.	38.000	-29.56	0.80
3963016	390075.	636050.	117.000	-13.53	0.85
3963017	391280.	639400.	53.035	-13.05	0.30
3963018	393040.	639025.	43.000	-21.82	0.55
3963019	394875.	638663.	114.605	-45.93	0.81
3963020	396988.	639250.	128.930	-58.98	0.37
3963021	398950.	637575.	124.000	-71.73	0.42

NT 94

3964001	395950.	649500.	50.292	-43.35	0.28
3964002	398175.	649050.	86.868	-45.80	0.42
3964003	396688.	647225.	69.494	-53.94	0.26
3964004	398263.	646100.	52.730	-65.87	0.12
3964005	396550.	645525.	73.152	-56.79	0.12
3964006	397250.	643438.	75.286	-54.98	0.17
3964007	395263.	642650.	66.446	-48.79	0.30
3964008	395738.	641755.	97.231	-48.30	0.28
3964009	397538.	641438.	106.070	-54.37	0.37
3964010	393613.	641038.	51.816	-37.79	0.56
3964011	392588.	642600.	63.094	-24.94	0.16
3964012	390463.	643025.	46.939	-6.47	0.15

3964013	390380.	640695.	54.559	-4.41	0.31
3964014	394150.	642775.	69.190	-41.79	0.21
3964015	393825.	644475.	81.686	-45.24	0.19
3964016	391650.	644513.	45.720	-11.53	0.15
3964017	390700.	646250.	51.816	-8.05	0.23
3964018	391063.	647575.	40.538	-14.04	0.19
3964019	392363.	648075.	44.806	-16.14	0.12
3964020	393875.	649325.	54.559	-18.23	0.24
3964021	394575.	647957.	55.169	-36.13	0.19
3964022	394325.	646432.	81.382	-42.96	0.33
3964023	392425.	645625.	53.645	-18.49	0.11
		NT 95			
3965001	394625.	655600.	93.944	7.45	0.68
3965002	394692.	654100.	43.276	-11.51	0.56
3965003	395900.	653700.	68.200	-14.27	0.74
3965004	393450.	656025.	88.388	7.40	0.65
3965005	393505.	657200.	124.700	16.26	0.84
3965006	393515.	658305.	150.300	19.11	1.22
3965007	392450.	659363.	90.800	20.72	0.60
3965008	391475.	658825.	96.049	16.11	0.49
3965009	390200.	657820.	124.322	-13.00	0.57
3965010	391175.	657850.	132.893	9.84	0.76
3965011	392100.	657450.	136.830	16.73	0.78
3965012	392250.	656050.	80.541	-1.88	0.52
3965013	390900.	655900.	77.781	-14.63	0.28
3965014	393575.	650275.	35.800	-15.94	0.16
3965015	392725.	651075.	30.800	-10.96	0.22
3965016	391675.	651375.	41.951	-9.71	0.14
3965017	390530.	650975.	47.936	-10.44	0.13
3965018	392375.	651900.	40.234	-10.03	0.17
3965019	393275.	652538.	38.342	-9.24	0.21
3965020	394700.	652475.	24.054	-19.66	0.37
3965021	395738.	652600.	9.749	-18.91	0.68
3965022	393325.	653715.	56.752	-9.81	0.37
3965023	391875.	653725.	59.590	-6.60	0.20
3965024	390825.	653790.	61.132	-13.80	0.18
3965025	392050.	652763.	48.974	-9.21	0.17
3965026	396750.	658013.	112.471	-26.90	2.46
3965027	398425.	655538.	72.238	-38.04	1.12
3965028	397588.	651467.	17.983	-36.58	0.71
		NT 96			
3966001	390075.	665688.	80.167	-9.18	0.92
3966002	390188.	666300.	82.186	-7.04	0.97
3966003	391225.	667188.	50.292	-5.27	1.29
3966004	391875.	667200.	23.891	0.30	1.02
3966005	391525.	666538.	21.176	3.63	1.27
3966006	391490.	665150.	66.247	13.88	0.66
3966007	392275.	664750.	66.984	14.18	0.70
3966008	392550.	663425.	72.238	11.93	0.53
3966009	391450.	663575.	83.168	12.15	0.44
3966010	390688.	664945.	87.587	10.13	0.65
3966011	390075.	663927.	109.429	6.44	0.55
3966012	391900.	662275.	71.985	-2.42	0.33
3966013	390530.	662750.	90.830	-5.96	0.52
3966014	390982.	661750.	60.655	-11.97	0.33
3966015	392125.	661200.	52.073	0.28	0.41
3966016	391675.	660325.	44.143	-0.64	0.84

3966017	390375.	660725.	65.532	-18.26	0.41
3966018	393250.	660410.	88.521	20.05	0.83
3966019	394057.	662090.	65.227	16.11	0.62
3966020	394400.	663150.	28.251	18.03	0.72
3966021	394425.	664045.	11.279	15.43	0.68
3966022	393175.	663900.	58.826	10.77	0.61
3966023	395682.	660425.	97.416	-0.08	2.57

APPENDIX D

PROGRAMS AND ROUTINES USED

In the following section, apart from small programs written mainly for the data manipulation, a brief summary of the programs and routines used will be given.

1. GRAVØ1, GRAVØ3, ..., GRAV12: Different output versions of the general reduction program of gravity data. See detailed description in Chapter II.

2. FTERCOR: Filing program, checking the digitised topography for errors and storing it into a file as data input to TERCOR program; written initially by C J Swain.

3. TERCOR: Calculates the terrain coefficient of gravity stations (see description in Chapter II), written by C J Swain.

4. DENS1, DENS2, DENS3: Programs calculating the Bouguer density fitting by least squares first, second and third degree surface, to the Bouguer anomaly. See description in Chapter II. DENS1, DENS2 were written by R G Hipkin and DENS3 by the author. DENS3 is listed in Appendix E.

5. NETWORK: Performs the least squares adjustment of a gravity base station network (see detailed description in Chapter III).

6. IRSPAC: Converts irregularly spaced data observations into a regular grid, Swain (1976).

7. TRIANG: Plotting routine which plots irregularly spaced data using the triangle method (see description in paragraph 4.3.2), written by C Gold.

8. GPCP: Plotting routine; for details see CALCOMP's (1973) User's Manual.

9. SACM: Commercial package for plotting regularly or irregularly spaced data, performing trend surface analysis (regional-residual separation).

10. SYMAP: Computer mapping program, displaying graphically spatial data with variable density and texture, creating complete maps on a lineprinter and providing a method of interpolating irregularly spaced data (SYMAP user's reference manual, 1975).

11. SYMVU: Program producing three dimensional display of data on a graph plotter (SYMVU user's guide, 1977).

12. MODM2D: Program calculating the disturbance in the total intensity of the earth's magnetic field produced by a number of parallel horizontal prisms of infinite length, arbitrary polygonal cross-section and specified magnetisation, along a profile. (Marine Geophysics Unit (MGU) program.)

13. TALG2D: Program calculating the gravity anomaly in the earth's field along a profile perpendicular to parallel horizontal prisms of infinite length and of arbitrary polygonal cross-section (specified by the co-ordinates of their corners) with a specified density contrast. For details see Talwani et al (1959). (MGU program.)

14. PARKG2D: Two dimensional program written as an iterative procedure and based on Parker's (1972) paper to calculate the 2-D gravitational anomaly caused by an uneven layer of material, whose upper boundary is defined by the equation $Z = h(\vec{r})$.

Then the iterative scheme is:

$$F\left[h_1(\vec{r})\right] = \frac{1}{2nG\rho} F\left[\Delta g(\vec{r}_o)\right] \exp(KZ_o) - \sum_{n=2} \frac{K^{n-1}}{n!} F\left[h_o^n(\vec{r})\right]$$

$$F\left[h_2(\vec{r})\right] = \frac{1}{2nG\rho} F\left[\Delta g(\vec{r}_o)\right] \exp(KZ_o) - \sum_{n=2} \frac{K^{n-1}}{n!} F\left[h_1^n(\vec{r})\right]$$

....

$$F\left[h_p(\vec{r})\right] = \frac{1}{2nG\rho} F\left[\Delta g(\vec{r}_o)\right] \exp(KZ_o) - \sum_{n=2} \frac{K^{n-1}}{n!} F\left[h_{p-1}^n(\vec{r})\right]$$

The notation $F\left[\ldots\right]$ denotes Fourier transform.

It was found that the series of the Fourier transforms was not converging in a satisfactory way. Convergence can be achieved when $h/z \leqslant 1$, something which was not satisfied in the Southern Uplands, trying to model the gravity low in terms of a granite batholith (Chapter V); by putting a value of more than 4-5km for 8, it caused problems on the term $\exp(KZ_o)$, and h in our case was as big as 12km. This might be overcome by attenuating the high frequencies in the term of $F\left[h^n(\vec{r})\right]$.

15. MODG3D: Three-dimensional iterative automatic inversion program calculating the gravity anomaly at grid points due to an interface with a given density contrast where its depth at one point is known. The interface is approximated by rectangular prisms with given length and width, but variable depth whose gravitational attraction is calculated by the use of the full prism formula. (Program written by R G Hipkin.)

16. MODG2D: This program calculates the gravity anomaly along a profile due to a given interface with a constant density contrast. The interface is approximated by prisms with a horizontal or sloping base extending infinitely perpendicular to the direction of the profile. The computation of the attraction of prisms is based on the full slab formula. (Program written initially by R G Hipkin.)

17. MAGRAV: Three-dimensional iterative routine which adjusts an initial model to fit given magnetic field data and calculates its gravitational attraction or vice versa. Program written by Dr D Powell, Geology Department, Glasgow University.

APPENDIX E

LISTING OF PROGRAM DENS3

```
C***************************************************************************
C
C
C                          THE PROGRAM DENS3
C
C
C***************************************************************************


C   PROGRAM DEN3 CALCULATES THE BOUGUER DENSITY FITTING A THIRD
C          DEGREE SURFACE TO THE BOUGUER ANOMALY

      DIMENSION GRV(1000), RHO(1000), X(1000), Y(1000), A(11,11), B(11)
     1 ,IREF(1000),ELEV(1000),TER(1000),ERR(1000),BOUGER(1000)
C           DATA INPUT ON CHANNEL 5
C    IREF=REFERENCE NUMBER OF GRAVITY STATION
C    X=EASTING OF GRAVITY STATION
C    Y=NORTHING OF GRAVITY STATION
C    ELEV=ELEVATION OF GRAVITY STATION
C    GRV=BOUGUER GRAVITY OF GRAVITY STATION
C    TER=TERRAIN COEFFICIENT OF GRAVITY STATION
C     EASTING, NORTHING, ELEVATION ARE
C             IN   METRES


      DO 1 I=1,2000
      READ(5,100,END=2) IREF(I),X(I),Y(I),ELEV(I),GRV(I),TER(I)
    1 RHO(I)=0.41928*ELEV(I)-TER(I)
    2 N=I-1
  100 FORMAT (I7,2F8.0,F9.3,F7.2,F6.2)
C           SET ARRAYS INITIALLY TO ZERO
      DO 3 I=1,11
      B(I)=0.0
      DO 3 J=1,11
    3 A(I,J)=0.0
C          NORMALISE THE VARIABLES
      CALL MAXMIN(N,X,XMAX,IXMAX,XMIN,IXMIN)
      CALL MAXMIN(N,Y,YMAX,IYMAX,YMIN,IYMIN)
      CALL MAXMIN(N,RHO,RHOMAX,IROMAX,RHOMIN,IROMIN)
      CALL MAXMIN(N,GRV,GMAX,IGMAX,GMIN,IGMIN)
      XSCALE = XMAX - XMIN
      YSCALE = YMAX - YMIN
      GSCALE = GMAX - GMIN
      RSCALE = RHOMAX - RHOMIN
      DO 4 I=1,N
      GRV(I)=(GRV(I)-GMIN)/GSCALE
      RHO(I)=(RHO(I)-RHOMIN)/RSCALE
      X(I)=(X(I)-XMIN)/XSCALE
    4 Y(I)=(Y(I)-YMIN)/YSCALE
C          EVALUATE THE ELEMENTS OF THE NORMAL EQUATION MATRICES
      DO 5 I=1,N
      X2=X(I)*X(I)
      XY=X(I)*Y(I)
```

```
Y2=Y(I)*Y(I)
X3=X(I)*X2
X2Y=X2*Y(I)
XY2=X(I)*Y2
Y3=Y2*Y(I)
X4=X3*X(I)
X3Y=X3*Y(I)
X2Y2=X2*Y2
XY3=X(I)*Y3
Y4=Y3*Y(I)

X5=X4*X(I)
X4Y=X4*Y(I)
X3Y2=X3*Y2
X2Y3=X2*Y3
XY4=Y4*X(I)
Y5=Y4*Y(I)

X6=X5*X(I)
Y6=Y5*Y(I)
X5Y=X5*Y(I)
XY5=Y5*X(I)
X3Y3=X3*Y3
X4Y2=X4*Y2
X2Y4=X2*Y4
XGRV=X(I)*GRV(I)
YGRV=Y(I)*GRV(I)
X2GRV=X2*GRV(I)
XYGRV=XY*GRV(I)
Y2GRV=Y2*GRV(I)
XRHO=X(I)*RHO(I)
YRHO=Y(I)*RHO(I)
X2RHO=X2*RHO(I)
XYRHO=XY*RHO(I)
Y2RHO=Y2*RHO(I)
X3RHO=X3*RHO(I)
Y3RHO=Y3*RHO(I)
X2YRHO=X2RHO*Y(I)
XY2RHO=Y2RHO*X(I)
X3GRV=X3*GRV(I)
Y3GRV=Y3*GRV(I)
X2YGRV=X2GRV*Y(I)
XY2GRV=Y2GRV*X(I)

X3GRV=X3*GRV(I)
X2YGRV=X2Y*GRV(I)
XY2GRV=XY2*GRV(I)
Y3GRV=Y3*GRV(I)
X3RHO=X3*RHO(I)
X2YRHO=X2Y*RHO(I)
XY2RHO=XY2*RHO(I)
Y3RHO=Y3*RHO(I)
A(1,2)=A(1,2)+X(I)
A(1,3)=A(1,3)+Y(I)
A(1,4)=A(1,4)+X2
```

```
A(1,5)=A(1,5)+XY
A(1,6)=A(1,6)+Y2
A(1,7)=A(1,7)+X3
A(1,8)=A(1,8)+X2Y
A(1,9)=A(1,9)+XY2
A(1,10)=A(1,10)+Y3
A(1,11)=A(1,11)+RHO(I)
A(2,4)=A(2,4)+X3
A(2,5)=A(2,5)+X2Y
A(2,6)=A(2,6)+XY2
A(2,7)=A(2,7)+X4
A(2,8)=A(2,8)+X3Y
A(2,9)=A(2,9)+X2Y2
A(2,10)=A(2,10)+XY3
A(2,11)=A(2,11)+XRHO
A(3,6)=A(3,6)+Y3
A(3,7)=A(3,7)+X3Y
A(3,8)=A(3,8)+X2Y2
A(3,9)=A(3,9)+XY3
A(3,10)=A(3,10)+Y4
A(3,11)=A(3,11)+YRHO
A(4,4)=A(4,4)+X4
A(4,5)=A(4,5)+X3Y
A(4,6)=A(4,6)+X2Y2
A(4,7)=A(4,7)+X5
A(4,8)=A(4,8)+X4Y
A(4,9)=A(4,9)+X3Y2
A(4,10)=A(4,10)+X2Y3
A(4,11)=A(4,11)+X2RHO

A(5,6)=A(5,6)+XY3
A(5,7)=A(5,7)+X4Y
A(5,8)=A(5,8)+X3Y2
A(5,9)=A(5,9)+X2Y3
A(5,10)=A(5,10)+XY4
A(5,11)=A(5,11)+XYRHO

A(6,6)=A(6,6)+Y4
A(6,7)=A(6,7)+X3Y2
A(6,8)=A(6,8)+X2Y3
A(6,9)=A(6,9)+XY4
A(6,10)=A(6,10)+Y5
A(6,11)=A(6,11)+Y2RHO

A(7,7)=A(7,7)+X6
A(7,8)=A(7,8)+X5Y
A(7,9)=A(7,9)+X4Y2
A(7,10)=A(7,10)+X3Y3
A(7,11)=A(7,11)+X3RHO
A(8,8)=A(8,8)+X4Y2
A(8,9)=A(8,9)+X3Y3
A(8,10)=A(8,10)+X2Y4
A(8,11)=A(8,11)+X2YRHO
A(9,10)=A(9,10)+XY5
A(9,11)=A(9,11)+XY2RHO
```

```
      A(10,10)=A(10,10)+Y6
      A(10,11)=A(10,11)+Y3RHO
      A(11,11)=A(11,11)+RHO(I)*RHO(I)

      B(1)=B(1)+GRV(I)
      B(2)=B(2)+XGRV
      B(3)=B(3)+YGRV
      B(4)=B(4)+X2GRV
      B(5)=B(5)+XYGRV
      B(6)=B(6)+Y2GRV
      B(7)=B(7)+X3GRV
      B(8)=B(8)+X2YGRV
      B(9)=B(9)+XY2GRV
      B(10)=B(10)+Y3GRV
5     B(11)=B(11)+RHO(I)*GRV(I)
      DO 6 I=1,11
      B(I)=B(I)/N
      DO 6 J=1,11
    6 A(I,J)=A(I,J)/N
      A(1,1)=1.0
      A(2,1)=A(1,2)
      A(2,2)=A(1,4)
      A(2,3)=A(1,5)
      A(3,1)=A(1,3)
      A(3,2)=A(1,5)
      A(3,3)=A(1,6)
      A(3,4)=A(2,5)
      A(3,5)=A(2,6)
      A(4,1)=A(1,4)
      A(4,2)=A(2,4)
      A(4,3)=A(3,4)
      A(5,1)=A(1,5)
      A(5,2)=A(2,5)
      A(5,3)=A(3,5)
      A(5,4)=A(4,5)
      A(5,5)=A(4,6)
      A(6,1)=A(1,6)
      A(6,2)=A(2,6)
      A(6,3)=A(3,6)
      A(6,4)=A(4,6)
      A(6,5)=A(5,6)
      A(7,1)=A(1,7)
      A(7,2)=A(2,7)
      A(7,3)=A(3,7)
      A(7,4)=A(4,7)
      A(7,5)=A(5,7)
      A(7,6)=A(6,7)
      A(8,2)=A(2,8)
      A(9,2)=A(2,9)
      A(10,2)=A(2,10)
      A(8,3)=A(3,8)
      A(9,3)=A(3,9)
      A(8,1)=A(1,8)
      A(9,1)=A(1,9)
      A(10,1)=A(1,10)
      A(11,1)=A(1,11)
      A(6,6)=A(3,10)
```

```
      A(11,2)=A(2,11)
      A(11,3)=A(3,11)
      A(11,4)=A(4,11)
      A(11,5)=A(5,11)
      A(11,6)=A(6,11)
      A(11,7)=A(7,11)
      A(11,8)=A(8,11)
      A(11,9)=A(9,11)
      A(11,10)=A(10,11)
      A(8,4)=A(4,8)
      A(8,5)=A(4,9)
      A(8,6)=A(4,10)
      A(9,4)=A(5,8)
      A(9,5)=A(6,8)
      A(9,6)=A(6,9)
      A(10,4)=A(5,9)
      A(10,5)=A(5,10)
      A(10,6)=A(6,10)
      A(10,3)=A(3,10)
       A(8,7)=A(7,8)
       A(8,8)=A(7,9)
       A(8,9)=A(7,10)
       A(9,9)=A(8,10)
       A(9,8)=A(7,10)
      A(10,7)=A(7,10)
      A(10,8)=A(8,10)
      A(10,9)=A(9,10)
      A(9,7)=A(7,9)
C          SOLVE THE NORMAL EQUATIONS USING THE SSP ROUTINE SIMQ
      CALL SIMQ(A,B,11,ISING)
      IF (ISING.EQ.1) GO TO 9991
C          CONVERT TO UN-NORMALISED VARIABLES AND DETERMINE SIGMA
      DO 7 I=1,N
      ERR(I)=GRV(I)-(B(1)+B(2)*X(I)+B(3)*Y(I)+B(4)*X(I)*X(I)
     1 +B(5)*X(I)*Y(I)+B(6)*Y(I)*Y(I)+B(7)*X(I)*X(I)*X(I)+B(8)*X(I)*X(
     1  I)*Y(I)+B(9)*X(I)*Y(I)*Y(I)+B(10)*Y(I)*Y(I)*Y(I)+B(11)*RHO(I))
    7 ERR(I)=ERR(I)*GSCALE
      DENSE=B(11)*GSCALE/RSCALE
      A02=B(6)*GSCALE/(YSCALE*YSCALE)
      A11=B(5)*GSCALE/(XSCALE*YSCALE)
      A20=B(4)*GSCALE/(XSCALE*XSCALE)
      A01=B(3)*GSCALE/YSCALE-2.0*A02*YMIN-A11*XMIN
      A10=B(2)*GSCALE/XSCALE-2.0*A20*XMIN-A11*YMIN
      A00=B(1)*GSCALE+GMIN-A10*XMIN-A01*YMIN-A20*XMIN*XMIN
     1  -A11*XMIN*YMIN-A02*YMIN*YMIN-DENSE*RHOMIN
      VAR=0.0
      DO 8 I=1,N
      X(I)=X(I)*XSCALE+XMIN
      Y(I)=Y(I)*YSCALE+YMIN
      GRV(I)=GRV(I)*GSCALE+GMIN
      RHO(I)=RHO(I)*RSCALE+RHOMIN
      BOUGER(I)=A00+A10*X(I)+A01*Y(I)+A20*X(I)*X(I)+A11*X(I)*Y(I)
     1  +A02*Y(I)*Y(I)+RHO(I)*DENSE
    8 VAR=VAR+ERR(I)*ERR(I)/(RHO(I)*RHO(I))
      SIGMA=SQRT(VAR/N)
```

```
C           OUTPUT   CHANNEL 6
      WRITE (6,200) (IREF(I),X(I),Y(I),ELEV(I),GRV(I),BOUGER(I),ERR(I)
     1  ,I=1,N)
  200 FORMAT (' DETERMINATION OF THE BOUGUER DENSITY BY FITTING A
     1 3RD DEGREE TREND SURFACE TO THE GRAVITY ANOMALY'//' REFERENCE
     1 EASTING
     2  NORTHING    HEIGHT    OBSERVED   CALCULATED   RESIDUAL'/'    NUMBER
     3  (METRES)  (METRES)  (METRES)    ANOMALY    ANOMALY'
     4   //(I10,2F10.0,F10.3,3F10.3))
      WRITE (6,300) DENSE,SIGMA,N
  300 FORMAT  (///' DENSITY CORRECTION = ', F10.5,'   STANDARD DEVIATION
     1  = ', F10.5,'  WITH ',I4,' OBSERVATIONS')
C     WRITE (6,400) A00,A10,A01,A20,A11,A02
C 400 FORMAT (' '///' POLYNOMIAL FOR THE REGIONAL FIELD'/E25.10,' + ',
C    1 E12.5,'X + ',E12.5,'Y + ',E12.5,'X*X + ',E12.5,'X*Y + ',E12.5,
C    2 'Y*Y')
      STOP
 9991 WRITE (6,99910)
99910 FORMAT (' NO SOLUTION POSSIBLE: SINGULAR MATRIX')
      STOP
      END
C*************************************************************************
C
C
C          THE SUBROUTINE MAXMIN
C
C
C*************************************************************************
      SUBROUTINE MAXMIN(N,F,FMAX,IMAX,FMIN,IMIN)
      DIMENSION F(N)
      FMAX=-1.0E40
      FMIN=1.0E40
      I=0
    1 I=I+1
      IF (FMAX.GT.F(I)) GO TO 2
      FMAX=F(I)
      IMAX=I
    2 IF (FMIN.LT.F(I)) GO TO 3
      FMIN=F(I)
      IMIN=I
    3 CONTINUE
      IF(I.EQ.N) GO TO 4
      GO TO 1
    4 RETURN
      END
```

GEOLOGICAL SKETCH MAP
OF
SE SCOTLAND

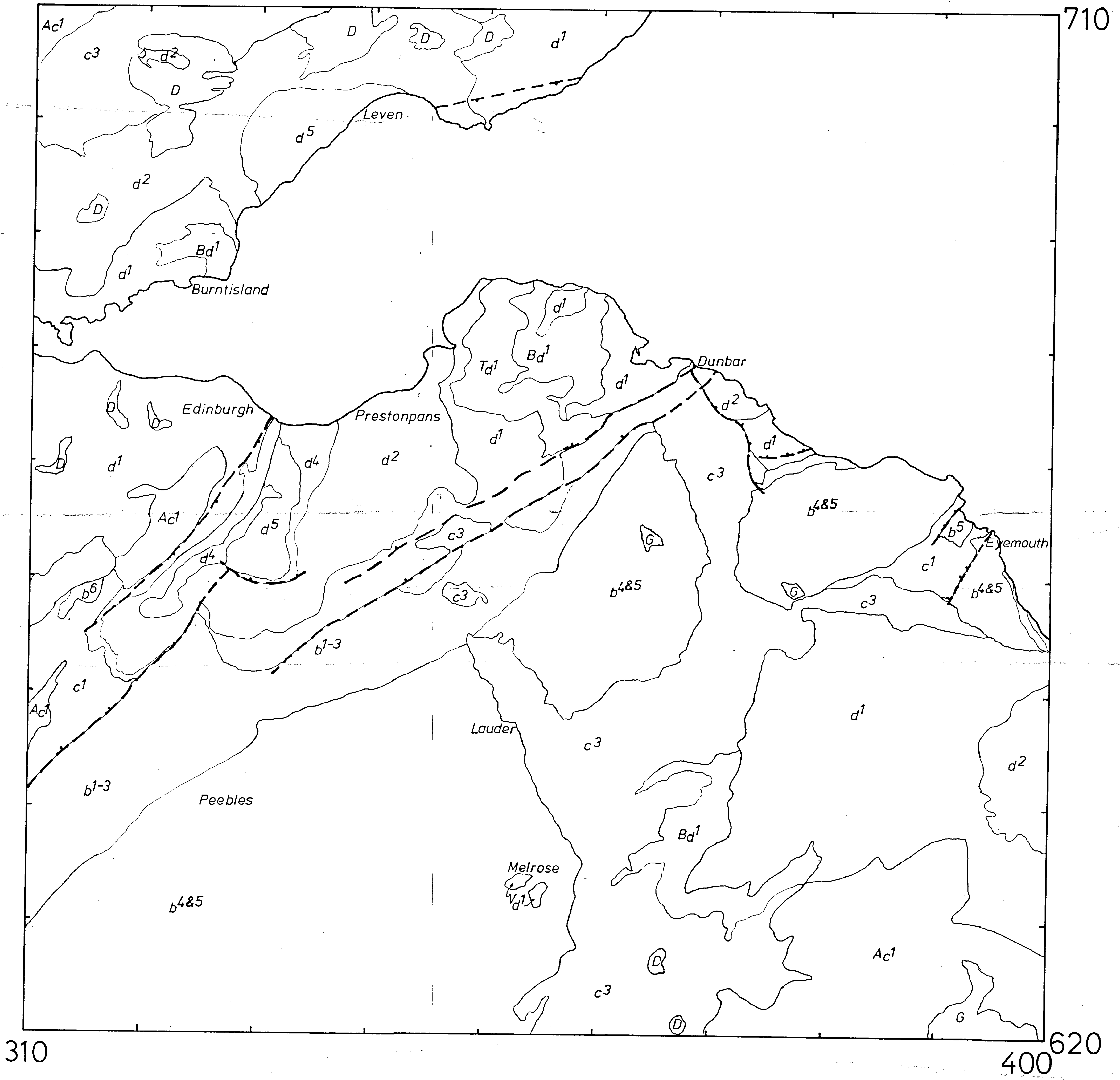

d^5	Coal Measures	Carboniferous		A	Andesite & Mugearite	Extrusive Lavas
d^4	Millstone Grit			B	Basaltic	
d^2	Limestone Series			T	Trachyte, Keratophyre & Rhyolite	
d^1	Calciferous Sandstone Series					
c^3	Upper	Devonian		G	Granite	Intrusive
c^1	Lower			D	Dolerite	
b^{4-6}		Silurian		V	Agglomerate in 'Necks'	
b^{1-3}		Ordovician		—+—	Fault	

BOUGUER GRAVITY ANOMALY MAP
OF SOUTH EAST SCOTLAND

Contour interval 10 gu

Bouguer density 2.67 g cm⁻³

Terrain corrections applied within a radius of 22 km

Anomalies calculated against the International Gravity Formula 1967 and referred to the National Gravity Reference Net 1973